Zeolite Catalysis for Mandelic Acid Conversion and Cyclic Monomer Synthesis

SAMUEL GEORGE MEACHAM

Zeolite Catalysis for Mandelic Acid Conversion and Cyclic Monomer Synthesis

Durham University

Thesis for the degree of PhD

By Samuel George Meacham

Department of Chemistry

June 2024

Table of Contents

Abstract

Petroleum-based plastics are ubiquitous, but their persistence in the environment due to slow (or even the absence of) degradation pathways has resulted in a desire to seek alternative materials with a lower environmental impact. Polyesters of alpha hydroxy acids (AHAs) are one such alternative, as they can be biodegradable and, in some cases, bioderived. Mandelic acid, an AHA bearing a phenyl substituent, can be synthesised into biodegradable polymers with high glass transition temperatures. Poly(mandelic acid) (PMA) has been described as a biodegradable alternative to polystyrene, as a result of the similarities in their structure and their thermal properties. Poly(AHAs) are often best synthesised by ring opening polymerisation (ROP) of a cyclic monomer. In the case of PMA, this has posed some challenges to researchers, requiring the investigation of various novel synthetic strategies, with a particular focus on the nature of the cyclic monomer. The role of catalysis in the synthesis of cyclic monomers from mandelic acid is comparably under-explored, with all reports thus far using the homogeneous catalyst, *p*-TSA. In this thesis, the use of heterogeneous zeolite catalysts in the synthesis of cyclic monomers of mandelic acid is investigated.

The synthesis of the cyclic dimer of mandelic acid, mandelide, was investigated over a range of Brønsted acidic zeolites. The conversion of mandelic acid over these catalysts was found to give rise to a wider variety of products than the previously reported conversion of lactic acid, under similar conditions. The effects of zeolite properties such as framework type, silica:alumina ratio and porosity were investigated.

The use of zeolites in the synthesis of 5-membered 1,3-dioxolan-4-ones of mandelic acid was also investigated. Zeolites performed comparably to p-TSA in batch reactions. After an initial catalyst screening, the best catalyst (H-Y-30) was taken forward for testing in a liquid phase flow reactor. Results varied depending on the monomer synthesised, with the best results achieved for 2-methyl-5-phenyl-1,3-dioxolan-4-one (MePhDOX).

Following the successful synthesis of MePhDOX over USY zeolites in the liquid phase flow reactor, ROP of this monomer using catalysts previously reported for the related monomers PhDOX and Me_2PhDOX was investigated but a successful synthesis of PMA was not achieved.

Chapter 1: Literature Background and Project Aims

1.1 Zeolites

1.1.1 Discovery and Early Work

Zeolites are crystalline microporous minerals. Cronstedt was the first to identify them, discovering zeolite stilbite in 1756.[1] It was a long time before the unique pore structure began to be understood. Just before the turn of the 20th century, Friedel observed that zeolites could adsorb a range of organic molecules, inferring from this that they have a sponge-like structure.[2] It was not until the 1940s that the first synthetic zeolites were made, opening up the field of zeolite synthesis. Some of these first synthetic zeolites were made by conversion of minerals by heating in the presence of salt solutions.[3] Later, synthesis of zeolites from aluminosilicate gels (the basis of most modern zeolite syntheses) was demonstrated.[4, 5] Another key discovery for modern zeolite synthesis was the use of quaternary ammonium compounds as "templates" around which the zeolite structure forms, opening the door to the synthesis of a diverse range of different zeolites from the early 1960s onwards.[5, 6]

1.1.2 Framework

Zeolites are made up of TO_4 tetrahedra, where T is a tetrahedrally-coordinated atom of silicon or aluminium. Adjacent TO_4 tetrahedra are joined through corner-sharing oxygen atoms, leading to a long-range structure referred to as the "framework" of the zeolite. The tetrahedra can be arranged into different secondary buildings units (SBUs), resulting in a diverse range of framework types. There are several aspects of the zeolite structure that vary between different framework types. According to the IUPAC definition, micropores have a diameter of less than 2 nm, mesopores have a diameter of 2-50 nm, and macropores have a diameter of more than 50 nm.[7] Zeolites contain pores in the micropore range. The ring size of the micropores can be expressed in terms of the number of tetrahedral atoms present in the ring. Micropore size in zeolites can be generally categorised as small, medium, large and extra-large pore based on the size of the largest ring, as shown in Table 1.

Table 1 Pore size categorisation of zeolites.[8] ("8MR" = 8-membered ring, etc)

Pore Size	Largest Ring Size	Micropore Diameter / nm	Example of Framework
Small	8MR	0.30-0.45	Zeolite A
Medium	10MR	0.45-0.60	ZSM-5
Large	12MR	0.60-0.80	Zeolites X and Y
Extra Large	14MR	> 0.80	UTD-1

Table 2 Zeolite frameworks and their pore dimensions. The IZA assigns each framework a 3-letter code, shown in brackets here in the "Type" column. Pictures and framework data taken from the IZA database.[9]

Type	Structure	Dimensions	Ring sizes	Pore dimensions / Å	Maximum sphere / Å	
					Included	Diffuses
Beta (BEA)	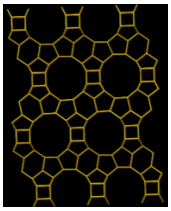	3D	12, 6, 5, 4	6.7	6.68	5.95 (a,b,c)
Faujasite / zeolite Y (FAU)	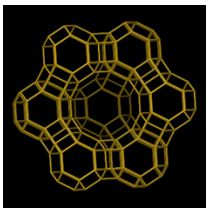	3D	12, 6, 4	7.4	11.24	7.35 (a,b,c)
ZSM5 (MFI)	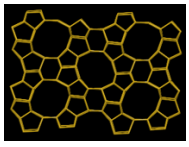	3D	10, 6, 5, 4	5.6	6.36	4.7 (a) 4.46 (b,c)
Mordenite (MOR)	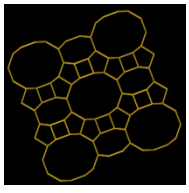	1D	12, 8, 5, 4	7.4 x 6.5	6.7	1.57 (a) 2.95 (b) 6.45 (c)

The International Zeolite Association (IZA) maintains a database of zeolite frameworks[9] which, at the time of writing, contains over 250 different framework topologies. The database is also published periodically as the *Atlas of Zeolite Structure Types*.[10] Whilst a large number of frameworks are known, a much smaller fraction of these are sold and used commercially. Table 2 shows the structures and pore dimensions of some common commercial zeolite frameworks: beta (BEA), faujasite (also known as zeolite Y, FAU), ZSM-5 (MFI) and mordenite (MOR). The 3-letter codes in brackets correspond to the 3-letter code assigned to the framework by the IZA. The number of dimensions of the pore network is shown. For example, mordenite is a one-dimensional (1D) framework, whereas zeolite Beta is a three-dimensional (3D) framework containing three intersecting channels. The data in Table 2 also shows the size of a sphere that can be included within, and can diffuse within, each of the frameworks. These are both key parameters which govern a phenomenon in zeolites known as shape selectivity (which will be discussed in more detail in section 1.1.4).

1.1.3 Acid Sites

Silica is made up of SiO_4 tetrahedra with the bridging oxygen atom shared between adjacent tetrahedra, resulting in a general formula of $(SiO_2)_x$. This ratio of silicon (+4) to oxygen (2-) results in a material with a neutral overall charge. Isomorphous substitution of silicon in SiO_2 with Group III metals such as boron, aluminium, gallium and iron results in a framework with a net negative charge, which requires a charge balancing cation in order to satisfy charge neutrality. As shown in Figure 1b, association of a proton with this negative charge balances the charge and gives rise to Brønsted acid sites. Other cations are possible including ammonium and alkali metals. As a result of these acid sites, zeolites are an important class of heterogeneous catalyst that have been used in a variety of industrial reactions, including fluidized catalytic cracking, alkylation and in the production of aromatics.[11-14]

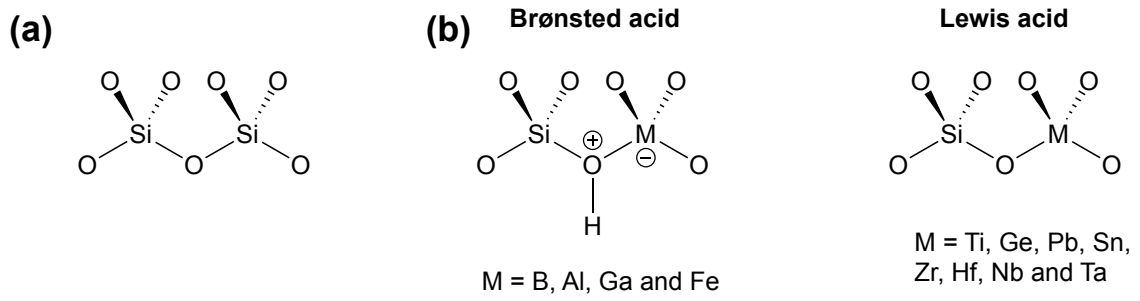

Figure 1 Structure of (a) silica and (b) Brønsted and Lewis acid sites in metallosilicates, such as aluminosilicate zeolites.

Isomorphous substitution of T-atoms by Lewis acidic metals with a +4 oxidation state (e.g., titanium, tin) can give rise to Lewis acid sites. In this case, the framework has a net

neutral charge and therefore no charge balancing cations are present. The nature of tetrahedral atoms introduced into the framework can affect framework stability and acid strength.[15]

Extra-framework species, that are not part of the tetrahedrally-coordinated framework, may also be present. These can form as a result of framework modification such as selective removal of aluminium (known as dealumination) that creates extra-framework species such as octahedral aluminium, $Al(OH)_6$.[16-20] These extra-framework species are known to be Lewis acidic.[21]

1.1.4 Shape Selectivity

Zeolites possess acid sites that are predominantly confined within the micropore network. As a result, the pore structure of zeolites is highly influential on reaction outcomes. The size of the micropores relative to reactants, intermediates and products can lead to shape selectivity. If the pores are too small, diffusion in and out may be slow. This can lead to undesirable effects such as low rates of reaction, or deactivation of the zeolite through formation of carbonaceous deposits (known as “coke”) and pore blockage.

There are three classical types of shape selectivity (illustrated in Figure 2): (a) reactant shape selectivity, (b) product selectivity and (c) transition state selectivity.[22-24] Reactant shape selectivity originates from the confinement of catalytic sites within the internal micropores of zeolites. These sites can only catalyse reactions involving substrates which are sufficiently small to diffuse into the zeolite micropores, and therefore the zeolite is selective for particular substrates based on their size. In transition state shape selectivity, the formation of transition states or molecules which are too large to fit within the micropores are disfavoured. After the products are formed within the zeolite micropore, the next step is desorption out of the pore system. This is only possible if the products are sufficiently small that this diffusion is possible. In some cases, the internal pores may be larger than the pore opening at the surface of the zeolite crystal. As a result, products can form within the internal pores of the zeolite that are too large to exit the crystal back into the bulk reaction medium. Such products can become trapped in the zeolite and may undergo further reaction. Selectivity towards products that are small enough to diffuse out of the zeolite is known as product shape selectivity.

Para-xylene can be produced by xylene isomerisation or toluene disproportionation using medium pore zeolites such as ZSM5.[22] In ZSM5, the undesired meta- and ortho-xylene isomers are also formed, but are too large to diffuse out of the zeolite. Para-xylene on the other hand has a smaller cross-sectional area, due to the para-substitution of the

methyl groups. As a result, m- and o-xylene have to be converted to the p-xylene in order to diffuse out of ZSM5. This is a classical example of product selectivity.

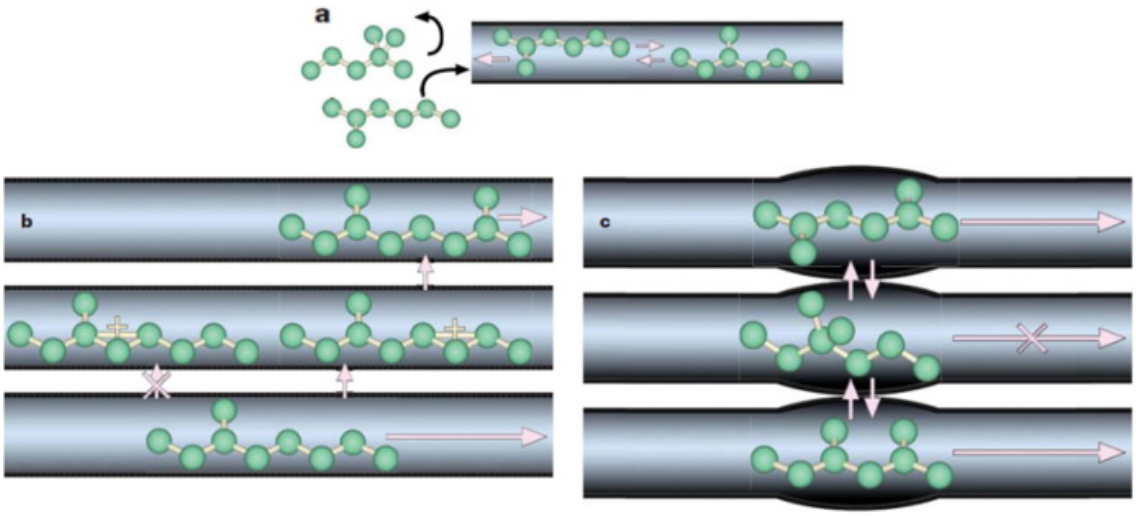

Figure 2 Three forms of shape selectivity in zeolites: (a) reactant shape selectivity, (b) transition state selectivity and (c) product shape selectivity. Figure reproduced with permission from Jia, X. C.; Khan, W.; Wu, Z. J.; Choi, J.; Yip, A. C. K., *Adv. Powder Technol.* **2019,** 30 (3), 467-484.[25]

1.1.5 Micropore Geometry – 1D vs 2D vs 3D Connectivity

In addition to the size (i.e. pore width) of the micropores, the connectivity of the channels is also important. Figure 3 shows the micropore voids of zeolites mordenite, ZSM5 and beta. Mordenite has a one-dimensional (1D) pore structure comprising straight 12MR channels. Adjacent channels are not interconnected. In contrast, zeolites ZSM-5, beta and faujasite all have three-dimensional (3D) pore structures. In practice, this means that adsorbates have many more available diffusion pathways in a 3D pore system than in a 1D pore system. This can influence catalyst deactivation. In a 1D system, pore mouth blockage[26] results in obstruction of the diffusion pathway. In a 3D system on the other hand, a pore blockage is less consequential, as multiple diffusion pathways exist and molecules can diffuse sideways via the interconnected 3D channels. Therefore, in reactions where catalyst deactivation occurs readily due to pore blockage, zeolites with 3D channels are often favoured over 1D channels (described in section 1.1.6).[27, 28]

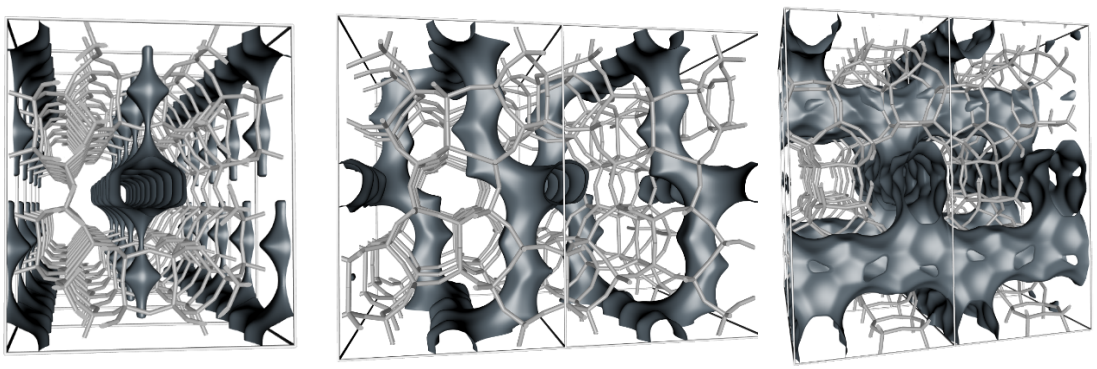

Figure 3 Pore connectivity in Mordenite, ZSM5 and Beta zeolites. The zeolite framework is represented by the light grey lines and the micropores are represented by the dark grey shaded areas. Images were generated using iRASPA software.[29]

1.1.6 Drawbacks

In order for zeolite catalysis to be fully exploited, products need to be able to formed inside the micropores of the zeolite and subsequently desorb out of the micropore system. This can present challenges in the synthesis of bulky molecules.[30] These reactions can be subject to significant diffusion limitations. Possible solutions to this problem include: (i) utilising extra-large pore zeolites;[31] (ii) reducing the zeolite crystal size in order to decrease diffusion path lengths;[32-35] and (iii) introducing pores with a larger size than the micropores listed in Table 1, such as meso- and macropores. In these larger pores, diffusion limitation is less severe than in the zeolite micropores.[36-39] Diffusion is often rate-limiting, as the time scale for the diffusion of reactants from the bulk to the active site within zeolite micropores is greater than the time scale for the reaction itself to take place. If residence time within the zeolite is high, desired product selectivity can decrease due to generation of secondary products through overreaction.[39, 40] Zeolite catalysts can be deactivated in a variety of ways, which can lead to changes in both activity and selectivity. Some common causes of zeolite deactivation are summarised in Table 3.

Table 3 Common causes of zeolite catalyst deactivation.[27, 41]

Cause	Description	Example(s)
Poisoning	Irreversible chemisorption of species to catalytic active sites.	Adsorption of highly basic nitrogen-containing compounds on the zeolite acid sites causing neutralisation.
Fouling or coking	Formation of deposits on the zeolite, either by deposition of species present in the feed (fouling) or production of new species (coke) during the reaction that are deposited on the zeolite (coking). Can lead to pore blockage.	Formation of coke by oligomerisation in FCC catalysts.[27]
Chemical/ structural alteration	Changes in the chemical and structural properties of the zeolites, such as Si/Al ratio, acid sites and crystallinity.	Dealumination, framework collapse/loss of crystallinity.
Leaching	Loss of active species into the liquid phase.	Transfer of zeolite charge balancing cation into the liquid phase.

1.1.7 Hierarchical Zeolites

As discussed earlier, zeolites are microporous materials, and this gives rise to shape selectivity. Zeolites containing both micropores and mesopores are known as "hierarchical" zeolites, due to the presence of two pore systems of different length scales.[42, 43] The presence of mesopores can enhance catalytic activity through improving mass transport to and from catalytic active sites.[44-47]

1.1.8 Generation of Hierarchical Zeolites

Methods for generating hierarchical zeolites can generally be categorised as either "bottom up" or "top down" methods.[48] "Bottom up" refers to strategies involving changes to the zeolite synthesis, such as hard or soft templating. "Top down" refers to strategies

involving modification of a previously synthesised zeolite, such as removal of aluminium or silicon from the framework, or recrystallisation in the presence of a secondary template.[25, 49] The term “post synthetic” is also used to refer to such methods due to the fact that they are carried out after initial synthesis of the zeolite. An example of a well-known and much studied post synthetic method is the steaming and acid washing of zeolite Y to produce ultra-stable zeolite Y (USY).[39, 50] USY zeolites are used industrially in fluid catalytic cracking (FCC).[27, 40, 51, 52] Synthesising zeolite Y with Si/Al greater than 3 is challenging. Steaming removes aluminium from the framework, making it possible to access higher Si/Al ratios. In addition, steaming also increases thermal stability and generates mesopores in the zeolite.[53]

The steaming process can be broken down into two stages. The first stage involves hydrothermal treatment of the zeolite in the presence of steam. This is typically carried out at high temperatures, often up to 500 °C or higher.[54, 55] Dealumination occurs through hydrolysis of Si-O-Al bonds in the framework of the zeolite (illustrated in Figure 4). Initially, the breaking of Si-O-Al bonds results in Al extraction. The abstraction of an aluminium atom from the framework requires the breaking of four Si-O-Al bonds, generating a vacancy consisting of four Si-OH groups. These defects in the zeolite are known as silanol nests (shown in Scheme 1). Silicon within the zeolite framework is mobile under the conditions used (high temperatures in the presence of steam), meaning that Si atoms are able to migrate to heal some of the vacancies left after Al extraction. This process causes some of the vacancies to heal whilst others grow, ultimately generating mesopores in the zeolite.

Aluminium abstraction leads to deposition of extraframework material within the zeolite, known as extraframework aluminium species (EFAl). The second stage in the production of USY is acid washing to remove material (such as EFAl) that remains deposited within the mesopores after steaming. Acid washing also causes dealumination of the zeolite and the strength of the acid used determines the amount of aluminium removed.[50] Increasing the strength of the acid increases both the mesopore volume and the Si/Al ratio of the USY zeolite.

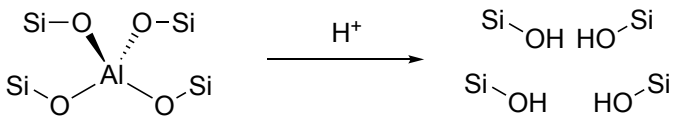

Scheme 1 Creation of silanol defects through dealumination.

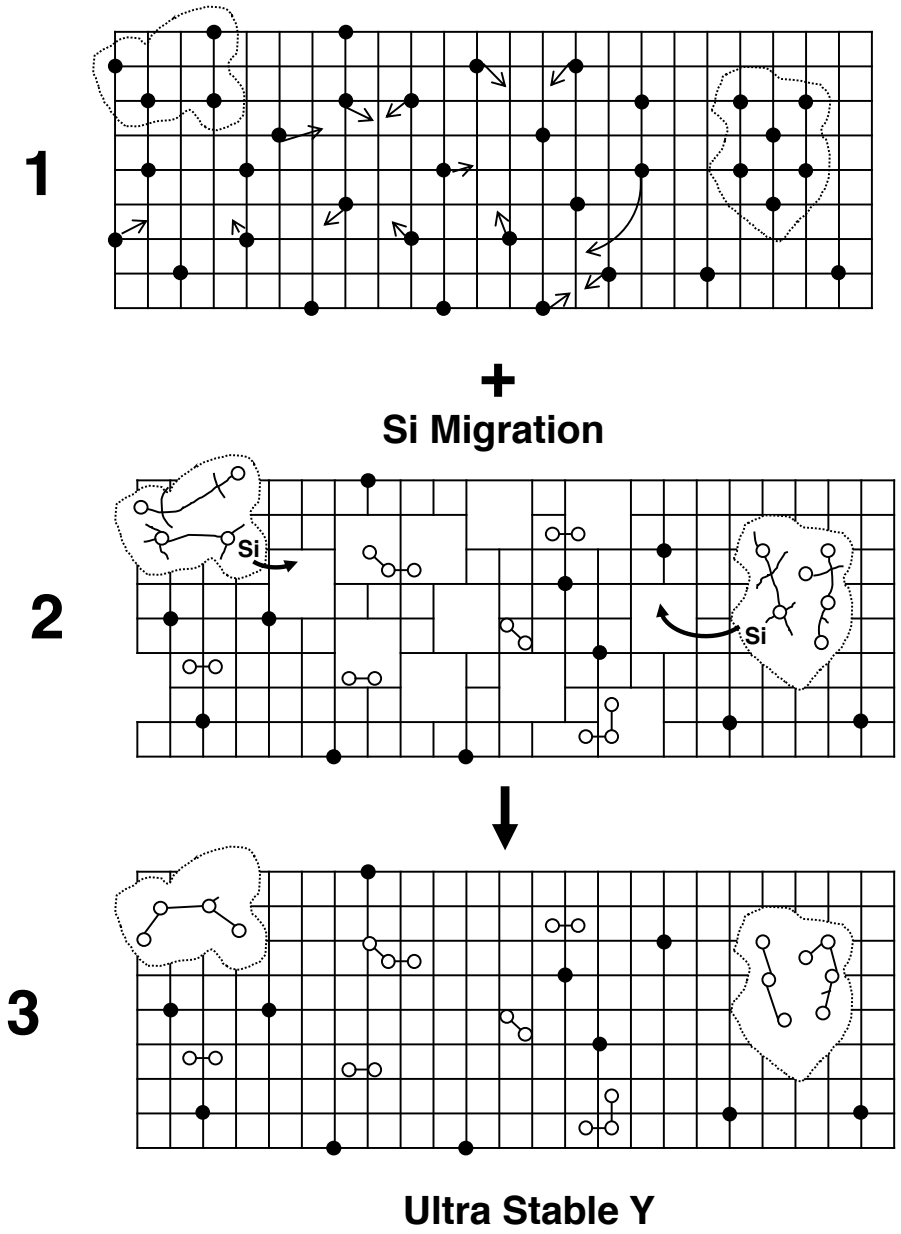

Figure 4 Reproduced with permission from van Donk, S.; Janssen, A. H.; Bitter, J. H.; de Jong, K. P., Generation, Characterization, and Impact of Mesopores in Zeolite Catalysts. Catalysis Reviews **2003,** 45 (2), 297-319.[39]

As well as generating mesopores, this steaming and acid washing process alters the acidity of the zeolite. Acid density is reduced due to increased Si/Al ratio, whilst strength of individual acid sites can increase, as reduction in next nearest neighbour Al can increase Brønsted acid strength.[39] Steaming and dealumination can also give rise to new types of acid sites. Some EFAl remains present in the zeolite after acid washing and is known to have Lewis acidic character.

Removal of silicon (known as desilication) is also commonly used to introduce mesoporosity in zeolites.[37, 44-47, 56] Whereas dealumination of zeolites requires acidic conditions, desilication occurs under alkaline conditions. These methods can be as

simple of exposing the zeolite to alkali solution, followed by filtering and washing of the zeolite.[57] However, the desilication in this manner can create amorphous regions within the zeolite, resulting in a loss of crystallinity. The inclusion of quaternary ammonium compounds such as tetrapropylammonium bromide (TPABr) in the alkali solution can help to preserve the microporous crystal structure of the zeolite.[47, 58]

As well as desilication, it is also possible to restructure the framework under mild alkali pH without significant loss of silicon.[40, 56, 59, 60] This process involves partial breaking of some Si-O-Si bonds, followed by hydrothermal treatment similar to the hydrothermal conditions used in zeolite synthesis. An organic structure directing agent (OSDA), such as a tetraalkylammonium halide, is included in the mild alkali solution. If the OSDA has surfactant properties, e.g. cetyl trimethyl ammonium bromide (CTAB), these OSDAs form self-assembled structures such as micelles within the zeolite, acting as a template for mesopores formation. When the alkali-treated zeolite is subjected to hydrothermal treatment in the presence of the OSDA, mesopores are formed.[40, 52, 60] The term "mesostructuring" has been suggested for this process to distinguish it from a true desilication process.

1.1.9 Aqueous Ion Exchange

As discussed earlier, isomorphous substitution of silicon can give rise to Brønsted and Lewis acid sits. The presence of framework tetrahedrally-coordinated atoms with a +3 oxidation state, such as aluminium, results in a net negative charge on the zeolite framework. This generates Brønsted acid sites when the negative charge is balanced by a proton, but other charge balancing cations are possible. These include ammonium and the alkali earth metals.[15, 61, 62] These cations can be introduced by suspending the zeolite in an aqueous salt solution of the desired cation, such as nitrate salts. This can lead to the creation of new types of catalytic sites within the zeolite, such as weak Lewis basic sites on the framework oxygen in the case of alkali metal exchanged zeolites.[63] The presence of Lewis acidic alkali metal can lead to acid-base catalysis involving the cation and framework basic sites.[64]

1.1.10 Zeolites as Catalysts in Sustainable Chemistry

The historic use of zeolites is predominated by applications in the oil refining and petrochemical industries,[14] such as the use of faujasite zeolites in fluid catalytic cracking discussed earlier in this chapter. However, zeolites have potential for much wider usage, as the fundamental concept of shape selectivity to control reaction outcomes is applicable to many different catalytic reactions. In particular, zeolites are a useful alternative to soluble acid catalysts, which often require rigorous separation from product

streams, generating significant waste.[65] In contrast, zeolites are much easier to separate and recycle. As a result, they can substitute traditional catalysts to increase the green credentials of existing industrial processes and also find potential use in a range of newer sustainable processes.[66] These include generating useful chemicals through catalytic conversion of biomass[67-74] and biopolymer monomer synthesis.[34, 75-81]

1.2 Polymers

1.2.1 Structure and Properties

The term polymer derives from Greek, meaning “many parts”. IUPAC defines a polymer as “a molecule of high relative molecular mass, the structure of which essentially comprises the multiple repetition of units derived, actually or conceptually, from molecules of low relative molecular mass”.[82] Polymers are made up of chains of repeat units and can have molecular weights of thousands of grams per mole or more. The molecular structure of polymers gives them their unique properties, resulting in a wide range of applications such as packaging, electronics and construction.

Properties of polymers can be tuned for various applications through modifying the chemical structure, such as molecular weight, and the type of repeat unit present.[83] Copolymers can be made by incorporating more than one type of repeat unit. Varying the side chains (i.e. monomer functional groups) on the polymer backbone can alter the barriers to rotation within the polymer, resulting in a change in the thermal properties. For example, polymers bearing bulkier groups will tend to experience higher barriers to rotation, increasing chain rigidity and phase transition temperatures as a result.[84] The glass transition is an example of a phase transition observed in amorphous polymers which corresponds to the transformation of the polymer from a hard, glassy state (at lower temperature) to a softer, rubbery state (at higher temperature). The temperature at which this transition occurs is known as the glass transition temperature (T_g). For example, polystyrene has a higher T_g (100 °C) than polyethylene (-60 °C), due to the presence of a bulky phenyl ring in place of an ethylene group (Figure 5). The glass transition temperature is an important property as it determines the processing window of a polymer and its suitability for certain applications. Polymers with higher T_g may be harder to process, as they require significant heating to transform them into a state in which they can be moulded into products. If a rigid product is required, the polymer’s T_g must be higher than the temperature at which it will be used, so polymers with a low T_g may be unsuitable for such applications.

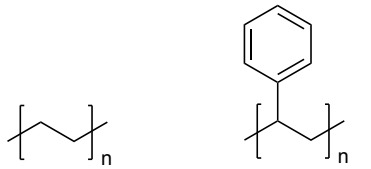

poly(ethylene) poly(styrene)

Figure 5 Structures of poly(ethylene) and poly(styrene).

Another key property of polymers is their tacticity. This term refers to the relative stereochemistry of the repeat units and Figure 6 shows three common types. In isotactic polymers, all the chiral centres have the same stereochemistry. In a syndiotactic polymer, the stereochemistry alternates from one chiral centre to the next. Finally, atactic polymers have a random assorted of stereochemistry. A common example of the significance of this property is polypropylene. The isotactic polymer is substantially crystalline and has good mechanical properties, making it useful in a range of applications. The atactic form on the other hand is a waxy amorphous material that lacks the useful mechanical properties of the isotactic form.[83]

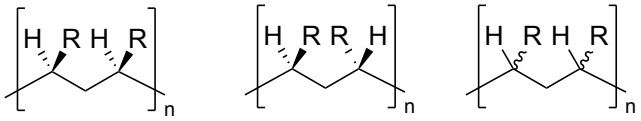

isotactic syndiotactic atactic

Figure 6 Tacticity of polymers.

In reality, a sample of a synthetic polymer consists of many individual chains. The molecular weight of each of the individual chains will usually vary within a given sample. As a result, the molecular weight is usually expressed in two ways: the average molecular weight and the range of molecular weights present in the sample. There are two ways to express average molecular weight, the weight average (M_w) (Equation 1) and the number average (M_n) (Equation 2). The distribution of molecular weight is expressed using a statistical measure called the polydispersity index (PDI). PDI is the ratio of M_W and M_N (Equation 3). These parameters are commonly determined using analytical techniques such as gel permeation chromatography (GPC).[85]

$$M_W = \frac{\sum(N_i {M_i}^2)}{\sum(N_i M_i)} \quad \textbf{(Equation 1)} \qquad M_N = \frac{\sum(N_i M_i)}{\sum N_i} \quad \textbf{(Equation 2)}$$

$$PDI = \frac{M_W}{M_N} \quad \textbf{(Equation 3)}$$

1.2.2 Petroleum-based Plastics

As much as 99% of the feedstock for plastic production is derived from fossil fuels. This presents challenges for the future of plastic production, due to the finite nature of fossil fuel resources and the negative environmental impact that the manufacturing of these plastics can have. For example, polyethylene is a highly inert polyolefin. In low sunlight environments, thermal oxidative degradation does not readily occur at temperatures below 100 °C and not below 350 °C when oxygen concentration is also low.[86] Plastic released into the environment is unlikely to experience such high temperatures and therefore last for significant periods without degradation.

1.2.3 Biodegradable Plastics

Biodegradable polymers, defined as polymers which are susceptible to degradation by biological activity,[87] represent a potential alternative to petroleum-based commodity plastics. Many classes of biodegradable polymers are known,[88] including polyesters,[89, 90] polycarbonates[91, 92], polyhydroxyalkanoates,[93] and polyamides,[94] some examples of which are shown in Figure 7. If polymers degrade to environmentally benign products, the problems of environment persistence and pollution can potentially be mitigated.[95] Furthermore, many of these polymers can also be biobased i.e. derived, at least in part, from biomass. It should be noted than not all biodegradable polymers are also biobased, and *vice versa*. The concept of a circular economy is a complex one, but minimising or eliminating waste and generating new products from nature are important aspects to realising this goal. As a result, polymers that are both biobased and biodegradable are likely to form an important part of a future circular economy.[96]

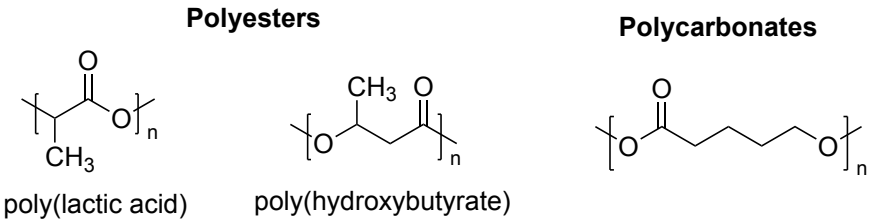

Figure 7 Structures of some common biodegradable polymers.

1.2.4 Poly(lactic acid) - A Common Commercial Biodegradable Polymer

Alpha hydroxy acids are carboxylic acids of the formula $R^1R^2(OH)COOH$ (Figure 8a). Lactic acid Is an example of an alpha hydroxy acid where R^1 and R^2 are H and CH_3. Poly(lactic acid) (PLA) is the polymer of lactic acid and many other poly(alpha hydroxy acid) polymers are known.PLA is proposed as a promising alternative to the petroleum-based commodity plastics that are so prominent in today's society. PLA is both biodegradable and bioderived. Lactic acid is a bioderived platform molecule that can be

produced from sugar feedstocks such as glucose or sucrose, via chemocatalytic routes[67-69] or by biocatalysis i.e. fermentation.[97] For example, Cargill Dow obtains lactic acid for the production of their Ingeo® PLA by enzymatic conversion of corn-derived starch to dextrose, followed by fermentation of dextrose to lactic acid (Figure 8b).[98, 99]

PLA biodegrades via hydrolytic degradation and cleavage of the ester bonds. The polymer chains undergo chain scission to produce shorter oligomers and the acidic COOH termini of these oligomers are able to catalyse further ester hydrolysis, making the process auto-catalytic.[100] Biodegradation occurs readily in the presence of oxygen and water at temperatures above 60 °C. This means that PLA lends itself to industrial composting, where these conditions can be easily achieved, but its degradation remains a challenge under ambient conditions, such as those found in landfill or the marine environment.[101, 102]

There are two main routes that can be used to synthesise PLA: (1) polycondensation of lactic acid; (2) ring opening polymerisation (ROP) of lactide, the cyclic dimer of lactic acid. ROP is favoured due to several drawbacks of polycondensation, including poor control over molecular weight, side reactions and use of forcing conditions.[90]

The current commercial production of PLA involves a multistep process (shown in Figure 8b)[99] starting with synthesis of low MW oligomers from lactic acid. This is followed by thermal decomposition in the presence of a Sn-based catalyst to depolymerise these chains, producing the cyclic lactide monomer via a “backbiting” mechanism. This process has several drawbacks. Heat is required for the depolymerisation process, consuming additional energy. During backbiting, some of the resultant chains become unreactive towards further depolymerisation and are wasted. Furthermore, some of the lactide produced has the undesired *L,L*-stereochemistry. The unreactive chains, *L,L*-lactide and the Sn catalyst, must then be removed, creating further processing steps.[75]

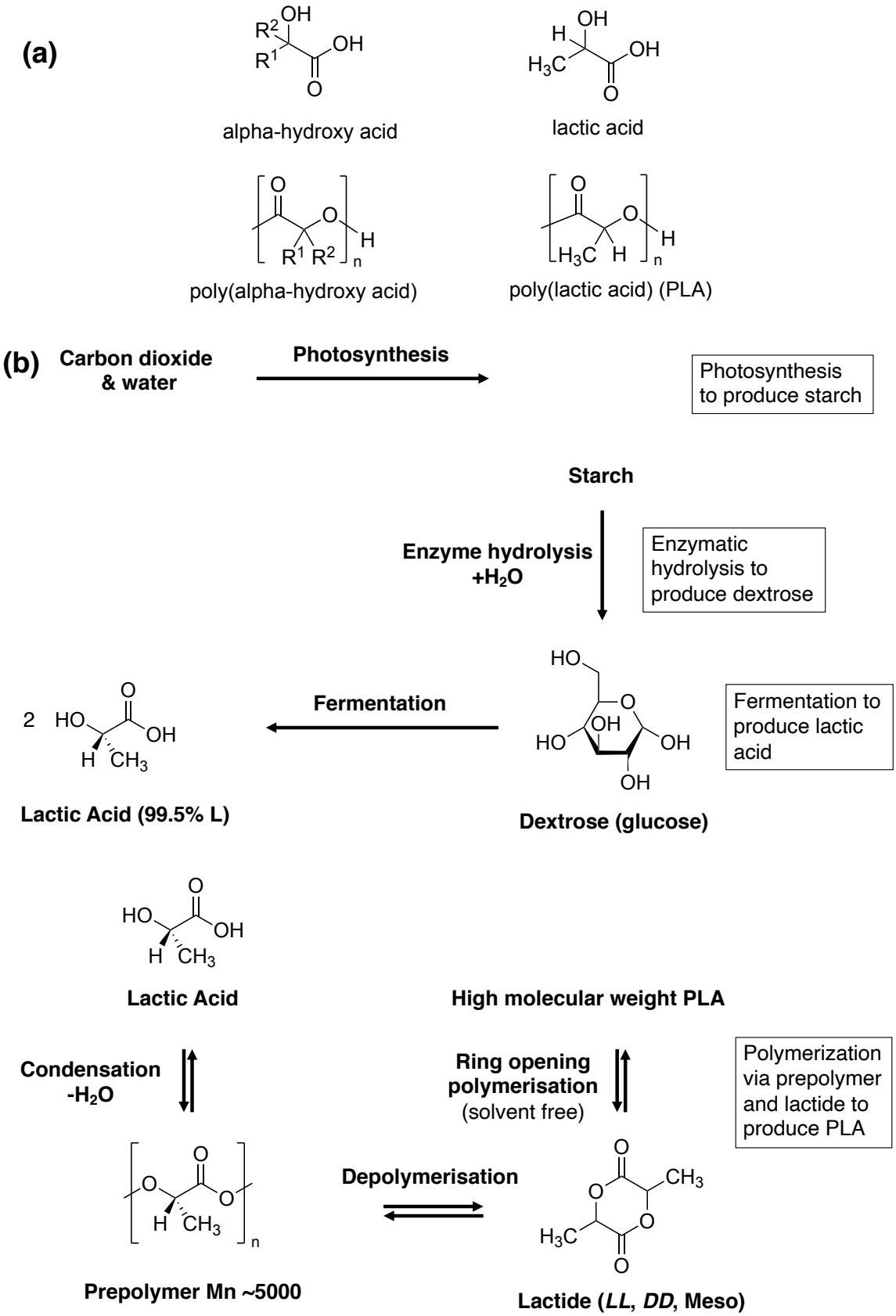

Figure 8 (a) Structure of alpha-hydroxy acids and poly(alpha-hydroxy acids. (b) Process used by Cargill Dow to produce Natureworks™ poly(lactic acid) (PLA).[98]

1.2.5 Heterogeneous Catalysts for Lactide (Monomer) Synthesis

The conversion of lactic acid over zeolite catalysts has been widely studied. Reactions such as esterification, decarbonylation, decarboxylation and dehydration lead to a variety of products including lactide,[34, 75, 77-79, 103, 104] acrylic acid[105-109] and acetaldehyde.[104] Of particular interest in the field of biodegradable polymers is the production of lactide, the cyclic monomer of lactic acid and precursor to PLA. Sels and coworkers[75] reported selective production of lactide from lactic acid in aromatic solvents using various zeolites as catalysts. The use of homogeneous catalysts H_2SO_4 or paratoluenesulfonic acid (*p*-TSA) in this process resulted in mostly linear oligomeric products formed by sequential esterification reactions of lactic acid. In the case of catalysis by H_2SO_4, the average oligomer length was as high as 14 repeat units. Of the heterogeneous catalysts tested, Beta and FAU zeolites were the most selective for lactide, with a maximum yield of approximately 80 % achieved after 3 hours at reflux in o-xylene in the presence of H-Beta zeolite (Si/Al = 12.5). The authors hypothesised that the microporous structure of the zeolite was crucial in inhibiting the formation of larger oligomeric species. This led to ©n increase in lactide selectivity and a decrease in both oligomer selectivity and average chain length compared to the other catalysts tested. This selectivity was much higher than observed for other heterogeneous, non-shape selective Brønsted-acidic catalysts tested, such as Nafion, Amberlyst-15 and H-Al-MCM-41. Whilst these catalysts performed better than the homogeneous catalysts in terms of lactide selectivity, selectivity remained lower than that achieved by the zeolites. Various aromatic solvents were tested. O-xylene resulted in the best combination of reaction rate, lactide selectivity and reduced oligomer length.[75]

Following this initial report of direct synthesis of lactide over commercial zeolites, further work has expanded the scope to other Brønsted acidic and Lewis acidic zeolites, as well as other types of heterogeneous catalysts. Aluminosilicate ITQ-47 zeolite was synthesised via an OSDA-free synthesis using borosilicate ITQ-47 as a seed. This zeolite was found to outperform commercial zeolite Beta under the same conditions.[77]

Lewis acidic zeolites have also been shown to be useful in the synthesis of lactide.[78] Dealumination of the commercial H-Beta zeolite followed by remetallation with $SnCl_4$ was used to synthesise Sn-Beta with various levels of Sn in the framework (Si/Sn ratios from 30 to 100). Whilst these catalysts were able to produce lactide in high selectivity under certain conditions, they required much higher reflux temperatures to achieve comparable selectivity to the commercial H-Beta zeolite. When Sn-Beta with a Si/Sn ratio of 30 was used with o-xylene as the solvent, lactic acid conversion was still above 90% but lactide yield was only around 60%, with a significant amount of linear oligomers formed. It was

only when the higher boiling propylbenzene or mesitylene solvents were used that the Sn-Beta zeolites achieved comparable results, with lactide yield of approximately 88% at 99% lactic acid conversion for Sn-Beta-30.

Whilst the above Brønsted and Lewis acidic zeolites perform well on relatively dilute lactic acid solutions (50 wt%), lactide selectivities have been found to be lower when lactic acid concentration is increased. Lactic acid solutions contain a mix of lactic acid and lactic acid oligomers in equilibrium with one another due to autocatalytic esterification reactions.[110, 111] As the concentration is increased, the concentration of oligomers present also increases. As a result, synthesis of lactide from concentrated lactic acid solutions requires a catalyst that can convert both lactic acid and lactic acid oligomers. For commercial Beta zeolites, as lactic acid concentration was increased, lactide selectivity decreased and oligomer selectivity increased, suggesting that conversion of oligomers was more challenging for these catalysts.[75]

Beta zeolites with nanosized particles (<100nm) have been synthesised via a method that utilises L-lysine in the synthesis gel.[34] These were tested as catalysts for the synthesis of lactide from highly concentrated lactic acid solutions and compared with conventional commercial Beta zeolites with larger crystal sizes. Lactide selectivity in toluene was between 61-74% for the nanosized beta zeolites, with the lactide selectivity being higher for the zeolite with higher acid density (lower Si/Al). A nanosized beta zeolite with Si/Al of 15 and average particle size of 10 nm achieved 74% lactide yield and 17% oligomers, whereas a commercial Beta zeolite with comparable Brønsted acid density (Si/Al = 12) achieved a 67% lactide yield and 24% oligomers. However, this is a small difference and suggests that other factors beyond the crystal size are important. Zeolites with a particle size less than 100 nm are referred to as nanosized zeolites.[32] Nanosized zeolites have also been synthesised via a steam-assisted crystallisation method, with a Beta zeolite with Si/Al of 10 achieving 78% lactide yield in toluene, compared with 69% for the commercial Beta zeolite (Si/Al = 12.5).[80]

As well as the batch synthesis methods discussed above, the synthesis of lactide over heterogeneous catalysts has also been reported in a fixed bed reactor using a gaseous feed. This process has been shown to work for a feed containing lactic acid[112] or the methyl ester of lactic acid, methyl lactate.[103, 104] As shown in Scheme 2, lactide forms from lactic acid via an esterification reaction, producing water as a byproduct. Lactide production from methyl lactate involves a transesterification reaction, producing methanol as a byproduct. The process starting from alkyl esters has been found to have broader applicability, with the same catalysts also shown to convert methyl glycolate (the methyl ester of glycolic acid) to glycolide.[113] Use of the methyl ester is favoured for the

gas phase process as they are more volatile, meaning feed concentrations can be higher. Side reactions such as decarbonylation and dehydration are also less favoured for the methyl ester.[104]

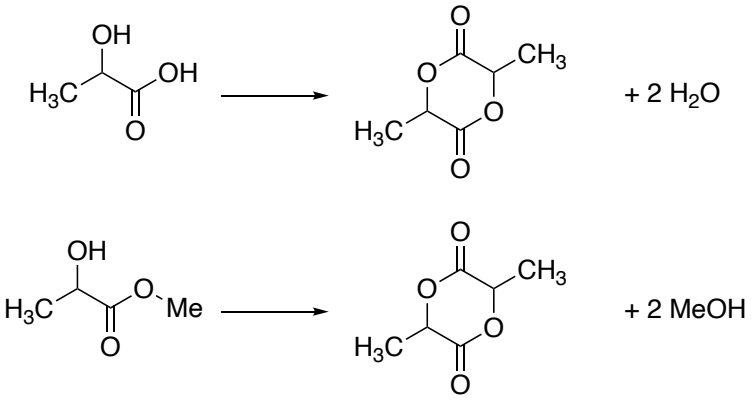

Scheme 2 Synthesis of lactide from lactic acid or methyl lactate.

Lactide synthesis from lactic acid in the gas phase has been reported over a SnO_2-SiO_2 "nanocomposite" catalyst.[112] This catalyst was synthesised by precipitation-deposition of $SnCl_4$ solution on colloidal silica (7 nm spherical particles), followed by calcination in air to form SnO_2 supported on the silica particles. Sn was found to exist as a highly dispersed Sn^{4+} tetragonal phase, giving rise to weak Lewis acid sites. Catalysts were loaded into a fixed bed reactor and a 75 wt% lactic acid feed was vaporised and mixed with N_2. H-ZSM5 zeolites and the SnO_2 nanocomposite catalysts were tested at 240 °C. Under these conditions, the best SnO_2 catalysts outperformed the best zeolite tested in terms of lactic acid conversion and *L*-lactide yield. However, this required high Sn loadings of at least 80 wt% of SnO_2 in SnO_2/SiO_2.

In contrast to the aforementioned synthesis of lactide from lactic acid in solution, low methyl lactate conversion was achieved when Brønsted acidic catalysts such as H-Beta zeolite were tested in flow.[104] Conversion was as low as 5% for H-Beta with the lowest acid density (Si/Al = 150). For the H-Beta zeolite with higher acid density (Si/Al = 12.5), conversion was higher (48%), but this was accompanied by a drop in lactide selectivity to 7% compared with 60% for H-Beta (Si/Al = 150) at 5% conversion. In this same study, several different heterogeneous catalysts based on TiO_2 supported on silica were synthesised to compare with Brønsted acidic Beta. Supports included a large pore SiO_2 gel and Si-MCM-41. Catalysts were synthesised by incipient wetness impregnation using titanium isopropoxide solution. Much higher lactide selectivities of around 90% were achieved for these catalysts at around 40% conversion (T = 240 °C) of methyl lactate and 5 wt% TiO_2 loading.[104] In a separate report by the same authors, these catalysts were also found to efficiently produce glycolide from methyl glycolate under similar conditions.[113] The authors also found that reaction temperature could be increased to

300 °C to increase methyl glycolate conversion and glycolide yield. This was not possible in the case of lactide, where increasing the temperature above 240 °C led to the formation of acetaldehyde as a byproduct.[104] This was suggested to occur via a decarbonylation reaction, either directly from methyl lactate or through decomposition of lactide (Scheme 3). In contrast, when methyl glycolate was used, no formaldehyde was detected.

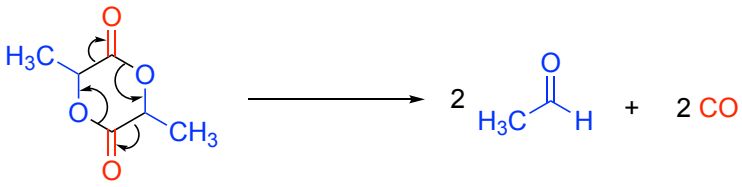

Scheme 3 Proposed mechanism for the formation of acetaldehyde in the synthesis of lactide from methyl lactate over titano-silicate catalysts.[104]

It would also be desirable to carry out similar heterogeneously catalysed processes to make different cyclic diesters, not just lactide and glycolide. The differences observed in the catalytic activity in the synthesis of the structurally very similar lactide and glycolide highlights the challenge associated with this. Whilst the synthesis of lactide and glycolide have been demonstrated over a range of heterogeneous catalysts under both batch and flow conditions, the synthesis of other cyclic diesters under analogous conditions has proved more difficult. In the synthesis of thiolactide from thiolactic acid (Scheme 4), zeolite catalysts performed poorly compared with homogeneous alternatives H_2SO_4 and p-TSA.[114] For all catalysts tested, thiolactide synthesis required higher temperatures and/or longer reaction times than lactide synthesis to achieve comparable conversion with the same catalysts. When H-Beta (Si/Al 12.5) was used, increasing the solvent boiling point resulted in increased conversion of thiolactic acid, but the yield of thiolactide remained similar. Rather, the yield and average chain length of oligomers increased, demonstrating that shape selectivity was not dictating the reaction outcome. The authors hypothesised that thiolactic acid adsorbed more strongly to Brønsted and Lewis acid sites than lactic acid (evidenced by FTIR experiments), resulting in poisoning of the catalyst.[114]

The synthesis of vinylglycolide (Scheme 5) over zeolites has also proved difficult.[75] The alkene group in this alpha-hydroxy acid was found to alkylate the aromatic solvent and, as a result, a maximum yield of only 24% of the cyclic diester was achieved. These examples show that, whilst the synthesis of lactide has been demonstrated over a range heterogeneous catalysts including zeolites, changing the alpha-hydroxy acid can have significant effects on cyclic diester selectivity.

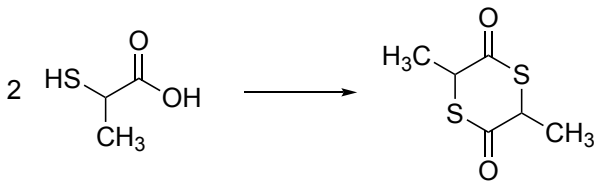

Scheme 4 Synthesis of thiolactide.

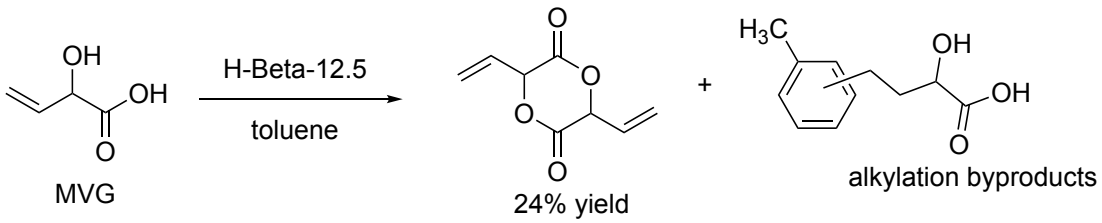

Scheme 5 Synthesis of the cyclic diester methylvinylglycolate (MVG) using H-Beta-12.5 zeolite as catalyst was hampered by the formation of byproducts through alkylation of the toluene solvent.[75]

1.2.6 Ring Opening Polymerisation of Lactides

A range of catalysts are reported in the literature for the ring opening polymerisation (ROP) of lactide, with most examples concerning metal complexes in the presence of alkoxide initiators. This is a living polymerisation that proceeds via a coordination-insertion mechanism.[115-117] More recently, the use of organocatalysts has become more common in the synthesis of biodegradable polymers.[118, 119] The coordination-insertion mechanism for the ROP of lactide catalysed by a metal complex, ML_n, is shown in Figure 9. Lactic acid is coordinated to the metal catalyst followed by attack on the lactide ester group by the alkoxide initiator, ^{-}OR. This alkoxide is either an alcohol initiator or the terminal alcohol group of a propagating polymer chain. This mechanism is common to many cyclic lactone monomers.[90, 115] Catalysts for ROP of cyclic lactones include tin octanoate ($Sn(Oct)_2$), aluminium alkoxides, basic organocatalysts such as pyridines, and metal complexes such as aluminium salens and zinc β-diiminates (Figure 10).[117, 120]

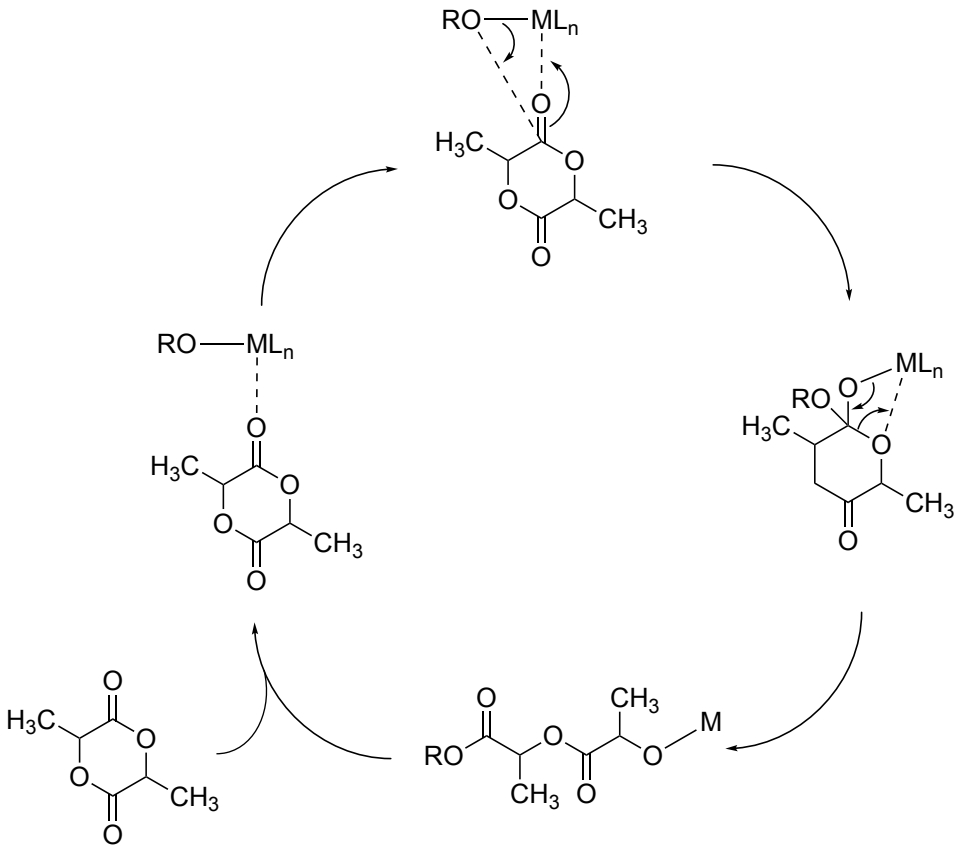

Figure 9 Coordination-insertion mechanism of lactide ring opening polymerisation (ROP). M = catalyst, OR = initiator or propagating chain.

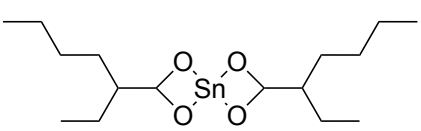

tin octanoate
$Sn(Oct)_2$

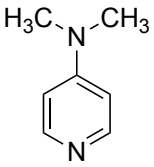

dimethylaminpyridine
DMAP

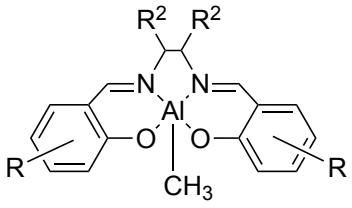

aluminium salen
Al(salen)

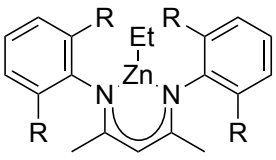

zinc β-diiminate
(BDI)ZnEt

Figure 10 Catalysts used for ring opening polymerisation (ROP) of cyclic monomers.[120]

1.3 Substituted Lactides and Functionalised Polyesters

There is a drive to incorporate more chemically diverse side chains into lactide monomers to impart different properties in the resultant polymers. PLA has a fairly low glass transition temperature (T_g) of 55 °C and is brittle, and therefore there is interest in

synthesising polymers with increased T_g or improved toughness.[94, 121, 122] Substituting the methyl groups of lactide to give substituted lactide is one such strategy. Examples of substituted lactides reported in the literature include those with groups such as isopropyl,[123] cyclohexyl,[124, 125] phenyl,[126-128] gluconic acid[129, 130], malic acid,[131] vinyl,[132, 133] alkyne[134] and alcohol.[89, 135, 136] The resultant polymers often have different properties to PLA. Bulkier groups such as phenyl or cyclohexyl rings can impart high glass transition temperatures by reducing the mobility of the polymer chains, however the presence of large groups in lactide monomers can slow rates of polymerisation[124] and the presence of electronic effects due to the aromatic rings can stabilise undesired intermediates.[127]

1.3.1 Poly(mandelic acid)

Varying the side chains present in a polymer can lead to changes in T_g, as discussed in the context of polystyrene in section 1.2.1. Increasing the length of the alkyl side chains of a polyester compared with poly(lactic acid) (Figure 11) from methyl to ethyl and to hexyl was found to decrease T_g.[124]

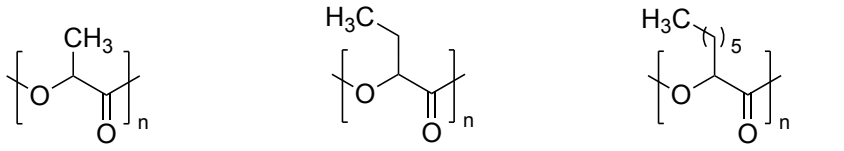

poly(lactic acid) (PLA) **T_g 55 ºC**

poly(ethylglycolide) **T_g 15 ºC**

poly(hexylglycolide) **T_g -37 ºC**

Figure 11 T_g of polyesters with different alkyl side chain length.[124]

A more effective method to increase T_g is to introduce bulky ring substituents. T_g was increased to 100 °C for poly(mandelic acid) (PMA), a polymer described as a biodegradable alternative to polystyrene (Figure 12).[126] This increase in T_g for PMA relative to PLA is proposed to be caused by increased chain rigidity due to the bulky phenyl ring.[126] In contrast to PMA, for poly(phenyllactide), the introduction of a CH_2 linker between the phenyl ring and the backbone (Figure 12) leads to greater chain flexibility and a comparably lower T_g of 50 °C.[128] Baker reported a poly(cyclohexyllactide) with a similar T_g (98 °C) to poly(mandelide), synthesised by reducing the aromatic ring of mandelic acid to a fully saturated cyclohexyl ring.[125] Mandelide readily racemises during polymerisation due to its labile methine hydrogen, which makes stereocontrolled ROP of mandelide difficult.[126, 127] This unwanted epimerisation is reduced in the polymerisation of cyclohexyllactide, leading to greater stereocontrol in the resultant polymer. These results show that synthesis of substituted polylactides is a complex challenge, as changing the nature of the substituents not only affects the polymer properties. It also presents challenges in terms of polymer synthesis by ring opening polymerisation and, as will be discussed later in section 1.3.2, cyclic monomer synthesis.

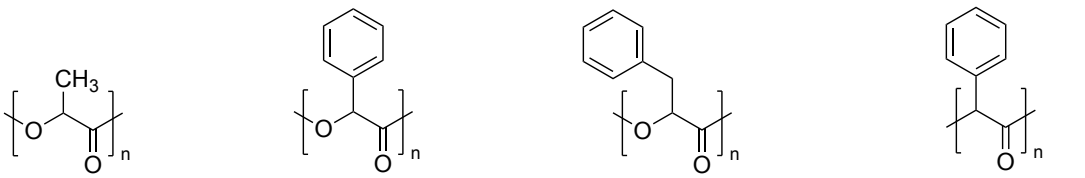

poly(lactic acid) (PLA) **7a** | poly(mandelic acid) (PMA) **7c** | poly(phenyllactide) (PPLA) | poly(styrene) (PS)

Figure 12 Structures of poly(lactic acid), poly(mandelic acid), poly(phenyllactide) and poly(styrene) polymers.

1.3.2 Ring Opening Polymerisation of Mandelide

As discussed earlier, poly(mandelide acid) is a biodegradable polymer with a higher T_g than polylactic acid. Homogenous acid catalysis has been used to synthesise linear oligomers and polymers of mandelic acid through polycondensation.[137] However, this process only gives low molecular weight polyesters. The polymerisation was hindered by the formation of the cyclic dimer of mandelic acid, mandelide, as a byproduct in the form of a precipitate. This precipitate was identified as (*S,S*)-3,6-diphenyl-1,4-dioxane-2,5-dione, formed due to poor solubility in the reaction solvent.[138] The authors attempted to synthesise poly(mandelic acid) by ring opening polymerisation of this cyclic dimer without success. Later, Baker and coworkers[126] synthesised mandelide from mandelic acid using p-TSA as the catalyst and mixed xylene as solvent. They used a much lower concentration of mandelic acid in order to favour dimerisation over oligomerisation. They found that mandelide was obtained as a mix of *rac (R,R-* and *S,S-)* and *meso* (*R,S-*) isomers (Figure 13). They found that the *meso* isomer had a lower melting point (137 °C vs 248 °C for the *rac*-isomer[126]) and better solubility than the *rac* isomers, making it a better prospective monomer for ring opening polymerisation both in the melt and in solution. However, it was only possible to synthesise mandelide as a statistical 50:50 mix of *rac* and *meso* isomers. Total yields of around 53% were achieved even after reflux for 3 days in the high boiling mixed xylenes solvent (T_b = 140 °C), highlighting the difficulty of synthesising this monomer.

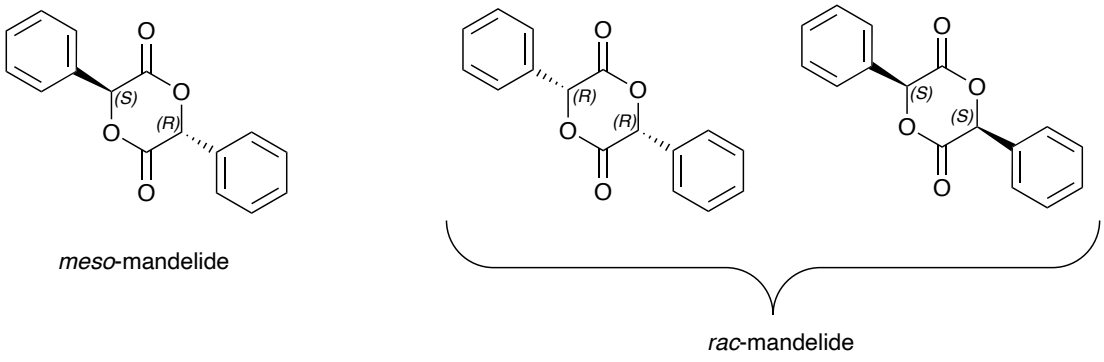

meso-mandelide

rac-mandelide

Figure 13 Structure of *rac*- and *meso*-mandelide.

More recent work by Graulus and coworkers[127] found that even after rigorous degassing of the mandelic acid/mixed xylenes solution prior to reflux, it was still only possible to achieve a modest overall mandelide yield of 57%. Despite some challenges with monomer and polymer synthesis, both papers showed that a biodegradable polymer with a higher glass transition temperature (T_g) compared with poly(lactic acid) could be synthesised from mandelide.[126, 127]

1.3.3 Alternative Monomers

As discussed in the previous section, the synthesis of poly(mandelic acid) from mandelide has some drawbacks. As well as ring opening, mandelide can be deprotonated by basic ROP catalysts (Figure 14a). The resulting enolate can give rise to side reactions that consume monomer, leading to lower-than-expected molecular weight.[127] This deprotonation can also lead to a lack of stereocontrol, as a stereopure monomer feed can be converted to a mixture of isomers by deprotonation to the enolate, followed by reprotonation to reform the mandelide monomer as a mix of *cis* and *trans* isomers (due to the planar geometry of the intermediate enolate). Alternative cyclic monomers have been reported based around the strategy of forming a 5-membered ring by insertion of a small molecule and subsequently releasing this molecule upon ring opening. These 5-membered monomers have higher ring strain than 6-membered lactides and can give more controlled polymerisation in terms of both molecular weight and tacticity. Figure 14b shows two alternative cyclic monomers: O-carboxyanhydrides (OCAs) and 1,3-dioxolan-4-ones (DOXs).

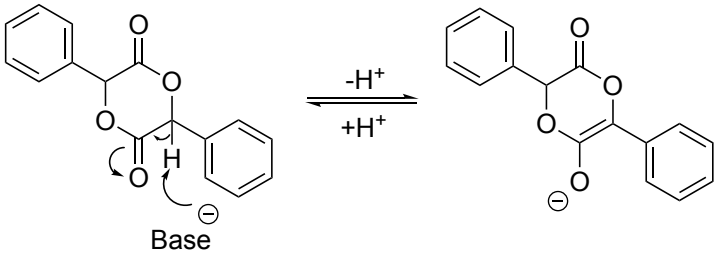

Figure 14 (a) Unwanted deprotonation of mandelide that occurs in the presence of basic ROP catalysts.

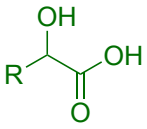

alpha-hydroxy acid

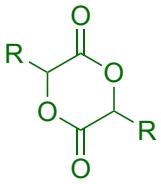

lactides/glycolides

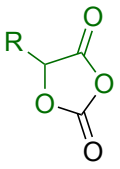

O-carboxyanhydrides (OCAs)

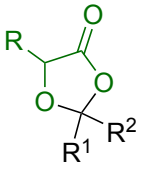

1,3-dioxolan-4-ones (DOX)

Figure 14 (b) Cyclic monomers of alpha-hydroxy acids used for ring opening polymerisation (ROP).

1.3.4 *O*-Carboxy Anhydrides (OCAs)

The first example of the use of OCAs for polylactide synthesis came from Bourissou *et al.*[139] They synthesised the so-called O-carboxy anhydride (OCA) of lactic acid by reaction with phosgene, to incorporate a carbon monoxide (CO) moiety. OCAs were chosen due to a pre-existing synthesis being available and the smaller 5-membered ring potentially leading to greater relief of ring strain upon ROP compared to the 6-membered lactide. These "activated equivalents of lactide" were proposed to allow ROP under milder conditions, with reduced transesterification side reactions. They were able to polymerise lac-OCA using a DMAP organocatalyst with alcohol initiators and found the L-lac-OCA monomer to polymerise much faster than L-lactide under similar conditions. The polymerisation of lac-OCA was found to be living by a second-feed experiment, where a first polymerisation was carried out to full conversion. A second monomer feed of an equivalent amount of monomer resulted in doubling of M_n, showing that the polymer chains were still active and polymerisation had living character. M_n up to 62,000 was achieved using neopentanol as the alcohol initiator, with a reasonable polydispersity of 1.18.

OCA monomers have been used in the synthesis of poly(mandelic acid) (PMA) and permits stereocontrolled polymerisations that are not possible in ROP of mandelide. It was found that the use of DMAP as an organocatalyst led to atactic PMA from a mandelic acid OCA (PhOCA), due to base-catalysed racemisation of the monomer.[140] However, the authors observed that polymers with high levels of stereoretention were formed when mandelic acid was detected in the reaction mixture (formed by hydrolysis of the manOCA monomer). They reasoned that the mandelic acid could be dictating the stereochemical outcome of the polymerisation. Subsequently, the polymerisation was initiated with a 1:1

adduct of pyridine and mandelic acid, resulting in the synthesis of isotactic poly (mandelic acid). PhOCA has been further investigated, both in the copolymerisation with lactic acid OCA[141] and for the preparation of stereocomplex PMA using synergetic organocatalysts.[142] Many other examples exist of OCAs with different functional groups for polyester synthesis.[140, 142-150]

1.3.5 1,3-dioxolan-4-ones (DOXs)

The synthesis of OCAs uses phosgene reagents which have some drawbacks, as they are both highly toxic and expensive. A cheaper and more sustainable route was proposed by Shaver *et al* involving the use of paraformaldehyde or acetone in place of phosgene, to give the 1,3-dioxalan-4-one monomer (DOX).[151] For example, they suggest that to synthesise the equivalent mass of PhDOX (mandelic acid derivative) as PhOCA, a 20 fold reduction in material cost is achieved. They were able to synthesise copolymers of lactide and glycolide by copolymerisation of a DOX of glycolic acid and lactide, catalysed by aluminium salen complexes. DOXs from a range of alpha hydroxy acids were prepared by reaction of the parent AHA with either paraformaldehyde or acetone, as shown in Scheme 6.[152]

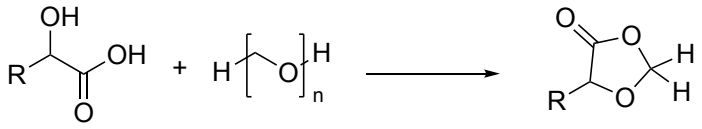

R = H, Ph, Me, *i*-Pr, Cy, *t*-Bu, *n*-Bu, *i*-Bu

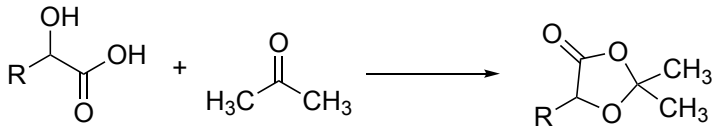

R = Me, Ph

Scheme 6 Synthesis of 1,3-dioxolan-4-ones from alpha-hydroxy acids.[152]

1.3.6 Routes to Mandelic Acid-based Polyesters

Many approaches to mandelic acid polymers have been reported in the literature which are summarised in Figure 15. In addition to ring opening polymerisation of mandelide, poly(mandelic acid) has been synthesised from an O-carboxyanhydride (2,4-dioxo-5-phenyl-1,3-dioxolane)[140, 142, 153] and 1,3-dioxolan-4-ones[151, 152] (5-phenyl-1,3-dioxolan-4-one and 2,2-dimethyl-5-phenyl-1,3-dioxolan-4-one) (Figure 15a). In addition to high T_g poly(mandelic acid), it is also possible to synthesise copolymers of mandelic acid and other alpha-hydroxy acids, either from a mixed monomer feed containing both lactic acid

and mandelic acid based monomers (Figure 15b)[127, 141, 152, 154] (e.g., lactide and mandelide) or by ring opening polymerisation of a cyclic dimer of mandelic acid and either glycolic or lactic acid (Figure 15c).[155-157] In copolymers with other alpha hydroxy acids, the T_g increases as a function of mandelic acid content, making it possible to tune the thermal properties.[127, 155, 156] The synthesis route also has implications in terms of environmental impact, with a recent life cycle analysis suggesting the synthesis of PMA via DOXs monomers could lead to at least 20% reduction in environmental impact compared with synthesis via OCAs.[158]

(a) homopolymerisation

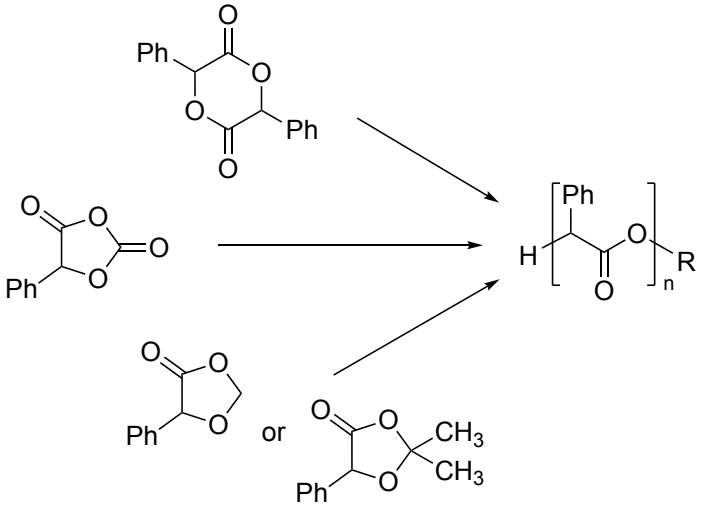

(b) copolymerisation

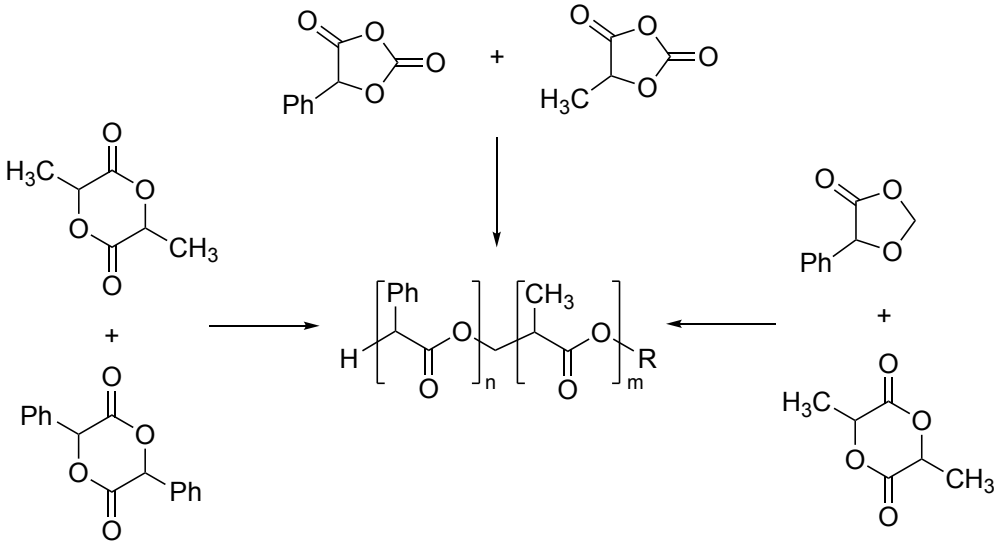

(c) polymerisation of mixed monomers

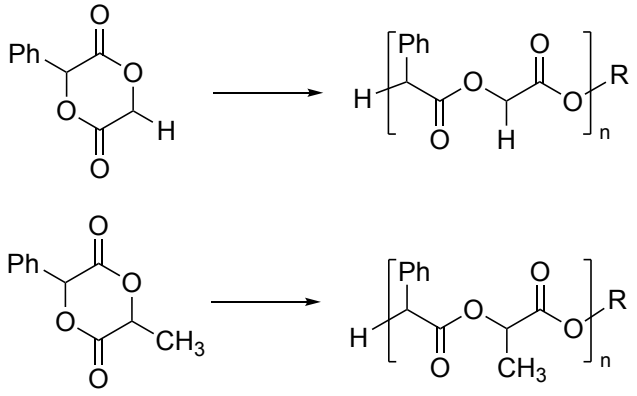

Figure 15 Routes to mandelic acid-based polymers. (a) Poly(mandelic acid) by ring opening polymerisation of mandelic acid-based cyclic monomers, (b) copolymers of lactic acid and mandelic acid through copolymerisation of different cyclic monomers. (c) Copolymers of mandelic acid with glycolic and lactic acid through ring opening polymerisation of mixed cyclic monomers.

1.4 Conclusions

Heterogeneous catalysis is a common approach used in industry, often suitable to scale up due to ease of catalyst separation and reuse. Zeolites are common heterogeneous catalysts employed in many organic reactions, from activation of small molecules such as methane to cracking of hydrocarbons. Their ability to host a variety of different catalytic active sites along with their shape-selective properties aids this versatility. Optimising the chemical and textural properties of the zeolite can lead to high product selectivity. Recently, the use of heterogeneous catalysis has been applied to the synthesis of cyclic monomers for biopolymers, such as lactide and, less commonly, glycolide. The parent alpha hydroxy acids of these cyclic monomers can be obtained by fermentation of sugars and the cyclic monomers have been shown to form from either the acid or its methyl ester in the presence of various heterogeneous catalysts, such as zeolites and various Lewis acid-functionalised silica species. The application of heterogeneous catalysts to functionalised lactide monomers is less well-documented. Whilst many functionalised alpha-hydroxy acids are not bioderived like lactic and glycolic acids, the range of chemical properties give them potential importance in achieving biodegradable plastics that are capable of replacing common commodity materials, such as petroleum-based plastics.

As well as 6-membered lactides, some 5-membered cyclic monomers have been investigated for ring opening polymerisation. These are proposed to give more controlled polymerisations, with reduction in both epimerisation and unwanted side reactions allowing control over both tacticity and molecular weight. Of these 5-membered monomers, the 1,3-dioxalan-4-ones appear the most promising, due to the use of

available, low cost and non-toxic starting materials in their synthesis along with their apparent wide substrate scope. By accessing these functionalised comonomers it has been shown that important properties such as phase transitions can be controlled through careful copolymerisations with lactide.

Overall, heterogeneous catalysis can be seen as a useful method to improve the efficiency of bioplastics production, and by applying it to a wider range of substrates can in turn broaden the properties of commercially viable options. Progress in chemo- and bio-catalysis for biomass conversion to useful platform molecules may lead to an increase in the chemical variety of bio-available molecules such as the alpha-hydroxy acids, making these functional polymers both biodegradable and bioderived.

1.5 Project Aims

Heterogeneous catalysts including zeolites are becoming more common in green chemistry and one such proposed use is in the acid-catalysed synthesis of cyclic bioplastic monomers such as lactide.[75] These cyclic monomers can be used to prepare biodegradable polyesters by ring opening polymerisation (ROP). A range of functionalised lactide monomers are known in the literature.[90, 159, 160] One such monomer is mandelide, the cyclic dimer of mandelic acid. ROP of mandelide yields biodegradable poly(mandelic acid) (PMA) which has a similar glass transition temperature, T_g, to polystyrene.[126, 127] As a result, PMA is an interesting alternative to PLA. Furthermore, there is a general trend in green chemistry to replace traditional homogeneous molecular acids with heterogeneous catalysts such as zeolites, due to recyclability and ease of catalyst separation. This project was concerned with the use of heterogeneous zeolite catalysts in the synthesis of biodegradable plastics and cyclic monomers based on mandelic acid.

Zeolites have already been applied to the synthesis of lactide.[34, 75, 77, 79, 103, 104, 112, 161] However, whilst this has been successful for lactide, applying it to alpha hydroxy acid substrates with greater functionality, such as methyl vinyl glycolate (MVG), has proved more challenging.[75, 113, 114] The synthesis of the cyclic monomer mandelide using a homogeneous para-toluenesulfonic acid catalyst is not straightforward, requiring up to 3 days of reaction time in high boiling xylene solvent to achieve only modest yields of approximately 50%.[126, 127] Alternative catalysts have not been investigated for the synthesis of mandelide. In this project, the synthesis of mandelide using zeolite catalysts has been attempted. The effect of zeolite framework on product distribution and mandelide yield was investigated.

In addition to modest overall yields, the synthesis of mandelide also produces a significant amount of the less desirable *rac*-mandelide isomer. The *meso* isomer is more desirable, as it has higher solubility in common organic solvents and a higher thermal stability. The previously reported syntheses of lactide using zeolites reported high selectivity towards the desired L,L-lactide isomer. In this project, the effect of zeolite catalysts on the *meso:rac* ratio of mandelide has also been investigated, as it would be advantageous to develop a catalyst that could synthesise the desirable *meso* isomer in higher selectivity.

As a result of some of the drawbacks associated with the synthesis and ring opening polymerisation of mandelide, poly(mandelic acid) has been prepared from other cyclic monomers.[120] These include O-carboxyanhydrides (OCAs) and 1,3-dioxolan-4-ones (DOXs). OCA synthesis requires the use of expensive, toxic phosgene reagents. As a result, synthesis of poly(mandelic acid) from DOX monomers is proposed to have a lower environmental impact compared with the OCA route.[158] All impact factors reported in the study were estimated to decrease for the DOX route compared with the OCA route. Some factors were reported to decrease significantly, with a greater than 50% decrease in climate change potential, human-toxicity (non-cancer), terrestrial ecotoxicity and ozone depletion. However, the DOX route was still estimated to have a greater environmental impact than polystyrene. This suggests that simply switching to a biodegradable polymer does not necessarily lead to a more environmentally-friendly manufacturing process. The production of novel biodegradable polymers is a comparatively new science compared the well-established and optimised production of petroleum-based plastics, and this life cycle analysis reported in the literature suggests PMA production has room for improvement and optimisation. As the reported DOX monomer synthesis uses homogeneous catalysis, the use of zeolites to synthesise DOX monomers was also investigated in this project.

Several of the reports of lactide synthesis using heterogeneous catalysts use gas-phase flow chemistry.[103, 104] The physical properties of mandelic acid differ from those of lactic acid, such as higher melting and boiling points. In addition, mandelide has poor solubility in common organic solvents and decomposes when heated above its melting point.[126] As a result, it is not known whether flow chemistry, such as has been used for lactide synthesis, would also be appropriate for the synthesis of cyclic monomers of mandelic acid. In this project, the use of flow chemistry has been investigated for the synthesis of cyclic monomers of mandelic acid, such as mandelide and 5-phenyl-1,3-dioxolan-4-ones.

Previous reports of DOX polymerisation show that the reactions are highly sensitive to the monomer structure[151, 152, 162], and that even under optimised conditions still suffer

from side reactions.[152] Whilst the synthesis of a broad scope of polymers from DOX monomers has been demonstrated,[151] the effect of monomer structure on ROP is still not fully understood. In this project, previously unreported ROP of DOX monomer, 2-methyl-5-phenyl-1,3-dioxolan-4-one (MePhDOX), has been investigated.

1.6 References

1. Cronstedt, A. F., *Akad. Handl. Stockholm* **1756,** *17*.

2. Friedel, G., Sur quelques propriétés nouvelles des zéolithes. *Bulletin de la Société française de Minéralogie* **1896,** *19* (3), 94-118.

3. Barrer, R. M., Synthesis of a zeolitic mineral with chabazite-like sorptive properties. *J. Chem. Soc.* **1948**, 127-132.

4. Feijen, E. J. P.; Martens, J. A.; Jacobs, P. A., Zeolites and their Mechanism of Synthesis. In *Zeolites and Related Microporous Materials: State of the Art 1994 - Proceedings of the 10th International Zeolite Conference, Garmisch-Partenkirchen, Germany, 17-22 July 1994*, 1994; pp 3-21.

5. Cundy, C. S.; Cox, P. A., The Hydrothermal Synthesis of Zeolites: History and Development from the Earliest Days to the Present Time. *Chem. Rev.* **2003,** *103*, 663-701.

6. Kerr, G. T., Chemistry of Crystalline Aluminosilicates. II. The Synthesis and Properties of Zeolite ZK-4. *Inorg. Chem.* **1966,** *5*, 1537-1539.

7. Burwell Jr., R. L., Manual of Symbols and Terminology for Physicochemical Quantities and Units - Appendix II. Definitions, Terminology and Symbols in Colloid and Surface Chemistry. Part II: Heterogeneous Catalysis. *Pure Appl. Chem.* **1976,** *46*, 71-90.

8. *Zeolites in Industrial Separation and Catalysis*. Wiley: 2010.

9. (IZA), I. Z. A. Database of Zeolite Structures. http://www.iza-structure.org/databases/ (accessed 18/11/2023).

10. Baerlocher, C.; McCusker, L. B.; Olson, D. H., *Atlas of Zeolite Framework Types*. 6 ed.; Elsevier: 2007.

11. Ejka, J.; Morris, R. E.; Nachtigall, P., *Zeolites in Catalysis: Properties and Applications*. 2017.

12. Vermeiren, W.; Gilson, J. P., Impact of Zeolites on the Petroleum and Petrochemical Industry. *Top. Catal.* **2009,** *52* (9), 1131-1161.

13. Vogt, E. T.; Weckhuysen, B. M., Fluid catalytic cracking: recent developments on the grand old lady of zeolite catalysis. *Chem. Soc. Rev.* **2015,** *44* (20), 7342-70.

14. Martínez, C.; Corma, A., Inorganic molecular sieves: Preparation, modification and industrial application in catalytic processes. *Coord. Chem. Rev.* **2011,** *255* (13-14), 1558-1580.

15. Shamzhy, M.; Opanasenko, M.; Concepcion, P.; Martinez, A., New trends in tailoring active sites in zeolite-based catalysts. *Chem. Soc. Rev.* **2019,** *48* (4), 1095-1149.

16. Corma, A.; Fornés, V.; Rey, F., Extraction of extra-framework aluminium in ultrastable Y zeolites by (NH4)2SiF6 treatments: I. Physicochemical Characterization. *Appl. Catal.* **1990,** *59* (1), 267-274.

17. Xu, B.; Bordiga, S.; Prins, R.; van Bokhoven, J. A., Effect of framework Si/Al ratio and extra-framework aluminum on the catalytic activity of Y zeolite. *Appl. Catal. Gen.* **2007,** *333* (2), 245-253.

18. Silaghi, M.-C.; Chizallet, C.; Raybaud, P., Challenges on molecular aspects of dealumination and desilication of zeolites. *Microporous Mesoporous Mater.* **2014,** *191*, 82-96.

19. Pu, X.; Liu, N.-w.; Shi, L., Acid properties and catalysis of USY zeolite with different extra-framework aluminum concentration. *Microporous Mesoporous Mater.* **2015,** *201*, 17-23.

20. Silaghi, M.-C.; Chizallet, C.; Sauer, J.; Raybaud, P., Dealumination mechanisms of zeolites and extra-framework aluminum confinement. *J. Catal.* **2016,** *339*, 242-255.

21. Sartori, G.; Maggi, R., Use of Solid Catalysts in Friedel–Crafts Acylation Reactions. *Chem. Rev.* **2006,** *106*, 1077-1104.

22. Weisz, P. B., Molecular shape selective catalysis. *Studies in Surface Science and Catalysis* **1981,** *7*, 3-20.

23. Csicsery, S. M., Shape-selective catalysis in zeolites. *Zeolites* **1984,** *4* (3), 202-213.

24. Davis, M. E., Zeolites and Molecular Sieves: Not Just Ordinary Catalysts. *Ind. Eng. Chem. Res.* **1991,** *30*, 1675-1683.

25. Jia, X. C.; Khan, W.; Wu, Z. J.; Choi, J.; Yip, A. C. K., Modern synthesis strategies for hierarchical zeolites: Bottom-up versus top-down strategies. *Adv. Powder Technol.* **2019,** *30* (3), 467-484.

26. Alaithan, Z. A.; Harrison, N.; Sastre, G., Diffusivity of Propylene in One-Dimensional Medium-Pore Zeolites. *J. Phys. Chem. C* **2021,** *125* (35), 19200-19208.

27. Cerqueira, H. S.; Caeiro, G.; Costa, L.; Ramôa Ribeiro, F., Deactivation of FCC catalysts. *J. Mol. Catal. A: Chem.* **2008,** *292* (1-2), 1-13.

28. Rahimi, N.; Karimzadeh, R., Catalytic cracking of hydrocarbons over modified ZSM-5 zeolites to produce light olefins: A review. *Appl. Catal. Gen.* **2011,** *398* (1-2), 1-17.

29. Dubbeldam, D.; Calero, S.; Vlugt, T. J. H., iRASPA: GPU-accelerated visualization software for materials scientists. *Mol. Simul.* **2018,** *44* (8), 653-676.

30. Jacobs, P. A.; Flanigen, E. M.; Jansen, J. C.; van Bekkum, H., *Introduction to zeolite science and practice*. Elsevier: 2001.

31. Jiang, J.; Yu, J.; Corma, A., Extra-large-pore zeolites: bridging the gap between micro and mesoporous structures. *Angew. Chem. Int. Ed. Engl.* **2010,** *49* (18), 3120-45.

32. Hong, L.; Zang, J.; Li, B.; Liu, G.; Wang, Y.; Wu, L., Research Progress on the Synthesis of Nanosized and Hierarchical Beta Zeolites. *Inorganics* **2023,** *11* (5).

33. Kalvachev, Y.; Todorova, T.; Popov, C., Recent Progress in Synthesis and Application of Nanosized and Hierarchical Mordenite—A Short Review. *Catalysts* **2021,** *11* (3).

34. Zhang, Q.; Xiang, S.; Zhang, Q.; Wang, B.; Mayoral, A.; Liu, W.; Wang, Y.; Liu, Y.; Shi, J.; Yang, G.; Luo, J.; Chen, X.; Terasaki, O.; Gilson, J.-P.; Yu, J., Breaking the Si/Al Limit of Nanosized β Zeolites: Promoting Catalytic Production of Lactide. *Chem. Mater.* **2019**.

35. Serrano, D. P.; van Grieken, R.; Melero, J. A.; García, A.; Vargas, C., Nanocrystalline ZSM-5: A catalyst with high activity and selectivity for epoxide rearrangement reactions. *J. Mol. Catal. A: Chem.* **2010,** *318* (1-2), 68-74.

36. Tao, Y.; Kanoh, H.; Abrams, L.; Kaneko, K., Mesopore-Modified Zeolites: Preparation, Characterization, and Applications. *Chem. Rev.* **2006,** *106*, 896-910.

37. Groen, J. C.; Peffer, L. A.; Moulijn, J. A.; Perez-Ramirez, J., Mechanism of hierarchical porosity development in MFI zeolites by desilication: the role of aluminium as a pore-directing agent. *Chemistry* **2005,** *11* (17), 4983-94.

38. Groen, J. C.; Jansen, J. C.; Moulijn, J. A.; Pérez-Ramírez, J., Optimal Aluminum-Assisted Mesoporosity Development in MFI Zeolites by Desilication. *J. Phys. Chem. B* **2004,** *108*, 13062-13065.

39. van Donk, S.; Janssen, A. H.; Bitter, J. H.; de Jong, K. P., Generation, Characterization, and Impact of Mesopores in Zeolite Catalysts. *Catal. Rev.* **2003,** *45* (2), 297-319.

40. García-Martínez, J.; Johnson, M.; Valla, J.; Li, K.; Ying, J. Y., Mesostructured zeolite Y—high hydrothermal stability and superior FCC catalytic performance. *Catal. Sci. Tech.* **2012,** *2* (5), 987-994.

41. Guisnet, M.; Ram a Ribeiro, F., *Deactivation and Regeneration of Zeolite Catalysts*. World Scientific: 2011.

42. Egeblad, K.; Christensen, C. H.; Kustova, M.; Christensen, C. H., Templating Mesoporous Zeolites. *Chem. Mater.* **2008,** *20*, 946-960.

43. Chen, L. H.; Sun, M. H.; Wang, Z.; Yang, W.; Xie, Z.; Su, B. L., Hierarchically Structured Zeolites: From Design to Application. *Chem. Rev.* **2020,** *120* (20), 11194-11294.

44. Verboekend, D.; Pérez-Ramírez, J., Design of hierarchical zeolite catalysts by desilication. *Catal. Sci. Tech.* **2011,** *1* (6), 879-890.

45. Verboekend, D.; Pérez-Ramírez, J., Desilication Mechanism Revisited: Highly Mesoporous All-Silica Zeolites Enabled Through Pore-Directing Agents. *Chem. Eur. J.* **2011,** *17* (4), 1137-1147.

46. Verboekend, D.; Vile, G.; Perez-Ramirez, J., Hierarchical Y and USY Zeolites Designed by Post-Synthetic Strategies. *Adv. Funct. Mater.* **2012,** *22* (5), 916-928.

47. Verboekend, D.; Vile, G.; Perez-Ramirez, J., Mesopore Formation in USY and Beta Zeolites by Base Leaching: Selection Criteria and Optimization of Pore-Directing Agents. *Cryst. Growth Des.* **2012,** *12* (6), 3123-3132.

48. Zhang, H.; Samsudin, I. b.; Jaenicke, S.; Chuah, G.-K., Zeolites in catalysis: sustainable synthesis and its impact on properties and applications. *Catal. Sci. Tech.* **2022,** *12* (19), 6024-6039.

49. Shamzhy, M.; Opanasenko, M.; Concepcion, P.; Martinez, A., New trends in tailoring active sites in zeolite-based catalysts. *Chem. Soc. Rev.* **2019**, 1095-1149.

50. Kenvin, J.; Mitchell, S.; Sterling, M.; Warringham, R.; Keller, T. C.; Crivelli, P.; Jagiello, J.; Pérez-Ramírez, J., Quantifying the Complex Pore Architecture of Hierarchical Faujasite Zeolites and the Impact on Diffusion. *Adv. Funct. Mater.* **2016,** *26* (31), 5621-5630.

51. Martinez, C.; Verboekend, D.; Perez-Ramirez, J.; Corma, A., Stabilized hierarchical USY zeolite catalysts for simultaneous increase in diesel and LPG olefinicity during catalytic cracking. *Catal. Sci. Tech.* **2013,** *3* (4), 972-981.

52. García-Martínez, J.; Li, K.; Krishnaiah, G., A mesostructured Y zeolite as a superior FCC catalyst – from lab to refinery. *Chem. Commun.* **2012,** *48* (97), 11841-11843.

53. Townsend, R. P.; Harjula, R., Dealumination Techniques for Zeolites. In *Post-Synthesis Modification I*, Springer, Berlin, Heidelberg: 2002; Vol. 3.

54. Lutz, W., Zeolite Y: Synthesis, Modification, and Properties—A Case Revisited. *Adv. Mater. Sci. Eng.* **2014,** *2014*, 1-20.

55. Wouters, B. H.; Chen, T.; Grobet, P. J., Steaming of Zeolite Y: Formation of Transient Al Species. *J. Phys. Chem. B* **2001,** *105*, 1135-1139.

56. Verboekend, D.; Milina, M.; Mitchell, S.; Perez-Ramirez, J., Hierarchical Zeolites by Desilication: Occurrence and Catalytic Impact of Recrystallization and Restructuring. *Cryst. Growth Des.* **2013,** *13* (11), 5025-5035.

57. Van Aelst, J.; Verboekend, D.; Philippaerts, A.; Nuttens, N.; Kurttepeli, M.; Gobechiya, E.; Haouas, M.; Sree, S. P.; Denayer, J. F. M.; Martens, J. A.; Kirschhock, C. E. A.; Taulelle, F.; Bals, S.; Baron, G. V.; Jacobs, P. A.; Sels, B. F., Catalyst Design by NH4OH Treatment of USY Zeolite. *Adv. Funct. Mater.* **2015,** *25* (46), 7130-7144.

58. Fernandez, S.; Ostraat, M. L.; Lawrence, J. A.; Zhang, K., Tailoring the hierarchical architecture of beta zeolites using base leaching and pore-directing agents. *Microporous Mesoporous Mater.* **2018,** *263*, 201-209.

59. Sachse, A.; Garcia-Martinez, J., Surfactant-Templating of Zeolites: From Design to Application. *Chem. Mater.* **2017,** *29* (9), 3827-3853.

60. Garcia-Martinez, J.; Xiao, C. H.; Cychosz, K. A.; Li, K. H.; Wan, W.; Zou, X. D.; Thommes, M., Evidence of Intracrystalline Mesostructured Porosity in Zeolites by Advanced Gas Sorption, Electron Tomography and Rotation Electron Diffraction. *ChemCatChem* **2014,** *6* (11), 3110-3115.

61. Valtchev, V.; Majano, G.; Mintova, S.; Perez-Ramirez, J., Tailored crystalline microporous materials by post-synthesis modification. *Chem. Soc. Rev.* **2013,** *42* (1), 263-90.

62. Townsend, R. P.; Harjula, R., Ion Exchange in Molecular Sieves by Conventional Techniques. In *Post-Synthesis Modification I*, Springer, Berlin, Heidelberg: 2002; Vol. 3.

63. Corma, A., State of the art and future challenges of zeolites as catalysts. *J. Catal.* **2003,** *216* (1-2), 298-312.

64. Keller, T. C.; Isabettini, S.; Verboekend, D.; Rodrigues, E. G.; Pérez-Ramírez, J., Hierarchical high-silica zeolites as superior base catalysts. *Chem. Sci.* **2014,** *5* (2), 677-684.

65. Sheldon, R. A.; Arends, I.; Hanefeld, U., *Green Chemistry and Catalysis*. John Wiley & Sons: 2007.

66. Li, Y.; Li, L.; Yu, J., Applications of Zeolites in Sustainable Chemistry. *Chem* **2017,** *3* (6), 928-949.

67. Holm, M. S.; Pagán-Torres, Y. J.; Saravanamurugan, S.; Riisager, A.; Dumesic, J. A.; Taarning, E., Sn-Beta catalysed conversion of hemicellulosic sugars. *Green Chem.* **2012,** *14* (3), 702.

68. Dusselier, M.; Van Wouwe, P.; de Clippel, F.; Dijkmans, J.; Gammon, D. W.; Sels, B. F., Mechanistic Insight into the Conversion of Tetrose Sugars to Novel α-Hydroxy Acid Platform Molecules. *ChemCatChem* **2013,** *5* (2), 569-575.

69. De Clercq, R.; Dusselier, M.; Christiaens, C.; Dijkmans, J.; Iacobescu, R. I.; Pontikes, Y.; Sels, B. F., Confinement Effects in Lewis Acid-Catalyzed Sugar Conversion: Steering Toward Functional Polyester Building Blocks. *ACS Catal.* **2015,** *5* (10), 5803-5811.

70. Yamaguchi, S.; Baba, T., A Novel Strategy for Biomass Upgrade: Cascade Approach to the Synthesis of Useful Compounds via C-C Bond Formation Using Biomass-Derived Sugars as Carbon Nucleophiles. *Molecules* **2016,** *21* (7).

71. Zhang, J.; Wang, L.; Wang, G.; Chen, F.; Zhu, J.; Wang, C.; Bian, C.; Pan, S.; Xiao, F.-S., Hierarchical Sn-Beta Zeolite Catalyst for the Conversion of Sugars to Alkyl Lactates. *ACS Sustain. Chem. Eng.* **2017,** *5* (4), 3123-3131.

72. Dapsens, P. Y.; Mondelli, C.; Perez-Ramirez, J., Design of Lewis-acid centres in zeolitic matrices for the conversion of renewables. *Chem. Soc. Rev.* **2015,** *44* (20), 7025-43.

73. Yang, H.; Guo, Q.; Yang, P.; Liu, X.; Wang, Y., Synthesis of hierarchical Sn-Beta zeolite and its catalytic performance in glucose conversion. *Catal. Today* **2020**.

74. Al-Naji, M.; Schlaad, H.; Antonietti, M., New (and Old) Monomers from Biorefineries to Make Polymer Chemistry More Sustainable. *Macromol. Rapid Commun.* **2021,** *42* (3), e2000485.

75. Dusselier, M.; Van Wouwe, P.; Dewaele, A.; Jacobs, P. A.; Sels, B. F., Shape-selective zeolite catalysis for bioplastics production. *Science* **2015,** *349*, 78-80.

76. Van Wouwe, P.; Dusselier, M.; Vanleeuw, E.; Sels, B., Lactide Synthesis and Chirality Control for Polylactic acid Production. *ChemSusChem* **2016,** *9* (9), 907-921.

77. Huang, Q.; Chen, N.; Liu, L.; Arias, K. S.; Iborra, S.; Yi, X.; Ma, C.; Liang, W.; Zheng, A.; Zhang, C.; Hu, J.; Cai, Z.; Liu, Y.; Jiang, J.; Corma, A., Direct synthesis of the organic and Ge free Al containing BOG zeolite (ITQ-47) and its application for transformation of biomass derived molecules. *Chem. Sci.* **2020,** *11* (44), 12103-12108.

78. Xu, Y.; Fang, Y.; Cao, J.; Sun, P.; Min, C.; Qi, Y.; Jiang, W.; Zhang, Q., Controlled Synthesis of l-Lactide Using Sn-Beta Zeolite Catalysts in a One-Step Route. *Ind. Eng. Chem. Res.* **2021,** *60* (37), 13534-13541.

79. Xu, Y.; Yang, L.; Si, C.; Zhang, S.; Zhang, Q.; Zeng, G.; Jiang, W., Direct Synthesis of Lactide from Lactic Acid by Sn-beta Zeolite: Crucial Role of the Open Sn Site. *Ind. Eng. Chem. Res.* **2022,** *61* (48), 17457-17466.

80. Ma, Z.; Zhang, Q.; Li, L.; Chen, M.; Li, J.; Yu, J., Steam-assisted crystallization of highly dispersed nanosized hierarchical zeolites from solid raw materials and their catalytic performance in lactide production. *Chem. Sci.* **2022,** *13* (27), 8052-8059.

81. Yakabi, K.; Mathieux, T.; Milne, K.; López-Vidal, E. M.; Buchard, A.; Hammond, C., Continuous Production of Biorenewable, Polymer-Grade Lactone Monomers through Sn-β-Catalyzed Baeyer–Villiger Oxidation with H2O2. *ChemSusChem* **2017,** *10* (18), 3652-3659.

82. Jenkins, A. D.; Kratochvíl, P.; Stepto, R. F. T.; Suter, U. W., Glossary of basic terms in polymer science (IUPAC Recommendations 1996). *Pure Appl. Chem.* **1996,** *68*, 2287-2311.

83. Young, R. J.; Lovell, P. A., *Introduction to Polymers*. 3rd ed.; CRC Press: 2011.

84. Azapagic, A.; Emsley, A.; Hamerton, I., Chapter 1 The Environment and Sustainable Development An Integrated Strategy for Polymers. In *Polymers: The Environment and Sustainable Development*, John Wiley and Sons: 2007.

85. Barth, H. G.; Mays, J. W., *Modern Methods of Polymer Characterization*. John Wiley & Sons: 1991.

86. Chamas, A.; Moon, H.; Zheng, J.; Qiu, Y.; Tabassum, T.; Jang, J. H.; Abu-Omar, M.; Scott, S. L.; Suh, S., Degradation Rates of Plastics in the Environment. *ACS Sustain. Chem. Eng.* **2020,** *8* (9), 3494-3511.

87. Horie, K.; Barón, M.; Fox, R. B.; He, J.; Hess, M.; Kahovec, J.; Kitayama, T.; Kubisa, P.; Maréchal, E.; Mormann, W.; Stepto, R. F. T.; Tabak, D.; Vohlídal, J.; Wilks, E. S.; Work, W. J., Definitions of terms relating to reactions of polymers and to functional

polymeric materials (IUPAC Recommendations 2003). *Pure Appl. Chem.* **2004,** *76*, 889-906.

88. Ünkel, A. N. K.; Se, B.; Chlegel, K. A. S.; Se, B., Polymers , Biodegradable. **2016**.

89. Leemhuis, M.; van Nostrum, C. F.; Kruijtzer, J. A. W.; Zhong, Z. Y.; ten Breteler, M. R.; Dijkstra, P. J.; Feijen, J.; Hennink, W. E., Functionalized Poly(α-hydroxy acid)s via Ring-Opening Polymerization: Toward Hydrophilic Polyesters with Pendant Hydroxyl Groups. *Macromol.* **2006,** *39* (10), 3500-3508.

90. Williams, C. K., Synthesis of functionalized biodegradable polyesters. *Chem. Soc. Rev.* **2007,** *36*, 1573-1580.

91. Brignou, P.; Gil, M. P.; Casagrande, O.; Carpentier, J. F.; Guillaume, S. M., Polycarbonates Derived from Green Acids: Ring-Opening Polymerization of Seven-Membered Cyclic Carbonates. *Macromol.* **2010,** *43* (19), 8007-8017.

92. Zhang, X.; Fevre, M.; Jones, G. O.; Waymouth, R. M., Catalysis as an Enabling Science for Sustainable Polymers. *Chem. Rev.* **2018,** *118* (2), 839-885.

93. Lu, J.; Tappel, R. C.; Nomura, C. T., Mini-review: Biosynthesis of poly(hydroxyalkanoates). *Polym. Rev.* **2009,** *49*, 226-248.

94. Nguyen, H. T. H.; Qi, P. X.; Rostagno, M.; Feteha, A.; Miller, S. A., The quest for high glass transition temperature bioplastics. *J. Mater. Chem. A* **2018,** *6* (20), 9298-9331.

95. Fiandra, E. F.; Shaw, L.; Starck, M.; McGurk, C. J.; Mahon, C. S., Designing biodegradable alternatives to commodity polymers. *Chem. Soc. Rev.* **2023,** *52* (23), 8085-8105.

96. Rosenboom, J. G.; Langer, R.; Traverso, G., Bioplastics for a circular economy. *Nat. Rev. Mater.* **2022,** *7* (2), 117-137.

97. Dusselier, M.; Van Wouwe, P.; Dewaele, A.; Makshina, E.; Sels, B. F., Lactic acid as a platform chemical in the biobased economy: the role of chemocatalysis. *Energy Environ. Sci.* **2013,** *6* (5), 1415.

98. Vink, E. T. H.; Rábago, K. R.; Glassner, D. A.; Gruber, P. R., Applications of life cycle assessment to NatureWorks™ polylactide (PLA) production. *Polym. Degrad. Stab.* **2003,** *80* (3), 403-419.

99. Vink, E. T. H.; Davies, S.; Kolstad, J. J., ORIGINAL RESEARCH: The eco-profile for current Ingeo® polylactide production. *Ind. Biotechnol.* **2010,** *6* (4), 212-224.

100. Lyu, S.; Schley, J.; Loy, B.; Lind, D.; Hobot, C.; Sparer, R.; Untereker, D., Kinetics and Time–Temperature Equivalence of Polymer Degradation. *Biomacromol.* **2007,** *8*, 2301-2310.

101. Haider, T. P.; Völker, C.; Kramm, J.; Landfester, K.; Wurm, F. R., Plastics of the Future? The Impact of Biodegradable Polymers on the Environment and on Society. *Angew. Chem. Int. Ed.* **2019,** *58*, 50-62.

102. Martin, R. T.; Camargo, L. P.; Miller, S. A., Marine-degradable polylactic acid. *Green Chem.* **2014,** *16* (4), 1768-1773.

103. De Clercq, R.; Dusselier, M.; Poleunis, C.; Debecker, D. P.; Giebeler, L.; Oswald, S.; Makshina, E.; Sels, B. F., Titania-Silica Catalysts for Lactide Production from Renewable Alkyl Lactates: Structure–Activity Relations. *ACS Catal.* **2018,** *8* (9), 8130-8139.

104. De Clercq, R.; Dusselier, M.; Makshina, E.; Sels, B. F., Catalytic Gas-Phase Production of Lactide from Renewable Alkyl Lactates. *Angew. Chem. Int. Ed. Engl.* **2018,** *57* (12), 3074-3078.

105. Sun, P.; Yu, D.; Tang, Z.; Li, H.; Huang, H., NaY Zeolites Catalyze Dehydration of Lactic Acid to Acrylic Acid: Studies on the Effects of Anions in Potassium Salts. *Ind. Eng. Chem. Res.* **2010,** *49* (19), 9082-9087.

106. Yan, B.; Tao, L. Z.; Liang, Y.; Xu, B. Q., Sustainable production of acrylic acid: alkali-ion exchanged beta zeolite for gas-phase dehydration of lactic acid. *ChemSusChem* **2014,** *7* (6), 1568-78.

107. Yan, B.; Mahmood, A.; Liang, Y.; Xu, B.-Q., Sustainable production of acrylic acid: Rb+- and Cs+-exchanged Beta zeolite catalysts for catalytic gas-phase dehydration of lactic acid. *Catal. Today* **2016,** *269*, 65-73.

108. Yan, B.; Tao, L.-Z.; Mahmood, A.; Liang, Y.; Xu, B.-Q., Potassium-Ion-Exchanged Zeolites for Sustainable Production of Acrylic Acid by Gas-Phase Dehydration of Lactic Acid. *ACS Catal.* **2017,** *7* (1), 538-550.

109. Yan, B.; Liu, Z.-H.; Liang, Y.; Xu, B.-Q., Acrylic Acid Production by Gas-Phase Dehydration of Lactic Acid over K+-Exchanged ZSM-5: Reaction Variable Effects, Kinetics, and New Evidence for Cooperative Acid–Base Bifunctional Catalysis. *Ind. Eng. Chem. Res.* **2020,** *59* (39), 17417-17428.

110. Espartero, J. L.; Rashkov, I.; Li, S. M.; Manolova, N.; Vert, M., NMR Analysis of Low Molecular Weight Poly(lactic acid)s. *Macromol.* **1996,** *29* (10), 3535-3539.

111. Vu, D. T.; Kolah, A. K.; Asthana, N. S.; Peereboom, L.; Lira, C. T.; Miller, D. J., Oligomer distribution in concentrated lactic acid solutions. *Fluid Phase Equilib.* **2005,** *236* (1), 125-135.

112. Upare, P. P.; Yoon, J. W.; Hwang, D. W.; Lee, U. H.; Hwang, Y. K.; Hong, D.-Y.; Kim, J. C.; Lee, J. H.; Kwak, S. K.; Shin, H.; Kim, H.; Chang, J.-S., Design of a heterogeneous catalytic process for the continuous and direct synthesis of lactide from lactic acid. *Green Chem.* **2016,** *18* (22), 5978-5983.

113. De Clercq, R.; Makshina, E.; Sels, B. F.; Dusselier, M., Catalytic Gas-Phase Cyclization of Glycolate Esters: A Novel Route Toward Glycolide-Based Bioplastics. *ChemCatChem* **2018,** *10* (24), 5649-5655.

114. Narmon, A. S.; Leys, E.; Khalil, I.; Ivanushkin, G.; Dusselier, M., Brønsted acid catalysis opens a new route to polythiolesters via the direct condensation of thiolactic acid to thiolactide. *Green Chem.* **2022,** *24* (24), 9709-9720.

115. Gregory, G. L.; López-Vidal, E. M.; Buchard, A., Polymers from sugars: cyclic monomer synthesis, ring-opening polymerisation, material properties and applications. *Chem. Commun.* **2017,** *53* (14), 2198-2217.

116. Stanford, M. J.; Dove, A. P., Stereocontrolled ring-opening polymerisation of lactide. *Chem. Soc. Rev.* **2010,** *39* (2), 486-94.

117. Dechy-Cabaret, O.; Martin-Vaca, B.; Bourissou, D., Controlled Ring-Opening Polymerization of Lactide and Glycolide. *Chem. Rev.* **2004,** *104*, 6147-6176.

118. Khalil, A.; Cammas-Marion, S.; Coulembier, O., Organocatalysis applied to the ring-opening polymerization of β-lactones: A brief overview. *J. Polym. Sci. A: Polym. Chem.* **2019,** *57* (6), 657-672.

119. He, W.; Tao, Y.; Wang, X., Functional Polyamides: A Sustainable Access via Lysine Cyclization and Organocatalytic Ring-Opening Polymerization. *Macromol.* **2018,** *51* (20), 8248-8257.

120. Gregory, G. L.; Lopez-Vidal, E. M.; Buchard, A., Polymers from sugars: cyclic monomer synthesis, ring-opening polymerisation, material properties and applications. *Chem. Commun.* **2017,** *53*, 2198-2217.

121. Jing, F.; Hillmyer, M. A., A bifunctional monomer derived from lactide for toughening polylactide. *J. Am. Chem. Soc.* **2008,** *130* (42), 13826-7.

122. Liu, H.; Zhang, J., Research progress in toughening modification of poly(lactic acid). *J. Polym. Sci., Part B: Polym. Phys.* **2011,** *49* (15), 1051-1083.

123. Arıcan, M. O.; Mert, O., Synthesis and properties of novel diisopropyl-functionalized polyglycolide–PEG copolymers. *RSC Adv.* **2015,** *5* (87), 71519-71528.

124. Yin, M.; Baker, G. L., Preparation and Characterization of Substituted Polylactides. *Macromol.* **1999,** *32*, 7711-7718.

125. Jing, F.; Smith, M. R.; Baker, G. L., Cyclohexyl-Substituted Polyglycolides with High Glass Transition Temperatures. *Macromol.* **2007,** *40* (26), 9304-9312.

126. Liu, T. Q.; Simmons, T. L.; Bohnsack, D. A.; Mackay, M. E.; Smith, M. R.; Baker, G. L., Synthesis of polymandelide: A degradable polylactide derivative with polystyrene-like properties. *Macromol.* **2007,** *40* (17), 6040-6047.

127. Graulus, G. J.; Van Herck, N.; Van Hecke, K.; Van Driessche, G.; Devreese, B.; Thienpont, H.; Ottevaere, H.; Van Vlierberghe, S.; Dubruel, P., Ring opening copolymerisation of lactide and mandelide for the development of environmentally degradable polyesters with controllable glass transition temperatures. *React. Funct. Polym.* **2018,** *128*, 16-23.

128. Simmons, T. L.; Baker, G. L., Poly(phenyllactide): Synthesis, Characterization, and Hydrolytic Degradation. *Biomacromol.* **2001,** *2* (3), 658-663.

129. Marcincinova Benabdillah, K.; Coudane, J.; Boustta, M.; Engel, R.; Vert, M., Synthesis and Characterization of Novel Degradable Polyesters Derived from d-Gluconic and Glycolic Acids. *Macromol.* **1999,** *32* (26), 8774-8780.

130. Marcincinova-Benabdillah, K.; Boustta, M.; Coudane, J.; Vert, M., Novel Degradable Polymers Combining d-Gluconic Acid, a Sugar of Vegetal Origin, with Lactic and Glycolic Acids. *Biomacromol.* **2001,** *2* (4), 1279-1284.

131. Pounder, R. J.; Dove, A. P., Synthesis and organocatalytic ring-opening polymerization of cyclic esters derived from l-malic acid. *Biomacromol.* **2010,** *11* (8), 1930-9.

132. Kuroishi, P. K.; Delle Chiaie, K. R.; Dove, A. P., Polylactide thermosets using a bis(cyclic diester) crosslinker. *Eur. Polym. J.* **2019,** *120*, 109192.

133. Leemhuis, M.; Akeroyd, N.; Kruijtzer, J. A. W.; van Nostrum, C. F.; Hennink, W. E., Synthesis and characterization of allyl functionalized poly(α-hydroxy)acids and their further dihydroxylation and epoxidation. *Eur. Polym. J.* **2008,** *44* (2), 308-317.

134. Coumes, F.; Darcos, V.; Domurado, D.; Li, S.; Coudane, J., Synthesis and ring-opening polymerisation of a new alkyne-functionalised glycolide towards biocompatible amphiphilic graft copolymers. *Polym. Chem.* **2013,** *4* (13), 3705-3713.

135. Leemhuis, M.; Kruijtzer, J. A. W.; van Nostrum, C. F.; Hennink, W. E., In Vitro Hydrolytic Degradation of Hydroxyl-Functionalized Poly(α-hydroxy acid)s. *Biomacromol.* **2007,** *8* (9), 2943-2949.

136. Seyednejad, H.; Vermonden, T.; Fedorovich, N. E.; van Eijk, R.; van Steenbergen, M. J.; Dhert, W. J. A.; van Nostrum, C. F.; Hennink, W. E., Synthesis and Characterization of Hydroxyl-Functionalized Caprolactone Copolymers and Their Effect

on Adhesion, Proliferation, and Differentiation of Human Mesenchymal Stem Cells. *Biomacromol.* **2009,** *10* (11), 3048-3054.

137. Whitesell, J. K.; Pojman, J. A., Homochiral and heterochiral polyesters: polymers derived from mandelic acid. *Chem. Mater.* **1990,** *2* (3), 248-254.

138. Lynch, V. M.; Pojman, J.; Whitesell, J. K.; Davis, B. E., Structure of (S,S)-3,6-diphenyl-1,4-dioxane-2,5-dione. *Acta Crystallogr.* **1990,** *46* (6), 1125-1127.

139. Thillaye du Boullay, O.; Marchal, E.; Martin-Vaca, B.; Cossio, F. P.; Bourissou, D., An activated equivalent of lactide toward organocatalytic ring-opening polymerization. *J. Am. Chem. Soc.* **2006,** *128* (51), 16442-3.

140. Buchard, A.; Carbery, D. R.; Davidson, M. G.; Ivanova, P. K.; Jeffery, B. J.; Kociok-Kohn, G. I.; Lowe, J. P., Preparation of stereoregular isotactic poly(mandelic acid) through organocatalytic ring-opening polymerization of a cyclic O-carboxyanhydride. *Angew. Chem. Int. Ed. Engl.* **2014,** *53* (50), 13858-61.

141. Vagenende, M.; Graulus, G.-J.; Delaey, J.; Van Hoorick, J.; Berghmans, F.; Thienpont, H.; Van Vlierberghe, S.; Dubruel, P., Amorphous random copolymers of lacOCA and manOCA for the design of biodegradable polyesters with tuneable properties. *Eur. Polym. J.* **2019,** *118*, 685-693.

142. Li, M.; Tao, Y.; Tang, J.; Wang, Y.; Zhang, X.; Tao, Y.; Wang, X., Synergetic Organocatalysis for Eliminating Epimerization in Ring-Opening Polymerizations Enables Synthesis of Stereoregular Isotactic Polyester. *J. Am. Chem. Soc.* **2019,** *141* (1), 281-289.

143. Bonduelle, C.; Martin-Vaca, B.; Cossio, F. P.; Bourissou, D., Monomer versus alcohol activation in the 4-dimethylaminopyridine-catalyzed ring-opening polymerization of lactide and lactic O-carboxylic anhydride. *Chemistry* **2008,** *14* (17), 5304-12.

144. Pounder, R. J.; Fox, D. J.; Barker, I. A.; Bennison, M. J.; Dove, A. P., Ring-opening polymerization of an O-carboxyanhydride monomer derived from l-malic acid. *Polym. Chem.* **2011,** *2* (10), 2204.

145. Lu, Y.; Yin, L.; Zhang, Y.; Zhonghai, Z.; Xu, Y.; Tong, R.; Cheng, J., Synthesis of water-soluble poly(alpha-hydroxy acids) from living ring-opening polymerization of O-benzyl-L-serine carboxyanhydrides. *ACS Macro Lett.* **2012,** *1* (4), 441-444.

146. Xia, H.; Kan, S.; Li, Z.; Chen, J.; Cui, S.; Wu, W.; Ouyang, P.; Guo, K., N-heterocyclic carbenes as organocatalysts in controlled/living ring-opening polymerization of O-carboxyanhydrides derived from L-lactic acid and L-mandelic acid. *J. Polym. Sci. A: Polym. Chem.* **2014,** *52* (16), 2306-2315.

147. Yin, Q.; Yin, L.; Wang, H.; Cheng, J., Synthesis and biomedical applications of functional poly(alpha-hydroxy acids) via ring-opening polymerization of O-carboxyanhydrides. *Acc. Chem. Res.* **2015,** *48* (7), 1777-87.

148. Wang, R.; Zhang, J.; Yin, Q.; Xu, Y.; Cheng, J.; Tong, R., Controlled Ring-Opening Polymerization of O-Carboxyanhydrides Using a beta-Diiminate Zinc Catalyst. *Angew. Chem. Int. Ed. Engl.* **2016,** *55* (42), 13010-13014.

149. Bexis, P.; De Winter, J.; Coulembier, O.; Dove, A. P., Isotactic degradable polyesters derived from O -carboxyanhydrides of l -lactic and l -malic acid using a single organocatalyst/initiator system. *Eur. Polym. J.* **2017,** *95*, 660-670.

150. Sun, Y.; Jia, Z.; Chen, C.; Cong, Y.; Mao, X.; Wu, J., Alternating Sequence Controlled Copolymer Synthesis of alpha-Hydroxy Acids via Syndioselective Ring-Opening Polymerization of O-Carboxyanhydrides Using Zirconium/Hafnium Alkoxide Initiators. *J. Am. Chem. Soc.* **2017,** *139* (31), 10723-10732.

151. Cairns, S. A.; Schultheiss, A.; Shaver, M. P., A broad scope of aliphatic polyesters prepared by elimination of small molecules from sustainable 1,3-dioxolan-4-ones. *Polym. Chem.* **2017,** *8* (19), 2990-2996.

152. Xu, Y.; Perry, M. R.; Cairns, S. A.; Shaver, M. P., Understanding the ring-opening polymerisation of dioxolanones. *Polym. Chem.* **2019,** *10* (23), 3048-3054.

153. Jiang, J.; Cui, Y.; Lu, Y.; Zhang, B.; Pan, X.; Wu, J., Weak Lewis Pairs as Catalysts for Highly Isoselective Ring-Opening Polymerization of Epimerically Labile rac-O-Carboxyanhydride of Mandelic Acid. *Macromol.* **2020,** *53* (3), 946-955.

154. Xu, Y.; Șucu, T.; Perry, M. R.; Shaver, M. P., Alicyclic polyesters from a bicyclic 1,3-dioxane-4-one. *Polym. Chem.* **2020**.

155. Otsugu, S.; Kimura, Y.; Nakajima, H.; Loos, K., Enhancement of Tg of Poly(l-lactide) by Incorporation of Biobased Mandelic-Acid-Derived Phenyl Groups by Polymerization and Polymer Blending. *Macromol. Chem. Phys.* **2019,** *221* (3), 1900392.

156. Nakajima, H.; Loos, K.; Ishizu, S.; Kimura, Y., Ring-Opening Polymerization of a New Diester Cyclic Dimer of Mandelic and Glycolic Acid: An Efficient Synthesis Method for Derivatives of Amorphous Polyglycolide with High Tg. *Macromol. Rapid Commun.* **2018,** *39* (12), e1700865.

157. Wang, Y.; Jia, Z.; Jiang, J.; Mao, X.; Pan, X.; Wu, J., Highly Regioselective Ring-Opening Polymerization of Cyclic Diester for Alternating Sequence-Controlled Copolymer Synthesis of Mandelic Acid and Glycolic Acid. *Macromol.* **2019,** *52* (20), 7564-7571.

158. Jeswani, H. K.; Perry, M. R.; Shaver, M. P.; Azapagic, A., Biodegradable and conventional plastic packaging: Comparison of life cycle environmental impacts of poly(mandelic acid) and polystyrene. *Sci. Total Environ.* **2023,** *903*, 166311.

159. Kageyama, K.; Ogino, S.; Aida, T.; Tatsumi, T., Mesoporous zeolite as a new class of catalyst for controlled polymerization of lactones. *Macromol.* **1998,** *31* (13), 4069-4073.

160. Gerhardt, W. W.; Noga, D. E.; Hardcastle, K. I.; García, A. J.; Collard, D. M.; Weck, M., Functional Lactide Monomers: Methodology and Polymerization. *Biomacromol.* **2006,** *7* (6), 1735-1742.

161. Ghadamyari, M.; Chaemchuen, S.; Zhou, K.; Dusselier, M.; Sels, B. F.; Mousavi, B.; Verpoort, F., One-step synthesis of stereo-pure l,l lactide from l-lactic acid. *Catal. Commun.* **2018,** *114*, 33-36.

162. Gazzotti, S.; Ortenzi, M. A.; Farina, H.; Silvani, A., 1,3-Dioxolan-4-Ones as Promising Monomers for Aliphatic Polyesters: Metal-Free, in Bulk Preparation of PLA. *Polymers (Basel)* **2020,** *12* (10).

Chapter 2: Experimental

2.1 Materials

D,L-Mandelic acid (99+%, Acros Organics), acetonitrile (HPLC grade), acetone (AR grade), benzaldehyde (Alfa Aesar, 99+%), cyclohexane (99.5%, Thermo Scientific), methylcyclohexane (99%) toluene (AR grade), o-xylene (99%), p-xylene (99%), m-xylene (99%), mixed xylenes (AR grade), magnesium nitrate hexahydrate (Alfa Aesar, 98%) and potassium nitrate (Acros Organics, 99%) were purchased from Fisher Scientific. Chlorobenzene, para-toluenesulfonic acid monohydrate (p-TSA), and ammonium nitrate (98%) were purchased from Sigma Aldrich.

Zeolite Y (CBV series) materials were purchased from Alfa Aesar or supplied by Johnson Matthey. ZSM5, Beta, L and Mordenite zeolites were supplied by Clariant. Further details of catalyst properties are given in Section S4 below. Unless otherwise stated, all zeolites were purchased in the H-form and used as commercially supplied, without a pre-drying step or a calcination step. Where zeolites were purchased in the NH_4-form, they were calcined in air in a muffle furnace at 550 °C for 6 hours to convert them to the protic form.

The shorthand naming convention used for the commercial zeolites within this work follows the following: X-YYY-ZZ, where YYY is the zeolite framework, X is the stated countercation and ZZ is the Si/Al ratio, all as reported by the zeolite manufacturer.

2.2 Molecule Numbering System

Alpha-hydroxy acids and their derivatives referred to in this thesis are numbered using a reference. Each molecule is given a reference comprising at least a number and a letter. The number corresponds to the type of compound (e.g., hydroxy acid, dimer of the hydroxy acid etc) and the letter corresponds to the alpha-hydroxy acid (e.g., lactic acid, mandelic acid etc). For example, dimers are given the numeral “2”, and lactic acid is given the letter “a”, therefore a lactic acid dimer is given the reference numeral “2a”. Where more than one example exists, the two-letter reference is suffixed with “-1”, “-2” etc. Where a compound can exist as different stereoisomers, the reference is prefixed with a letter to indicate the relative stereochemistry. For example, the racemic isomer of lactide (3a) is labelled “*r*-3a”.

For a full list of reference numerals, see Table 1.

Table 1 Molecule numbers used in this thesis.

Compound name	Abbreviation	Compound Structure	Reference Numeral
Lactic acid	LA	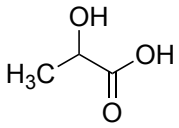	1a
Lactic acid dimer	L_2A	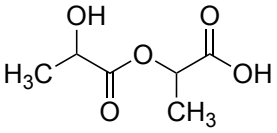	2a
Lactide	LD	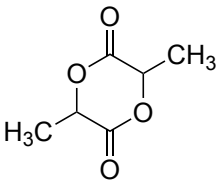	3a
Acetaldehyde	CH_3CHO	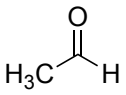	4a
5-methyl-1,3-dioxolan-4-one	Me-DOX	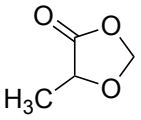	5a-1
2,5-dimethyl-1,3-dioxolan-4-one	Me_2-DOX	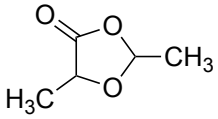	5a-2
2,2,5-trimethyl-1,3-dioxolan-4-one	Me_3-DOX	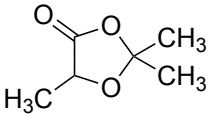	5a-3
Poly(lactic acid)	PLA	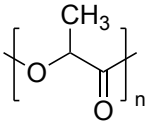	7a
Mandelic acid	MA	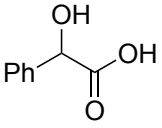	1b

Mandelic acid dimer	M_2A	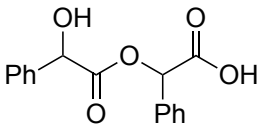	2b
Mandelide	MD	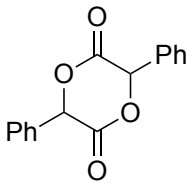	3b
Benzaldehyde	PhCHO	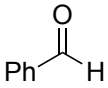	4b
5-phenyl-1,3-dioxolan-4-one	Ph-DOX	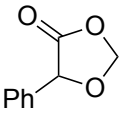	5b-1
2-methyl-5-phenyl-1,3-dioxolan-4-one	MePh-DOX	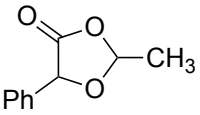	5b-2
2,2-dimethyl-5-phenyl-1,3-dioxolan-4-one	Me_2Ph-DOX	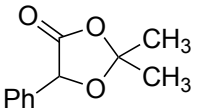	5b-3
2,5-diphenyl-1,3-dioxolan-4-one	diPh-DOX	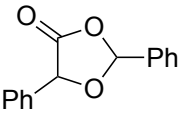	5b-4
2-tert-butyl-5-phenyl-1,3-dioxolan-4-one	^{t}BuPh-DOX	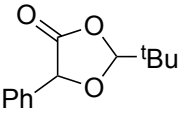	5b-5
Diarylactetic acid	DAA	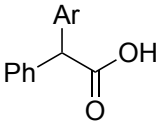	6b
Poly(mandelic acid)	PMA	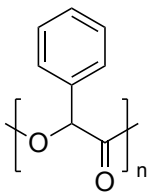	7b

Benzylic acid	BA	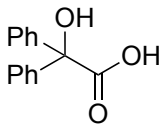	1c
Benzylide	BD	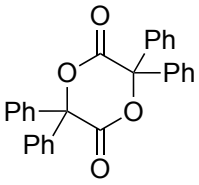	3c
Triarylacetic acid	TAA	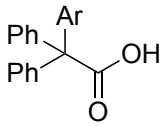	6c
Methylvinylglycolate	MVG	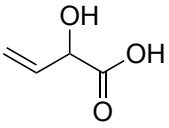	1d
Methylvinylglycolide	-	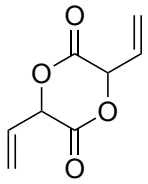	3d
Thiolactic acid	TLA	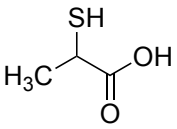	1e
Thiolactide	TD	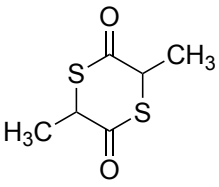	3e

2.3 Zeolite Modification

2.3.1 Ion-exchange

For alkali metal exchange, zeolite was added to centrifuge tube along with an aqueous solution of metal nitrate (various concentration, 1 g of zeolite per 100 mL solution). Ion exchange was carried out by placing centrifuge tubes of a tube roller for various times. After ion exchange, zeolites were washed with deionised water, dried overnight at 80 °C then calcined air at 550 °C (5 °C min^{-1} ramp rate) for 5 hours.

2.3.2 Base Leaching

H-Beta-75 zeolite was modified by base leaching to generate mesopores, based on a method reported in the literature[1] involving: (i) treating the zeolite with an alkaline solution in the presence of tetrapropylammonium bromide (TPABr); (ii) calcination to remove TPABr; (iii) ion exchange to obtain a Brønsted acid zeolite. This method was reproduced as follows: an aqueous solution (40 mL) containing NaOH (various concentrations from 0.05 to 0.3 M) and TPABr (0.2 M) was heated to 65 °C with stirring (500 rpm). Zeolite (1.32 g, approximately 33 g L^{-1}) was added and the temperature and stirring was maintained for 30 minutes. At the end of this time period, the flask was cooled with ice to quench. Next, the suspension was filtered to isolate the zeolite. The zeolite was then washed using distilled water until the filtrate measured pH 8. The zeolite was then dried overnight in an 80 °C oven followed by calcination in air in a muffle furnace at 150 °C for 1 hour (heating rate of 5 °C min^{-1}), then 550 °C for 6 hours (heating rate of 5 °C min^{-1}). The washed and calcined zeolites were exchanged into the ammonium form by three consecutive ion exchanges in 0.3 M NH_4NO_3. Ammonium-form were subsequently calcined again according to the same procedure as above to convert the NH_4 cation into a proton and obtain the protic form zeolite.

2.3.3 Washing and Centrifugation

Washing of modified zeolites (i.e. those modified by ion exchange or base leaching as described in 2.3.1 and 2.3.2, respectively) was achieved by suspending the zeolite in deionised water in 40 mL centrifuge tubes. The tubes were placed on a tube roller to ensure adequate washing. Zeolite was separated from the wash water by centrifugation on a Heraeus™ Megafuge™ from Thermo Scientific.

2.4 Mandelic Acid Conversion

2.4.1 Catalyst Testing - Batch

Zeolite catalyst testing reactions were carried out without the use of inert atmosphere techniques. For overnight catalyst screening tests (16-18 hours), a round bottom flask (100 mL) was charged with mandelic acid (0.5 g), 3 mol% H^+ (p-TSA) or 3 mol% Al (zeolites), solvent (50 mL) and a stirrer bar. For time-dependent conversion plots, a round bottom flask (50 mL) was charged with mandelic acid (0.2 g), 3 mol% (relative to mandelic acid) H^+ (in p-TSA) or 3 mol% (relative to mandelic acid) of Al (in zeolites), solvent (20 mL) and a stirrer bar was used (catalyst masses are given in Table S6). The flask was connected to a homemade phase separator with a water or air condenser above (Figure 1). This is a similar apparatus as used by Sels.[2] The inner part of the phase separator has an opening which allows solvent vapour to transfer from the

reaction flask to the reservoir (outer part of the phase separator). Prior to starting the reaction, the reservoir of the phase separator was pre-filled with the same solvent as was used for the reaction, to avoid a reduction in reaction volume upon reflux (due to transfer of solvent from the flask to the phase separator - the capacity of the phase separator was around 10-15 mL, compared to a solvent volume of around 20 mL in the reaction flask). The dimerisation of mandelic acid is a condensation reaction which generates water as a byproduct. Upon reflux, any water generated is removed (along with reaction solvent) from the reaction as a vapour (step 1 in the schematic diagram shown in Figure 1). Water separates from the organic solvent in the phase separator (due to the immiscibility of the two phases). Due to its higher density, water sinks to the bottom of the reservoir (step 2 in the schematic diagram shown in Figure 1) and cannot return to the reaction flask. The flask was contacted with a pre-heated hotplate set 20 °C above the solvent boiling point and stirred at 500 rpm. This was taken as time = 0.

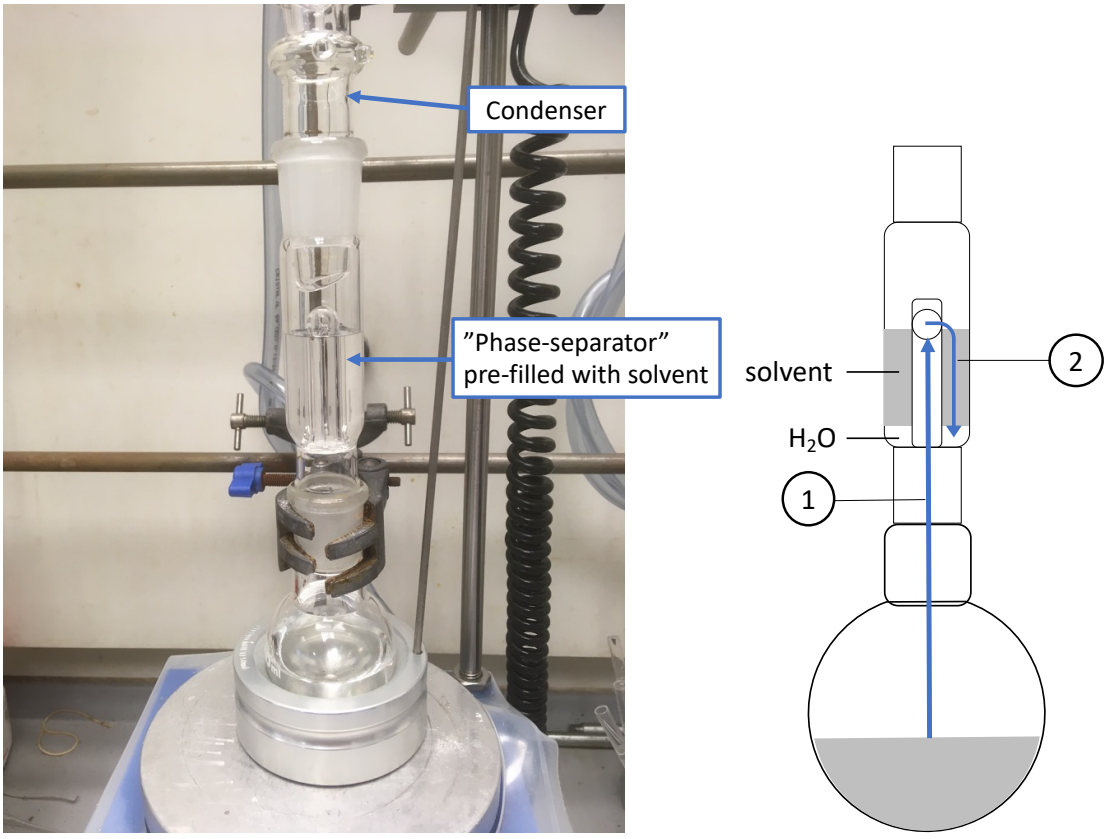

Figure 1 Reaction setup used for catalytic conversion of mandelic acid. A phase separator is used between the flask and condenser to remove water produced during the reaction. The phase separator is pre-filled with reaction solvent to avoid a reduction in the reaction volume upon reflux.

To analyse the product distribution, the reaction mixture was allowed to cool to room temperature (approximately 10 mins) and an equal volume of acetonitrile was added to

dissolve any insoluble species. The reaction mixture was then filtered by vacuum filtration (Buchner flask and filter paper or sinter funnel) to remove the zeolite and a small sample (*ca.* 1 mL) of the filtrate was taken forward for analysis. Solvent was removed *in vacuo* and the crude sample dissolved in $CDCl_3$ for analysis by ^1H NMR spectroscopy, to calculate the composition of products. For each compound, the methine proton (the proton alpha to the phenyl ring) was used as the diagnostic proton. The products and methine protons are shown in Table 2, along with their respective chemical shifts in $CDCl_3$. For NMR analysis, the integrals of resonances of all the known compounds in the ^1H NMR spectra were summed to nominally determine a total integral of "100%". This method has limitations, as it assumes that all products present in the product mixture have been assigned and integrated. Additionally, a carbon balance was not calculated, so the effects of adsorption of products within the zeolite were not accounted for. As such, the values of conversion and yield determined by this method are not absolute values. However, we believe that these results show the trends in catalytic activity between the different zeolites tested.

An additional NMR sample was also made by diluting a couple of drops of the filtrate with 1 mL $CDCl_3$. This sample was used to check for the presence of volatile benzaldehyde that would otherwise be removed by rotary evaporation. When benzaldehyde was present, this sample could be used to account for this in the final quantification by determining the relative integral of the benzaldehyde peak relative to the other known product peaks in the spectrum. This NMR sample (with protic reaction solvent present) was not suitable for analysis of all the product peaks, as the lower intensity resonance not resolvable above the baseline in this sample. Hence, a first sample with the protic solvent and benzaldehyde removed (rotary evaporation), and a second sample with protic solvent and benzaldehyde present, were used in conjunction for complete analysis.

For the conversion-time plots, individual reactions of different durations were carried out rather than sampling a single reaction over time. This was done to avoid issues associated with the poor solubility of some of the products at room temperature which would have adversely affected the selectivity calculations should products precipitate during sampling.

Table 2 Diagnostic protons and chemical shifts used for quantification.

Molecule and diagnostic proton used for analysis (red)	**^{1}H Chemical Shift in $CDCl_3$ / ppm**	**Further information**
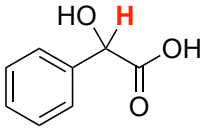	5.25	Racemic D,L-mandelic acid was used.
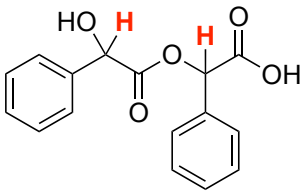	5.40, 5.96 (*D,L*) 5.33, 6.01 (*L,L*)	*D,L* and *L,L* assignment taken from the literature. Ref: [3]
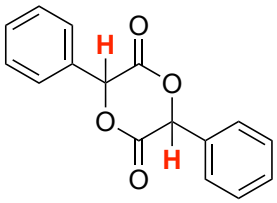	5.87 (*meso*-mandelide, *R,S* isomer) 6.13 (*rac*-mandelide, racemic mixture of *S,S* and *R,R* enantiomers)	*Meso* and *rac* assignment taken from the literature. Ref: [4] For further information on the synthesis of mandelide see also ref [5].
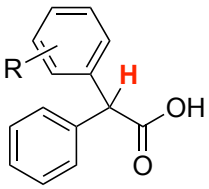	Various between around 5-5.25 ppm. The chemical shift of the methine proton (red) in diarylacetic acids is influenced by the nature of the aromatic ring substitutents.	More detail of the characterisation of these compounds is given in in the appendices.
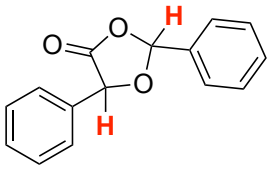	6.58, 5.43 (*cis*) 6.70, 5.53 (*trans*)	*Cis/trans* assignment taken from the literature. Ref: [6]
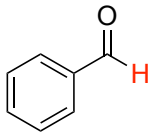	10.02	

2.4.2 Quantification Method and an Example Product Mixture Quantification

The method of quantification employed was based on the ^{1}H NMR method reported by Sels *et al.*[2] The amount of each compound was quantified in terms of the amount of mandelic acid incorporated into the products by integrating all of the methine resonances of mandelic acid (1b), mandelide linear dimer (2b), cyclic mandelide (3b), diarylacetic acid (6b), diphenyldioxolanone (5b-4) and the aldehyde resonance of benzaldehyde (4b). The quantity of each compound is then calculated by:

$$compound\ A\ (\%) = 100\%\ x\ \frac{sum\ of\ methine\ integrals\ for\ compound\ A}{sum\ of\ methine\ integrals\ and\ benzaldehyde\ aldehyde\ integral}$$

$$benzaldehyde\ (\%) = 100\%\ x\ \frac{benzaldehyde\ aldehyde\ integral}{sum\ of\ methine\ integrals\ and\ benzaldehyde\ aldehyde\ integral}$$

From this, the terms conversion and selectivity as used in this thesis were defined as:

$$conversion\ (\%) = 100\% - mandelic\ acid\ (\%)$$

$$selectivity\ compound\ A\ (\%) = 100\%\ x\ \frac{compound\ A\ (\%)}{conversion\ (\%)}$$

The reproducibility of catalytic tests was evaluated by 3-fold repetition of a test run with the following reaction conditions: mandelic acid (0.2 g), 3 mol% Al (H-Beta-75), mixed xylenes (20 ml), 1 hour of reaction time. The deviation of the arithmetic mean of obtained conversion and selectivity results was below 3%, as shown in Table 3 below.

Table 3 Individual conversion and selectivity data used to determine the standard deviation of catalytic tests. All values given as %.

	Conversion	**2b**	**3b**	**6b**	**5b-4**	**4b**
Run 1	45	21	24	27	10	15
Run 2	44	20	21	28	9	19
Run 3	48	24	24	26	8	17
Mean	45	21	23	27	9	17
Standard Deviation	2	2	2	1	1	2

2.4.3 Catalyst Testing – Flow

Flow reactions were carried out in a ThalesNano X-Cube flow reactor (Figure 2a). The flow reactor can operate at temperatures up to 200 °C, flow rates of 0.1-3.0 mL min^{-1} and pressure up to 150 bar. The feed solution containing the reagents can be introduced via HPLC pumps (see Figure 2c - 1 or 2 pumps can be used depending on the nature of the reaction). The reactor has a touch screen interface which allows pressure, flow rate and temperature to be adjusted manually to allow screening of different reaction conditions. Zeolites were pressed and sieved to 60-80 mesh and 300 mg was packed into a CatCart catalyst bed along with 200 mg and 100 mg of silicon carbide as shown in Figure 2b. Feed solutions were prepared by dissolving mandelic acid in MeCN (1 g per 100 mL MeCN) and delivered into the flow reactor via a single HPLC pump. ^{1}H NMR spectroscopy analysis of the products was conducted as described in section 2.4.1.

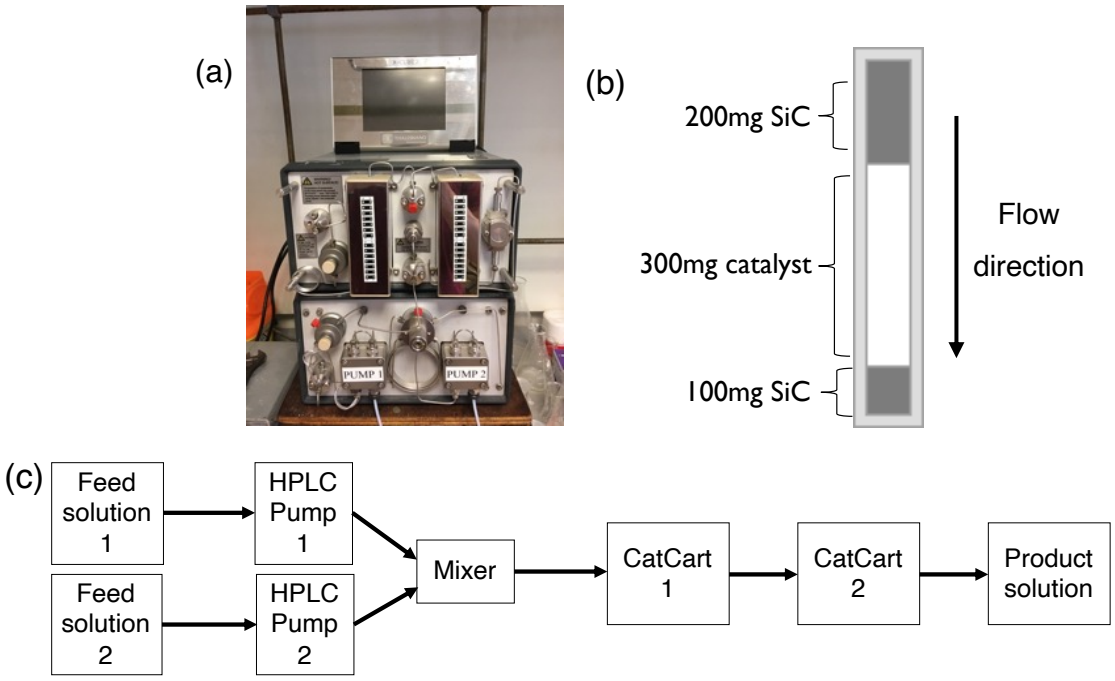

Figure 2 (a) X-Cube flow reactor. (b) Loading of the catalyst cartridge ("CatCart") used in these experiments. (c) Flow diagram summarising the process of the X-Cube flow reactor.

2.5 1,3-Dioxolan-4-one Synthesis

2.5.1 Catalyst Testing – Batch

Zeolite catalyst testing reactions were carried out without the use of inert atmosphere techniques. A round bottom flask (50 mL) was charged with mandelic acid (various amounts), 10 mol% H+ (p-TSA) or 2.5-10 mol% Al (zeolites), cyclohexane (10 mL, solvent), a stirrer bar and either paraformaldehyde or paraldehyde (various amounts). The flask was connected to a homemade phase separator with a water or air condenser

(Figure 1). The flask was contacted with a pre-heated hotplate set 20 °C above the solvent boiling point and stirred at 500 rpm. This was taken as time = 0.

2.5.2 Catalyst Testing – Flow

Catalyst testing in a flow reactor (Thales Nano X-Cube) was carried out using the same reaction set up as described in section 2.4.3. In the case of 1,3-dioxolan-4-one synthesis, the feed additionally contained carbonyl compound or a carbonyl source (Figure 3) selected from: trioxane (source of formaldehyde), paraldehyde (source of acetaldehyde) or acetone. Feed solutions were made by dissolving mandelic acid in MeCN (4 g per 100 mL MeCN) and trioxane, paraldehyde or acetone (various amounts depending on desired stoichiometry). Mesitylene was added as an internal standard (0.8 g per 100 mL MeCN).

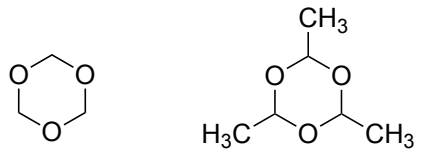

trioxane paraldehyde

Figure 3 Structure of carbonyl sources trioxane and paraldehyde.

A small sample (*ca.* 1-2 mL) of eluent from the flow reactor was taken for each data point in the analysis. Approximately 1-2 drops of this crude sample was taken and diluted in $CDCl_3$ for analysis by ^1H NMR spectroscopy, to calculate the composition of products.

To analyse the product distribution, the reaction mixture was allowed to cool to room temperature (approximately 10 mins) and an equal volume of acetone was added to dissolve any insoluble species. The reaction mixture was then filtered by vacuum filtration (Buchner flask and filter paper or sinter funnel) to remove the zeolite and a small sample (*ca.* 1 mL) of the filtrate was taken forward for analysis. Solvent was removed *in vacuo* and the crude sample dissolved in $CDCl_3$ for analysis by ^1H NMR spectroscopy, to calculate the relative concentration of mandelic acid and dioxolanone products. As described in 2.4.1 above, the integral of the resonance of the methine proton in the ^1H NMR spectra was used for quantification. The chemical shifts of these methine protons are listed in Table 4, along with the chemical shifts of mesitylene used as an internal standard in flow.

Table 4 Diagnostic protons and chemical shifts used for quantification in 1,3-dioxolan-4-one synthesis.

Molecule and diagnostic proton used for analysis (red)	**^{1}H Chemical Shift in $CDCl_3$ / ppm**	**Further information**
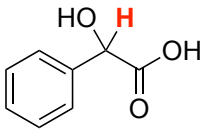	5.25	Racemic D,L-mandelic acid was used.
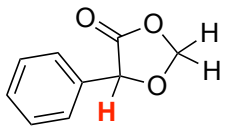	5.23	Ref for full NMR assignment: [7]
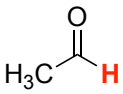	9.79	
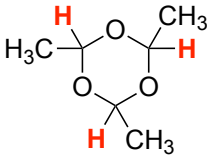	4.92	
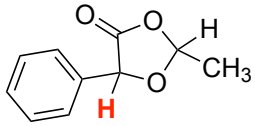	5.43 (*cis*), 5.25 (*trans*)	Ref for cis/trans assignment: [18]
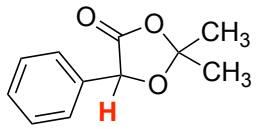	5.42	Ref for full NMR assignment: [7]
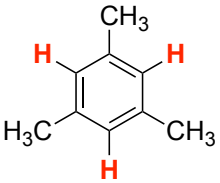	6.78	

2.5.3 Scaled Up Synthesis and Purification

2-methyl-5-phenyl-1,3-dioxolan-4-one (MePhDOX, 5b-2) was synthesised using the same reaction set up as described in section 2.4.1. Mandelic acid (8 g, 53 mmol), paraldehyde (15 g, 114 mmol) were added to cyclohexane (200 mL) in a 500 mL round

bottom flask. Zeolite H-Y-30 (2 g) was added, a phase separator and condenser were fitted (as in Figure 1) and the mixture was heated at reflux for 6 hours. The reaction mixture was allowed to cool to room temperature and washed with aqueous sodium bicarbonate (10%, 3 x 200 mL), water (3 x 200 mL) and aqueous sodium chloride (saturated, 3 x 200 mL). The organic layer was dried with magnesium sulphate and the solvent removed *in vacuo*. The crude 5b-2 was further purified by stirring over calcium hydride for approximately 16 hours followed by vacuum distillation to give a clear, colourless oil. Yield: 3.87 g, 42%. The flask containing distilled 5b-2 was sealed under vacuum and transferred to a glovebox for further use. The product was obtained as a 1:1 mixture (by NMR integration) of *cis* and *trans* isomers (according to the literature assignment[18]) and the NMR spectra were in accordance with the literature.[18]

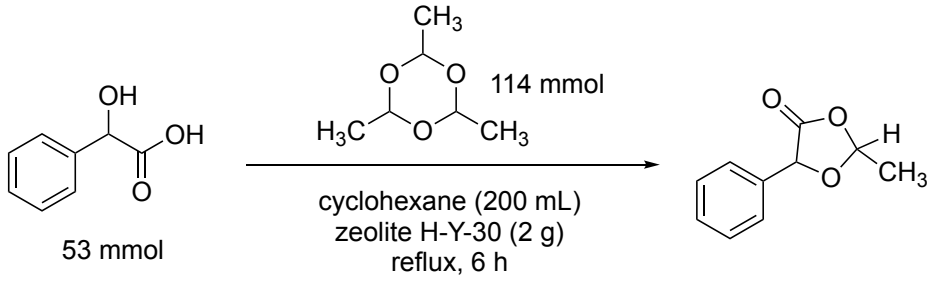

Scheme 1 Synthesis of PhMeDOX (5b-2).

^{1}H NMR (400 MHz, $CDCl_3$) δ 7.50-7.34 (m, 10H, Ar), 5.92 (qd, J = 5.0, 0.9 Hz, 1H, OC*H*CH_3 *cis*), 5.83 (qd, J = 5.0 Hz, 1.2 Hz, 1H, OC*H*CH_3 *trans*), 5.43 (d, J = 0.9 Hz, 1H, ArC*H cis*), 5.25 (d, J = 1.1 Hz, 1H, ArC*H trans*), 1.70 (d, J = 5.0 Hz, 3H, OCHC*H*$_3$ *trans*), 1.64 (d, J = 5.0 Hz, 3H, OCHC*H*$_3$ *cis*). ^{13}C NMR (100 MHz, $CDCl_3$) δ 171.83, 171.64, 133.71, 133.39, 129.36, 129.10, 129.08, 128.90, 126.98, 126.00, 103.02, 102.07, 20.88, 20.65.

^{1}H NMR (400 MHz, toluene-d8) δ 7.32-7.27 (m, 4H), 7.13-7.01 (m, 6H) 5.23 (qd, *J* = 5, 0.8 Hz, 1H), 5.07 (qd, *J* = 5.0, 1.1, 1H), 4.91 (q, J = 0.8 Hz, 1H), 4.54 (q, *J* = 0.8 Hz, 1H), 1.16 (d, *J* = 5.0 Hz, 3H), 1.09 (d, *J* = 5.0 Hz, 3H). ^{13}C NMR (100 MHz, toluene-d8) δ 170.89, 170.82, 134.58, 134.19, 133.52, 130.40, 128.91, 128.77, 128.66, 128.61, 128.19, 127.71, 127.02, 126.12, 125.34, 124.86, 102.35, 101.25, 76.67, 75.18.

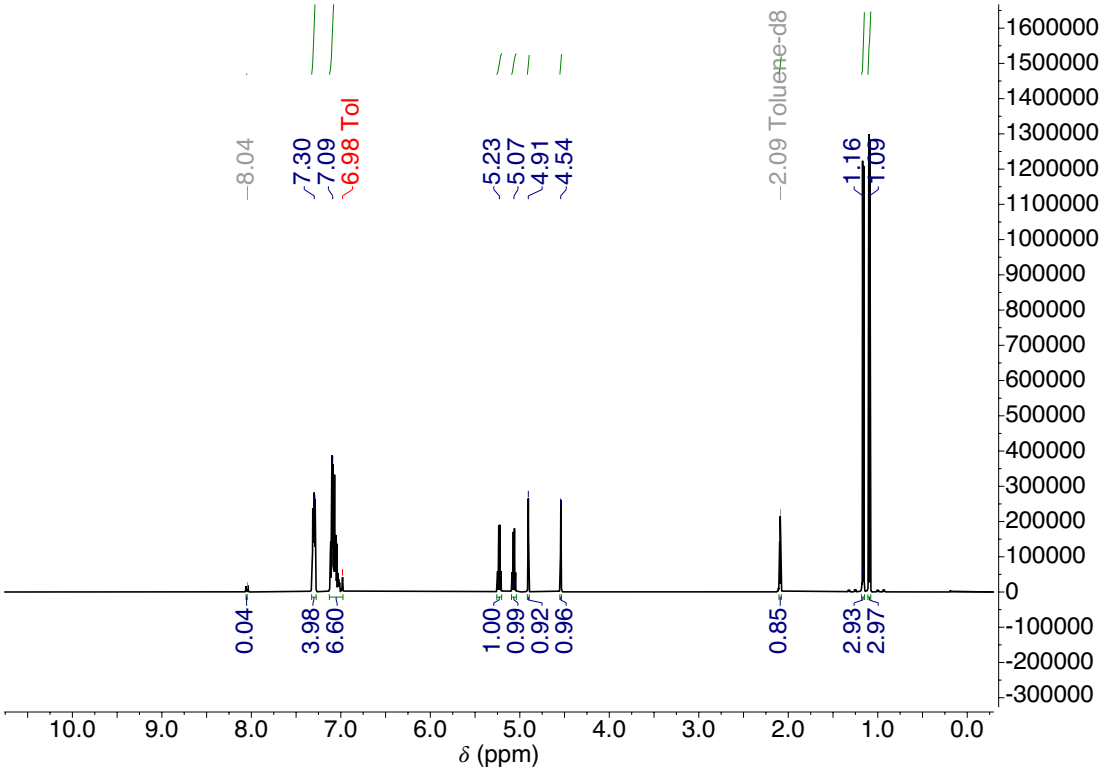

Figure 4 ^{1}H NMR (400 MHz, toluene-d8) spectrum of the mixture of *cis* and *trans* PhMeDOX (5b-2) after vacuum distillation.

2.6 Ring Opening Polymerisation (ROP) of 1,3-dioxolanones (DOX)

2.6.1 Al(salen) synthesis

The Al(salen) catalyst used in this work was synthesised according to a slightly modified literature procedure.[8, 9]

Synthesis of salen ligand 1,3-diamino-N,N'-bis(3,5-di-tert-butylsalicylidene)-2,2-dimethylpropane (Scheme 2): 2,2-dimethyl-1,3-propane diamine (0.54 g, 5.29 mmol) was added rapidly to a stirring solution of 3,5-ditert-butylsalicaldehyde (2.34 g, 9.97 mmol) in ethanol (25 mL). After refluxing for 5 hours at 78 °C, the precipitated solid was filtered, washed with cold methanol and dried under vacuum. Yield: 2.42 g, 4.21 mmol, 80%.

NMR spectra were in accordance with the literature.[9]

^{1}H NMR (400 MHz, $CDCl_3$) δ 13.87 (s, 2H, ArO*H*), 8.37 (s, 2H, ArC*H*N), 7.39 (d, J = 2.4 Hz, 2H, Ar*H*), 7.11 (d, J = 2.4 Hz, 2H, Ar*H*), 3.48 (s, 4H, $CH_2CMe_2CH_2$), 1.47 (s, 18H, $ArC(CH_3)_3$), 1.31 (s, 18H; $ArC(CH_3)_3$), 1.10 (s, 6H, $CH_2C(CH_3)_2CH_2$). ^{13}C NMR (100 MHz, $CDCl_3$) δ 166.89, 158.33, 140.12, 136.79, 127.04, 126.07, 118.0 (Ar and Ar*C*HN), 68.41 ($CH_2CMe_2CH_2$), 36.48 ($CH_2CMe_2CH_2$), 35.21, 34.28 ($C(CH_3)_3$), 31.65, 29.57 ($C(CH_3)_3$), 24.57 ppm ($CH_2C(CH_3)_2CH_2$).

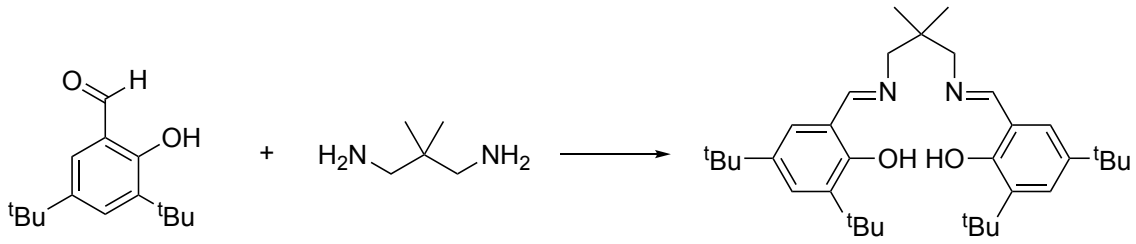

Scheme 2 Synthesis of salen ligand.

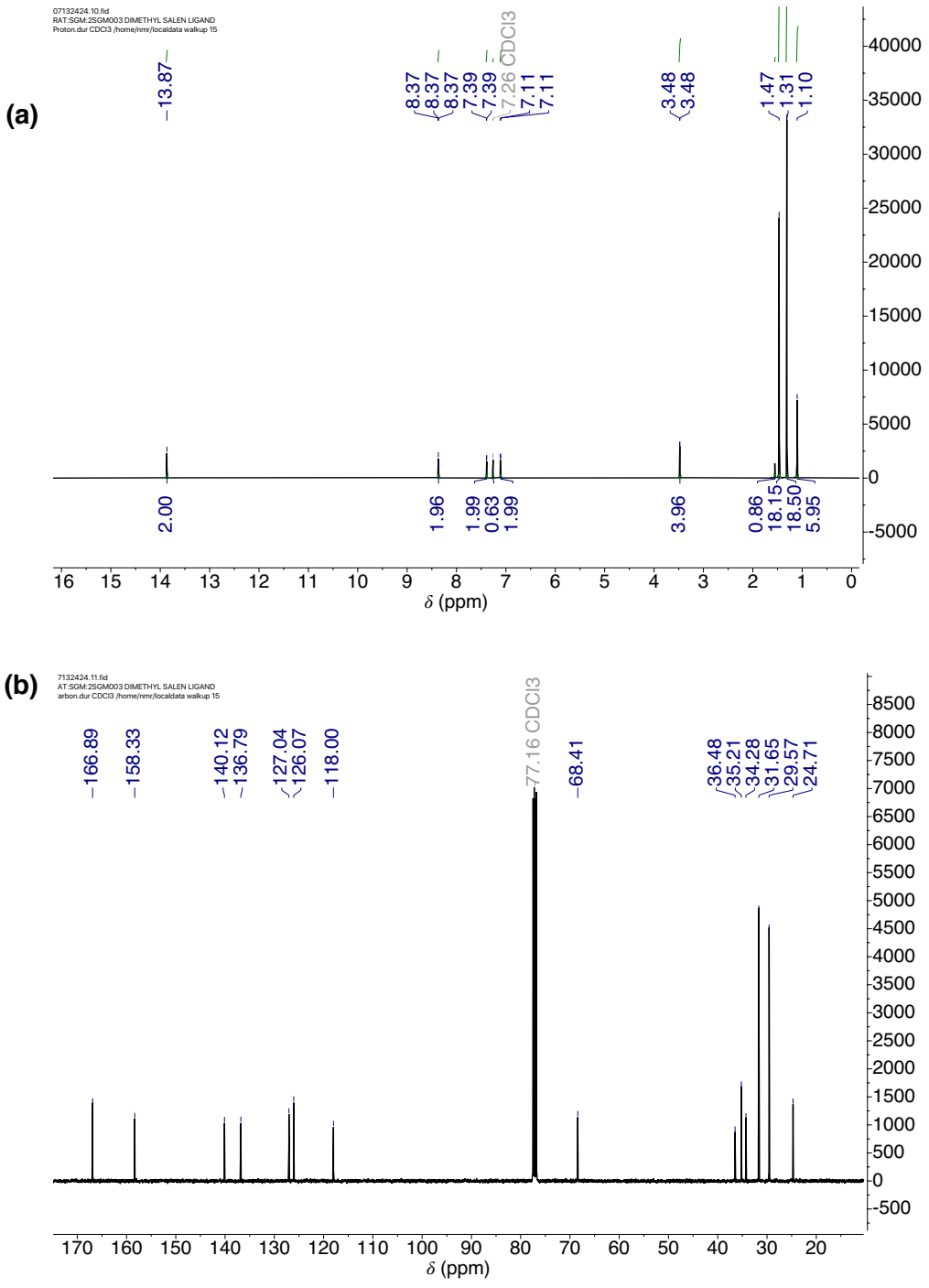

Figure 5 (a) ^{1}H (400 MHz, $CDCl_3$) and (b) ^{13}C (100 MHz, $CDCl_3$) NMR spectra of 1,3-diamino-*N,N'*-bis(3,5-di-tert-butylsalicylidene)-2,2-dimethylpropane.

Synthesis of Al(salen) (Scheme 3): To a stirring solution of salen ligand (0.75 g) in toluene (15 mL) was added (slowly) a solution of $AlMe_3$ in toluene (2.0 M, 0.70 mL). After the solution had stopped bubbling, the reaction was heated to reflux overnight under N_2. The reaction was allowed to cool to room temperature and Al(salen) precipitated as a yellow crystalline solid. Solvent was removed via cannula and the solid allowed to dry overnight under vacuum. The flask was sealed under vacuum and transferred to a glovebox for further use. NMR spectra were in accordance with the literature.[8, 10]

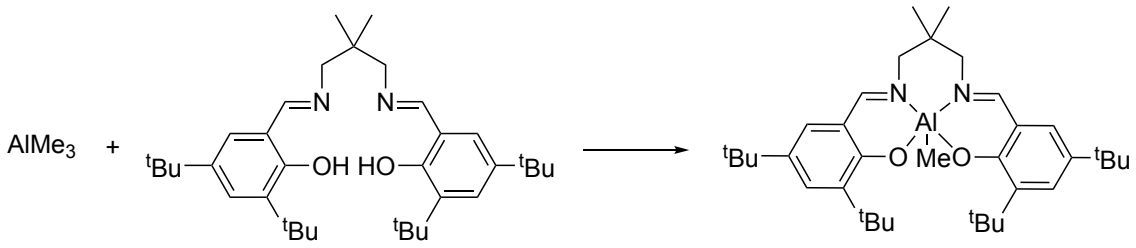

Scheme 3 Synthesis of Al(salen) catalyst.

^{1}H NMR (400 MHz, toluene-d8) δ 7.71 (d, J = 2.7 Hz, 2H, Ar), 7.55 (s, 2H, NC*H*) 7.52 (s, 2H, Ar), 7.00 (d, J = 2.6 Hz, 2H, Ar), 2.92 (dd, J = 12.1, 1.0 Hz, 2H, CH_2), 2.67 (m, 2H, CH_2), 1.78 (s, 19H, (CH_3)$_3$), 1.35 (s, 19H, (CH_3)$_3$), 0.63 (s, 3H, (CH_3)$_2$), 0.47 (s, 3H, (CH_3)$_2$), -0.57 (s, 3H, AlCH_3). ^{13}C NMR (100 MHz, toluene-d8) δ 170.08, 164.11, 141.54, 137.55, 130.50, 127.30, 119.02, 67.07, 36.01, 35.82, 34.16, 31.64, 30.11, 25.49, 25.01.

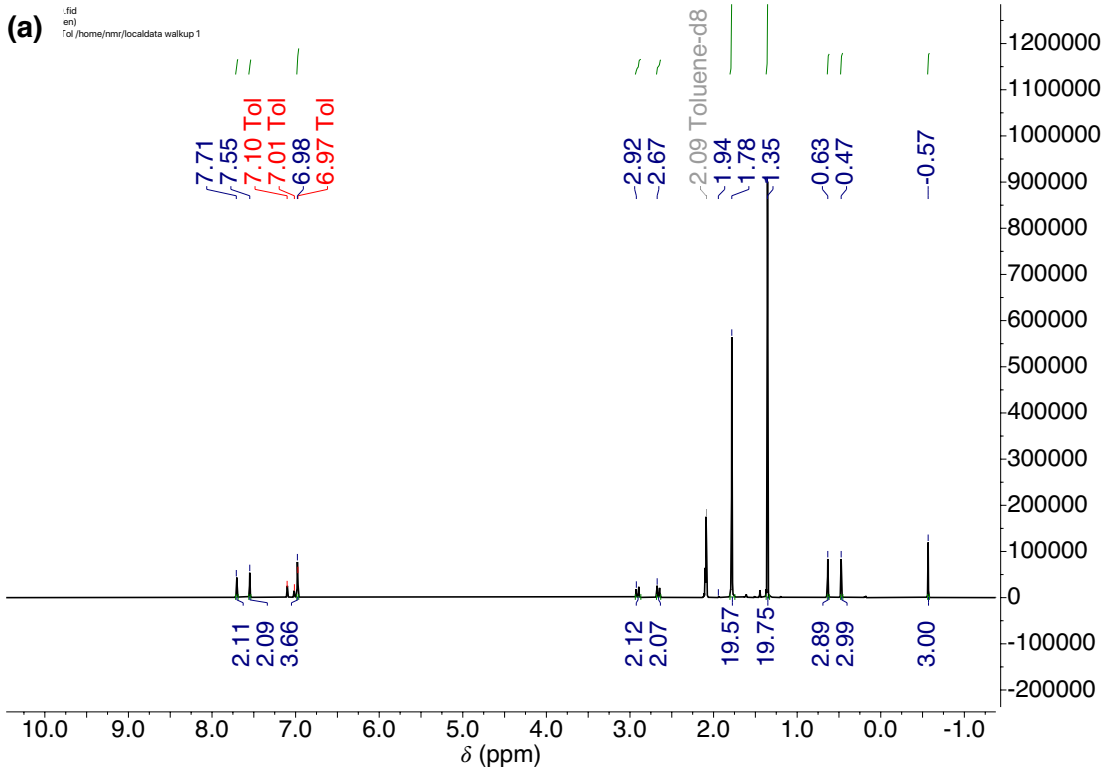

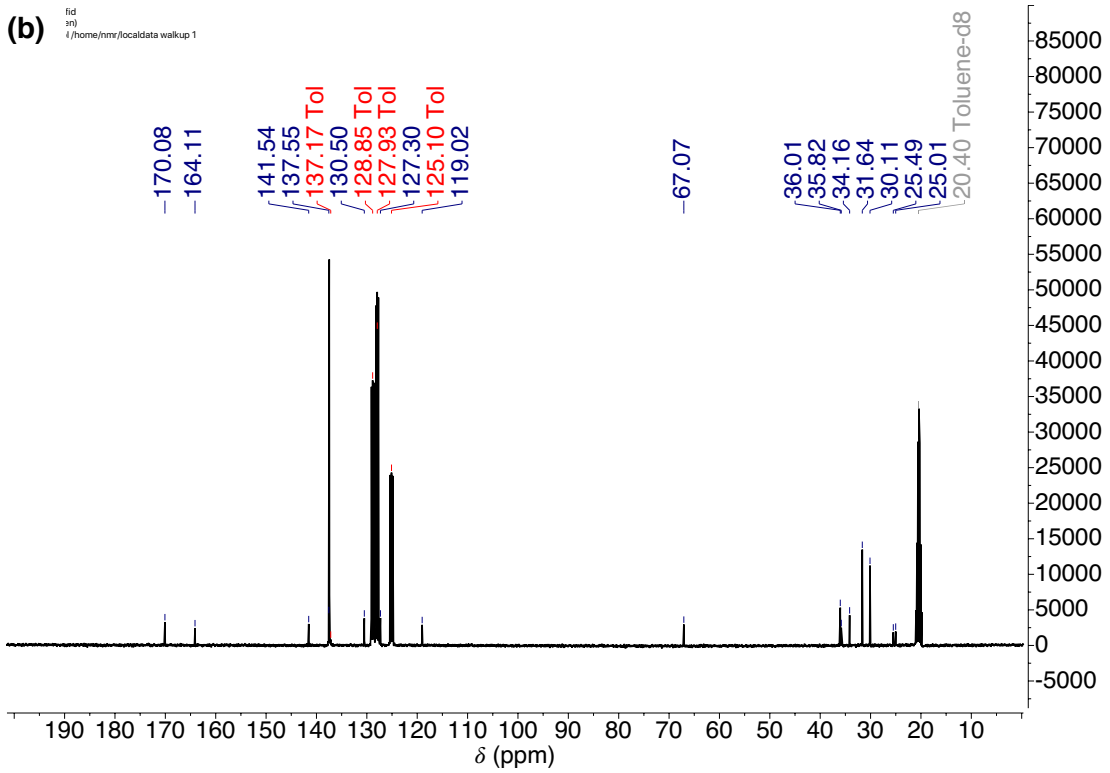

Figure 6 (a) ^{1}H (400 MHz, $CDCl_3$) and (b) ^{13}C (100 MHz, $CDCl_3$) NMR spectra of aluminium salen catalyst (Scheme 2).

2.6.2 Solvent-Free ROP

In a glovebox, the catalyst, initiator and monomer were added to a Schlenk flask in the desired ratio. The flask was sealed and removed from the glovebox and immediately submerged in a pre-heated oil bath - this was taken as time = 0. At the end of the reaction, the flask was removed from the oil bath and quenched with methanol (3–4 drops). A sample was taken and the conversion quantified by ^{1}H NMR spectroscopy ($CDCl_3$).

2.6.3 Solution Phase ROP

In a glovebox, the catalyst, initiator, monomer and toluene were added to a jacketed Schlenk flask (Figure 7) in the desired ratio. The flask was sealed and removed from the glovebox. The flask was connected via the Young's tap to a Schlenk line and the jacket of the flask was connected to a water supply for continuous cooling. The flask was submerged in a pre-heated oil bath - this was taken at time = 0. The oil bath was set to 130 °C to reflux toluene and the reaction was carried out under flowing nitrogen gas. At the end of the reaction, the flask was removed from the oil bath and quenched with methanol (3–4 drops). A sample was taken and the conversion quantified by ^{1}H NMR spectroscopy ($CDCl_3$).

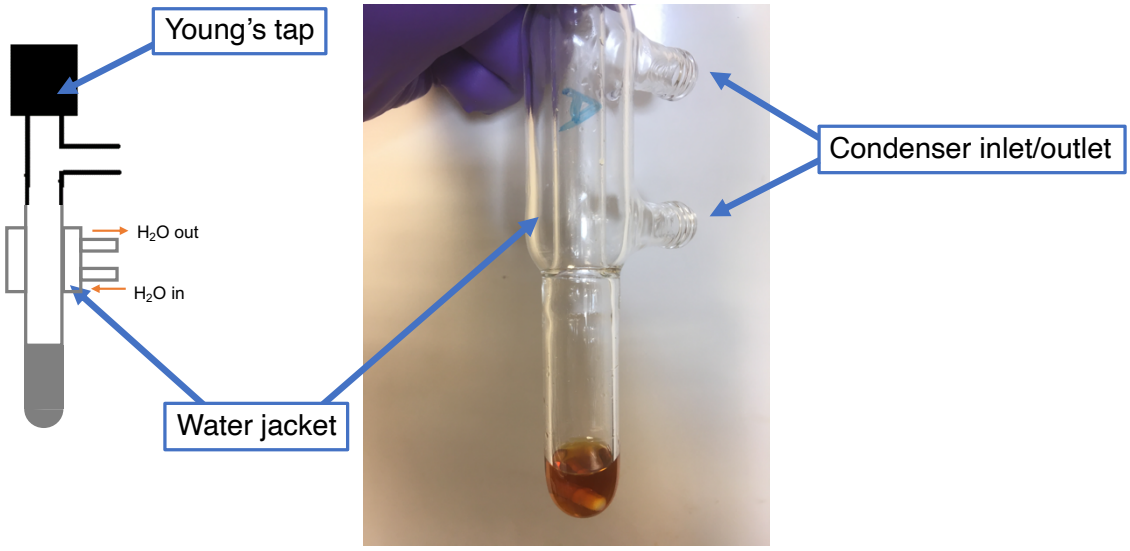

Figure 7 Flask used for ring opening polymerisation of MePhDOX.

2.7 Characterisation

2.7.1 Analysis of Zeolites

Elemental microanalyses of carbon, hydrogen and nitrogen (CHN) content of zeolites were obtained on an Exeter Analytical Inc. E-440 elemental analyser using a dynamic flash combustion method.

Zeolite Si/Al ratios and degree of ion exchange were determined using energy dispersive X-ray fluorescence (ED-XRF). EDXRF measurements were performed using a Malvern Panalytical Epsilon 1 ED-XRF with a 50 kV silver anode X-ray tube. Zeolite powders were pressed into discs in a sample cup containing a polypropylene film. The results are reported as an average of 3 measurements of the same sample.

Powder X-Ray Diffraction (pXRD) diffractograms were collected on a Bruker D8 Avance X-ray diffractometer using a step of 0.02 ° over a range of 2θ = 5–70 °. A knife edge was utilised for low angle scattering. Samples were mounted onto glass or silicon slide holders and rotated during data acquisition.

2.7.2 Solution-state NMR Spectroscopy

Solution-state ^{1}H and ^{13}C NMR spectra were recorded Bruker Avance III-HD-400 or Bruker Neo-400 spectrometers. Chemical shifts are reported in ppm using the residual solvent signal as an internal reference. All NMR spectra were manipulated using MestReNova software.

2.7.3 Liquid Chromatography-Mass Spectrometry (LC-MS)

Samples for electron ionisation (EI) tandem liquid chromatography mass spectra (LC-MS) were prepared by dissolution in acetonitrile at ~1mg mL^{-1} and submitted via mass

spectrometry service. Samples were separated on an Acquity UPLC BEH C18 column (1. 7μm, 2.1mm x 50mm) using acetonitrile/water gradient. Mass spectra were recorded on Waters triple quadrupole mass spectrometer, using electrospray ionisation.

2.8 Critical Diameter Calculations

Approximations of the size of some of the key molecules were modelled using an approach that has been successfully reported recently.[11, 12] Molecular sizes were approximated by first carrying out an energy minimisation at the B3LYP level using Scigress[13] then transferred into the VMD visualisation program. The energy minimised molecules were rotated to find and calculate the minimum projection area using the separation between the two furthest atoms (from van der Waal's radii).

2.9 References

1. Verboekend, D.; Vile, G.; Perez-Ramirez, J., Mesopore Formation in USY and Beta Zeolites by Base Leaching: Selection Criteria and Optimization of Pore-Directing Agents. *Cryst. Growth Des.* **2012,** *12* (6), 3123-3132.

2. Dusselier, M.; Van Wouwe, P.; Dewaele, A.; Jacobs, P. A.; Sels, B. F., Shape-selective zeolite catalysis for bioplastics production. *Science* **2015,** *349*, 78-80.

3. Kuisle, O.; Quiñoá, E.; Riguera, R., A General Methodology for Automated Solid-Phase Synthesis of Depsides and Depsipeptides. Preparation of a Valinomycin Analogue. *J. Org. Chem.* **1999,** *64* (22), 8063-8075.

4. Graulus, G. J.; Van Herck, N.; Van Hecke, K.; Van Driessche, G.; Devreese, B.; Thienpont, H.; Ottevaere, H.; Van Vlierberghe, S.; Dubruel, P., Ring opening copolymerisation of lactide and mandelide for the development of environmentally degradable polyesters with controllable glass transition temperatures. *React. Funct. Polym.* **2018,** *128*, 16-23.

5. Liu, T. Q.; Simmons, T. L.; Bohnsack, D. A.; Mackay, M. E.; Smith, M. R.; Baker, G. L., Synthesis of polymandelide: A degradable polylactide derivative with polystyrene-like properties. *Macromol.* **2007,** *40* (17), 6040-6047.

6. Shcherbinin, V. A.; Konshin, V. V., Convenient synthesis of O-functionalized mandelic acids via Lewis acid mediated transformation of 1,3-dioxolan-4-ones. *Tetrahedron* **2019,** *75* (26), 3570-3578.

7. Cairns, S. A.; Schultheiss, A.; Shaver, M. P., A broad scope of aliphatic polyesters prepared by elimination of small molecules from sustainable 1,3-dioxolan-4-ones. *Polym. Chem.* **2017,** *8* (19), 2990-2996.

8. Hormnirun, P.; Marshall, E. L.; Gibson, V. C.; Pugh, R. I.; White, A. J., Study of ligand substituent effects on the rate and stereoselectivity of lactide polymerization using aluminum salen-type initiators. *Proc. Natl. Acad. Sci. U S A* **2006,** *103* (42), 15343-8.

9. Nomura, N.; Ishii, R.; Yamamoto, Y.; Kondo, T., Stereoselective ring-opening polymerization of a racemic lactide by using achiral salen- and homosalen-aluminum complexes. *Chemistry* **2007,** *13* (16), 4433-51.

10. Cairns, S. Ring-Opening Polymerisation of 1,3-Dioxolan-4-ones. Ph.D. Thesis, University of Edinburgh, 2018.

11. Keller, T. C.; Isabettini, S.; Verboekend, D.; Rodrigues, E. G.; Pérez-Ramírez, J., Hierarchical high-silica zeolites as superior base catalysts. *Chem. Sci.* **2014,** *5* (2), 677-684.

12. Hendriks, F. C.; Valencia, D.; Bruijnincx, P. C. A.; Weckhuysen, B. M., Zeolite molecular accessibility and host–guest interactions studied by adsorption of organic probes of tunable size. *Phys. Chem. Chem. Phys.* **2017,** *19* (3), 1857-1867.

13. Fujitsu: Integrated Platform for Computational Chemistry SCIGRESS. https://www.fujitsu.com/global/solutions/business-technology/tc/sol/scigress/.

Chapter 3: Conversion of Mandelic Acid over Brønsted Acidic Zeolite Catalysts

3.1 Introduction

As discussed earlier, the conversion of lactic acid (1a) by zeolites is not limited to esterification chemistry. The formation of acetaldehyde (4a) is also possible under similar conditions as those used for lactide (3a) synthesis.[1] Dehydration of lactic acid to produce acrylic acid is also well known, albeit usually conducted at higher temperature and using alkali-exchanged rather than Brønsted acidic zeolites.[2-5] The process is more challenging for AHA substrates with greater functionality, such as methylvinylglycolate (MVG, 1d)[6] or different reactive groups, such as thiolactic acid (1e).[7] In addition, the conversion of benzylic acid (1c) over heterogeneous catalysts was found to give rise to a range of different products, with the product distribution highly dependent on catalyst selection.[8]

Sels and Dusselier found that lactide can be produced in high yield using zeolite catalysts.[6] Figure 1 shows the data from their catalyst screening. The only products identified under these conditions were lactide and linear oligomers (L_nA). The product distributions shown were calculated based on relative integrals in the ^{1}H-NMR spectra of the crude products and the number average oligomer length was determined by end group analysis (integration of the centre lactyl units relative to the end groups in lactic acid oligomers[9]).

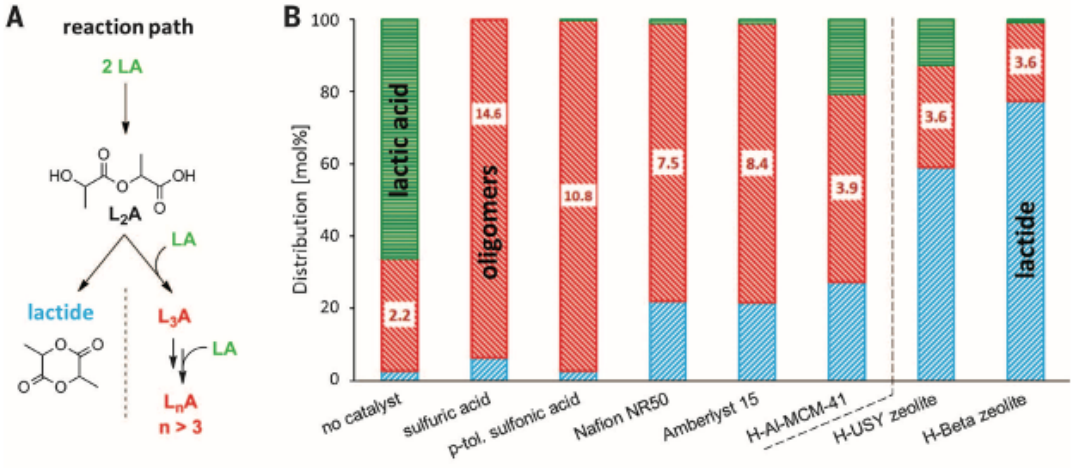

Figure 1 (A) Reaction pathways for the shape-selective reaction of lactic acid to lactide. (B) Product distribution after reaction with selected catalysts (0.565 mmol H^+, 6 mol% wrt. lactic acid, e.g., 0.5 g for H-Beta zeolite Si/Al = 12.5) on 1.67 g of aqueous L-LA (50 wt %) in 10 ml of toluene refluxed for 3 hours with water removal. Product [oligomers (red) and lactide (blue)] and reagent [LA (green)] distribution based on ^{1}H-NMR yields. Labels indicate the number-average length of the oligomer fraction (L_nA, with $n \geq 2$). Reproduced with permission from Dusselier, M.; Van Wouwe, P.; Dewaele, A.; Jacobs, P. A.; Sels, B. F., *Science*, 2015, 349, 78-80.

The previously reported syntheses of mandelide (3b) [10, 11] use similar conditions as the catalytic reactions to produce lactide (3a) shown in Figure 1. Both use Brønsted acid catalysts, organic solvents such as toluene and xylene, and reflux with azeotropic water removal. As shown in Figure 1, *p*-TSA has a tendency to produce lactic acid oligomers. *p*-TSA has also been used as a catalyst in the synthesis of oligomers of mandelic acid.[12] Compared with oligomer synthesis, the reported syntheses of cyclic dimer mandelide use a lower mandelic acid concentration. This favours dimerisation over oligomerisation. Scheme 1 shows the conditions used and the reported mandelide yields (reported as mass yields after purification). As discussed in the introduction to this thesis, mandelide forms as a mix of *meso*- and *rac*-mandelide. *rac*-Mandelide (*r*-3b) was recovered by filtration (it precipitates on cooling of the reaction mixture) and *meso*-mandelide (*m*-3b) was recovered by organic-aqueous extraction. This purification would remove any unreacted mandelic acid and oligomers of mandelic acid present in the crude products. As this work in the literature was focussed on polymerisation of mandelide, analysis of the byproducts of the monomer synthesis was not reported. The reported yields suggest that almost half of the mandelic acid added would have been either unreacted or converted to byproducts.

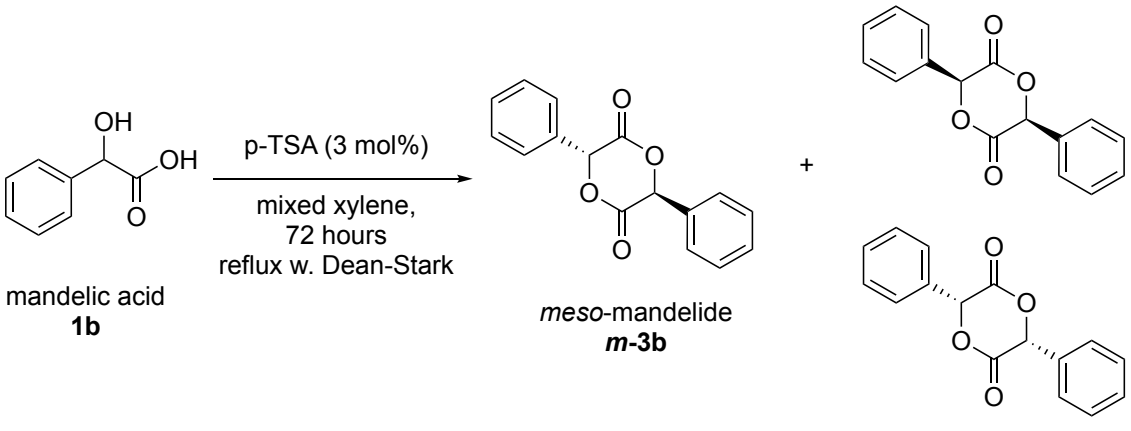

mandelic acid
1b

meso-mandelide
***m*-3b**

rac-mandelide
***r*-3b**

Ref	mandelide yield / %	*meso* yield / %	*rac* yield / %
[9]	53	24	28
[10]	57	25	32

Scheme 1 Reported syntheses of mandelide (3b). Yields were reported as mass of isolated products after work up and recrystallisation.

It is known from the reported syntheses of mandelide that the ^{1}H NMR chemical shifts corresponding to the methine proton of *rac*-mandelide, *meso*-mandelide, mandelic acid oligomers and mandelic acid (shown in Table 1) are well resolved. As a result, we

believed that we could conduct a screening of different zeolite catalysts to synthesise mandelide and quantify the products using ^{1}H NMR spectroscopy, in a similar manner for lactide synthesis as reported by Sels and Dusselier.[6]

Table 1 Chemical shifts of reactants, intermediates and products in poly(mandelide) synthesis.[10, 11]

Compound	Chemical shift (400 MHz, $CDCl_3$) / ppm
mandelic acid (1b)	5.25
meso-mandelide (*m*-3b)	5.87
rac-mandelide (*r*-3b)	6.13
oligo-/poly(mandelide)	6.00

The reaction of mandelic acid over heterogeneous catalysts (including zeolites) has not been reported in the literature. Conversion of the structurally similar benzylic acid (1c) was reported over Amberlyst-15 and zeolite H-Beta (Si/Al = 12).[8] The reactions were carried out at reflux in several aromatic solvents: toluene (110 °C), chlorobenzene (130 °C), p-chlorotoluene (150 °C) and o-dichlorobenzene (180 °C). A range of products were observed, dependent on catalyst and solvent used. These products included the cyclic ester dimer of benzylic acid, benzilide (3c), and the product of the reaction of benzylic acid and the aromatic solvent, triarylacetic acids (6c) (Scheme 2). Some products, including 6c, were proposed to form via a carbocation intermediate resulting from dehydration of the alpha-hydroxyl group of 1c. The formation of this carbocation was proposed to occur due to the electronic stabilisation through conjugation to the pi-systems of the adjacent aromatic rings, but the existence of a carbocation was not confirmed by any analysis. The authors also suggested that the presence of the bulky aromatic rings would make 3c and 6c too large to be accommodated within the zeolite micropores, and that these reactions may occur on external rather than internal acid sites. The reported selectivity data for 3c and 6c is shown in Table 2. Selectivity towards these products was highest for the non-zeolite catalysts Amberlyst-15 and Filtrol.

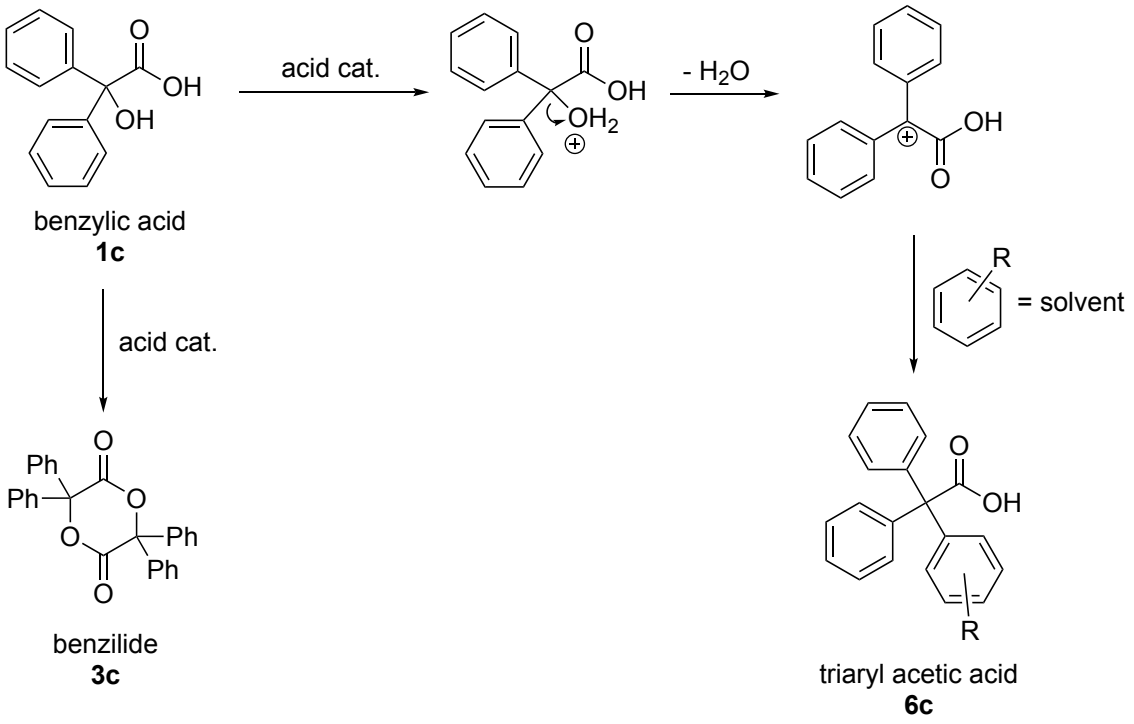

Scheme 2 Formation of triaryl acetic acids (6c) catalysed by H-Beta zeolite and benzilide (3c) catalysed by Amberlyst-15.[8] Triaryl acetic acids (6c) were proposed to form from benzylic acid (1c) via a carbocation intermediate.

Table 2 Selectivity for benzilide (3c) and triarylacetic acid (6c) from Hoefnagel, A. J.; van Bekkum, H., *Microporous Mesoporous Mater.* **2000,** *35-36*, 155-161.[8]

Catalyst	Solvent	Boiling point / °C	Selectivity[a] / %	
			3c	6c
None	*p*-Chlorotoluene	162	30	2
Amberlyst-15	Toluene	110	70	30
H-Beta-12	Toluene	110	7	8
Amberlyst-15	Chlorobenzene	130	28	2
H-Beta-12	Chlorobenzene	130	2	-
Amberlyst-15[c]	*p*-Chlorotoluene	150	1	5
H-Beta-12	*p*-Chlorotoluene	162	3	-
Filtrol[d]	*p*-Chlorotoluene	162	62	1
Amberlyst-15	*o*-Dichlorobenzene	150	1	-
H-Beta-12	*o*-Dichlorobenzene	180	1	-

[a]The paper does not state the conversion at which these selectivity measurements were obtained. Several other products were also formed in these reactions, but they are not of relevance to this thesis, so are not discussed here.

[c]Sulfonic acid-functionalised polystyrene

[d]A type of acidic clay

Based on previous reports of stereoselective synthesis of *L,L*-lactide from lactic acid using zeolite catalysts[6], we hypothesised that it might be possible to selectively synthesise the more desired *meso*-mandelide isomer using zeolites as catalysts (compared with the statistical mixture of *meso*- and *rac*-mandelide obtained using homogeneous p-TSA). We reasoned that the *trans* configuration of the phenyl rings in the *meso* isomer compared with the *cis* configuration in the *rac* isomers could result in a smaller cross-sectional area for the *meso* isomer. In turn, this could result in greater selectivity when zeolites are used, due to suppression of the formation of the larger *rac* isomers through product shape selectivity. The low selectivity of H-Beta towards benzilide (3c) (Scheme 2, Table 2) suggested that synthesis of larger cyclic dimers would be more challenging. However, given that mandelic acid possesses only one aromatic ring, it has an intermediate size between lactic acid and benzylic acid. This size might permit mandelic acid to access the internal micropores of the zeolite when benzylic acid cannot.

We have investigated the reactions of mandelic acid in the presence of Brønsted acidic zeolites. The effect of reaction conditions such as solvent choice and zeolite properties such as framework type, silicon to aluminium ratio on the product distribution have been investigated under batch conditions. Zeolite catalysts were modified by aqueous ion-exchange with alkali metals to investigate the effect of the charge balancing cation. Hierarchical zeolites containing both micropores and mesopores were made by top-down modification of commercial zeolites, using reported methods such as base leaching. Reactions were also attempted using a liquid-phase flow reactor. The kinetic diameter of the key reactants, intermediates and products were evaluated in order to aid the interpretation of the catalytic results.

3.2 Results and Discussion

3.2.1 Shape-Selective Heterogeneous Catalysis in the Synthesis of Mandelide – Initial Screening

In our initial screening, we tested zeolites H-Beta-75 and H-Y-30 against the benchmark *p*-TSA synthesis of mandelide from the literature.[10, 11] We found that the products of the conversion of mandelic acid using these Brønsted acidic zeolites included additional compounds not observed when using the *p*-TSA catalyst. Figure 2 shows the ^{1}H NMR spectra obtained for the products of reactions using these three catalysts. Figure 2a and Figure 2d show the products of the *p*-TSA catalysed reaction. These included unreacted mandelic acid (ca. 5.2 ppm), dimer (5.30, 5.40, 5.98, 6.00 ppm), *rac*-mandelide (5.87 ppm) and *meso*-mandelide (6.13 ppm). In contrast, Figure 2b and Figure 2e show that

the products of H-Beta catalysed reaction included the same products, along with additional compounds (corresponding to peaks 5.0-5.2, 5.44, 5.52, 6.58 and 6.69 ppm). These additional peaks are labelled with an asterisk on Figure 3. Finally, the products observed for zeolite H-Y-30 (shown in Figure 2c and Figure 2f) consisted almost entirely of the products in the 5.0-5.2 ppm range, with very little mandelide or oligomeric products. The peak corresponding to mandelic acid should appear at around 5.25 ppm (it is slightly shifted in the p-TSA spectrum to 5.2 ppm). Very little mandelic acid was observed in the zeolite-catalysed products. Later, reactions were conducted with shorter reaction times which confirmed that the reactions approached full conversion after around 3 hours for H-Beta-75 and 1 hour for H-Y-30 (see section 5.2.2).

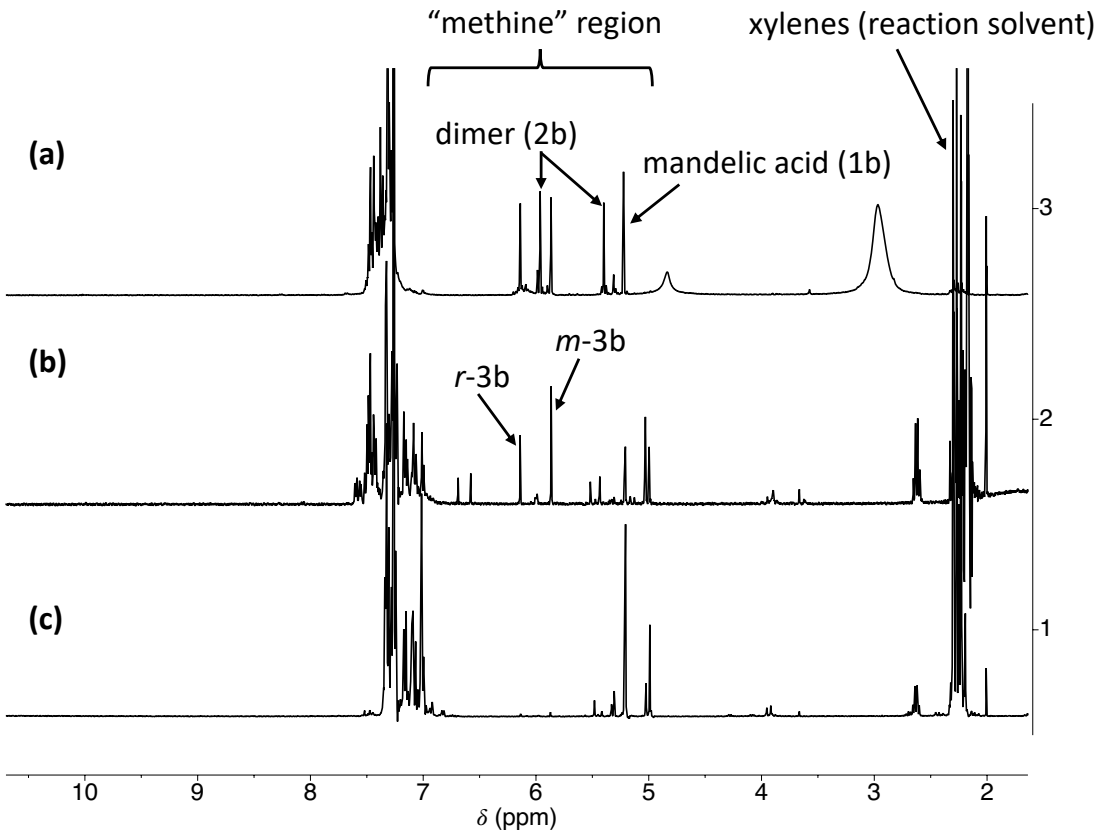

Figure 2a-c ^{1}H NMR spectra (400 MHz, $CDCl_3$) of the products from the initial screening. (a)-(c) show the full spectra for the crude products using catalysts: (a) p-TSA, (b) H-Beta-75 and (c) H-Y-30.

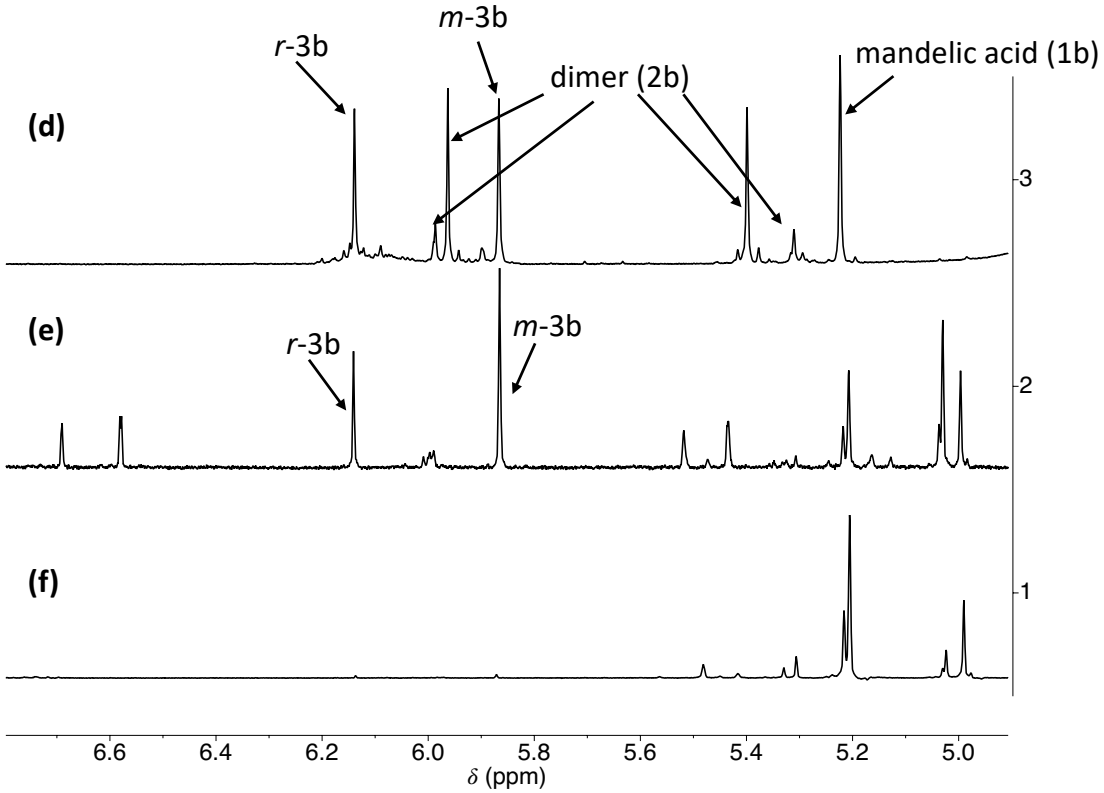

Figure 2d-f ^{1}H NMR spectra (400 MHz, $CDCl_3$) of the products from the initial screening. (d)-(f) show the same spectra as in Figure 2(a)-(c), zoomed in on the methine region from about 5.0 ppm to 6.8 ppm. Conditions: 0.5 g mandelic acid in 50 ml mixed xylenes, ~3.5 mol% H^+, reflux with Dean Stark trap overnight (ca. 20 hours), stirring rate = 500 rpm.

In their earlier work on lactide synthesis (see Figure 1B), Dusselier and Sels reported that H-Y-2.6 zeolite was an effective catalyst. In our screening, H-Y-30 zeolite produced products that we did not expect, corresponding to the series of resonances in the ^{1}H NMR spectra between 5-5.24 ppm and very little mandelide. Both H-Y-2.5 and H-Y-30 are ultrastable Y zeolites (USY) belonging to the CBV series of zeolites sold by Zeolyst. These USY zeolites are synthesised by steaming, followed by acid washing.[13] Both of these stages extract aluminium from the framework, increasing the Si/Al ratio of the zeolite. Generation of mesopores occurs simultaneously with aluminium extraction. Increasing the strength of the acid used in the acid washing step generally increases the Si/Al ratio and the total mesopore volume. USY catalysts are hierarchical materials containing both micro- and mesoporosity.

Similar to the results previously reported for lactide, mandelide was produced by H-Beta-75. However, mandelide selectivity (ca. 26%) of was much lower than lactide selectivity (ca. 80%[6]) under similar conditions. Figure 3 shows the product spectrum from the H-Beta-75 catalysed reaction, with the peaks corresponding to mandelide, oligomers and unknown products (*) labelled.

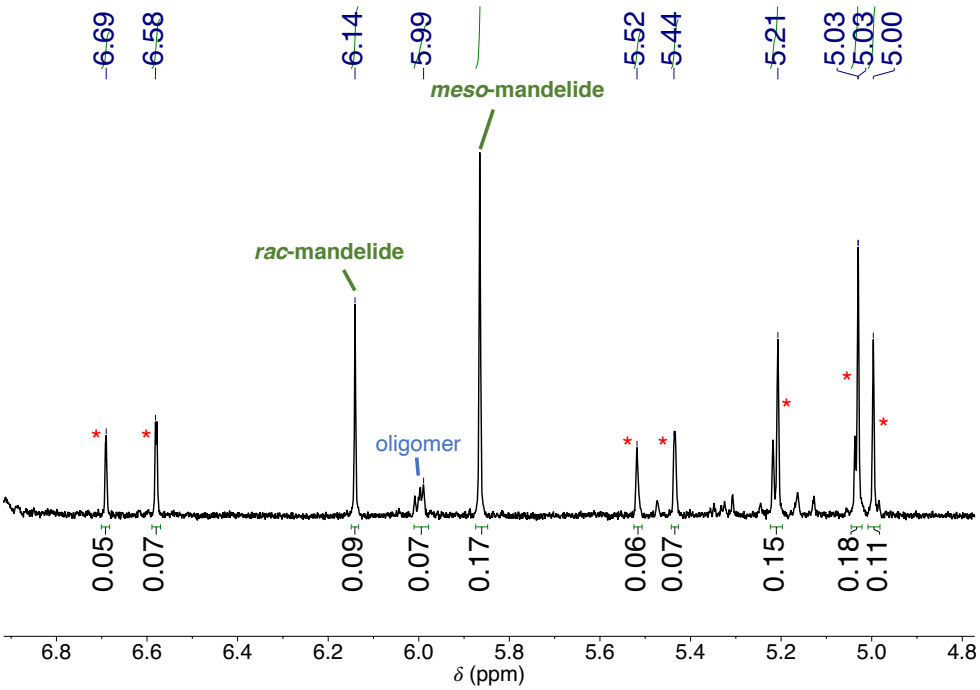

Figure 3 ^{1}H NMR (400 MHz, $CDCl_3$) spectrum of the products obtained during the initial overnight catalyst screening (catalyst = H-Beta-75, solvent = mixed xylenes), annotated to show the known (mandelide and oligomers) and unknown (*) products.

After identifying the additional products (see Appendix 1 for details) we were able to ascertain that zeolite-catalysed reactions of mandelic acid involved three distinct reaction pathways (shown in Figure 4): (1) esterification, (2) aromatic substitution and (3) decarboxylation or decarbonylation. The esterification pathway was the desired reaction, based on the literature on dimerisation of mandelic acid to mandelide using acid catalyst p-TSA[10, 11] and zeolite catalysed lactic acid to lactide.[6,14-18] Oligomerisation was also expected given literature on polycondensation of mandelic acid to give oligo- and polyesters.[10, 12] The aromatic substitution and decarbonylation pathways were unexpected based on our knowledge of the key literature available at the time.

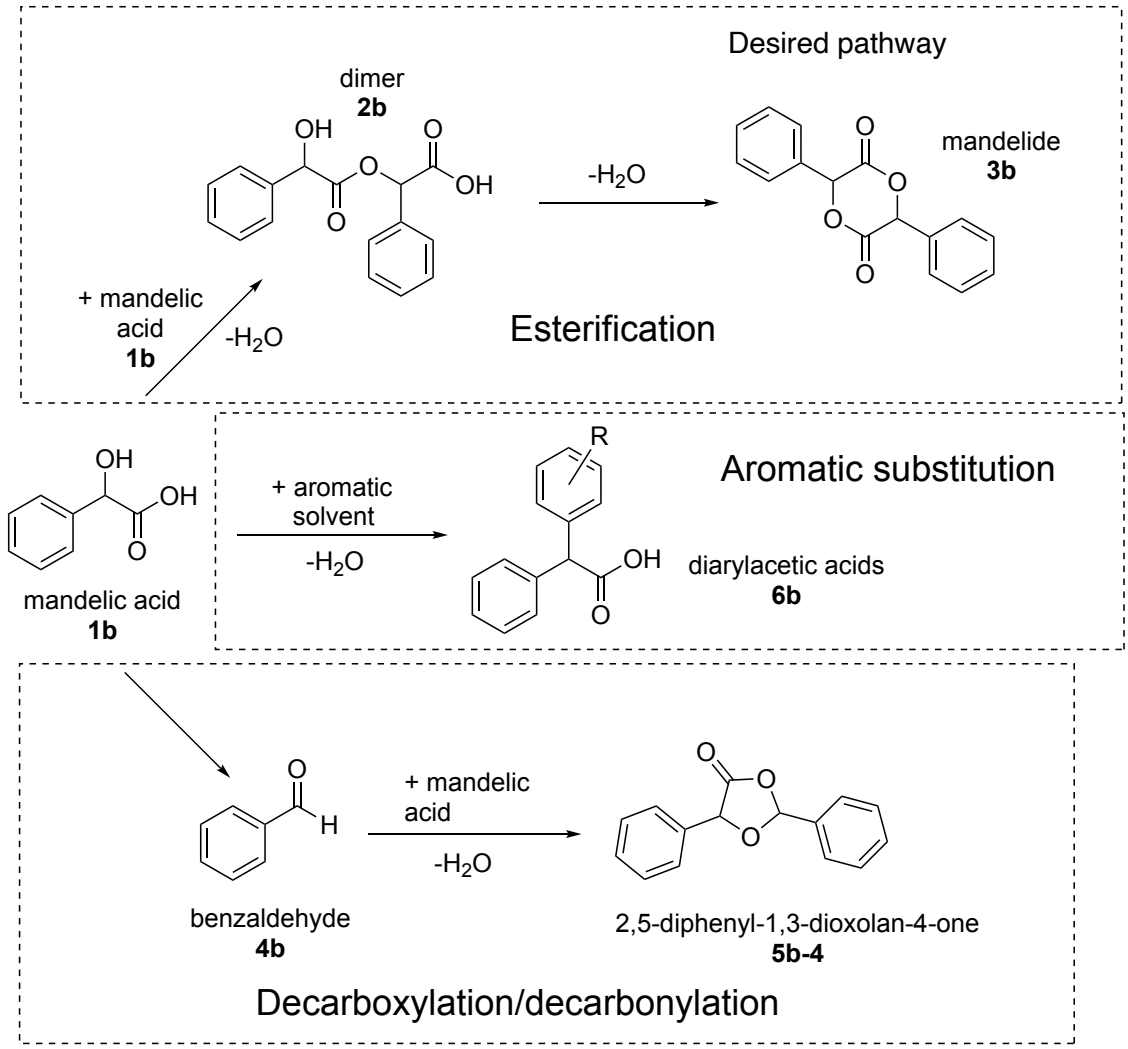

Figure 4 Zeolite-catalysed reaction pathways of mandelic acid identified in this work.

3.2.2 Effect of Zeolite Framework Type and Si/Al ratio on Mandelic Acid Conversion

After our initial screening of the zeolites Beta and Y reported by Sels and Dusselier for lactide synthesis and with our better understanding of the reaction pathways of mandelic acid in hand, we expanded the scope of the catalyst screening to other zeolite frameworks.

Table 3 Si/Al ratios of commercial Brønsted acidic zeolites.

Zeolite	Nominal Si/Al	Si/Al[(a)]
H-Beta-12.5	12.5	18.1
H-Beta-15	15	16.5
H-Beta-75	75	53.0
H-ZSM5-15	15	-

H-ZSM5-45	45	40.6
H-Y-2.5	2.55	3.0
H-Y-15	15	15.0
H-Y-30	30	26.5
H-Y-40	40	46.1
H-L-3	3	2.9
H-MOR-10	10	-
H-MOR-97	97	-

(a) By EDXRF

Different zeolite frameworks and Si/Al ratios were tested in the conversion of mandelic acid in mixed xylenes and the product distributions are shown in Figure 5. The product distribution was found to be highly dependent on both the zeolite framework type and Si/Al ratio, with differences in mandelic acid conversion and product selectivity observed. Beta zeolites were found to catalyse all three reaction pathways, with similar selectivity for each product. Increasing Beta Si/Al was found to increase the rate of conversion of mandelic acid, as can be seen in Figure 5 by comparing the series of catalysts from Si/Al = 12.5 to 75. H-Y-30 reached full conversion in this overnight reaction and was highly selective for the diarylacetic acid products. The medium pore ZSM-5 zeolites showed lower conversion than the large pore H-Beta, H-Y and H-MOR zeolites, which may be due to the reactant being too large to enter the medium micropore system of ZSM5.

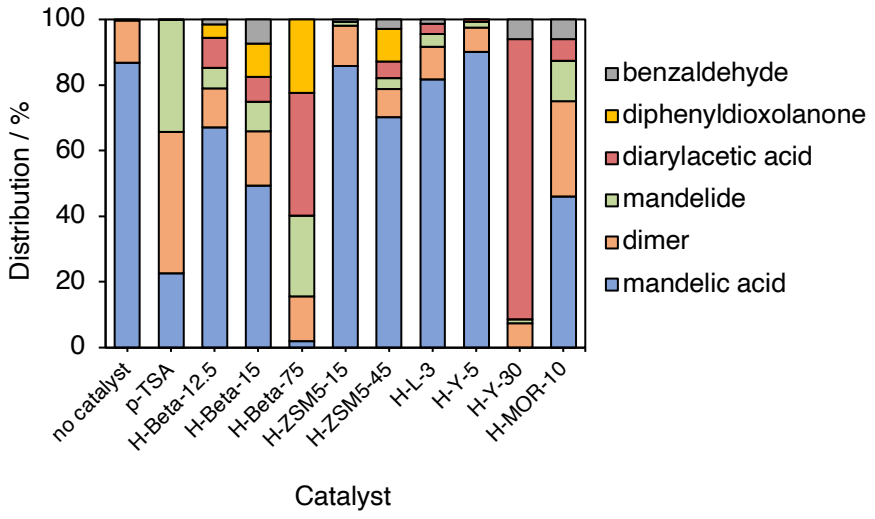

Figure 5 Effect of zeolite catalyst framework and silicon:aluminium ratio on product distribution. Conditions: 0.5 g mandelic acid in 50 ml mixed xylenes, ~3.5 mol% H^+ in zeolite, reflux with Dean Stark trap overnight (ca. 20 hours), stirring rate = 500 rpm. Product distributions calculated based on integration of ^1H NMR spectra recorded at 400 MHz in $CDCl_3$.

Catalysts H-ZSM5-45, H-Beta-75, H-Y-30 and H-MOR-97 were further investigated by varying the reaction time in mixed xylene solvent to determine the reaction profiles (Figure 6). In the case of zeolite H-Beta-75, conversion reaches approximately 80% after 3.5 hours. Conversion of mandelic acid was fastest for H-Y-30, reaching around 90% conversion after a 1-hour reaction. ZSM5 and MOR showed the slowest conversion, requiring overnight reactions for conversion to increase above 20%. When H-ZSM-5, H-Beta and H-MOR catalysts were used, all three reaction pathways (shown in Figure 6) occur simultaneously. In the case of H-Beta, after 2.5 hours a significant amount of benzaldehyde had been formed. This was not observed in the initial catalyst screening, as after the overnight reaction used in the initial screening, the benzaldehyde had been converted to diphenyldioxolanone. In contrast, for the zeolite H-Y-30, the major product is the diarylacetic acid, with greater than 90 % selectivity. At shorter reaction time, a small amount of linear dimer is present, but at longer reaction times the concentration decreases relative to the diarylacetic acid product, suggesting that dimer formation may be reversible.

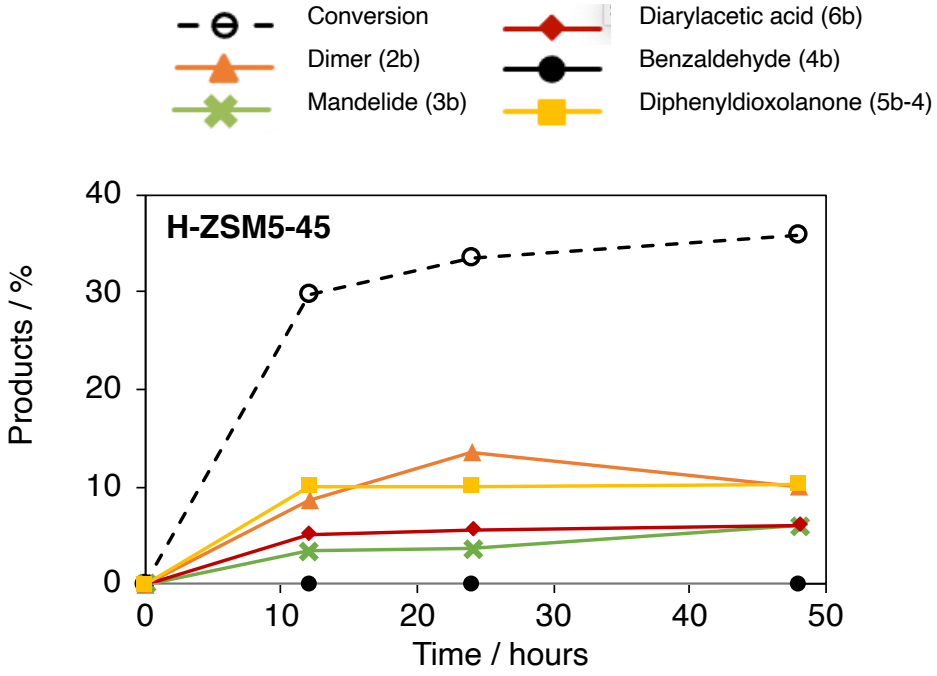

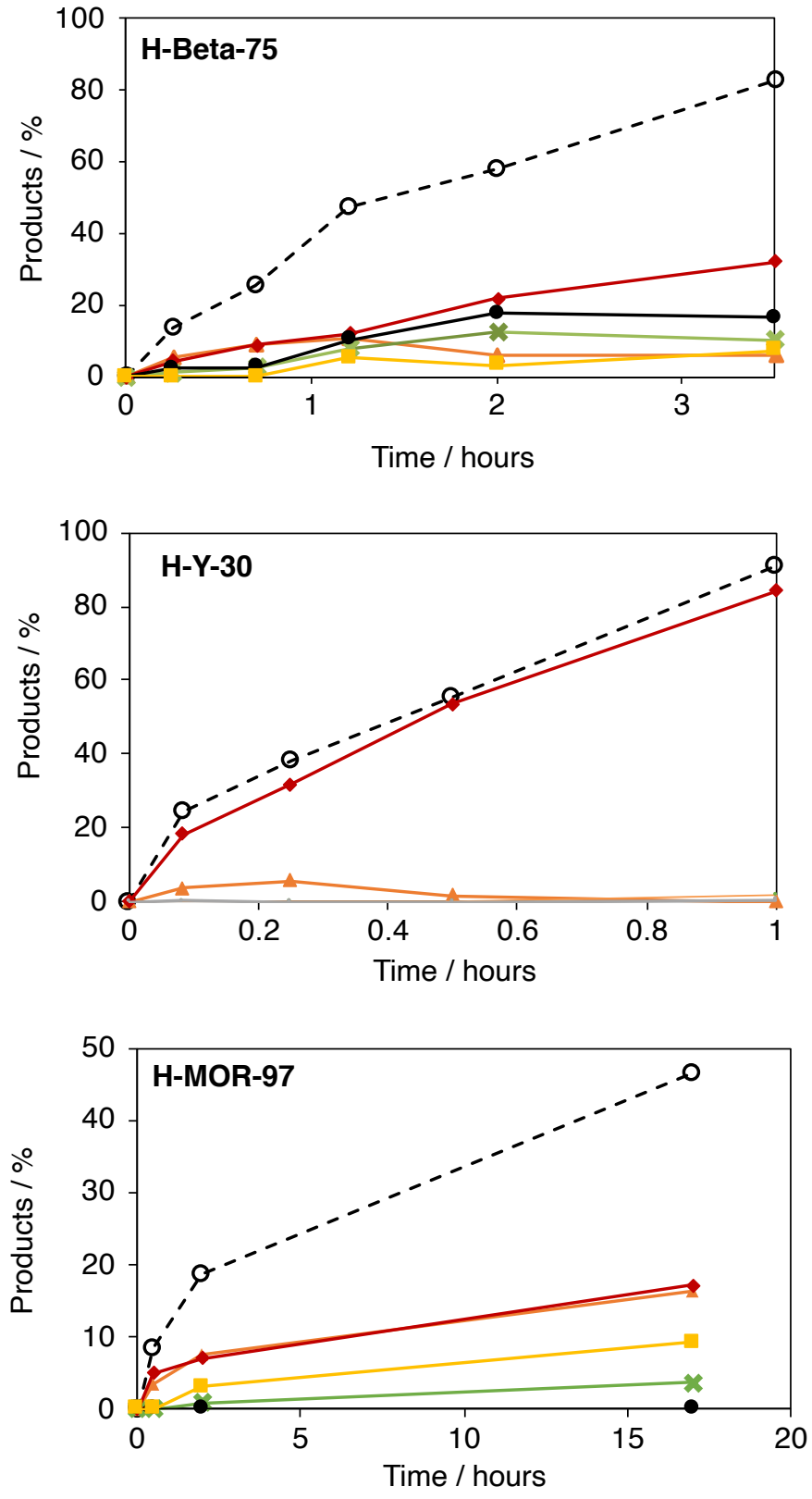

Figure 6 Reaction profile for the mandelic acid conversion in mixed xylenes. Conditions: 0.2 g mandelic acid, zeolite adjusted to give approximately 3 mol% H^+ relative to mandelic acid, 20 ml mixed xylenes, oil bath T = 160 °C (T_b + 20 °C), Dean Stark. Quantification by ^1H NMR spectroscopy in $CDCl_3$. Black = conversion, orange = dimer (2b), green = mandelide (3b), = red = diarylacetic acid (6b), grey = benzaldehyde (4b), yellow = 2,5-diphenyl-1,3-dioxolan-4-one (5b-4).

H-ZSM5-45, H-Beta-75 and H-MOR-97 turned a dark brown colour during the reaction, suggesting carbon deposition on the catalyst (see the spent H-Beta-75 zeolites in Figure 7). This might suggest that deactivation of the zeolite catalysts was occurring due to coke formation and this might account for the limited conversion with H-ZSM5-45 and H-MOR-97. The results of the CHN analysis of the spent H-Beta-75 zeolites in Figure 7 is shown in Figure 8. Approximately 9 wt% carbon at 50% mandelic acid conversion (30 minute reaction) and around 12 wt% at almost 100% mandelic acid conversion (3 hour reaction). Given that the reaction solvent used was xylenes (T_b = 140 °C), it is possible that the drying protocol (80 °C to constant weight) prior to CHN analysis did not remove all of the solvent. As a result, some of the carbon measured by CHN may have been due to residual adsorbed solvent rather than mandelic acid-based coke species.

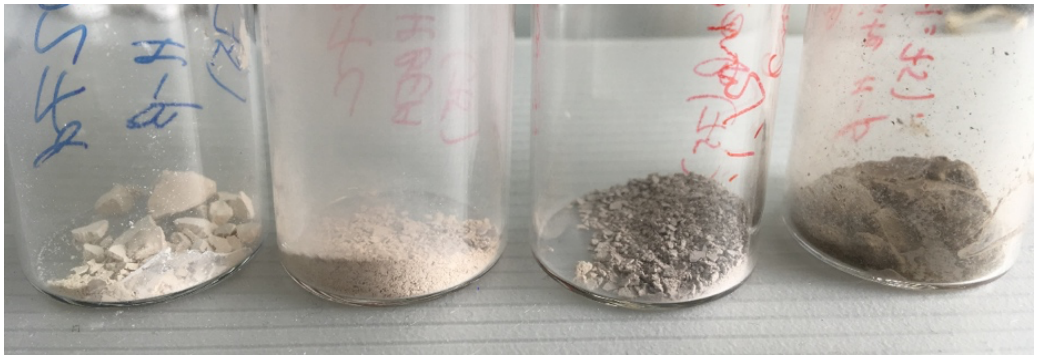

Figure 7 Spent H-Beta-75 zeolites from reactions of mandelic acid in mixed xylenes. Reaction time (from left to right): 30 minutes, 3 hours, 24 hours, 72 hours.

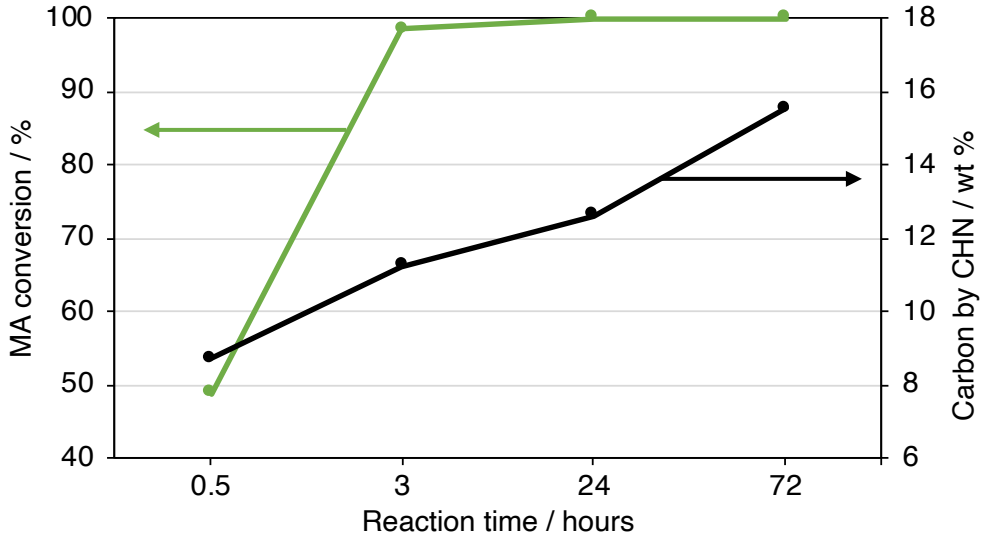

Figure 8 Conversion (green) and carbon content (black) by CHN analysis of spent zeolite H-Beta-75 after different reaction times. Conditions: 0.2 g mandelic acid, H-Beta-75 (mass adjusted to give approximately 3 mol% H^+ relative to mandelic acid), 20 ml mixed xylenes, oil bath T = 160 °C (Tb + 20 °C), Dean Stark. At the end of the reaction, the reaction mixtures were filtered and the spent zeolite obtained. The zeolite was dried at 80 °C in a drying oven over 72 hours. Note: the boiling point of the reaction solvent used mixed xylenes is 140 °C, so some of the carbon

content may be due to adsorbed solvent, as this would not be fully removed under the drying protocol used.

A negligible colour change was observed (if at all) for zeolite H-Y-30. When the reaction was run to 91% conversion using zeolite H-Y-30 (the longest reaction time shown for this catalyst in Figure 6), the amount of recovered products and starting material equated to 1.09 mmol (approximated from the recovered mass and product distribution by ^{1}H NMR). In comparison, 1.31 mmol of mandelic acid added at the start of the reaction. Therefore, approximately 0.22 mmol (17%) of the added mandelic acid was not recovered in the products. This could be attributed to losses during filtration or mandelic acid remaining adsorbed on the zeolite.

Considering the pore structures, ZSM5 has a 3D channel system with 10MR pore openings. It has the smallest pore diameter of any of the zeolites tested, which may mean that its internal acid sites are inaccessible to bulky mandelic acid molecules. MOR on the other hand has larger pore diameter, containing 12MR openings, meaning it may be able to accommodate the bulky molecules within its internal micropore network. However, MOR possesses a 1D channel structure. Considering the distinct colour changes of the spent catalysts compared with fresh ZSM5 and MOR, it seems likely that the limited conversion of these catalysts is at least in part caused by coke deposition. This may be attributed to the small pores of ZSM5 and the 1D channel system of MOR. Zeolites Beta and Y on the other hand possess 12MR channels with 3D connectivity. The increased mandelic acid conversion for these catalysts, and increased selectivity in the case of Y, may suggest that a pore system with large openings and 3D connectivity is advantageous in the reactions studied here. However, it is unclear whether the internal zeolite pore structure of the zeolites is accessible to the bulky molecules studied here, but efforts to understand this will be discussed in more detail in Section 5.2.8.

An increase in the pore size of the zeolite will increase accessibility for large substrates such as mandelic acid. Greater accessibility results in a greater number of available acid sites within the zeolites. If accessibility to internal acid sites is limited, external acid sites play a larger role in dictating the reaction outcome. As these sites are not located within the zeolite micropores, the outcome will not be governed by shape selectivity. This may be evident in our results, as all reaction pathways occur simultaneously for zeolites ZSM5, Beta and MOR, suggesting shape selectivity does not play a role. However, this does not explain the high selectivity of the Y zeolite.

BET analysis of some of the fresh zeolite catalysts is given in Table 4. BET surface area ranged from around 400-650 $m^2\ g^{-1}$, depending on the zeolite. The mesopore volume of the zeolite was estimated based on the difference between the total pore volume and

the micropore volume, determined by t-plot and BJH methods, respectively. The micropore volumes obtained from this analysis are in good agreement with values reported in the literature for these same commercial materials (see Table 5). The total pore volumes obtained our measurements are slightly lower than reported elsewhere, but nevertheless both sets of data suggest that the high-silica zeolites ZSM5-45, H-Beta-75, H-Y-30 and H-Y-40 all contain a significant pore volume that cannot be attributed to micropores. This suggests that these catalysts are hierarchical materials containing both micro- and mesopores. Selected N_2 adsorption isotherms are also shown in Figure 9.

Table 4 BET surface area and pore volume of H-ZSM5, H-Beta and H-Y catalysts.

Zeolite	Si/Al[(a)]	BET Surface Area / $m^2\ g^{-1}$	V_{micro}[(b)] / $cm^3\ g^{-1}$	V_{meso}[(c)] / $cm^3\ g^{-1}$	V_{total}[(d)] / $cm^3\ g^{-1}$
H-ZSM5-45	40.6	420	0.091	0.22	0.31
H-Beta-12.5	18.0	560	0.16	0.27	0.43
H-Beta-75	53.0	635	0.19	0.10	0.29
H-Y-30	26.5	651	0.20	0.11	0.31
H-Y-40	46.1	519	0.21	0.04	0.25

(a) By EDXRF; (b) t-plot method; (c) $V_{meso} = V_{total}(BJH) - V_{micro}(t\text{-plot})$; (d) BJH method, volume adsorbed at $p/p_0 = 0.95$.

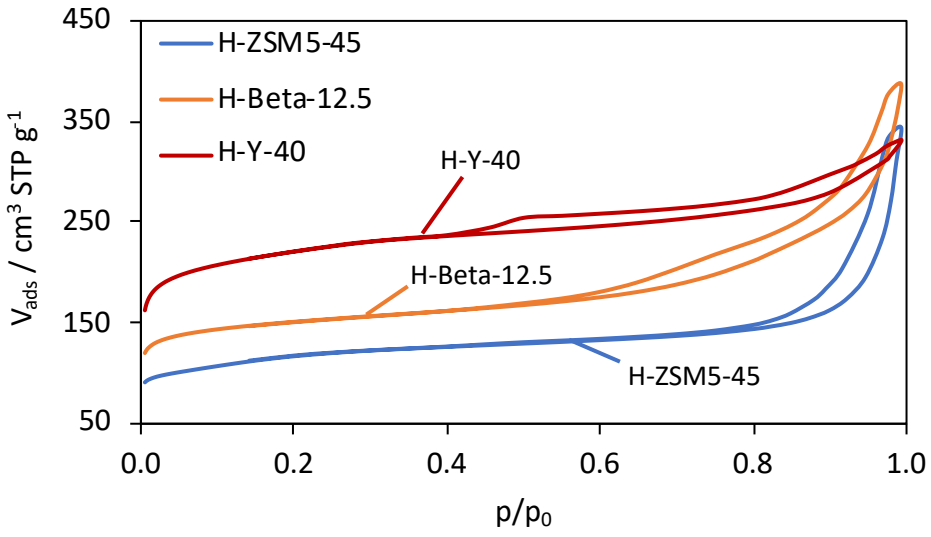

Figure 9 N_2 adsorption isotherm of selected commercial zeolites.

Table 5 Comparative BET analysis of commercial zeolites.

Zeolite	Si/Al[a]	BET Surface Area / m^2 g^{-1}	V_{micro}[b] / cm^3 g^{-1}	V_{meso}[c] / cm^3 g^{-1}	V_{total}[d] / cm^3 g^{-1}	Ref
H-ZSM5-45	42	359	0.089	-	0.5341	19
H-Beta-12.5	-	478	0.164	-	-	6
H-Beta-75	78	563	0.176	-	0.3721	19
H-Y-30	31	548	0.2445	-	0.5233	19
H-Y-40	32	606	0.1966	-	0.4819	19

3.2.3 Effect of Reaction Solvent on Mandelic Acid Conversion Catalysed by H-Beta-75 Zeolite

Next, a solvent screening study was conducted to investigate the effect of reaction solvent on the product selectivity. The occurrence of the competing Friedel-Crafts reaction (Figure 4, reaction to form the diarylacetic acid product 6b) could vary in different aromatic solvents, particularly given that the solvent is also a substrate in this reaction. For example, the different electronics of the aromatic rings caused by the different substituents could alter the selectivity. This solvent screening was initially designed to investigate the possibility of improving H-Beta-75 selectivity towards the mandelide product, by suppressing the competing Friedel-Crafts reaction. However, we also found that diarylacetic acids could be synthesised selectively over H-Y-30 in a range of solvents (described later in section 5.2.6).[20]

Figure 10 shows the product distribution for the reaction of mandelic acid in various aromatic and non-aromatic solvents catalysed by H-Beta-75. In each of the aromatic solvents tested, diarylacetic acids formed. The selectivity to these products was slightly lower in p-xylene and ethylbenzene in comparison with toluene, chlorobenzene and mixed xylene. The non-aromatic solvents tested (acetonitrile, cyclohexane, methylcyclohexane) are not capable of participating in the Friedel-Crafts reaction to produce diarylacetic acids. Solvent choice was limited as many common solvents, such as alcohols or ethers, would be reactive to the zeolite catalysts and the mandelic acid substrate. For example, alcohol solvents could form self-condensation products or form esters with the carboxylic acid group of mandelic acid. Cyclohexane and acetonitrile were tested first. No appreciable conversion was observed in these solvents in an overnight reaction, probably due to their relatively low boiling points (ca. 80 °C). Methylcyclohexane was chosen in place of cyclohexane, due to its higher boiling point (100 °C), which is

similar to toluene (111 °C). As shown in Figure 10, mandelide was the major product in methylcyclohexane. By extending the reaction time to 3 days, it was possible to increase the mandelide yield to around 63%. However, this reaction also gave a 28% yield of diphenyldioxolanone, which was the highest yield of this product observed in this solvent screening (along with the reaction in p-xylene).

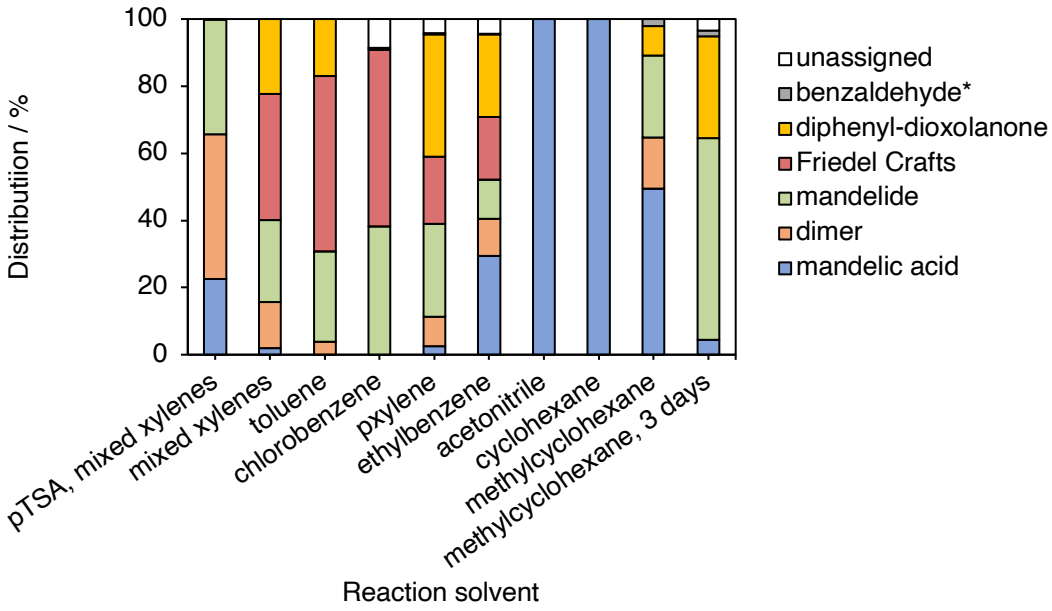

Figure 10 Product distribution for H-Beta-75-catalysed mandelic acid conversion in various solvents. In some solvents, a small amount of unknown products were formed. The peaks corresponding to these unknowns were intergrated and included in the quantification. They are labelled “unassigned”. At this stage of the project, we had not modified the quantification method to properly quantify benzaldehyde. Some small peaks were present in the spectra, but it is unlikely that it was accurately quantified in these experiments. These reactions were not repeated. Reaction conditions: 0.5g mandelic acid, 50 ml solvent, reflux in Dean Stark overnight, 3 mol% catalyst.

Shorter reaction time (1 hour) was also investigated for some aromatic solvents and the product distribution data is shown in Figure 11. In m-xylene, a significant amount of benzaldehyde was formed early in the reaction. In comparison, less benzaldehyde was formed in o-xylene, and a greater proportion was converted to 2,5-diphenyl-dioxolan-4-one. Conversion in chlorobenzene and toluene was lower for this 1-hour reaction, reflecting the lower reflux temperature of these solvents (132 °C and 111 °C, respectively).

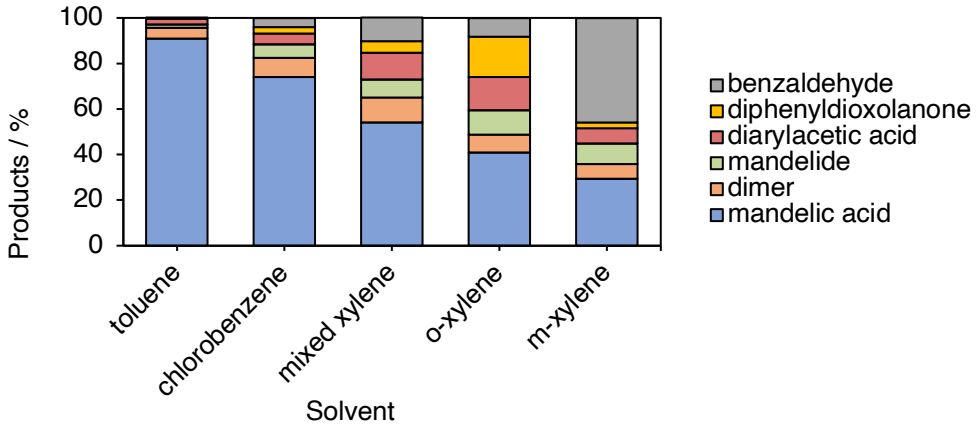

Figure 11 Effect of aromatic solvent on conversion of mandelic acid. Conditions: 0.2 g mandelic acid, 20 ml solvent, 0.13 g H-Beta-75 zeolite (approx. 3 mol % H^+ relative to mandelic acid), reflux for 1 hour.

Table 6 shows results of the reaction of mandelide in methylcyclohexane and toluene catalysed by H-Beta-12.5, H-Beta-75 and H-Y-30. The structures corresponding to the compound references in Table 6 are shown in Figure 12. Comparison of the results in these two solvents may show the effect of competition from the Friedel-Crafts pathway. In methylcyclohexane, conversion of mandelic acid was observed for all three catalysts tested, albeit at a fairly slow rate. In the case of both H-Beta-75 and H-Y-30, the rate of overall conversion was considerably higher in toluene compared with methylcyclohexane. For example, the reaction catalysed by H-Y-30 reached 30 % conversion after 3 hours in toluene but took 22 hours to reach the same conversion in methylcyclohexane. This is unsurprising given that a significant amount of mandelic acid is converted by Friedel-Crafts reaction in toluene, and this reaction is not possible in methylcyclohexane. Comparing mandelide yield over H-Beta-75 in toluene and methylcyclohexane at a given reaction time (e.g., comparing entries 6 and 9 in Table 6) shows that rate of mandelide production in similar in the two solvents. These results also show that without the competing arylation reaction in methylcyclohexane, H-Y-30 was capable of catalysing the mandelic acid esterification reaction, achieving a much higher yield of the dimer product than in any of the other aromatic solvents tested (Table 6 Entry 3). Comparing the results for H-Y-30 and H-Beta-75 (entries 3 and 9) shows that the overall activity of the H-Beta-75 catalyst was higher than H-Y-30, reaching higher conversion after 22 hours of 52% compared with 29% for H-Y-30. After 22 hours, mandelide yield was also higher for H-Beta-75. This might suggest that H-Beta-75 was also more active for the ring closing to mandelide. However, given that the formation of mandelide is a step process via the linear dimer, this may be a result of the different overall conversion in entries 3 and 9. Instead, comparing entries 3 and 8 shows that are more comparable conversion, the mandelide yield for the two catalysts is similar. This suggests that the

formation of mandelide must be preceded by some accumulation of the linear dimer. A longer reaction using H-Y-30 in methylcyclohexane to compare with H-Beta-75 at around 50% conversion was not conducted. The results in Table 6 are not sufficient to conclude whether the higher mandelide yield in entry 9 is a result of the higher overall conversion or improved ring closing by H-Beta-75 catalyst compared with H-Y-30. H-Beta-12.5 required increased catalyst loading to approximately 6 mol% of Al relative to the amount of mandelic acid to achieve measurable conversion in a 24 hour reaction (Table 6, entry 4).

Table 6 Reaction data for zeolite catalysed reactions in toluene and methylcyclohexane.

Entry	Cat	Sol*	t / h	Conversion / %	Yield / %				
					2b	3b	4b	5b-4	6b
1	H-Y-30	Tol	3	30	6	<1	0	0	24
2	H-Y-30	Tol	22	100	<1	4	<1	0	95
3	H-Y-30	MeCyc	22	29	24	5	0	0	N/A
4	H-Beta-12.5†	MeCyc	24	19	10	4	<0.5	4	N/A
5	H-Beta-75	Tol	3	22	10	5	0	0	7
6	H-Beta-75	Tol	20	100	4	27	0	17	52
7	H-Beta-75	MeCyc	1	13	10	3	0	0	N/A
8	H-Beta-75	MeCyc	2	21	15	6	<1	0	N/A
9	H-Beta-75	MeCyc	22	52	17	25	1	9	N/A
10	H-Beta-75	MeCyc	72	96	3	63	2	28	N/A

Conditions: 0.2 g mandelic acid, 20 mL solvent, reflux at T_b + 20 °C.
*MeCyc = methylcyclohexane, Tol = toluene.
†6 mol% catalyst. MD = mandelide, diPh-DOX = diphenyldioxolanone, DAA = diarylacetic acid

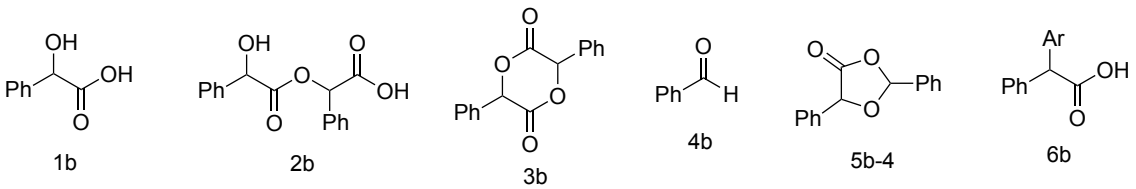

Figure 12 Compounds corresponding to the yield data in Table 6.

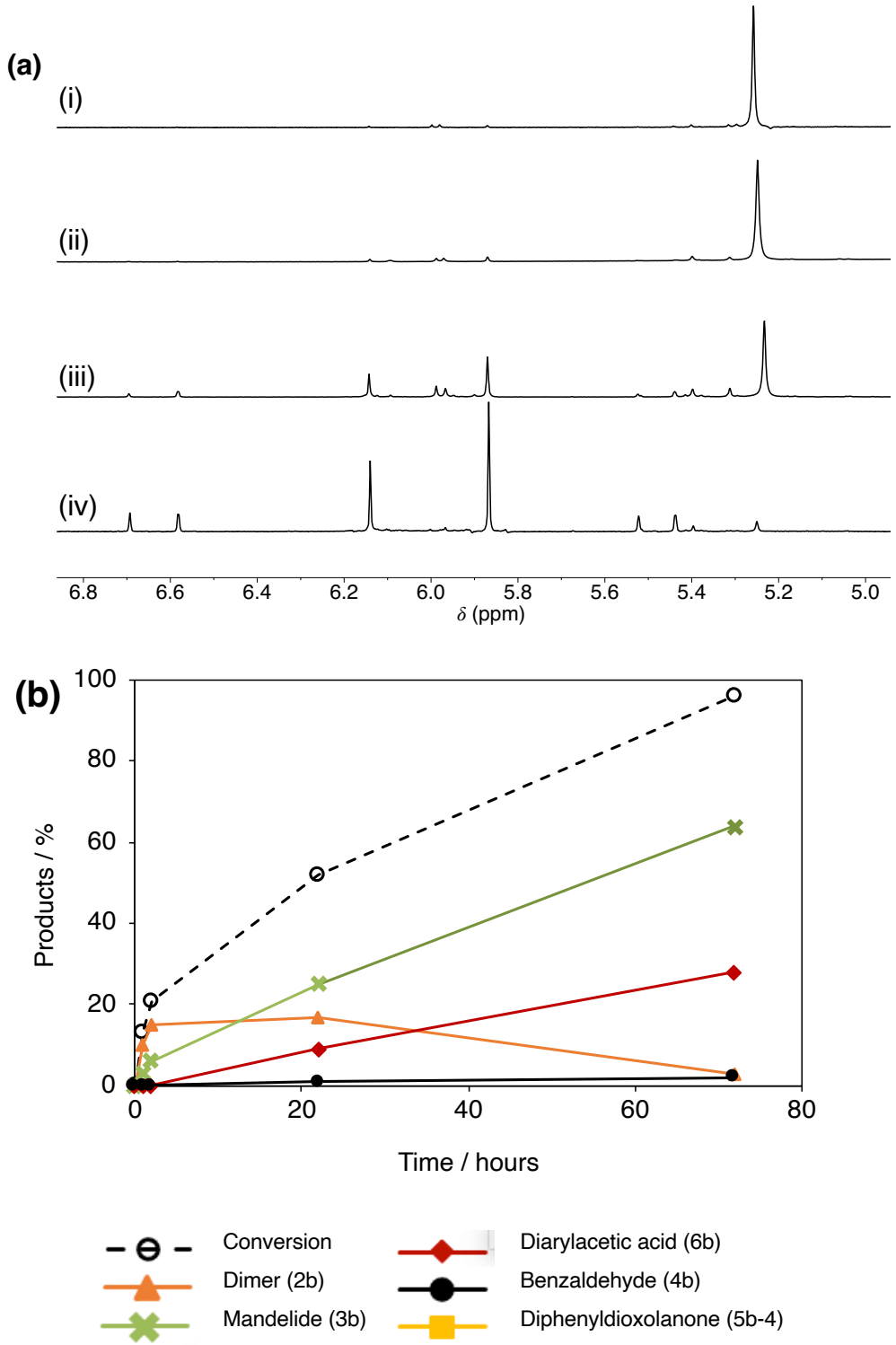

Figure 13 (a): ^{1}H NMR spectra of H-Beta-75 catalysed conversion of mandelic acid in methylcyclohexane at different reaction times: (i) 1 hour, (ii) 2 hours, (iii) 22 hours and (iv) 72 hours. (b): Reaction-time profile for the same set of reactions.

The rate of mandelic acid conversion in methylcyclohexane was highest for the H-Beta-75 catalyst, reaching 52% conversion after 22 hours at approximately 3 mol% loading. Reaction times of up to 72 hours were tested for this catalyst, showing that it was possible to achieve near full conversion of mandelic acid in methylcyclohexane. Figure 13 shows

the time dependence of conversion and product yield for these reactions. These results show that mandelide increased steadily over time. The concentration of linear dimer increased initially, then remained fairly constant from 2 to 22 hours while mandelide yield grew. This suggests that the rates of dimer formation and subsequent ring closure to mandelide were fairly equal, maintaining the dimer concentration constant at around 15%. At the longest reaction time of 72 hours, most of the dimer present had been converted to mandelide. Diphenyldioxolanone yield increases simultaneously with mandelide yield, at approximately half the rate, reaching 28% yield after 72 hours compared with 63% for mandelide. Interestingly, negligible amounts of benzaldehyde were detected at all reaction times tested. From the constant increase in diphenyldioxolanone yield with reaction time, we can deduce that benzaldehyde was formed and subsequently rapidly converted to diphenyldioxolanone by reaction with mandelic acid.

The reaction catalysed by H-Beta-75 in methylcyclohexane gave the best mandelide yield of any zeolite-catalysed reaction. Table 7 shows the mandelide yield from the literature and this work. One of the aims of this work was to synthesise *meso*-mandelide selectively, potentially by suppression of the *rac*-mandelide isomer through product shape selectivity. The data in Table 7 shows that the homogenous *p*-TSA catalyst gives roughly a 1:1 mix of *meso* and *rac* isomers. However, zeolite H-beta leads to approximately 2:1 mix of *meso* and *rac*. This ratio was consistent for the different solvents and reaction times tested for this catalyst, suggesting that the change in ratio was the result of a framework effect. Whilst the NMR yields in our work were higher than the isolated yields of mandelide reported for the *p*-TSA-catalysed syntheses in the literature, it is likely that actual isolated yields would be lower due to losses during work up. Furthermore, both reported syntheses of mandelide used organic-aqueous extraction to isolate mandelide. If this work up was used for the zeolite-catalysed reaction, the organic fraction would contain 2,5-diphenyl-1,3-dioxolan-4-one. This compound would require further purification, such as column chromatography, to separate it from mandelide. Therefore, the zeolite-catalysed synthesis of mandelide appears to increase the *meso:rac*-mandelide ratio, along with general advantages associated with heterogeneous catalysts such as ease of catalyst separation. However, the zeolite-catalysed route still presents challenges in terms of reaction time and product separation.

Table 7 Comparison of mandelide (2c) yield catalysed by homogeneous and heterogeneous catalysts.

Catalyst	Solvent	Time	Yield type	2c yield / %	*meso* yield / %	*rac* yield / %	*meso:rac* ratio	Ref
p-TSA	mixed xylene	3 days	purified mass	53	24	28	0.9	[10]
p-TSA	mixed xylene	3 days	purified mass	57	25	32	0.8	[11]
p-TSA	mixed xylene	O/N	NMR	55	29	26	1.1	This work
H-Beta-75	methyl-cyclohexane	1 day	NMR	25	16	9	1.8	This work
H-Beta-75	methyl-cyclohexane	3 days	NMR	63	42	22	1.9	This work
H-Beta-75	toluene	O/N	NMR	29	19	10	1.9	This work
H-Beta-75	chloro-benzene	O/N	NMR	41	27	14	1.9	This work
H-Beta-75	mixed xylene	O/N	NMR	25	16	9	1.8	This work

3.2.4 Effect of Alkali-Metal Cation Exchange of Beta-75 Zeolite on Mandelic Acid Conversion

Alkali-metal exchanged zeolites have been shown to be effective for the dehydration of lactic acid to acrylic acid.[2-5, 21] This selectivity was reliant on suppression of decarbonylation, decarboxylation and esterification pathways. The authors of these reports proposed that the suppression of these reactions was possible due to neutralisation of the carboxylic acid group of lactic acid by basic sites in the ion exchanged zeolites, resulting in higher selectivity towards the dehydration reaction. As discussed earlier, dehydration of mandelic acid by acidic zeolites in aromatic solvents produces diarylacetic acids. By exchanging Bronsted acid sites for alkali cations, we hoped to probe the role of Brønsted acid sites in the dehydration pathways.

A series of ion-exchanged Beta-75 zeolites were prepared by aqueous ion exchange using nitrate salts and then tested for mandelic acid conversion. Table 8 shows the conditions used to prepare the various zeolites and their elemental analysis. Na, Mg, K, Zn and Rb exchanged Beta-75 zeolites were prepared, including K-exchanged zeolites with various degrees of exchange by varying the concentration of nitrate salt solution used. Figure 15 shows the pXRD patterns of the potassium exchanged Beta-75 zeolites. These patterns show that the crystallinity of the zeolites remained predominantly unchanged with increasing ion exchange.

Table 8 Ion-exchanged H-Beta-75 zeolites including nitrate solution concentration, time used for ion exchange, number of repetitions, silicon:aluminium ratio and exchange degree of ion-exchanged zeolite.

Salt	Concentration / M	time / h	repetitions[a]	Si/Al[b]	Metal/Al[c] / %
$MgNO_3$	0.3	1	10	51.8	144
KNO_3	0.3	1	10	58.3	105
$NaNO_3$	0.3	1	10	-	-
$ZnNO_3$	0.3	1	10	52.9	95
KNO_3	0.005	2	1	53.4	40
KNO_3	0.02	2	1	57.8	71
KNO_3	0.1	2	1	57.6	86
KNO_3	0.5	2	1	57.9	93
NH_4NO_3[b]	0.01	2.5	1	54.9	23
$RbNO_3$	0.5	1	4	51	90

(a) 1 repetition means the zeolite and indicated nitrate solution was added to a centrifuge tube and placed on a tube roller for the indicated time. For more details, see experimental chapter. (b) EDXRF – Na not determined due to instrumental limitations; (c) A further sample was made by exchanging the 93% K-exchanged beta with NH_4^+ to leave 23% K^+ content. The NH_4 were converted to H^+ through calcination at 550 °C for 5 hours.

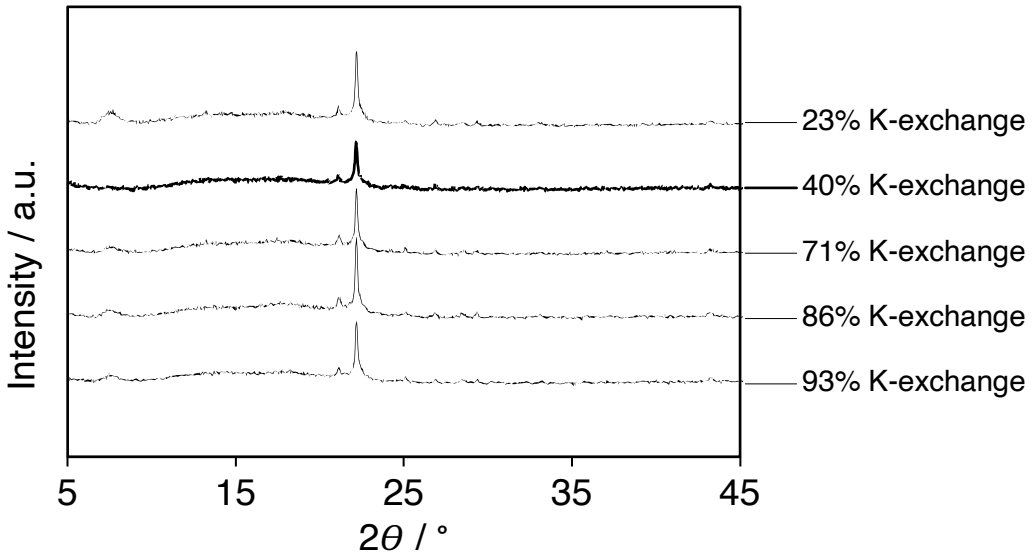

Figure 15 pXRD patterns from 2θ = 5 – 55° of the K-exchanged Beta-75 zeolites.

Isoconversion screening (at around 20-40% mandelic acid conversion) of the ion-exchanged H-Beta-75 zeolites showed small changes in selectivity compared to the H-form (Figure 16). In the case of K^+ and Na^+ exchange, a reduction in the selectivity towards diarylacetic acids and an increase in the selectivity towards diphenyldioxolanone

was observed. For Zn^{2+} exchange, the decrease in diarylacetic acid selectivity was less significant but the increase in diphenyldioxolanone selectivity was comparable. There was no diphenyldioxolanone observed at this conversion level for the H-form zeolite, but around 20% selectivity for each of the ion-exchange Beta zeolites. Rate of conversion decreased relative to the H-form zeolite when the same mass of catalyst was used, presumably due to the reduction in the concentration of acid sites in the ion exchanged catalysts.

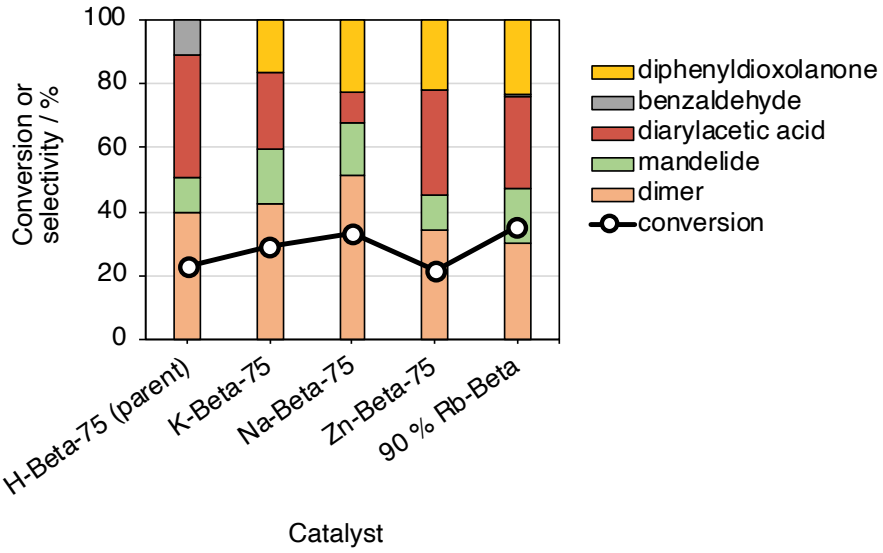

Figure 16 Selectivity at around 20-40% conversion (by changing the reaction time) in the conversion of mandelic acid catalysed by ion-exchanged zeolites. Solvent = mixed xylenes. The K-Beta-75 zeolite used was the 105% exchanged zeolite (Entry 2, Table 8).

Figure 17a shows the time dependence and product yield when 70% K-exchanged Beta-75 was used as catalyst. Figure 17b shows results for the parent zeolite at similar conversion for comparison. The results from this experiment show that when this zeolite was ion-exchanged, the overall rate of conversion was significantly decreased (compare the reaction time scale on the x-axes of Figure 17a and Figure 17b). Ion-exchange also caused a change in the conversion of benzaldehyde to diphenyldioxolanone. Benzaldehyde was detected in the products of the H-form zeolite, however negligible amounts were detected for the ion-exchanged zeolite. Additionally, the amount of diphenyldioxolanone formed was much higher for the ion-exchanged zeolite, and at 15 hours reaction and around 40% conversion, diphenyldioxolanone is the major product.

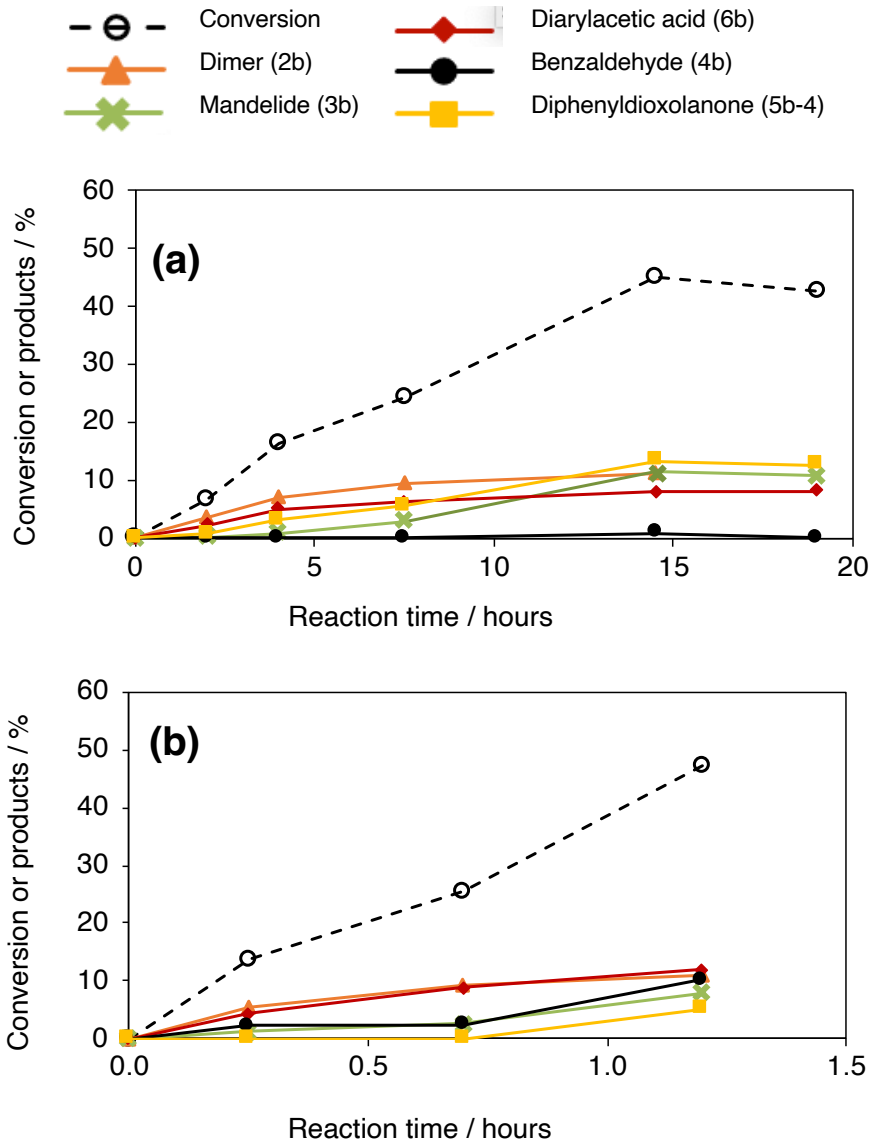

Figure 17 (a) Time dependence of conversion and product yield for the conversion of mandelic acid in mixed xylenes, catalysed by 70% K-exchanged Beta-75 zeolite. (b) Comparative data for the H-Beta-75 parent zeolite over similar range of conversion.

We also observed a change in selectivity as the extent of K^+ exchange was varied. Figure 18 compares the selectivity of K^+ exchanged Beta-75 at different exchange levels, and at low (Figure 18a), medium (Figure 18b) and high (Figure 18c) levels of conversion. The results in Figure 18 suggest that a change in selectivity occurs at higher extent of K^+-exchange. The results for the H-form parent, 23% and 40% K-exchanged samples appear similar. In contrast, the 70%, 86% and 105% K-exchanged zeolites appear to have a lower selectivity towards the diarylacetic acid product and higher selectivity for the diphenyldioxolanone. Previous reports of ion-exchanged zeolites for lactic acid conversion suggest that ion-exchange creates basic sites,[2-5] which may explain the difference in catalytic results for the K^+-exchanged zeolites in comparison to the H-form in our work. The K-exchanged zeolite also produced the highest quantity of unknown compounds, providing further evidence for a change in the nature of catalytic sites

compared with the H-form. Further characterisation of the nature and strength of acid sites present in the K-exchanged zeolites would have been informative here, but we did not do any further characterisation of this nature. For example, acidity and basicity of the zeolites can be measured by temperature-programmed desorption of probe molecules. Adsorption of ammonia can be used to probe acidity and adsorption of CO_2 can be used to probe basicity.[4, 22] The results of this characterisation method give an indication of the quantity and strength of the acid and base sites present in the zeolite. Ion-exchanged zeolites tend to have a decreased density of acid sites and an increased density of basic sites, which can influence reactions such as acrylic acid dehydration[2-5, 21], cracking of alkanes[23], Knoevenagel and aldol condensations of benzaldehyde.[22]

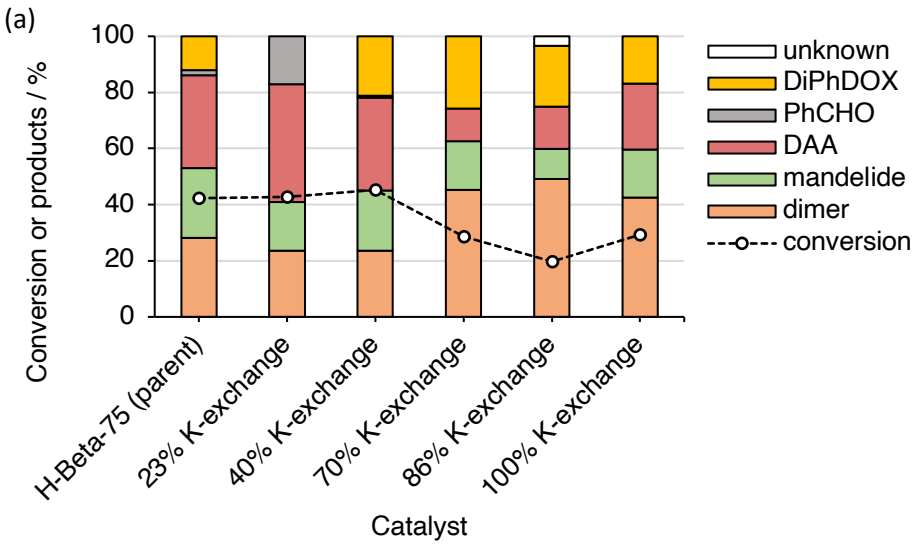

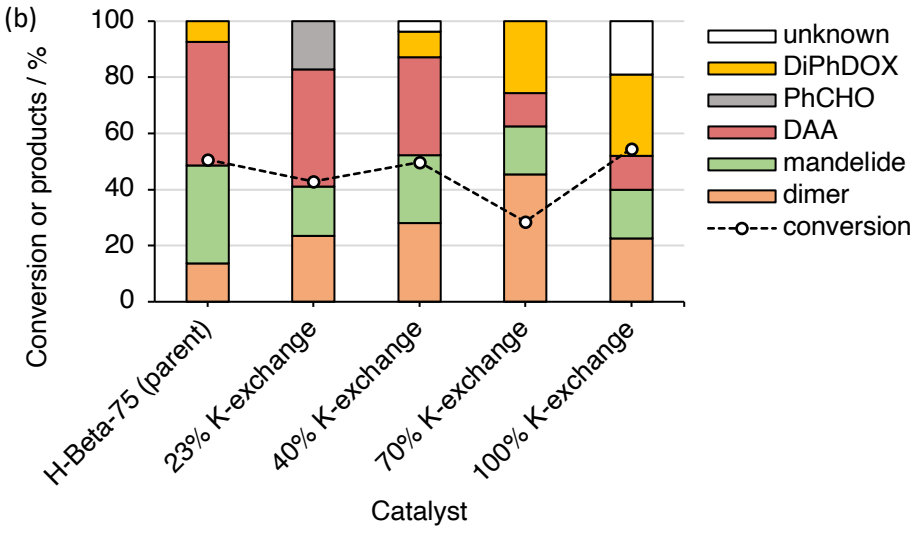

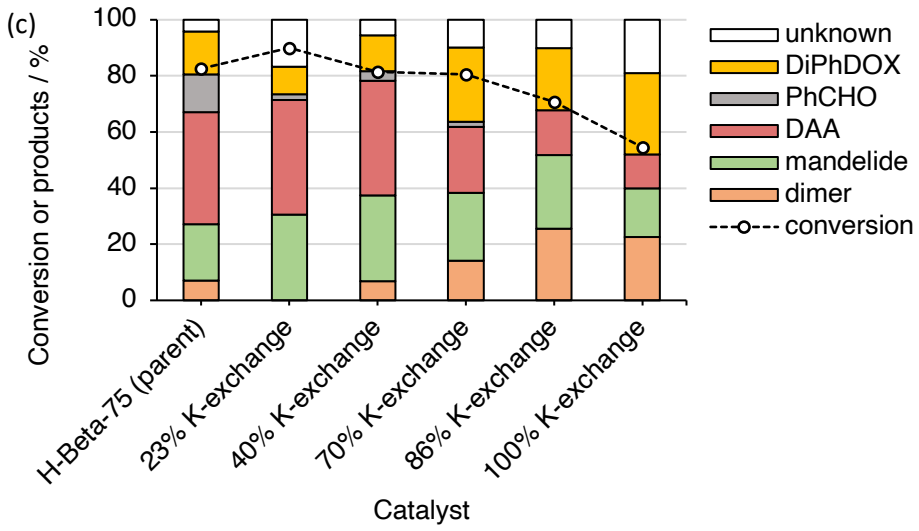

Figure 18 Selectivity at (a) low conversion (20-40%), (b) moderate conversion (30-60%) and (c) high conversion (up to 90%) conversion of mandelic acid catalysed by K-exchanged zeolite Beta-75 of varying extent of K^+-exchange from 0 to 100%. Different conversions were achieved by adjusting the reaction time. In the case of the high conversion reactions, some unknowns were formed that could not be assigned. The ^{1}H NMR peaks were integrated and are accounted for in the quantification. Conditions: 0.2 g mandelic acid, 0.13 g zeolite, 20 ml mixed xylenes, reflux at 160 °C.

3.2.5 Effect of Mesopore Treatment of H-Beta-75 Zeolite on Mandelic Acid Conversion

To assess the effect of the textural properties of zeolite H-Beta-75 on the conversion of mandelic acid, a series of catalysts were made using a top-down modification method known as “base leaching”.[24, 25] In this method, a base and a template are used. The base acts on the zeolite by breaking Si-O bonds and removing silicon from the zeolite by desilication. The removal of silicon creates voids in the zeolite framework and can result in mesopores through optimisation of the reagents and conditions used. The literature suggests that use of a template such as tetrapropylammonium bromide (TPABr) helps to preserve the original microporosity of the parent zeolite.[24, 25] The goal of this method is to make a zeolite with mesopores that are interconnected with the original microporosity, which can lead to improved accessibility to catalytic sites in the micropores and reduced deactivation.[26] Here, we used a previously reported method[25] to treat the H-Beta-75 zeolite. The zeolite is suspended in NaOH solution (concentrations from 0.05 M to 0.20 M), with constant amounts of TPABr (Figure 19) and stirred for 30 minutes at 65 °C. The results are shown in Table 9. As the base concentration was increased, the Si/Al of the zeolites decreased due to desilication. The Si/Al ratio of the zeolite also affects the degree of desilication, with greater Al content said to reduce the

degree of desilication due to repulsion between negatively charged Al in the zeolite framework and the negatively charged base, in this case hydroxide.[25, 27, 28]

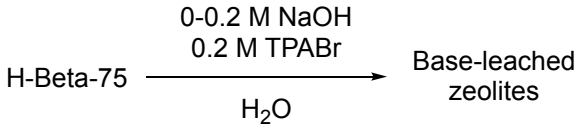

TPABr:

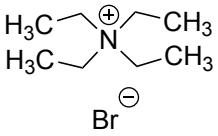

Figure 19 Reagents for base leaching of zeolite H-Beta-75. Conditions: stirred at 65 °C for 30 minutes.

Nitrogen porosimetry was used to analyse the textural properties of the base-leached zeolites, with the surface areas, micropore volume and mesopore volume calculated via BET, t-plot and BJH methods, respectively. Figure 20 shows the adsorption isotherms and Table 9 shows the surface area and pore volume data. For NaOH concentrations of 0.05 and 0.10 M, there was very little change in the textural properties relative to the parent zeolite despite EDXRF analysis suggesting that desilication had occurred. However, on increasing base concentration to 0.15 and 0.20 M, an increase in both the BET surface area and the mesopore volume were observed. Micropore volume remained similar, however a slight decrease may have occurred at 0.20 M NaOH, suggesting some loss of the zeolite micropore structure as a result of the higher base concentration and degree of desilication.

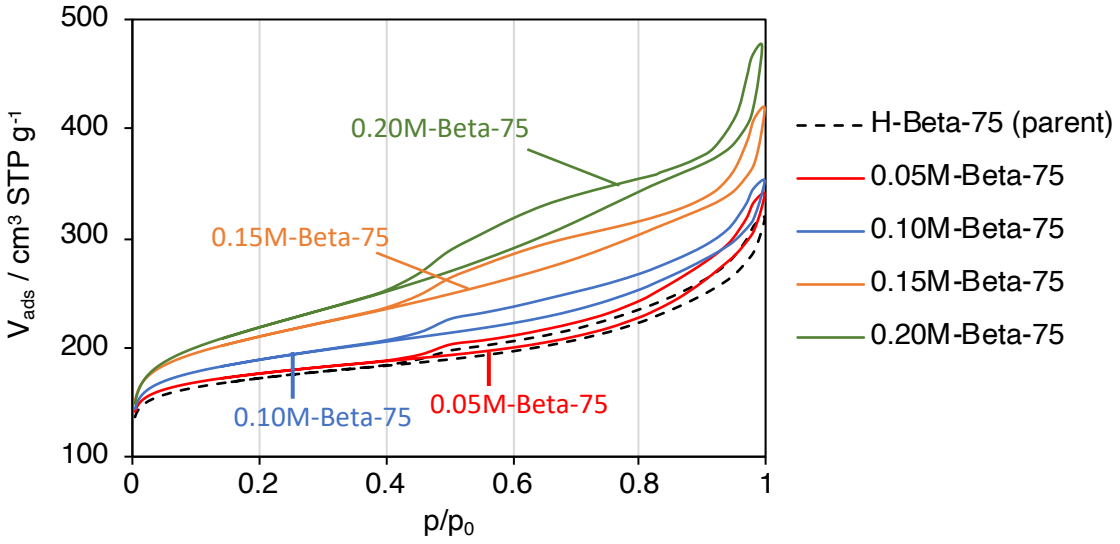

Figure 20 N_2 adsorption isotherms of the base-leached H-Beta zeolites.

Table 9 Base concentrations used in base leaching of H-Beta-75 zeolite and resultant Si/Al and textural properties of the zeolite.

Ref	NaOH conc^{n} / M	Si/Al [(a)]	BET Surface Area / $m^2\ g^{-1}$	V_{micro}[(b)] / $cm^3\ g^{-1}$	V_{meso}[(c)] / $cm^3\ g^{-1}$	V_{total}[(d)] / $cm^3\ g^{-1}$
H-Beta-75	-	53.0	635	0.19	0.10	0.29
0.05M-Beta-75	0.05	50.4	651	0.20	0.12	0.32
0.10M-Beta-75	0.10	47.5	696	0.19	0.12	0.31
0.15M-Beta-75	0.15	42.7	767	0.18	0.25	0.43
0.20M-Beta-75	0.20	39.1	790	0.16	0.38	0.54

(a) EDXRF; (b) t-plot method; (c) $V_{meso} = V_{total} - V_{micro}$; (d) BJH method.

Finally, these catalysts were tested for mandelic acid conversion using mixed xylene as the solvent. The results at around 60% conversion (2 hours reaction time) are shown in Figure 21. The amount of catalyst added was varied to account for the difference in Si/Al ratio caused by the desilication, such that the amount of Al present (and hence, Brønsted acid sites) remained roughly constant for all five reactions. The results show that the base leaching had very little effect on the selectivity of the catalysts. The slight variation in the ratio of products may be due to experimental variation, as the difference is small. Repeat runs were not carried out, so this cannot be said with certainty. The slight decrease in conversion for 0.20M-Beta-75 may be due to slight variation between reaction runs, but it could also be an effect of the base concentration used. As this was the strongest base concentration used, the degree of desilication was highest and this may have begun to affect the crystallinity of the zeolite. These results show that there is very little difference in the catalytic activity of the parent H-form zeolite and any of the base leached zeolites, despite the BET measurements showing that mesopores were present. This may infer that the accessibility to internal porosity plays little role in the reaction outcome and that external acid sites may be the predominant active site for these reactions, or that internal transport limitations are not a key factor limiting catalysis. Alternatively, given that the parent zeolite H-Beta-75 already contained a significant mesopore volume (as shown in Table 9), the generation of additional mesopore volume had little effect on activity. Calculations were later carried out to estimate the approximate cross-sectional area of the starting material and key reaction intermediates and products. These results are discussed in section 5.2.8 and give further insight into the role of zeolite porosity in the conversion of mandelic acid.

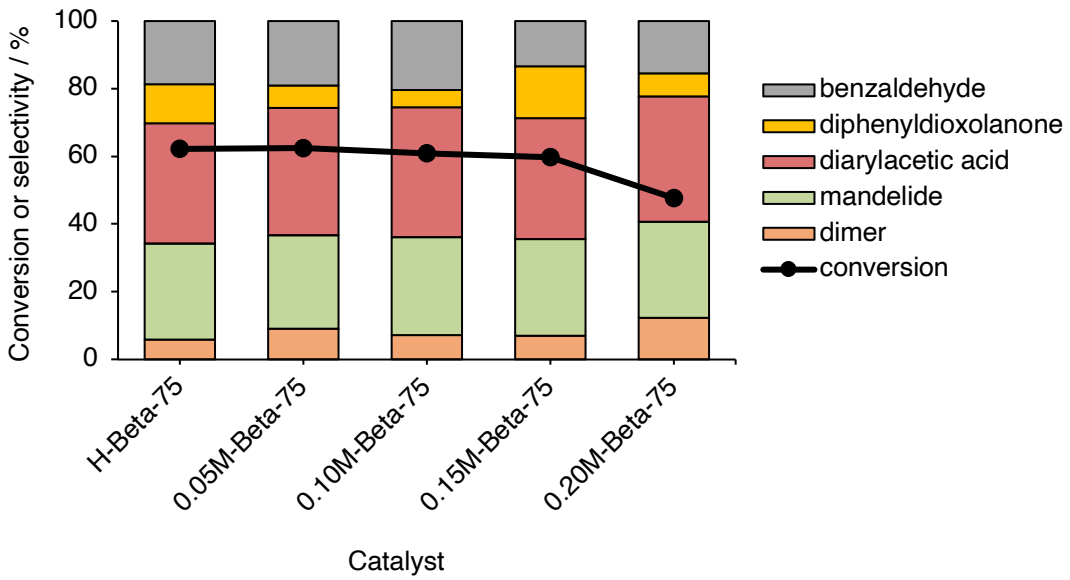

Figure 21 Product distributions for the conversion of mandelic acid by base-treated Beta-75 zeolites. Conditions: 0.2 g mandelic acid, 20 ml mixed xylenes, reflux with Dean-Stark trap (Oil bath T = 160 °C, T_b + 20 °C), zeolite mass added was proportional to Si/Al ratio to give 3 mol % Al relative to mandelic acid.

3.2.6 Effect of Reaction Solvent on Mandelic Acid Conversion of Catalysed by H-Y-30 Zeolite

Following the catalyst screening results, where we found that zeolite H-Y-30 showed high selectivity to diarylacetic acids in mixed xylene, we further investigated the reaction of mandelic acid with various other aromatic solvents. It was found that this reaction occurred in all aromatic solvents tested: toluene, m-xylene, o-xylene, p-xylene, chlorobenzene and mesitylene. The reaction profile was plotted for each solvent by conducting a series of reactions of various duration in each solvent. Each point in Figure 22 represents an individual reaction. It was found that both the selectivity to diarylacetic acids and the rate of conversion of mandelic acid were highly solvent-dependent. The lowest rate of conversion was observed when toluene was used as solvent, and the highest rate was observed in mixed xylene. This observed change in the rate of conversion correlated with the boiling point of the solvent, with higher boiling point solvents increasing the rate of conversion.

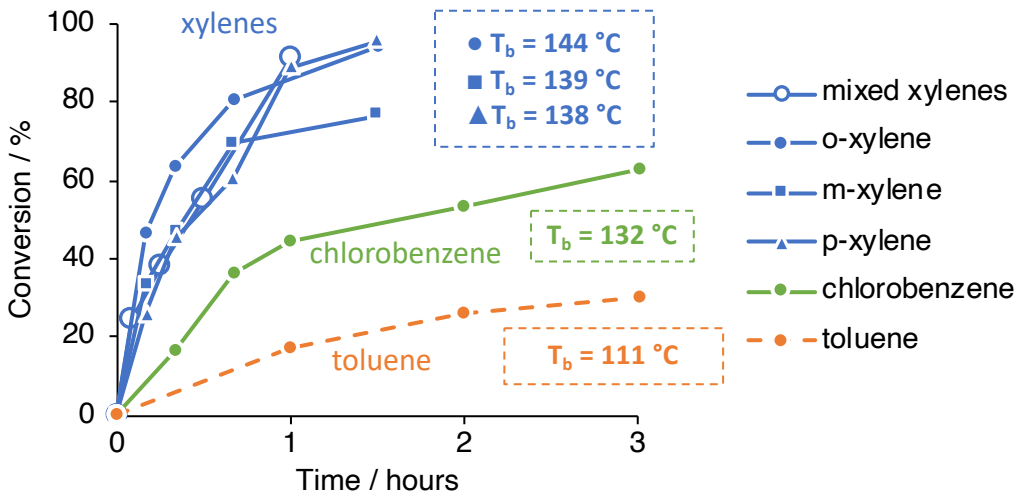

Figure 22 Reaction-time profiles for the zeolite-catalysed conversion of mandelic acid by H-Y-30 zeolite in various aromatic solvents. Solvent boiling points are annotated on the figure. Conditions: 0.2 g mandelic acid, 0.13 g zeolite H-Beta-75, 20 ml solvent, reflux at T_b + 20 °C.

Not only does the solvent choice affect the rate of reaction. Figure 23 shows product selectivity in different aromatic solvents at similar mandelic acid conversion of approximately 50%. These results suggest that the higher boiling solvents lead to higher selectivity to the diarylacetic acids.

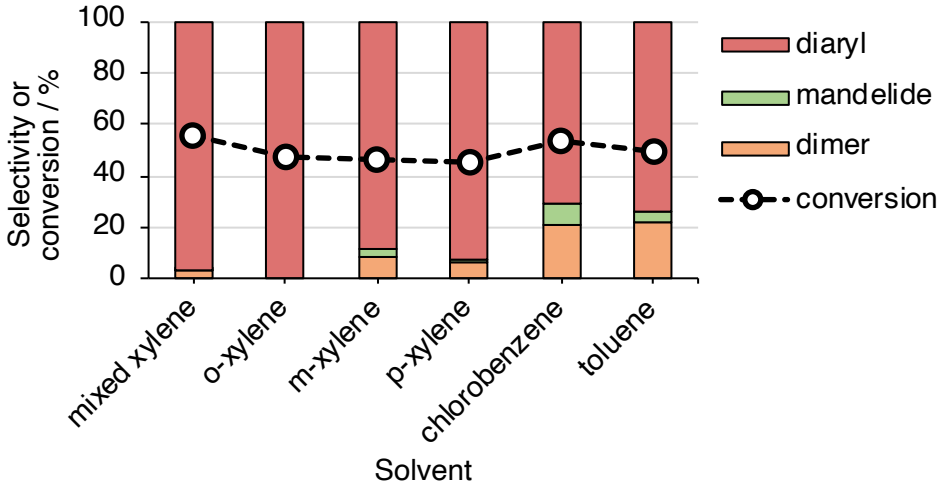

Figure 23 Selectivity towards different products at approximately 50 % conversion. Conditions: 0.2 g mandelic acid, 0.13 g zeolite H-Beta-75, 20 ml solvent, reflux at Tb + 20 °C.

As well as the trends in rate and selectivity with solvent boiling point, the presence of different substituent patterns on the aromatic ring could also influence the reaction. Methyl substituents are electron-donating and so activate the aromatic ring to make it a better nucleophile. Chlorine substituents are electron-withdrawing, so have the opposite effect. This may explain the lower selectivity to diarylacetic acids in chlorobenzene in comparison to xylene. As well as the type of substituents, the substitution pattern will affect how the substituents influence nucleophilicity of the ring. Methyl substituents are

ortho/para-directing. This means that the methyl substituents in para- and ortho-xylene would have an antagonistic effect (their directing effects cancel out) whilst in meta-xylene they will have a reinforcing or cooperative effect (Figure 24). However, this is not apparent in the results, with the highest selectivity observed in o-xylene and the lowest in m-xylene. This is the converse of what would be expected from purely electronic effects and suggests that this is not the only factor affecting the selectivity. For example, the higher boiling point solvents may facilitate more efficient removal of water generated in the reactions to push equilibria towards the products of the condensation reactions.

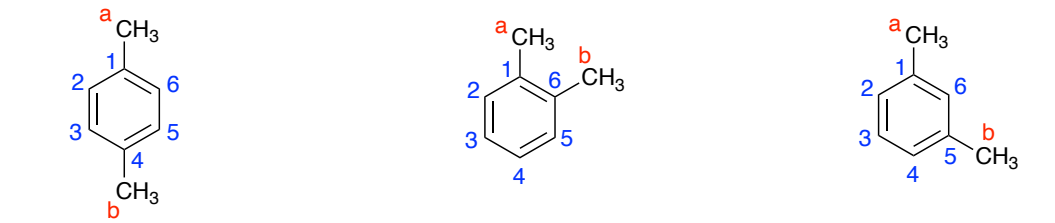

Figure 24 Origin of potential antagonistic and cooperative substituent effects when mixed xylene acts as a nucleophile in the synthesis of diarylacetic acids.

Adsorption of xylene isomers into zeolites varies depending on the isomer and has been widely studied in catalytic processes such as toluene disproportionation.[29, 30] The linear shape of p-xylene means that it is the smallest of the three isomers, and so will be least likely to suffer from diffusion limitations. As will be discussed in more detail later in this chapter (section 5.2.8), the accessibility of the reagents and products within the micropore networks of the zeolites studied is evaluated through computational methods.

Analysis of the mix of diarylacetic acid products in mixed xylene showed that the ratio of diarylacetic acids made from m-, p- and o-xylene very closely reflected the ratio of the isomers in the original mixed xylene solvent. This suggests that the trends in selectivity for reactions run in each of the xylenes (Figure 23) may be due to solvent boiling point or experimental variability, as the reaction in mixed solvent did not appear to be selective towards any particular isomer.

3.2.7 Mandelic Acid Conversion in an X-Cube Liquid Phase Flow Reactor

In our work investigating the zeolite-catalysed reactions of mandelic acid under batch conditions, we found that the zeolite framework type and reaction solvent were highly influential on the conversion and selectivity. Next, our attention turned to the possibility of conducting analogous reactions under flow conditions.

The conversion of glycolic acid to glycolide and lactic acid to lactide has been shown to work under flow conditions.[17, 31] As discussed earlier, this can be done via condensation of the free acid or transesterification of the methyl ester. Methyl glycolate and methyl lactate are liquids at room temperature, meaning that they can be fed into a flow reactor prior to vaporisation and mixing with inert gas. Methyl mandelate on the other hand is a solid at room temperature (m.p. = 56-58 °C[32]). Furthermore, previous reports suggest that *rac*-mandelide has poor solubility in common organic solvents and is not stable when heated above its melting point (248 °C)[10, 12], suggesting it would be likely to decompose at the elevated temperatures used for the gas phase processes (*ca*. 250-300 °C). As a result, we decided that gas phase flow reactions were not suitable for converting mandelic acid to mandelide, due to the constraints of the phase transition temperatures, decomposition of the products and potential for clogging the flow reactor with solid material. We decided instead to use a liquid phase reactor, a ThalesNano X-Cube (Figure 25a). In this reactor, the reagents are dissolved in a suitable solvent to make a feed solution which is then fed into the reactor via an HPLC pump.

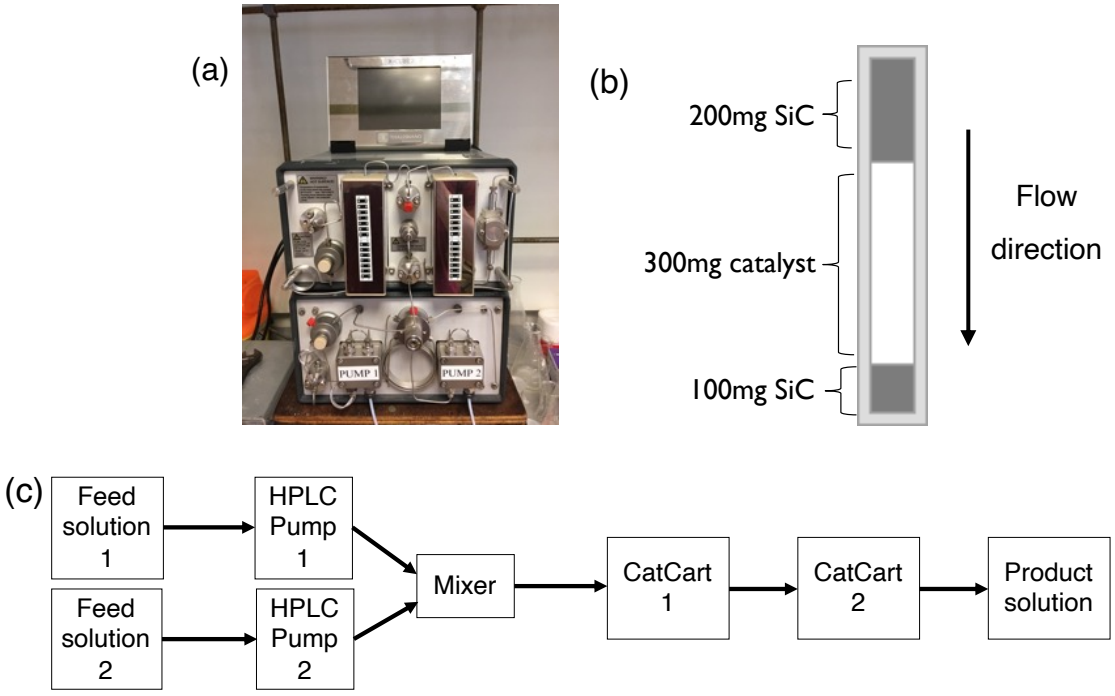

Figure 25 (a) X-Cube flow reactor. (b) Loading of the catalyst cartridge ("CatCart") used in these experiments. (c) Flow diagram summarising the process of the X-Cube flow reactor.

A suitable solvent for this process needed to fit several criteria. The solubility of mandelic acid needed to be sufficient for it to remain in solution through the reactor. The solvent should also dissolve any products that form in the catalyst bed, so that they also remain solubilised after the solution has left the heated zone of the catalyst bed. Insufficient solubility would lead to blockage of the reactor, particularly in the narrow stainless-steel tubing (1/6th inch) that connects the heated zones. Room temperature solubility wasn't a

necessary consideration for the batch (glassware) reactions described previously. Despite a lack of solubility at room temperature, when the temperature was increased to the reflux temperature of the solvents used, the solubility of mandelic acid was sufficient.

The non-polar solvents (cyclohexane, methylcyclohexane and aromatic solvents) previously explored for batch reactions were not suitable due to a lack of solubility at room temperature – mandelic acid and mandelide are only soluble in polar organic solvents. Acetonitrile was previously reported to solubilise mandelide and poly(mandelic acid)[9] and we found that it also dissolved mandelic acid. Other polar organic solvents such as ethers and alcohols may have been suitable in terms of solubility, but we reasoned that they were likely to undergo unwanted side reactions catalysed by the zeolite. Therefore, we chose acetonitrile as a solvent for these reactions.

When acetonitrile was tested as a solvent under batch conditions, we did not observe any conversion of mandelic acid in an overnight reaction at reflux (80 °C). However, the X-cube flow reactor used was able to handle solvents above their boiling point. Unlike the batch reactions, in the flow reactor we were not limited by the solvent boiling point and were able to increase the temperature above 80 °C.

We tested catalysts H-Beta-75, H-ZSM5-45 and H-Y-30. Catalysts were pressed and sieved to 60-80 mesh size (177-250 μm) and packed into an X-Cube CatCart (along with silicon carbide). These were added to the CatCart as follows (shown in Figure 25b): 200 mg of silicon carbide, then 300 mg pressed and sieved zeolite catalyst, then a further 100 mg silicon carbide. The cartridges were sealed and loaded into the second heating block of the X-Cube reactor. A blank cartridge containing only silicon carbide was used in the first heating block. Feed solutions of mandelic acid in acetonitrile were prepared at a concentration of 1 g per 100 ml.

Reactions were run over H-Beta-75 at temperatures between 100 °C and 180 °C and flow rates between 0.1 ml min^{-1} and 1.5 ml min^{-1}. At temperatures below 140 °C, no products were observed by ^{1}H NMR spectroscopy. At 140 °C and 0.1 ml min^{-1} we observed a small amount of dimer and mandelide in the product ^{1}H NMR spectrum (Figure 26). It was only at this lowest flow rate that any product peaks were observed, suggesting that the residence time possible in this flow set up was not sufficient to achieve significant conversion. The peaks in the methine region of the spectra (shown in Figure 26b) were indicative of residual mandelic acid 3a (5.25 ppm) dimer 3b (5.31, 5.40, 5.96, 5.98 ppm) and mandelide 3c (5.87 and 6.14 ppm).

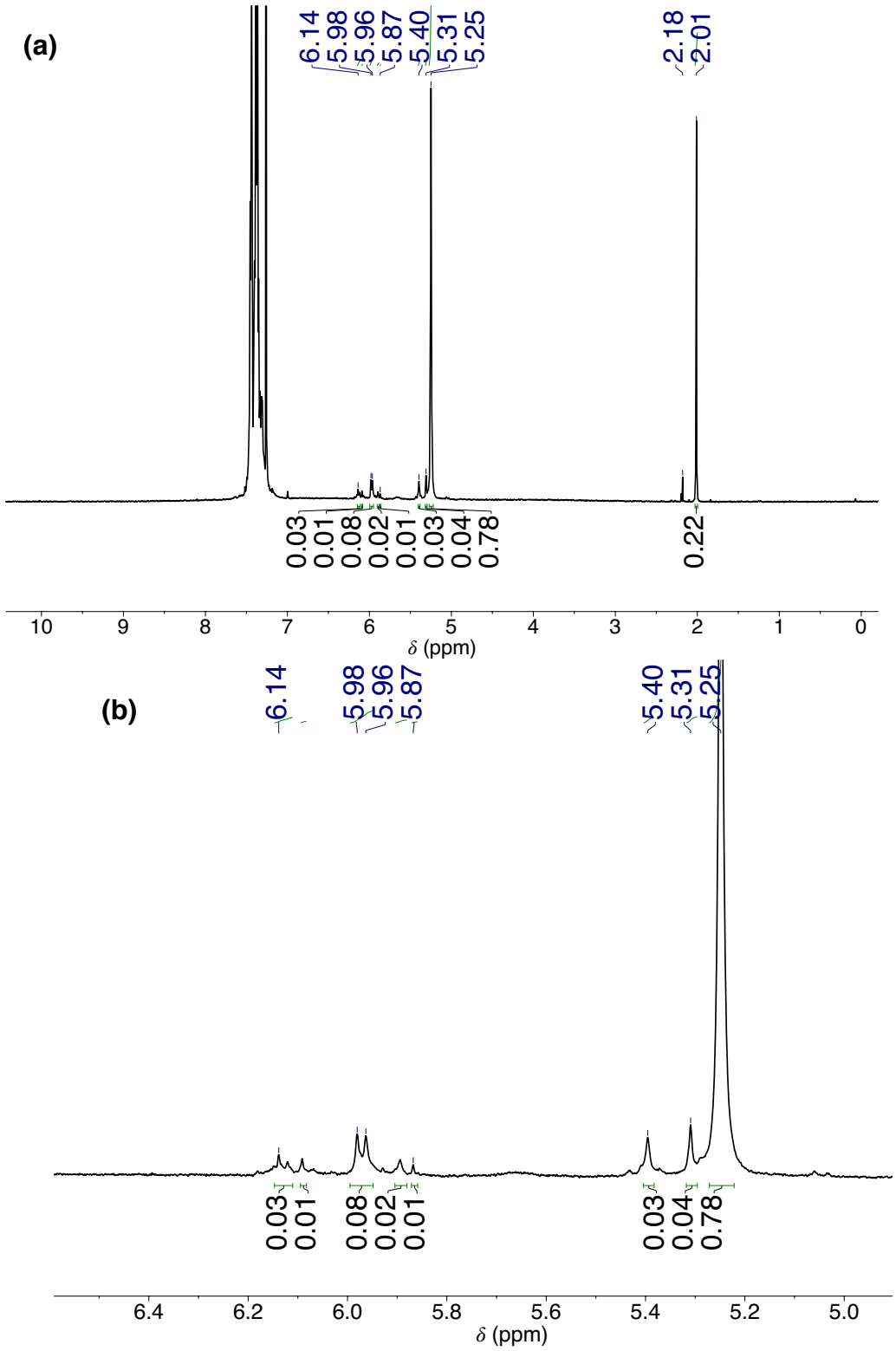

Figure 26 (a) ^{1}H NMR (400 MHz, $CDCl_3$) spectrum of the products obtained over H-Beta-75 at 140 °C and 0.1 mL min^{-1} flow rate. (b) the same spectrum zoomed in on 5-6.5 ppm methine region.

The acetonitrile solvent was removed from the crude product solution and the sample dissolved in $CDCl_3$. The peak at 2.18 corresponds to residual acetonitrile. The spectrum in Figure 26 contains another significant peak at 2.01 ppm, observed at greater intensity in the spectra of products obtained for reactions at higher temperatures. NMR spectroscopic analysis (^{1}H and ^{13}C) suggested that this peak corresponded to acetamide.

A small amount of dimerisation of mandelic had occurred (a condensation reaction liberating water) and acetamide could form from the reaction of acetonitrile with this water. However, the amount of acetamide present far exceeded the amount of mandelic acid conversion, so it is not clear what the source of the water would be in the flow reactor. A sample of acetamide was isolated from the crude products by washing with diethyl ether. The ^{13}C spectrum (in D_2O) of the dried aqueous layer is shown in Figure 27. This spectrum is consistent with a mixture of acetonitrile (1.47, 119.63 ppm)[33], mandelic acid (73.50, 127-138, 176.85 ppm) and acetamide (21.86, 177.99 ppm).[34]

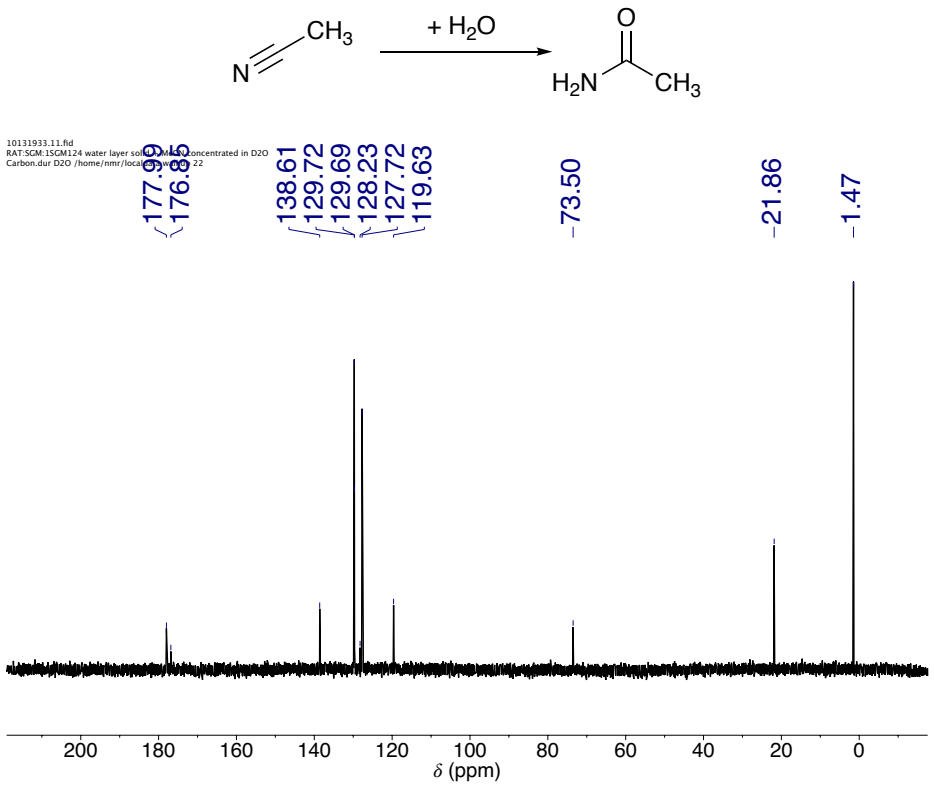

Figure 27 ^{13}C NMR (101 MHz, D_2O) spectrum of the compounds present in the aqueous layer after washing the products obtained over H-Beta-75 at 140 °C and 0.1 mL min^{-1} flow rate with diethyl ether. The peaks in the spectrum can be assigned to mandelic acid, acetonitrile (reaction solvent) and acetamide (byproduct).

Further experiments were run to assess the conversion of mandelic acid in the flow set up at temperatures above 140 °C, using a flow rate of 0.1 ml min^{-1}. The ^1H NMR spectra of the crude products are shown in Figure 28. Conversion was low (less than 20%) for temperatures below 190 °C. At 190 °C, conversion increased significantly with several peaks observed in the methine region of the ^1H NMR spectrum and at 10 ppm (benzaldehyde). The solutions collected from the reactor were dried by rotary evaporator before preparing NMR samples, so the size of the benzaldehyde peak is qualitative only, due to loss of benzaldehyde in the rotary evaporator. A sharp peak at 5.87 and a broad

peak at around 6-6.1 ppm were present. The sharp peak at 5.87 is consistent with *meso*-mandelide. Based on literature data for poly(mandelic acid), a broad resonance around 6 ppm suggests is typical for oligomers and polymers of mandelic acid.[10, 11, 35] The presence of the broad peak in our results suggested some oligomerisation may have occurred at this high temperature. As well as a change in product distribution at this high temperature, the occurrence of blockages in the reactor also became more frequent, possibly due to the presence of insoluble oligomers. Furthermore, even at this high temperature, measurable conversion was only achieved at a flow rate of 0.1 ml min^{-1}. Increasing the flow rate resulted in a drop in mandelic acid conversion back to low levels. As a result, it took a significant amount of time to collect product due to the combination of low flow rate and relatively low concentration of mandelic acid in the feed (0.1 ml min^{-1} and 0.01 g ml^{-1}, respectively). As the solution concentration was already at a level that resulted in frequent blockages of the reactor, it was not possible to increase the concentration.

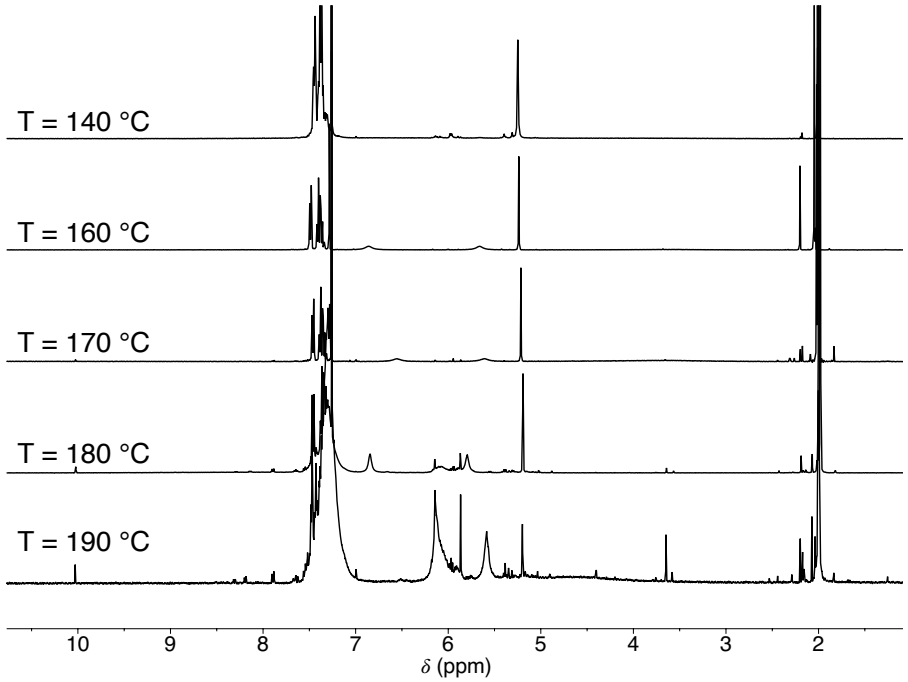

Figure 28 ^{1}H NMR (400 MHz, $CDCl_3$) of the products obtained between 140-190 °C using an X-Cube flow reactor. Conditions: 1g mandelic acid per 100 mL MeCN, flow rate = 0.1 ml min^{-1}, catalyst: 300 mg Zeolite H-Beta-75.

The use of H-ZSM5-45 as a catalyst lead to a small amount of dimer formation at 160 °C and approximately 20% mandelic acid conversion (Figure 29a). Increasing the temperature to 180 °C lead to an increase in benzaldehyde formation and the appearance of some unassigned peaks including 2 broad peaks at 5-6 ppm, a peak at 3.5 ppm and several peaks around 2-2.5 ppm (Figure 29b).

Increasing the reactor temperature further to 185 °C resulted in an immediate blockage of the reactor. It was possible to unblock the reactor by switching the feed to fresh solvent and purging the reactor at a flow rate of 1 ml min^{-1} for 10 minutes. An orange solution then eluted from the reactor, the ^{1}H NMR spectrum of which is shown in Figure 29c. Purging the reactor for a further 10 minutes was not sufficient to obtain a spectrum free of mandelic acid and products (Figure 29d), suggesting a significant amount of material had precipitated within the reactor or adsorbed to the catalyst. Acetamide was again present, particularly at a reaction temperature of 180 °C, which is shown clearly in the ^{13}C NMR spectrum of the products (Figure 30). The peaks at 22 and 273 ppm corresponding to acetamide were significantly larger than those corresponding to mandelic acid at 73 ppm and around 128 ppm. This suggested that the reaction of the acetonitrile solvent was the major process occurring at this temperature.

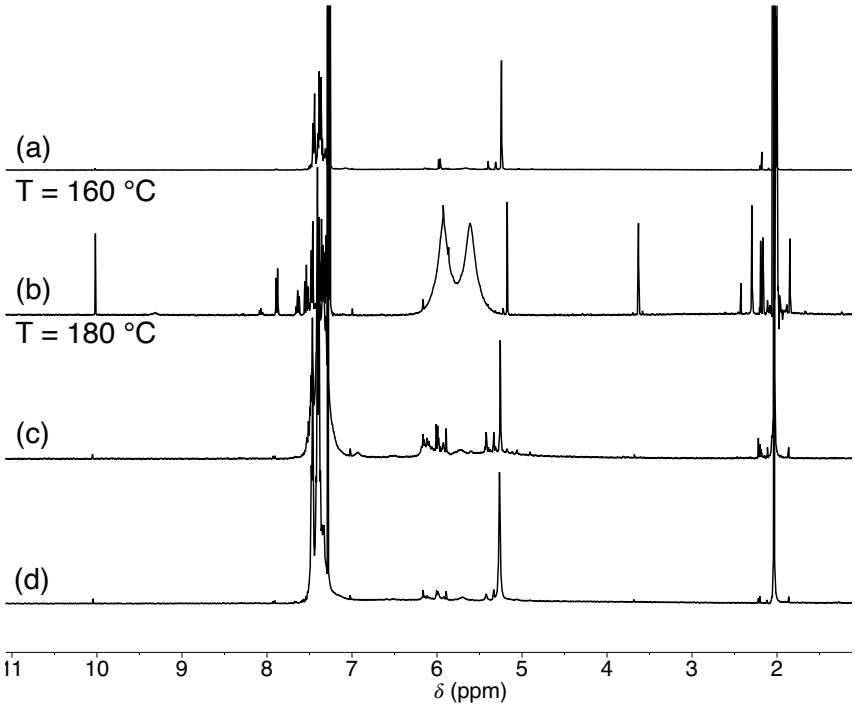

Figure 29 ^{1}H NMR (400 MHz, $CDCl_3$) of the products obtained at (a) 160 and (b) 180 °C using an X-Cube flow reactor. After increasing the temperature to 185 C, the reactor became blocked. Cleaning of the reactor with excess solvent yielded an orange solution. (c) and (d) show the ^{1}H NMR spectrum of the residue left after rotary evaporation of this solution. (c) shows the solution obtained initially after unblocking the reactor and (d) shows the solution obtained after 10 minutes of cleaning. Conditions: 1 g mandelic acid per 100 mL MeCN, flow rate = 0.1 ml min^{-1}, catalyst: 300 mg Zeolite H-ZSM5-45.

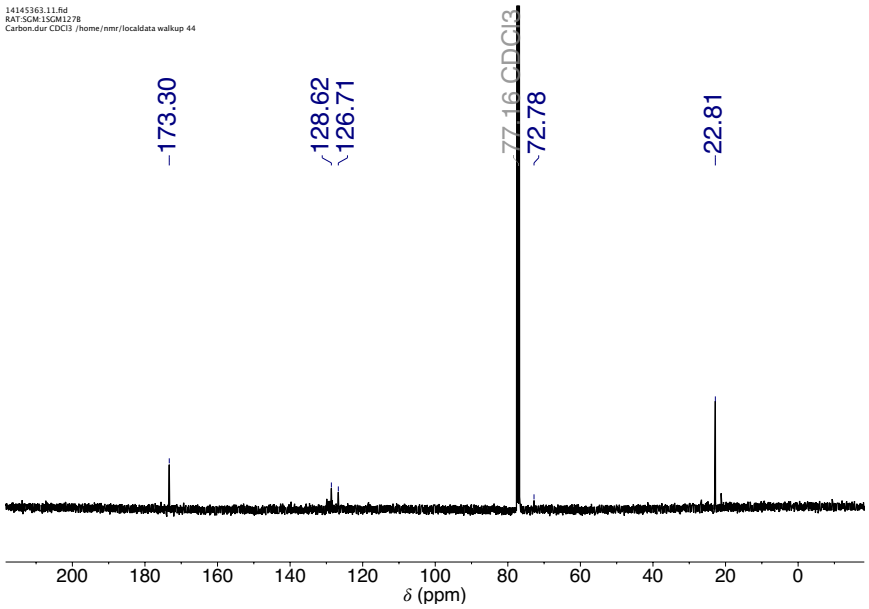

Figure 30 ^{13}C NMR (101 MHz, $CDCl_3$) of the products obtained at 180 °C using an X-Cube flow reactor. Conditions: 1 g mandelic acid per 100 mL MeCN, flow rate = 0.1 ml min^{-1}, catalyst: 300 mg Zeolite H-ZSM5-45.

As a result of the poor solubility, high temperatures required, solvent instability and poor selectivity of the catalysts tested, the use of liquid phase flow reactor to convert mandelic acid into mandelide did not appear promising and no further work was carried out.

3.2.8 Approximate Critical Diameter of Mandelic Acid and Key Products

We suspected that the size of mandelic acid and its products would be large in comparison to the size of the micropores of the zeolite frameworks screened in our experiments. When reactants are large relative to the pore size, accessibility to the active sites within the pores can be reduced. Furthermore, the shape-selective effects of the zeolite catalyst will not be realised.

We used Scigress to perform a structure minimisation using the B3LYP level of theory. The structures were then visualised using VMD visualisation software to manually determine an approximation of the critical diameter including the van der Waal's radii of the atoms. This diameter was then computed using some simple code developed by another member of our research group. The results are summarised in Table 10.

Table 10 Approximate critical diameter of mandelic acid and selected products.

Molecule	Critical Diameter / Å
mandelic acid	7.1
p-xylene	6.7
Benzaldehyde	6.7
meso-mandelide	7.3
diarylacetic acid (p-xylene)	8.4
2,5-diphenyl-1,3-dioxolan-4-one	7.4

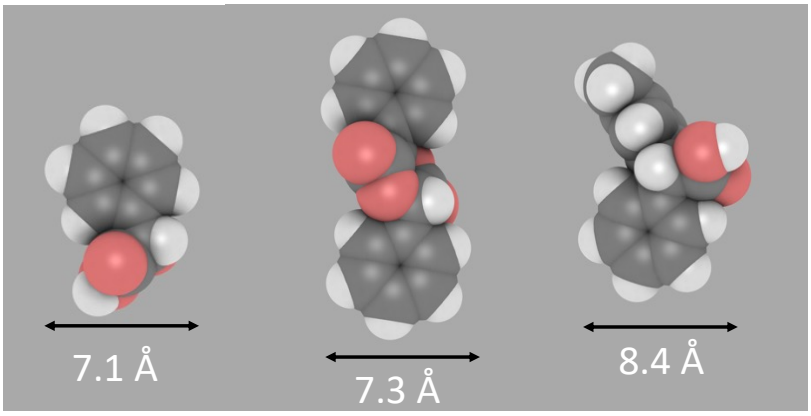

Figure 31 Approximate critical diameter perpendicular to long axis of the molecule. Image produced using iRASPA. Left: Mandelic acid (1b), middle: mandelide (3b), right: diarylacetic acid (6b, solvent = p-xylene).

The critical diameter approximated by our method for p-xylene is in good agreement with a value calculated by another method (6.62 Å[36]). The diameters of p-xylene and benzaldehyde in Table 10 were slightly smaller than the largest nominal pore widths of the zeolites possessing 12 membered rings (e.g., Beta at 6.7 Å and Y at 7.4 Å). Therefore, they are likely to be able to access the internal micropore system of these zeolites. Furthermore, mandelic acid is of a similar diameter (7.1 Å) as the pore width of zeolite Y (7.4 Å). One report showed that a probe with an approximate kinetic diameter of 7.2 Å adsorbed into zeolite Y (Si/Al 2.6) in reasonable amounts, whereas a larger 10.1 Å probe did not.[37] Therefore, it appears likely from our calculations that mandelic acid and xylenes, the reactants for the formation of diarylacetic acids, can access the micropores of zeolite Y. The nominal pore width of Beta zeolite is smaller than that of zeolite Y. The critical diameters calculated for mandelic acid, mandelide and the diarylacetic acid are all larger than the pore width of zeolite Beta, suggesting that none of these molecules can be accommodated within micropores of zeolite Beta. The 7.4 Å channels in zeolite Y are not large enough to accommodate the diarylacetic acids. However, these channels are connected with “supercages” in zeolite Y. These supercages are approximately 13 Å in

diameter[38] and therefore could accommodate the formation of diarylacetic acids. However, these products would be too large to exit the supercages via the narrower 7.4 Å channels that connect the supercages to the external surface of the zeolite.

This is interesting given that our catalytic results showed that H-Beta-75 can produce both mandelide and diarylacetic acids, both of which have critical diameters larger than the nominal pore width of Beta. As a result, it is unlikely these reactions over H-Beta are governed by the reactant, product and transition shape selectivity described earlier in the introduction to this thesis.[39-41] The higher silica (and hence, low Brønsted acid density) Beta and Y zeolites gave highest conversion. These zeolites also possess a high degree of mesoporosity (see Table 4 and Table 5) of this chapter and Appendix 2 for BET measurements). This suggests that presence of mesopores could be important for high catalytic activity. It is difficult to conclude that the increased activity is a result of improved transport to and from the micropores in these hierarchical catalysts given the approximate size of the products. An alternative explanation may be needed for the activity of H-Beta and the high selectivity of zeolite Y. Whilst traditional shape selectivity (reactant, product and transition state) requires the reactions to occur within the micropores, other modes of shape selectivity are known, including effects associated with reactions that occur on or near the external surface of the zeolite.[41] These include the pore mouth and key-lock mechanisms, the window effect and the nest effect. Work is ongoing in our group to investigate the origin of the high selectivity of USY zeolite towards diarylacetic acid products of mandelic acid.

One explanation for the lack of selectivity of ZSM5, Beta and MOR is that reactions were occurring mostly on the external surface of the zeolites (i.e. not in the micropores). Whilst the diarylacetic acids tended to be the major product in the case of zeolite Beta, the high concentration of solvent molecules compared with mandelic acid may have contributed to this rather than any property of the zeolite. Mandelic acid would more likely to encounter solvent molecules than another molecule of mandelic acid (to make a dimer) or a molecule of benzaldehyde (to make DOX), due to the abundance of solvent molecules present. Given the likelihood that mandelic acid was unable to access the internal microporosity of zeolite Beta, this would also explain the results obtained for the hierarchical zeolites in section 5.2.5 where the development of mesoporosity made little difference to the results of catalytic tests. As a result, improving access the micropores would not influence reactions occurring on the external surface.

It is unclear why the ratio of *meso*- and *rac*-mandelide differs for zeolite H-Beta compared with *p*-TSA-catalysed reactions. As with zeolite Y and the diarylacetic acid, it seems likely that a framework effect is causing this difference between the zeolite and *p*-TSA.

According to the literature, *rac*-mandelide is more thermodynamically stable than *meso*-mandelide,[10, 11] and this was provided as the reason for the observed product ratio.[10, 11] In addition to differences in product formation, it is also possible that the degree of racemisation of *meso*-mandelide to *rac*-mandelide (Figure 32) is different dependent on the catalyst used. This racemisation would affect the observed product ratio and has previously been reported to occur more readily at higher temperatures and under basic conditions.[10]

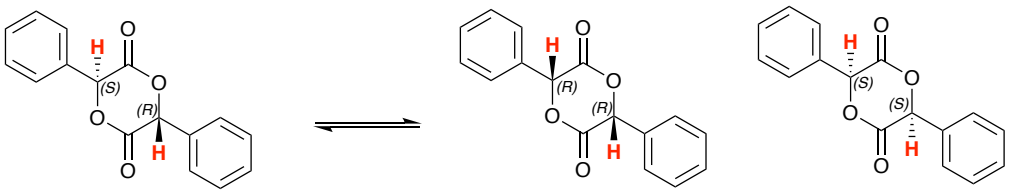

meso-mandelide

rac-mandelide

Figure 32 Racemisation of *meso*-mandelide due to labile methine protons (highlighted red).

3.3 Conclusions

The conversion of mandelic acid has been investigated over a range of commercial Brønsted acidic zeolites. It was found that a range of products can be formed, in contrast to lactic acid which can be selectively converted to lactide under the same conditions. In aromatic solvents, the zeolite-catalysed reactions of mandelic acid included dimerisation (by esterification), electrophilic aromatic substitution, decarbonylation to benzaldehyde, and reaction of benzaldehyde with mandelic acid to form 2,5-diphenyl-1,3-dioxolan-4-one. The activity and selectivity of zeolite catalysts was found to be highly framework-dependent.

The rate of conversion was significantly higher for H-Beta than for ZSM-5 under similar catalyst loading and Si/Al ratio. The conversion by ZSM-5 was found to plateau at around 35 % after 10 hours of reaction time, with no significant increase in conversion even when reaction time was increased up to 2 days. This was accompanied by a significant colour change of the catalyst, suggesting catalyst deactivation had occurred, which may explain the limited conversion. In the case of H-Beta, conversion was found to increase with increasing Si/Al ratio (the total amount of Al was kept roughly constant by adjusting the amount of zeolite added), with H-Beta-75 being the most active Beta zeolite tested. Whilst rate of conversion was improved compared with ZSM5, H-Beta was still not selective for any particular product.

In contrast to H-ZSM-5 and H-Beta, H-Y-30 was found to be highly selective in the conversion of mandelic acid, but not to the desired mandelide product. In aromatic solvents, the electrophilic aromatic substitution of the solvent by mandelic acid occurred,

with loss of water from the alpha-hydroxyl group of mandelic acid. This reaction occurred more rapidly than H-Beta catalysed conversion, with near full conversion achieved after 1 hour. This reaction was found to occur in a range of aromatic solvents, with the rate of largely dictated by the solvent boiling point, and hence reflux temperature. Lower selectivity was obtained in chlorobenzene compared with xylene and toluene, suggesting that the electron-withdrawing chloro-substituent may have influenced the reaction. However, as the reactions were run at reflux, this electronic effect was not studied for the different solvents at equivalent temperatures, so these results are not conclusive.

A non-aromatic solvent, methylcyclohexane, was tested and found to allow the highest mandelide yield of any solvent tested. The reaction time required was still long, in similarity with mandelide synthesis catalysed by p-TSA in mixed xylenes. The lack of aromatic solvent meant that the diarylacetic acids were not formed, which allowed for the increased mandelide yield. However, 2,5-diphenyl-1,3-dioxolan-4-one still formed simultaneously with mandelide. Analysis of the ratio of *meso* and *rac*-mandelide showed that the zeolite H-Beta-75 gave a higher proportion of the *meso* isomer in comparison to the reaction catalysed p-TSA reported in the literature and reproduced in our work (approximately 2:1 for H-Beta compared with 1:1 for p-TSA). Whilst changing the reaction solvent resulted in different conversion and selectivity for the H-Beta-75 zeolite, this ratio of *meso* and *rac*-mandelide remained unchanged in different solvents. This indicating that this ratio was specific to the Beta framework.

Zeolite modifications were also carried out, such as aqueous ion exchange with alkali metal cations and base leaching using basic conditions and organic templates. These modified zeolites were compared to the parent forms. We found that generation of mesopores in H-Beta through base leaching did not affect the conversion or selectivity, aside from a slight drop in conversion for the most severely desilicated catalyst. Aqueous ion exchange was found to be more influential. Exchanging the Brønsted acidic protons in the zeolite with various alkali metals led to a drop in conversion and, in most cases, a change in selectivity. Whilst the drop in conversion increased with increasing extent of ion exchange, probably due to loss of catalytically active Brønsted acid sites, we found that fully exchanged zeolites were still more active than a blank reaction run without catalyst. Non-Brønsted acidic sites in these materials may be able to catalyse reactions of mandelic acid, albeit at much slower rates, or aqueous ion exchange may not have fully removed all the Brønsted acid sites in the zeolite. Non-Brønsted acid sites could be those associated with the alkali metal introduced by ion exchange, or they could be silanol nests or extraframework alumina.

In addition to conversion of mandelic acid under batch conditions, we also attempted to use an X-Cube flow reactor. Acetonitrile was chosen as solvent and several catalysts were tested. We found that it was possible to catalyse some conversion of mandelic acid, but this required temperatures above 180 °C. At these temperatures, blockage of the reactor was frequent, probably due to the formation of oligomeric products and/or poor solubility of mandelic acid in acetonitrile. Obtaining any measurable conversion also required the lowest possible flow rate to be used, leading us to the conclusion that this flow reactor set up was not useful as a practical method for synthesising mandelide.

Finally, we used some simple calculations to approximate the critical diameter of mandelic acid and the observed products. We estimated that the aromatic solvents and benzaldehyde were small enough to access the zeolite micropores, but mandelic acid and all other products were larger than the pores of all zeolites tested, with the exception of the supercages of zeolite Y. A lack of selectivity in reactions catalysed by ZSM5, MOR and Beta could be explained by catalysis occurring predominantly on the external surface of the zeolite where shape selectivity effects would not dictate the reaction outcome.

We observed two changes for zeolite catalysts compared with homogeneous p-TSA. When H-Beta-75 zeolite was used, the *meso:rac*-mandelide ratio was higher than for p-TSA. Our calculations suggest that it is unlikely that these results can be attributed to shape selectivity of the internal micropore system, as the critical diameter of mandelide is larger than the nominal pore width of zeolite Beta. Mandelide and the diarylacetic acids would fit into the supercages of zeolite H-Y-30 but would be too large to exit the supercages via the 12MR (7.4 Å) windows. When H-Y-30 zeolite was used, diarylacetic acids were formed selectively. It is possible that alternative modes of shape selectivity such as the nest effect could be influential here given that diffusion via the 12MR channels seems implausible for these products and work to elucidate the origin of the selectivity in these reactions is ongoing.

3.4 References

1. De Clercq, R.; Dusselier, M.; Makshina, E.; Sels, B. F., Catalytic Gas-Phase Production of Lactide from Renewable Alkyl Lactates. *Angew. Chem. Int. Ed. Engl.* **2018,** *57* (12), 3074-3078.

2. Yan, B.; Liu, Z.-H.; Liang, Y.; Xu, B.-Q., Acrylic Acid Production by Gas-Phase Dehydration of Lactic Acid over K+-Exchanged ZSM-5: Reaction Variable Effects, Kinetics, and New Evidence for Cooperative Acid–Base Bifunctional Catalysis. *Ind. Eng. Chem. Res.* **2020,** *59* (39), 17417-17428.

3. Yan, B.; Tao, L.-Z.; Mahmood, A.; Liang, Y.; Xu, B.-Q., Potassium-Ion-Exchanged Zeolites for Sustainable Production of Acrylic Acid by Gas-Phase Dehydration of Lactic Acid. *ACS Catal.* **2017,** *7* (1), 538-550.

4. Yan, B.; Mahmood, A.; Liang, Y.; Xu, B.-Q., Sustainable production of acrylic acid: Rb+- and Cs+-exchanged Beta zeolite catalysts for catalytic gas-phase dehydration of lactic acid. *Catal. Today* **2016,** *269*, 65-73.

5. Sun, P.; Yu, D.; Tang, Z.; Li, H.; Huang, H., NaY Zeolites Catalyze Dehydration of Lactic Acid to Acrylic Acid: Studies on the Effects of Anions in Potassium Salts. *Ind. Eng. Chem. Res.* **2010,** *49* (19), 9082-9087.

6. Dusselier, M.; Van Wouwe, P.; Dewaele, A.; Jacobs, P. A.; Sels, B. F., Shape-selective zeolite catalysis for bioplastics production. *Science* **2015,** *349*, 78-80.

7. Narmon, A. S.; Leys, E.; Khalil, I.; Ivanushkin, G.; Dusselier, M., Brønsted acid catalysis opens a new route to polythiolesters via the direct condensation of thiolactic acid to thiolactide. *Green Chem.* **2022,** *24* (24), 9709-9720.

8. Hoefnagel, A. J.; van Bekkum, H., New zeolite-catalyzed ring-closure reaction of benzilic acid. *Microporous Mesoporous Mater.* **2000,** *35-36*, 155-161.

9. Espartero, J. L.; Rashkov, I.; Li, S. M.; Manolova, N.; Vert, M., NMR Analysis of Low Molecular Weight Poly(lactic acid)s. *Macromol.* **1996,** *29* (10), 3535-3539.

10. Liu, T. Q.; Simmons, T. L.; Bohnsack, D. A.; Mackay, M. E.; Smith, M. R.; Baker, G. L., Synthesis of polymandelide: A degradable polylactide derivative with polystyrene-like properties. *Macromol.* **2007,** *40* (17), 6040-6047.

11. Graulus, G. J.; Van Herck, N.; Van Hecke, K.; Van Driessche, G.; Devreese, B.; Thienpont, H.; Ottevaere, H.; Van Vlierberghe, S.; Dubruel, P., Ring opening copolymerisation of lactide and mandelide for the development of environmentally degradable polyesters with controllable glass transition temperatures. *React. Funct. Polym.* **2018,** *128*, 16-23.

12. Whitesell, J. K.; Pojman, J. A., Homochiral and heterochiral polyesters: polymers derived from mandelic acid. *Chem. Mater.* **1990,** *2* (3), 248-254.

13. Kenvin, J.; Mitchell, S.; Sterling, M.; Warringham, R.; Keller, T. C.; Crivelli, P.; Jagiello, J.; Pérez-Ramírez, J., Quantifying the Complex Pore Architecture of Hierarchical Faujasite Zeolites and the Impact on Diffusion. *Adv. Funct. Mater.* **2016,** *26* (31), 5621-5630.

14. Yin, M.; Baker, G. L., Preparation and Characterization of Substituted Polylactides. *Macromol.* **1999,** *32*, 7711-7718.

15. Van Wouwe, P.; Dusselier, M.; Vanleeuw, E.; Sels, B., Lactide Synthesis and Chirality Control for Polylactic acid Production. *ChemSusChem* **2016,** *9* (9), 907-921.

16. Upare, P. P.; Yoon, J. W.; Hwang, D. W.; Lee, U. H.; Hwang, Y. K.; Hong, D.-Y.; Kim, J. C.; Lee, J. H.; Kwak, S. K.; Shin, H.; Kim, H.; Chang, J.-S., Design of a heterogeneous catalytic process for the continuous and direct synthesis of lactide from lactic acid. *Green Chem.* **2016,** *18* (22), 5978-5983.

17. De Clercq, R.; Dusselier, M.; Poleunis, C.; Debecker, D. P.; Giebeler, L.; Oswald, S.; Makshina, E.; Sels, B. F., Titania-Silica Catalysts for Lactide Production from Renewable Alkyl Lactates: Structure–Activity Relations. *ACS Catal.* **2018,** *8* (9), 8130-8139.

18. Zhang, Q.; Xiang, S.; Zhang, Q.; Wang, B.; Mayoral, A.; Liu, W.; Wang, Y.; Liu, Y.; Shi, J.; Yang, G.; Luo, J.; Chen, X.; Terasaki, O.; Gilson, J.-P.; Yu, J., Breaking the Si/Al Limit of Nanosized β Zeolites: Promoting Catalytic Production of Lactide. *Chem. Mater.* **2019**.

19. Jiang, N.; Shang, R.; Heijman, S. G. J.; Rietveld, L. C., Adsorption of triclosan, trichlorophenol and phenol by high-silica zeolites: Adsorption efficiencies and mechanisms. *Sep. Purif. Technol.* **2020,** *235*.

20. Meacham, S. G.; Taylor, R. A., Selective alkylation of mandelic acid to diarylacetic acids over a commercial zeolite. *Chem. Commun. (Camb)* **2023,** *59* (60), 9243-9246.

21. Yan, B.; Tao, L. Z.; Liang, Y.; Xu, B. Q., Sustainable production of acrylic acid: alkali-ion exchanged beta zeolite for gas-phase dehydration of lactic acid. *ChemSusChem* **2014,** *7* (6), 1568-78.

22. Keller, T. C.; Isabettini, S.; Verboekend, D.; Rodrigues, E. G.; Pérez-Ramírez, J., Hierarchical high-silica zeolites as superior base catalysts. *Chem. Sci.* **2014,** *5* (2), 677-684.

23. Ji, Y.; Yang, H.; Yan, W., Effect of alkali metal cations modification on the acid/basic properties and catalytic activity of ZSM-5 in cracking of supercritical n-dodecane. *Fuel* **2019,** *243*, 155-161.

24. Zhang, K.; Fernandez, S.; Kobaslija, S.; Pilyugina, T.; O'Brien, J.; Lawrence, J. A.; Ostraat, M. L., Optimization of Hierarchical Structures for Beta Zeolites by Post-Synthetic Base Leaching. *Ind. Eng. Chem. Res.* **2016,** *55* (31), 8567-8575.

25. Verboekend, D.; Vile, G.; Perez-Ramirez, J., Mesopore Formation in USY and Beta Zeolites by Base Leaching: Selection Criteria and Optimization of Pore-Directing Agents. *Cryst. Growth Des.* **2012,** *12* (6), 3123-3132.

26. Verboekend, D.; Milina, M.; Mitchell, S.; Perez-Ramirez, J., Hierarchical Zeolites by Desilication: Occurrence and Catalytic Impact of Recrystallization and Restructuring. *Cryst. Growth Des.* **2013,** *13* (11), 5025-5035.

27. Groen, J. C.; Peffer, L. A.; Moulijn, J. A.; Perez-Ramirez, J., Mechanism of hierarchical porosity development in MFI zeolites by desilication: the role of aluminium as a pore-directing agent. *Chemistry* **2005,** *11* (17), 4983-94.

28. Thibault-Starzyk, F.; Stan, I.; Abelló, S.; Bonilla, A.; Thomas, K.; Fernandez, C.; Gilson, J.-P.; Pérez-Ramírez, J., Quantification of enhanced acid site accessibility in hierarchical zeolites – The accessibility index. *J. Catal.* **2009,** *264* (1), 11-14.

29. Suarez, N.; Perez-Pariente, J.; Mondragon, F.; Moreno, A., Generation of hierarchical porosity in beta zeolite by post-synthesis treatment with the cetyltrimethylammonium cationic surfactant under alkaline conditions. *Microporous Mesoporous Mater.* **2019,** *280*, 144-150.

30. Mesa, S.; Arboleda, J.; Echavarría, A.; López-Suárez, F. E., Ferrierite zeolite passivation and its catalytic application in toluene disproportionation. *Chem. Eng. Sci.* **2019,** *208*.

31. De Clercq, R.; Makshina, E.; Sels, B. F.; Dusselier, M., Catalytic Gas-Phase Cyclization of Glycolate Esters: A Novel Route Toward Glycolide-Based Bioplastics. *ChemCatChem* **2018,** *10* (24), 5649-5655.

32. Zheng, Y.; Zhao, Y.; Tao, S.; Li, X.; Cheng, X.; Jiang, G.; Wan, X., Green Esterification of Carboxylic Acids Promoted by tert-Butyl Nitrite. *Eur. J. Org. Chem.* **2021,** *2021*, 2713-2718.

33. Fulmer, G. R.; Miller, A. J. M.; Sherden, N. H.; Gottlieb, H. E.; Nudelman, A.; Stoltz, B. M.; Bercaw, J. E.; Goldberg, K. I., NMR Chemical Shifts of Trace Impurities: Common Laboratory Solvents, Organics, and Gases in Deuterated Solvents Relevant to the Organometallic Chemist. *Organometallics* **2010,** *29* (9), 2176-2179.

34. Tomas-Mendivil, E.; Suarez, F. J.; Diez, J.; Cadierno, V., An efficient ruthenium(IV) catalyst for the selective hydration of nitriles to amides in water under mild conditions. *Chem. Commun. (Camb)* **2014,** *50* (68), 9661-4.

35. Cairns, S. A.; Schultheiss, A.; Shaver, M. P., A broad scope of aliphatic polyesters prepared by elimination of small molecules from sustainable 1,3-dioxolan-4-ones. *Polym. Chem.* **2017,** *8* (19), 2990-2996.

36. Webster, C. E.; Drago, R. S.; Zerner, M. C., Molecular Dimensions for Adsorptives. *J. Am. Chem. Soc.* **1998,** *120* (22), 5509-5516.

37. Hendriks, F. C.; Valencia, D.; Bruijnincx, P. C. A.; Weckhuysen, B. M., Zeolite molecular accessibility and host–guest interactions studied by adsorption of organic probes of tunable size. *Phys. Chem. Chem. Phys.* **2017,** *19* (3), 1857-1867.

38. Lutz, W., Zeolite Y: Synthesis, Modification, and Properties—A Case Revisited. *Adv. Mater. Sci. Eng.* **2014,** *2014*, 1-20.

39. Davis, M. E., Zeolites and Molecular Sieves: Not Just Ordinary Catalysts. *Ind. Eng. Chem. Res.* **1991,** *30*, 1675-1683.

40. Csicsery, S. M., Shape-selective catalysis in zeolites. *Zeolites* **1984,** *4* (3), 202-213.

41. Degnan, T. F., The implications of the fundamentals of shape selectivity for the development of catalysts for the petroleum and petrochemical industries. *J. Catal.* **2003,** *216* (1-2), 32-46.

Chapter 4: Synthesis of 1,3-Dioxolan-4-one Monomers over Zeolite Catalysts under Batch and Flow conditions

4.1 Introduction

As discussed in the previous chapter, the synthesis of 6-membered lactide monomers is challenging. These monomers are typically synthesised by acid-catalysed condensation. For monomers other than glycolide and lactide, dilute solutions are needed to favour dimerisation over oligomerisaton. Even then, forcing conditions such as high temperatures and long reaction times in the order of days are still required. Even under these extreme conditions, yields are typically low. We have shown that zeolite catalysts could be used to produce mandelide, the cyclic dimer of mandelic acid, but selectivity was hampered by side reactions. In addition to the difficulty in synthesising mandelide, mandelide itself presents further problems when subjected to ring opening polymerisation. It has poor solubility in common polymerisation solvents such as toluene. Furthermore, the *rac*-isomers decompose on melting, meaning that both solution polymerisation and solvent-free polymerisation in the melt present problems with monomer solubility and stability, respectively.[1] Whilst this monomer has been polymerised using $Sn(Oct)_2$, tacticity control has not been possible, so only amorphous polymers have been synthesised from mandelide. Furthermore, molecular weights are lower than theoretical due to chain initiation by species formed during the reactions.[2]

Alternative monomers have been investigated that offer better control of molecular weight and polydispersity compared with 6-membered lactide-type monomers. These monomers are *O*-carboxyanhydrides (OCAs) and 1,3-dioxolan-4-ones (DOX) (Figure 1).[3-5] One of the drawbacks of 6-membered lactide-type monomers is that the ring strain is not high enough to provide a significant driving force for ring opening polymerisation. This means that highly active catalysts are required. Decreasing the ring size of the monomer to 5-membered ring OCAs and DOXs increases ring strain, leading to improved ring opening. The presence of a single repeat unit in each monomer also opens up new possibilities for copolymer sequences. Lactides being dimers, cannot be used to create copolymers with isolated repeat units, as two adjacent alpha hydroxy acid units will always be present in the polymer backbone. The reported monomer syntheses of OCAs and DOXs are also much more efficient than for lactide monomers such as mandelide. OCAs can be synthesised at room temperature[3] and DOXs can be synthesised by reflux in cyclohexane,[6] whereas mandelide synthesis uses reflux in high

boiling point xylenes.[1, 2] OCA and DOX syntheses also use much shorter reaction times than mandelide synthesis (a few hours for OCA and DOX vs a few days for mandelide).

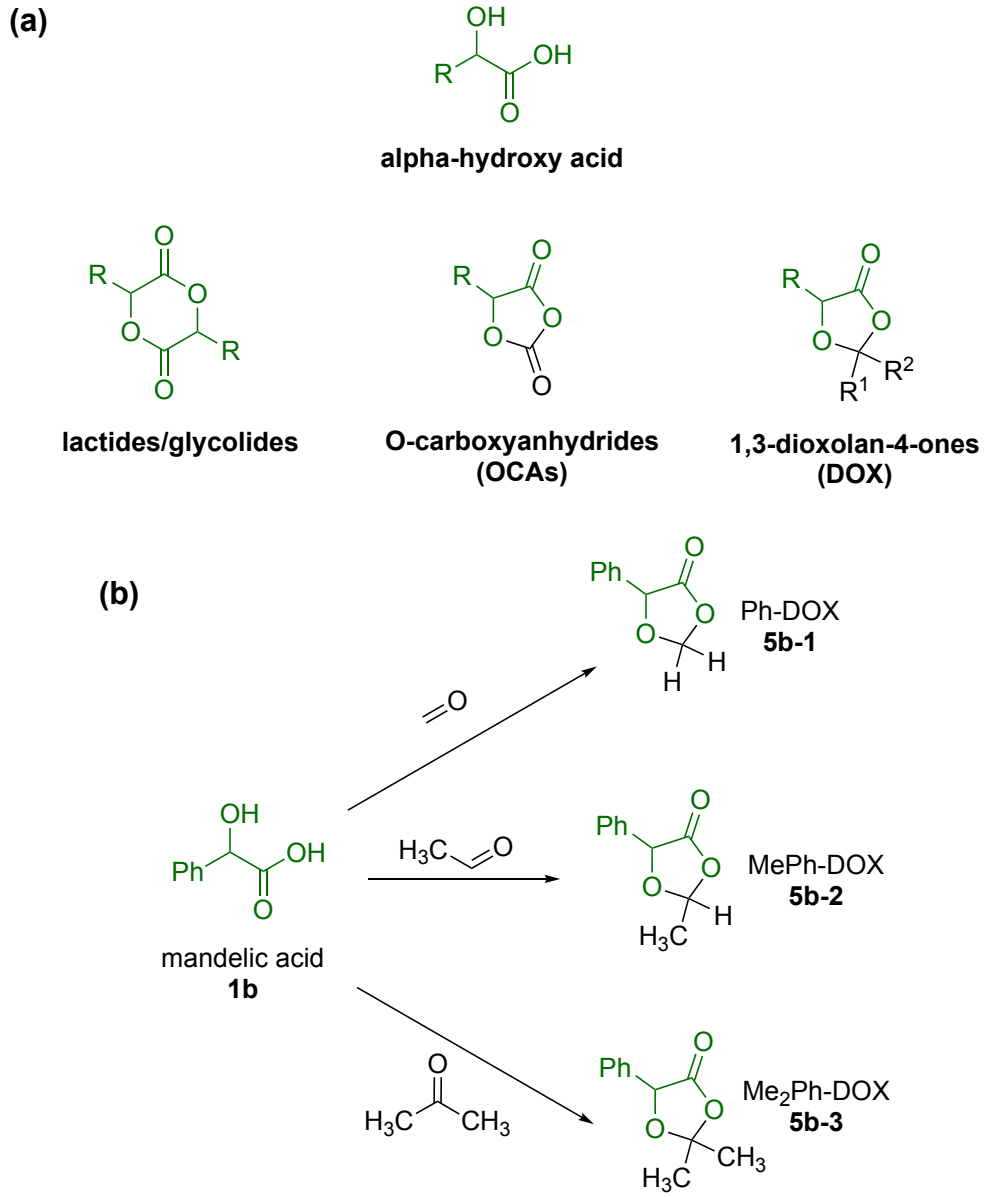

Figure 1 (a) Structures of cyclic monomers used to make poly(alpha-hydroxy acids) such as poly(mandelic acid) via ring opening polymerisation. R^1 and R^2 = H or CH_3. (b) Structures of 1,3-dioxolan-4-ones of mandelic acid with formaldehyde (Ph-DOX, 5b-1), acetaldehyde (MePh-DOX, 5b-2) and acetone (Me_2Ph-DOX, 5b-3).

The *O*-carboxyanhydride of mandelic acid (Ph-OCA) is typically synthesised by reacting mandelic acid with a phosgene reagent (such as diphosgene or triphosgene), using *p*-TSA as catalyst. Synthesis of Ph-OCA is much faster than the synthesis of mandelide, with 75% yield achieved after 18 hours[7] compared with around 50% yield for mandelide after 3 days.[1, 2] Compared with mandelide synthesis, higher mandelic acid concentration can be used (*ca*. 10-fold increase), resulting in lower solvent usage. Reaction time is shorter to achieve this higher monomer yield, and the reaction can be run at room temperature in THF compared with reflux in mixed xylenes (b.p. 140 °C) for mandelide.

Through optimisation of the synthesis procedure, Ph-OCA yield can be increased to around 84%[8] or even quantitative yields.[9]

The 1,3-dioxolan-4-ones of mandelic acid (1b) are synthesised by reacting mandelic acid with a carbonyl compound, again using *p*-TSA as catalyst.[5, 6] Examples in the literature use formaldehyde or acetone as the carbonyl compound to give 1,3-dioxolan-4-ones referred to as Ph-DOX (5b-1) or Me_2Ph-DOX (5b-3), respectively. As with OCAs, synthesis of DOXs is much faster than for mandelide, with 90% yield achieved after 3 hours and 95% after 6 hours. In contrast to the OCA synthesis, these reactions require reflux, but the solvents used are still comparably lower boiling (cyclohexane or benzene, b.p. 80 °C) than the mixed xylenes used for mandelide synthesis. These monomers also do not require the use of toxic reagents in their synthesis in comparison to the *O*-carboxyanhydrides which require a phosgene reagent. DOX monomers have been polymerised using a range of catalysts such as Al(salen) complexes and pyridine bases.[5, 6, 10, 11] Furthermore, their copolymerisation with lactide to form poly(lactic acid-co-mandelic acid) has been reported.[5, 12] Given that zeolite H-Beta catalysed the reaction of mandelic acid with benzaldehyde to make 2,5-diphenyl-1,3-dioxolan-4-one (5b-4), as discussed in the previous chapter of this thesis, we reasoned that zeolites may also be useful as catalysts for DOX monomer synthesis.

Outside of polymer chemistry, many examples of 1,3-dioxolan-4-one synthesis exist. Carbonylation of formaldehyde with carbon monoxide can be catalysed by H-ZSM-5 zeolite (Scheme 1).[13] Comparison of ZSM5 zeolites showed that increasing Si/Al resulted in a lower yield of DOX (Figure 2). No DOX was formed over silicalite, indicating that Brønsted acidity was required for the reaction. The temperature dependence was also investigated, with 40 – 80 °C giving low yields, with highest yields at 120 °C and 160 °C, and finally yield appears to decrease slightly again at higher temperatures. Finally, the effect of reaction time was studied and it was found that yield of 1,3-DOX-4 was maximised after around 5 hours, after which time the solid product yield increased, attributed to the formation of poly(glycolide) via ring-opening polymerisation of DOX. The reaction also requires extremely high pressures of 15-75 MPa CO in an autoclave.

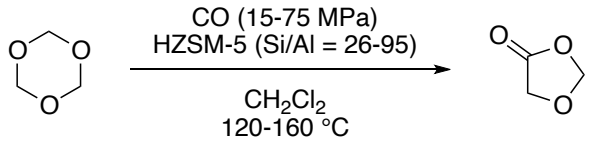

Scheme 1 Synthesis conditions used to synthesis 1,3-dioxolan-4-one via carbonylation of formaldehyde over various ZSM5 zeolites.

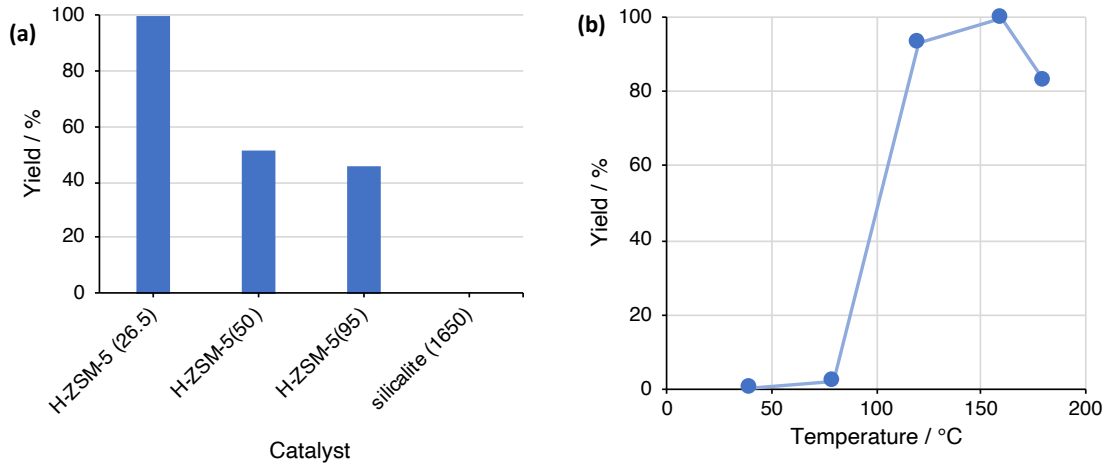

Figure 2 Synthesis of 1,3-dioxolan-4-one via carbonylation of formaldehyde over various ZSM5 zeolites. (a) Effect of ZSM-5 Si/Al ratio on DOX yield at 120 °C and 35 MPa CO after 2 hours. (b) Effect of temperature on DOX yield over H-ZSM-5 (95) zeolite at 35 MPa CO after 5 hours.[13]

The synthesis of dioxolanones over solid acids has also been investigated for the reaction of mandelic acid with various carbonyl compounds using silica sulfate as a catalyst.[13] SO_3H groups on the surface of silica gel acted as the catalyst. Reactions in diethyl ether gave good yields of the DOX product of mandelic acid and cyclohexanone, with a maximum yield of 88 % achieved after 20 hours of reaction time, albeit at high catalyst loading of 40 mol% SO_3H groups relative to mandelic acid. Faster reaction times were achieved by employing solvent-free conditions and pulverising the catalyst and reactants in a mortar. Under these conditions, 90 % yields were achieved after 25 minutes. Silica gel reference material gave no products, suggesting that the SO_3H groups are acting as the active catalytic species.[14] The DOX product of mandelic acid and acetone, 5-phenyl-2,2-dimethyl-1,3-dioxolan-4-one (Me_2Ph-DOX), was synthesised in 80 % yield after 2 hours using 25 mol% silica sulfate (Scheme 2).[14] Me_2Ph-DOX has been used for ring opening polymerisation to synthesise poly(mandelic acid)[5] and this is the only example of its synthesis via heterogenous catalysis that we are aware of.

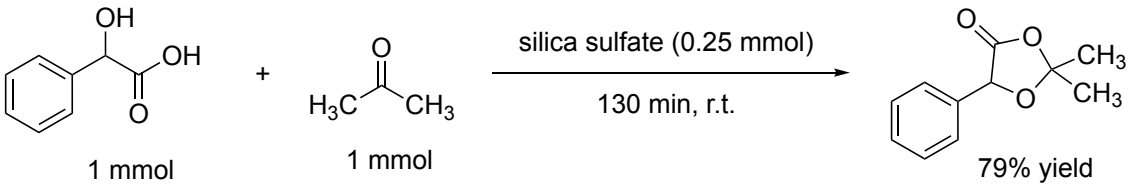

Scheme 2 Synthesis of 5-phenyl-2,2-dimethyl-1,3-dioxolan-4-one (Me_2Ph-DOX, 5b-3) using silica sulfate as catalyst.[14]

As discussed in the previous chapter, the DOX product of mandelic acid and benzaldehyde can be synthesised using a Lewis acidic catalyst such as BF_3OEt_2.[15] The reaction of acetaldehyde with lactic acid has been reported under batch conditions, by reaction of *L*-lactic acid with paraldehyde using para-toluene sulfonic acid as catalyst in

petroleum ether. The reaction was carried out under reflux with Dean Stark trap for an unspecified time, to yield 21% 2,5-dimethyl-1,3-dioxolan-4-one (5a-2), as a 70:30 mixture of diastereomers (the absolute stereochemistry of the major and minor diastereomers was not assigned).[16]

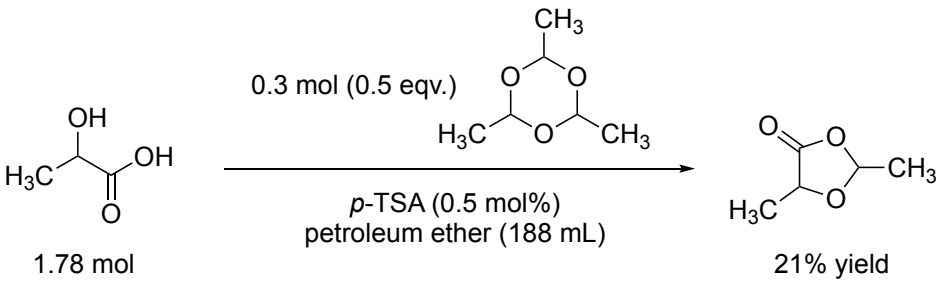

Scheme 3 Reaction of L-lactic acid with paraldehyde to give 2,5-dimethyl-1,3-dioxolan-4-one (5a-2).

Two different DOX monomers have been used to make poly(mandelic acid): 5-phenyl-1,3-dioxolan-4-one (Ph-DOX, 5b-1) and 2,2-dimethyl-5-phenyl-1,3-dioxolan-4-one (Me_2Ph-DOX, 5b-3).[5, 6] As discussed earlier, these monomers can be synthesised using homogeneous *p*-TSA and this method gives good yields after 6 hours at reflux in cyclohexane. These current DOX monomer synthesis conditions are sufficient to obtain monomer for the purpose of lab scale polymerisations. As DOX monomers have only been synthesised on the lab scale, it is not clear whether the current conditions would work at an industrial scale. As discussed in the context of lactide production in the previous chapter, heterogeneous catalysts can have advantages in industrial processes compared with homogeneous catalysts. Zeolites may be advantageous compared with *p*-TSA as they are temperature stable, easily separated from the products (e.g., by filtration) and, once separated, can be recycled and reused. Furthermore, the heterogeneous nature of zeolites makes it easier to implement a continuous flow process. In order to use a catalyst like *p*-TSA in a continuous process, the catalyst would need to be included in the feed solution and separated from the products at a later stage of the process, or immobilised on a support to generate a heterogeneous catalyst. A recent lifecycle analysis of the synthesis of poly(mandelic acid) suggested that the production of PMA could have up to 5 times the environment impact of the production of polystyrene, and the monomer synthesis was highlighted as one of the main contributing factors to this higher impact.[17] Using heterogeneous catalysts for monomer synthesis in PMA production could help reduce the environmental impact, making PMA more viable as a polystyrene substitute.

In the previous chapter, we also showed that the high temperatures needed for mandelide synthesis led to several problems in a liquid phase flow reactor including

acetonitrile solvent decomposition and reactor blocking. In comparison, the synthesis of dioxolanones is carried out at much lower temperatures than mandelide synthesis (80 °C (refluxing cyclohexane) versus 140 °C (refluxing xylene)) and the monomers themselves have better solubility in organic solvents, potentially leading to fewer practical issues in terms of reactor blocking.

In this part of the project, we investigated the synthesis of three different 1,3-dioxolan-4-one (DOX) monomers using both batch reaction in cyclohexane and liquid phase flow in acetonitrile (MeCN). The effect of different zeolite catalysts was investigated, as well as the effect of reaction parameters such as flow rate, temperature and reagent stoichiometry. The outcomes of batch and flow reactions were also compared.

4.2 Results and Discussion

4.2.1 Synthesis of previously reported DOX monomers

Taking the conditions reported[5, 6] for the preparation of 5b-1 and 5b-3, we substituted *p*-TSA with 3 different zeolites: H-ZSM-5, H-Beta and H-Y. We kept reactant stoichiometry and solvent the same as reported in the literature and evaluated the conversion of mandelic acid to DOX after 1 hour of reaction time (compared with 3 hours in the reported synthesis). After 1 hour, we did not observe any conversion of mandelic acid by *p*-TSA by ^{1}H-NMR spectroscopy – this catalyst required longer reaction times. In the case of Me_2Ph-DOX (5b-3), we also investigated the effects of lowering the zeolite catalyst loading, as 10 mol% gave high conversion even after just 1 hour. The results are summarised in Table 1 and Table 2. We found that selectivity was high for all three zeolites tested, with no significant byproducts apparent in the ^{1}H NMR spectra. Comparing the various catalyst loadings tested shows that there was not a linear relationship between catalyst loading and conversion. For example, 2.5 mol% H-Y-30 gave 25% conversion but doubling the loading to 5 mol% resulted in more than a 3-fold increase in conversion. This was an unusual result. It could possibly be attributed to poor mixing of the zeolite, meaning results were inconsistent – these reactions were not repeated. Once again, of the zeolites tested, the H-Y-30 catalyst proved to be the most useful in selectively converting mandelic acid. It's possible that some of the volatile reagents (e.g. formaldehyde or acetone) are lost from the flask, becoming concentrated in the phase separator rather than returning back into the flask with the refluxing solvent (an air condenser was used). This would reduce their concentration relative to mandelic acid over time. At higher catalyst loading, this effect might have been minimised due to the increased the rate of conversion. This explanation is plausible, as later experiments showed a plateau in conversion at longer reaction times, potentially also caused by

evaporation. It should also be noted that the higher conversion for acetone than paraformaldehyde was likely due to the differing conditions in the reported syntheses that were used here. Paraformaldehyde is added to give approximately 1.6 equivalents of formaldehyde relative to mandelic acid, whereas acetone is included in the solvent system, resulting in around 100 equivalents of acetone relative to mandelic acid. It is unsurprising that this large excess of acetone leads to higher conversion.

Table 1 Conversion of mandelic acid to $PhMe_2$-DOX using different zeolite catalysts. Conditions: mandelic acid (0.46 g, 3.02 mmol), zeolite (various amounts), cyclohexane (10 mL), acetone (10 mL, 45-fold excess), reflux for 1 hour with phase separator.

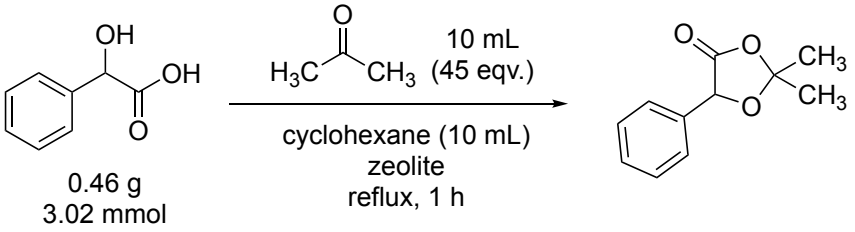

Catalyst	Catalyst loading relative to mandelic acid / mol%	Conversion / %
p-TSA	10	n.d.
H-ZSM5-15	2.5	n.d.
H-ZSM5-15	10	16
H-Beta-12.5	2.5	1
H-Beta-12.5	10	13
H-Y-30	2.5	25
H-Y-30	5	86
H-Y-30	10	92
H-Y-2.5	10	n.d.

Table 2 Conversion of mandelic acid to Ph-DOX using different zeolite catalysts. Conditions: mandelic acid (0.95 g, 6.24 mmol), zeolite (2.5 mol% H^+ relative to mandelic acid), cyclohexane (10 ml), paraformaldehyde (0.3 g, 1.6 eqv. CH_2O), reflux for 1 hour with phase separator.

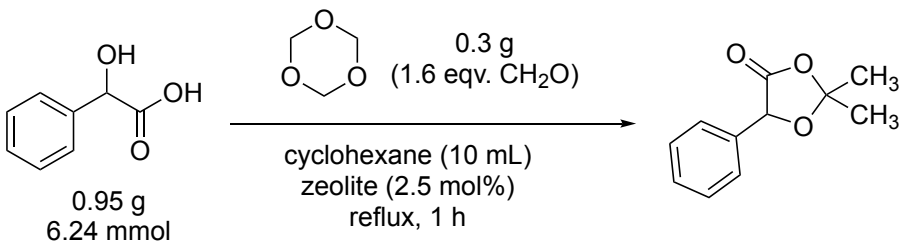

Catalyst	Conversion / %
H-ZSM5-15	n.d.
H-Beta-12.5	4
H-Y-30	36

4.2.2 Synthesis of 2-methyl-5-phenyl-1,3-dioxolan-4-one (MePh-DOX, 5b-2)

2-Methyl-5-phenyl-1,3-dioxolan-4-one (5b-2) is the dioxolanone product of the reaction of mandelic acid with acetaldehyde. This compound has been synthesised previously through acid catalysed reaction of mandelic acid with paraldehyde, the cyclic trimer of acetaldehyde[18] and has been investigated as a monomer in cationic polymerisation.[19] It did not undergo homopolymerisation but did copolymerise with cyclohexene oxide. We reproduced this synthesis to make a reference compound. Scheme 4 shows the conditions used for the synthesis.[18] 5b-2 was obtained in 46 % yield after washing the crude product 3 times with sodium bicarbonate. The reaction starts with decomposition of paraldehyde to form free acetaldehyde.

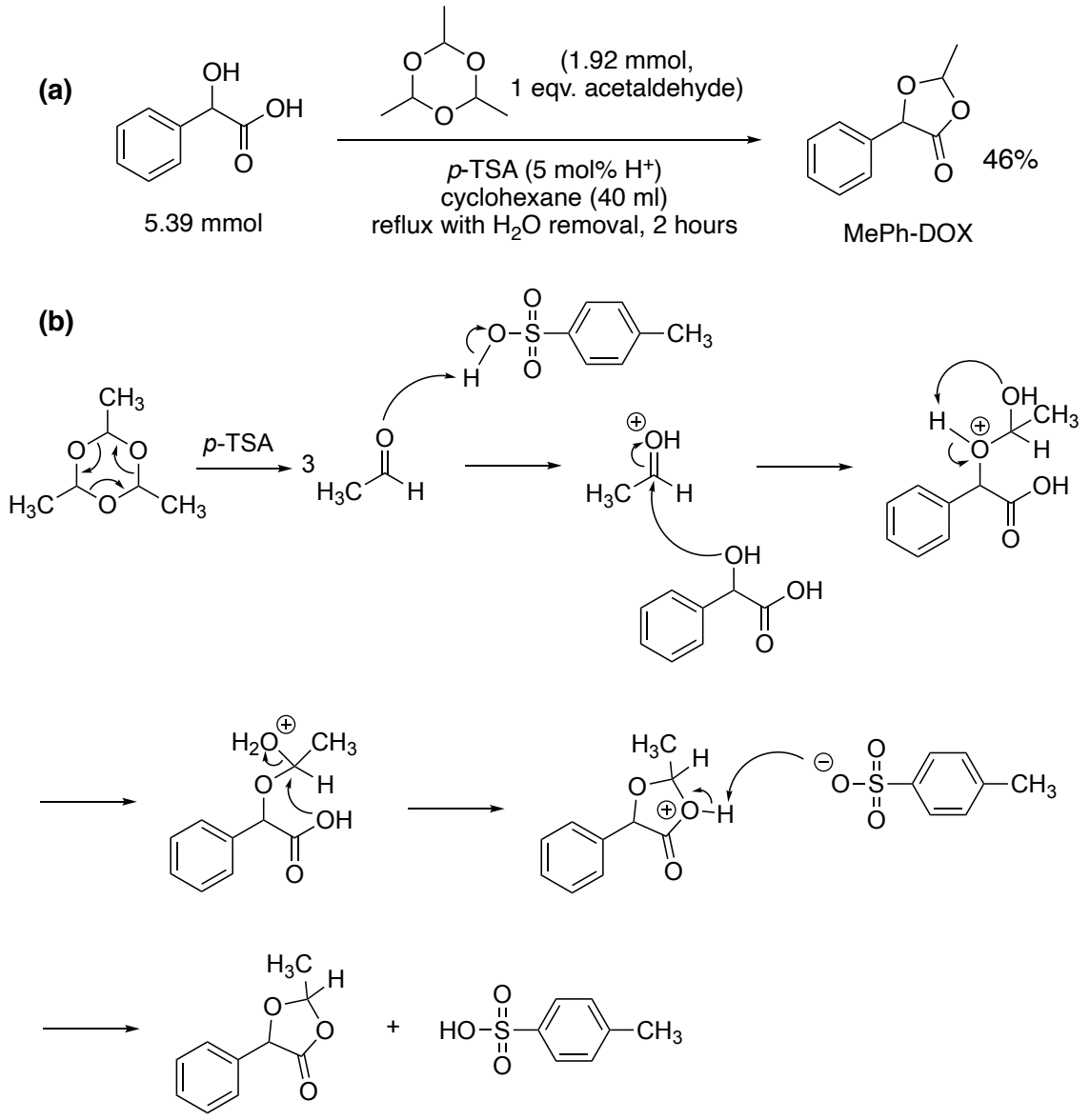

Scheme 4 (a) Reaction of mandelic acid with paraldehyde catalysed by paratoluene sulfonic acid (*p*-TSA) to give 2-methyl-5-phenyl-1,3-dioxolan-4-one (MePh-DOX, 5b-2). (b) Mechanism of formation of 5b-2 catalysed by *p*-TSA.

Figure 3 and Figure 4 show the characterisation obtained for the products of the reaction in Scheme 4. MePhDOX (5b-2) forms as a mix of two stereoisomers, indicated by two sets of chemical shifts in the ^{1}H NMR spectrum (Figure 3). The ratio of isomers was 0.58:0.42 according to the relative ^{1}H NMR integrals. The assignment of these chemical shifts is shown in Figure 4 and Table 3. Our results were consistent with reported chemical shift values.[18]

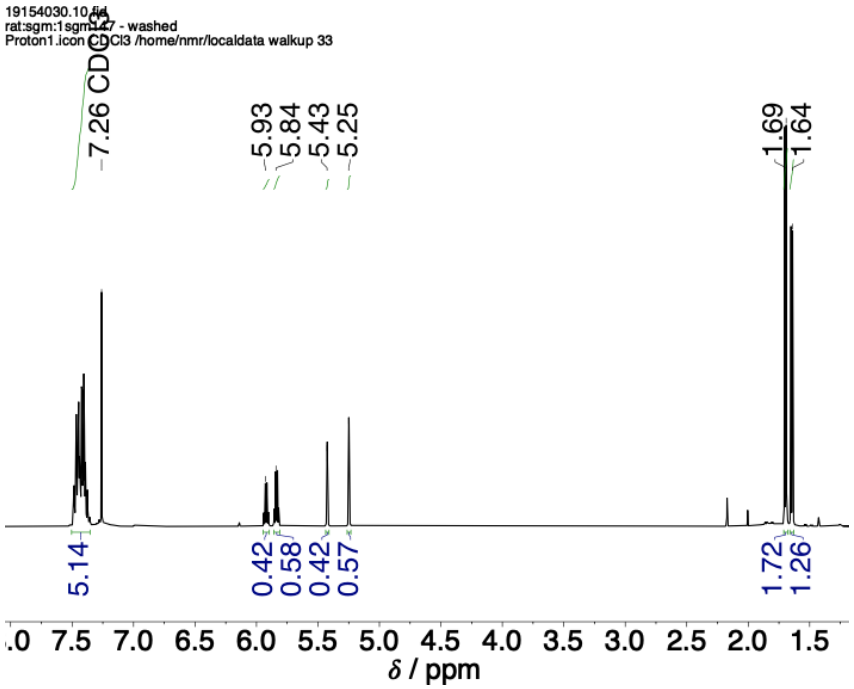

Figure 3 ^{1}H NMR spectrum (400 MHz, $CDCl_3$) of MePh-DOX.

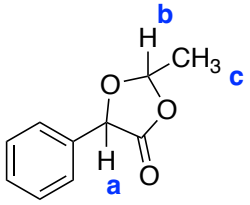

MePh-DOX

Figure 4 Proton environments in MePh-DOX (5b-2).

Table 3 Assignment of proton environments to chemical shifts observed in the ^{1}H spectrum of MePh-DOX, consisting of 2 isomers. For more details of the characterisation of this compound, see the experimental chapter of this thesis.

Proton environment	Isomer 1 (*trans* according to ref [18])	Isomer 2 (*cis* according to ref [18])
a	5.25	5.43
b	5.84	5.93
c	1.69	1.64
Ar-H	7.3-7.5	7.3-7.5

4.2.3 Effect of Catalyst Loading and Aldehyde Stoichiometry on the Synthesis of 1,3-dioxolan-4-ones

Variation of the catalyst loading was investigated for the reaction of mandelic acid with paraformaldehyde and paraldehyde using the H-Y-30 zeolite as catalyst. Loading was calculated based on the amount of H^+ in the zeolite, approximated from the Si/Al ratio.

Loadings of 1 mol%, 2.5 mol% and 5 mol% were used. Conversion and selectivity were monitored by ^{1}H NMR spectroscopy. As reported for Ph-DOX (5b-1) and Me_2Ph-DOX (5b-3) in the initial screening in section 6.2.1, selectivity remained high at different catalyst loading with no obvious byproducts present in the NMR spectra. Mandelic acid conversion was quantified through relative integration of mandelic acid and DOX methine peaks in ^{1}H NMR spectra in $CDCl_3$. For Ph-DOX (5b-1), conversion was found to plateau at around 16% at 1.0 mol% catalyst loading (Figure 5). Increasing the catalyst loading to 2.5 mol% increased the conversion. In the synthesis of MePh-DOX (5b-2), conversion also reached a plateau at around 20%, but in contrast, higher catalyst loadings only increased the conversion slightly (Figure 6). This difference is similar to the size of the variability between reaction runs, suggesting there was very little difference in conversion at the three catalyst loadings tested. It appeared that a factor other than catalyst loading was limiting the mandelic acid conversion in the synthesis of MePh-DOX (5b-2).

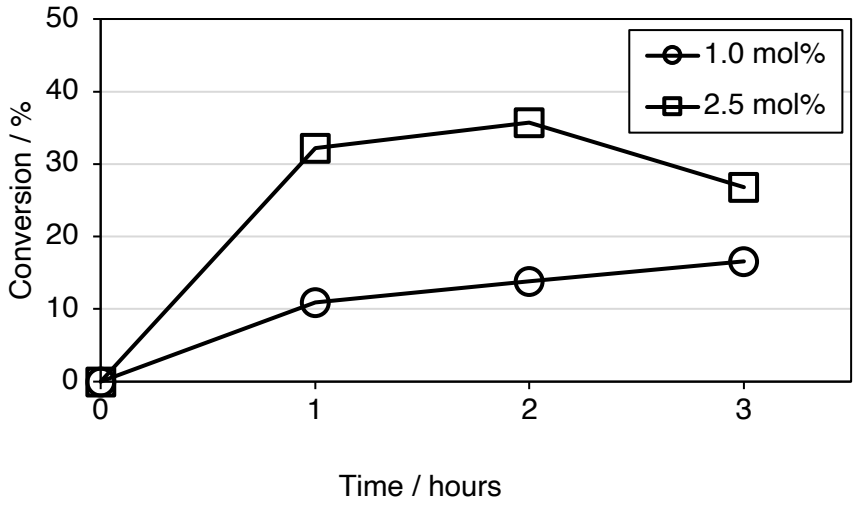

Figure 5 Effect of H-Y-30 catalyst loading on synthesis of Ph-DOX (5b-1). Conditions: mandelic acid (0.2 g), paraformaldehyde (0.0473 g, 1.2 eqv.) and cyclohexane (10 ml). Reflux for 1-3 hours with a phase separator. Mass of H-Y-30 zeolite: 0.0149 g (1 mol%), 0.0375 g (2.5 mol%)

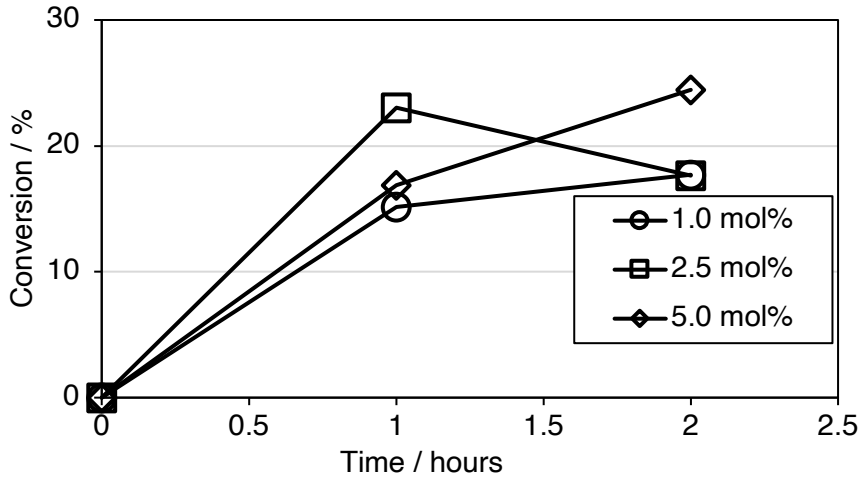

Figure 6 Effect of H-Y-30 catalyst loading on synthesis of MePh-DOX (5b-2). Conditions: mandelic acid (0.2 g), paraldehyde (0.0695 g, 1.2 eqv.) and cyclohexane (10 ml). Reflux for 1-2 hours with a phase separator. Mass of H-Y-30 zeolite: 0.0149 g (1 mol%), 0.0375 g (2.5 mol%), 0.0745 g (5 mol%).

Several factors may have been limiting conversion in the formation of DOX monomers. These reactions used around 1 equivalent of formaldehyde or acetaldehyde relative to mandelic acid, so the amount of acetaldehyde may have been insufficient. These reactions also used either paraformaldehyde (the polymeric form of formaldehyde) as a source of formaldehyde or paraldehyde (the cyclic trimer of acetaldehyde) as a source of acetaldehyde. These “masked” reagents (polymer or cyclic trimer) would need to dissociate sufficiently to the monomeric form. Another possibility was that acetaldehyde was lost from the reaction flask over the course of the reaction, due to its high volatility, and collected in the phase separator. We conducted further reactions, varying the amount of paraldehyde added and with catalyst loading kept constant at 5 mol%. A steady increase in conversion was observed when concentration was increased up to around 12 equivalents of acetaldehyde relative to mandelic acid. The data in Figure 7 shows that the plateau in conversion seen in Figure 6 above was at least in part due to the concentration of acetaldehyde being insufficient. This excess might minimise the effects of dissociation of paraldehyde or evaporation of acetaldehyde on the relative concentrations of free acetaldehyde to mandelic acid in the reaction flask. Product NMR spectra contained no paraldehyde or acetaldehyde. However, given the volatility of these compounds (b.p. 124 °C and 20 °C, respectively), they may have been removed during rotary evaporation prior to NMR sample preparation.

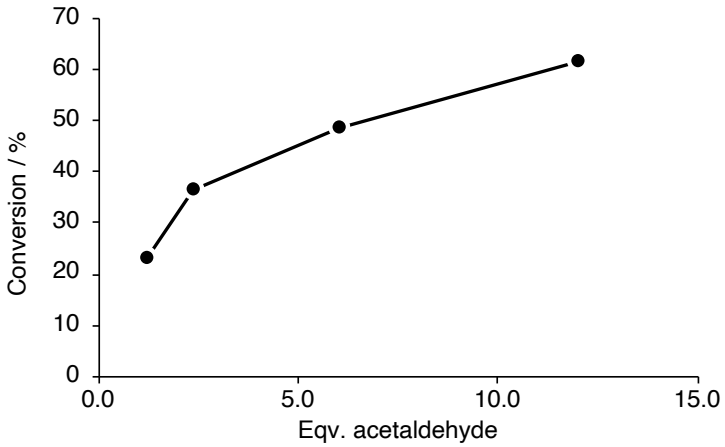

Figure 7 Effect of the ratio of acetaldehyde to mandelic acid from 0.5 equivalents to 12 equivalents. Conditions: mandelic acid (0.2 g), H-Y-30 (0.075 g, 5 mol% H^+), cyclohexane (10 ml), reflux with phase separator for 1 hour.

4.2.4 Synthesis of 1,3-dioxolan-4-ones in an X-Cube Flow Reactor

Having investigated the use of zeolites as catalysts for the synthesis of 1,3-dioxolan-4-one monomers under batch conditions (similar to those reported in the literature), we investigated the use of an X-cube flow reactor. Similar conditions were used as for mandelide synthesis in the same reactor, discussed in the previous chapter. In short, mandelic acid was dissolved in MeCN to use as a feed solution. This time, the carbonyl compound (trioxane, paraldehyde or acetone) was also included in the feed solution in order to synthesise the corresponding 1,3-dioxolan-4-one 5b-1, 5b-2 or 5b-3. In flow, an internal standard (mesitylene) was used to quantify the conversion of mandelic acid and the yield of the products.

Data in Figure 8a shows that changing the flow rate at a constant temperature of 80 °C affected the three reactions differently. Figure 8b shows the same conversion data plotted against residence time. In the case of 5b-1, the reaction temperature of 80 °C was too low (see Figure 8c) and so the flow rate did not affect conversion. In the case of 5b-2, increasing flow rate had a negative effect on conversion, with the best conditions being the lowest flow rate of 0.5 ml min^{-1}, suggesting that the residence time over the catalyst was not sufficient at high flow rate. The volume of the catalyst bed was 0.8 ml, so a flow rate of 0.5 ml min^{-1} equates to a 96 second residence time. Finally, the flow rate had little effect on conversion to 5b-3 at this reaction temperature.

We then used 0.5 ml min^{-1} flow rate to assess the temperature dependence of all three reactions. Figure 8c shows the results. In the case of 5b-2, temperatures of 80 °C or higher resulted in high conversion of around 90-95%. The slight decrease in conversion at higher temperatures than 80 °C could have been caused by catalyst deactivation

during the course of testing the different temperatures, as each temperature was carried out sequentially over the same catalyst bed. This was investigated in more detail later. The formation of 5b-3 shows only a small dependence on temperature under these conditions with a slight increase in conversion as the temperature was increased to 120 °C. There may be an equilibrium limitation on this reaction under the reagent quantities used here, as it appears to be unaffected by the reaction conditions. The conversion-temperature plot for the formation of 5b-1 shows that this reaction is highly dependent on the reaction temperature. These different reaction profiles may be related to both the thermal stability of the cyclic trimeric reagents used and the reactivity of the carbonyl compounds.

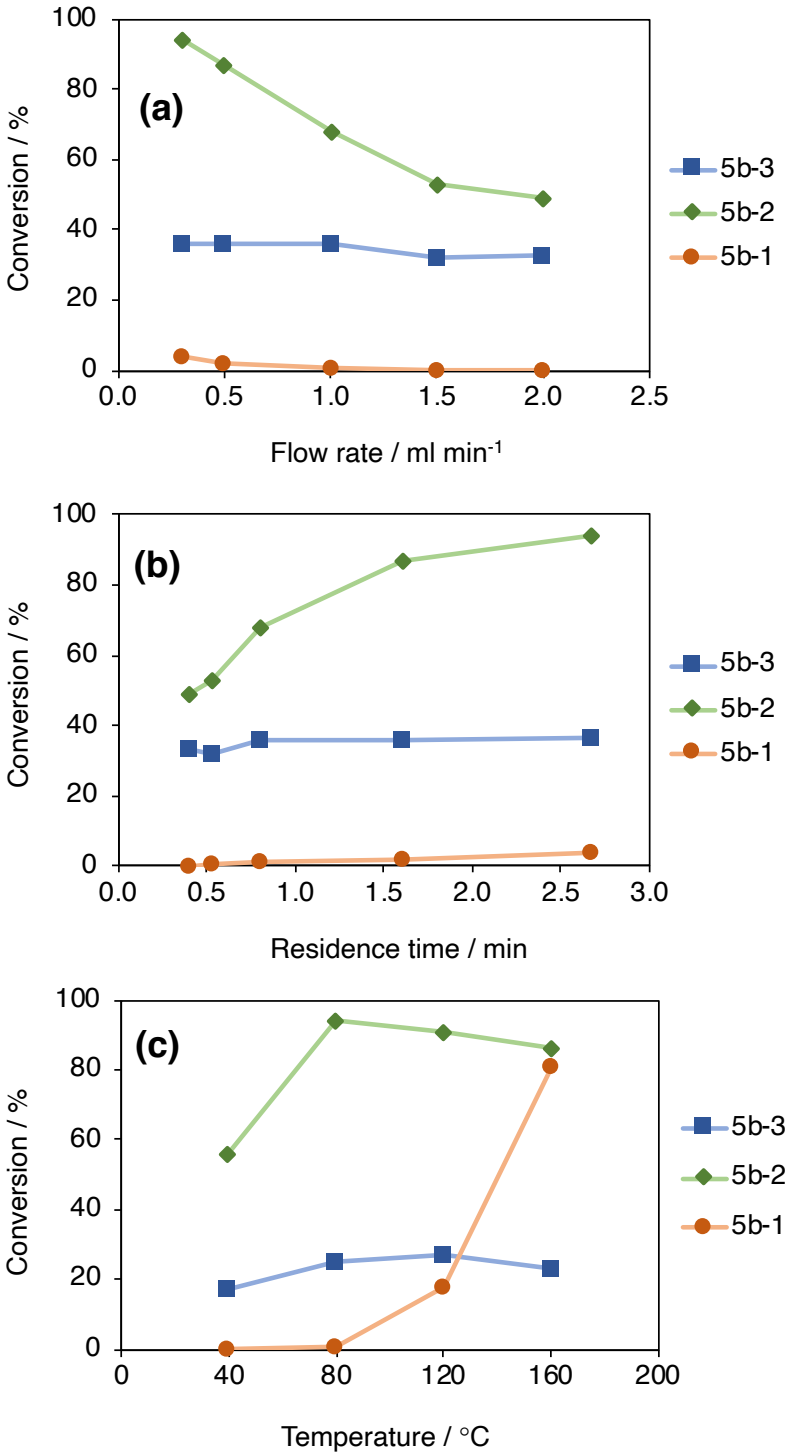

Figure 8 Effect of (a) flow rate and (b) residence time at 80 °C, and (c) temperature (at 0.5 ml min^{-1} flow rate) on the conversion of mandelic acid during the synthesis of 1,3-dioxolan-4-ones 5b-1, 5b-2 and 5b-3 over H-Y-30 zeolite in an X-Cube flow reactor. Catalyst: Zeolite H-Y-30 (300 mg, 60-80 mesh). Feed: mandelic acid (2 g), mesitylene (0.4 g, internal standard), MeCN (50 ml). Aldehyde source or acetone in feed: trioxane (3.45 g, 9 eqv.), paraldehyde (7.6 g, 13 eqv.) or acetone (4 g, 5 eqv.). Residence time (min) = CatCart volume (0.8 mL) / liquid flow rate (mL min^{-1}).

The first step in the formation of 5b-1 and 5b-2 will be the conversion of the cyclic trimers trioxane and paraldehyde to the monomeric forms formaldehyde and acetaldehyde,

respectively.[20, 21] The temperature-conversion profiles for the reactions using these cyclic trimer reagents show distinct trends. We observed a minimum temperature before the onset of increased conversion, which may have been caused by insufficient formation of the monomeric species at low temperatures. The temperature at which this conversion increased was lower for paraldehyde than trioxane. Paraldehyde is reported to undergo conversion to the monomeric form more readily than trioxane, which provides some further evidence for this explanation.[22] At 160 °C, conversion is comparable for trioxane and paraldehyde, suggesting that dissociation was comparable at these higher temperatures. Interestingly, a similar trend was reported for the carbonylation of formaldehyde to make 1,3-dioxolan-4-one over H-ZSM-5.[13] In this report, the source of formaldehyde was also the cyclic trimer, trioxane. Little or no conversion was observed at temperatures below 100 °C, whereas high conversion (> 80%) was observed at all three temperatures tested between 100 °C and 200 °C.

Figure 9 shows a possible mechanism for the reaction of mandelic acid with carbonyl compounds to form 5-phenyl-1,3-dioxolan-4-ones, catalysed by Brønsted acidic zeolites. It starts with nucleophilic attack by the alpha-hydroxyl group of mandelic acid on the partial positive carbonyl (formaldehyde, acetaldehyde or acetone), assisted by protonation of the carbonyl oxygen by the Brønsted acid sites of the zeolite. In terms of the trends in reactivity of the different carbonyls towards this nucleophilic attack, it is expected that reactivity would decrease in the order formaldehyde > acetaldehyde > acetone. This is due to the combined effects of sterics and electronics of the additional methyl group (Figure 10). As more methyl groups are added, the partial positive charge on the carbonyl would be decreased due to electron-donation (inductive effect) by the methyl groups, making it less susceptible to nucleophilic attack.[23] The presence of methyl groups in place of protons also increases steric hindrance around the carbonyl group, further impeding nucleophilic attack. Our results do not follow this trend, with acetaldehyde appearing to be the most reactive. Therefore, the difference in reactivity between trioxane and paraldehyde may have been due to different relative rates of formation of monomeric species from the cyclic trimer, as discussed earlier. In the case of acetone, similar conversion was observed at various temperatures, suggesting that the reaction may have been under equilibrium control under the conditions tested.

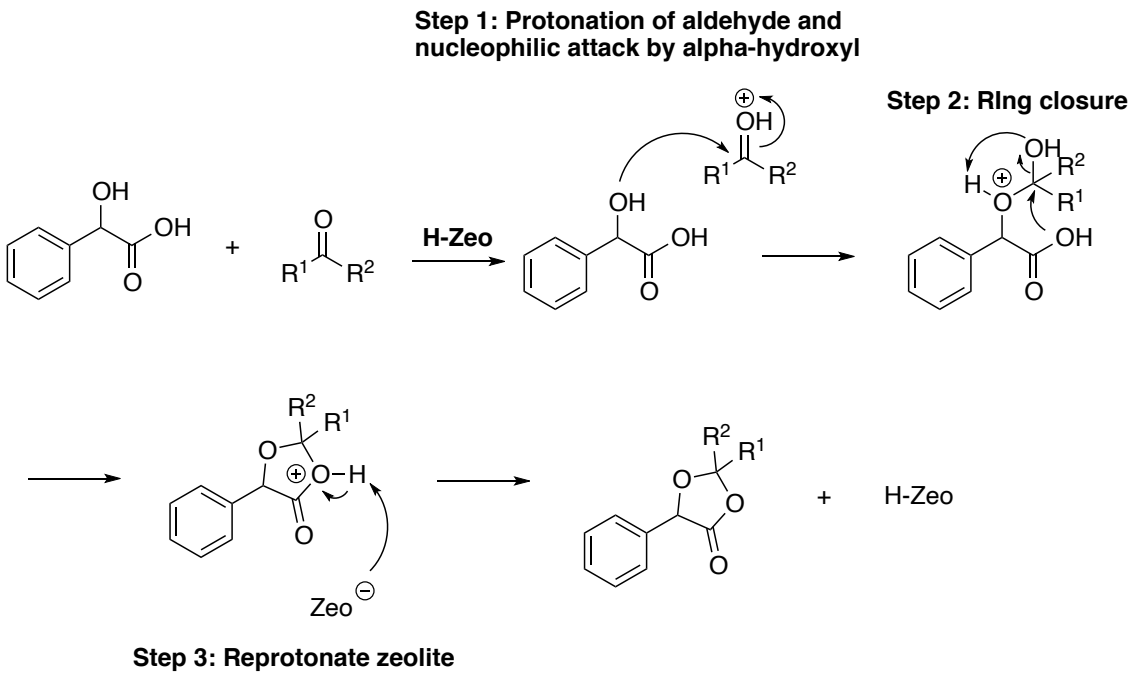

Figure 9 Possible mechanism of DOX formation over Brønsted acidic zeolites. In the case of use of trioxane and paraldehyde reagents, this mechanism would be preceded by an additional step of decomposition of the cyclic trimer to give free aldehyde (formaldehyde or acetaldehyde).

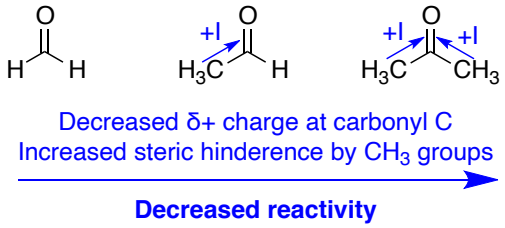

Figure 10 Reactivity trend for formaldehyde, acetaldehyde and acetone towards nucleophilic attack at the carbonyl carbon.

4.2.5 Effect of Time on Stream on Conversion

When assessing the synthesis of 5b-1, 5b-2 and 5b-3 in section 6.2.4, a fresh catalyst was used for each of the three monomers, but the same catalyst was used as we varied the temperature or flow rate in a given experimental run. As a result, as well as varying the temperature and the flow rate, the time on stream increased throughout the experiment for a given monomer. Therefore, the results in Figure 8 may have also shown some trends resulting from catalyst aging.

In Figure 8c for example, the trend for paraldehyde shows an increase in conversion between 40 °C and 80 °C, followed by a gradual decrease above 80 °C. After collecting the data in Figure 8c, we returned the temperature to 80 °C and monitored the conversion over time. The data is shown in Figure 11. T = 0 is the time at which the reactor had cooled back to 80 °C. The data shows a fairly rapid decrease in conversion, with almost

no activity after 2 hours on stream. This is likely due to catalyst deactivation. For the results shown in Figure 8c, the products were collected for 10 minutes at each temperature. Comparison of this time scale with Figure 11 shows that significant deactivation of the catalyst would have occurred by the time products had been collected at all four temperatures (*ca*. 50 minutes in total, including time to increase the reactor temperature between samples). For example, in Figure 11, 30 minutes time on stream at 80 °C led to a decrease in conversion from around 80% to less than 60%, and further decrease to less than 40% after 60 minutes.

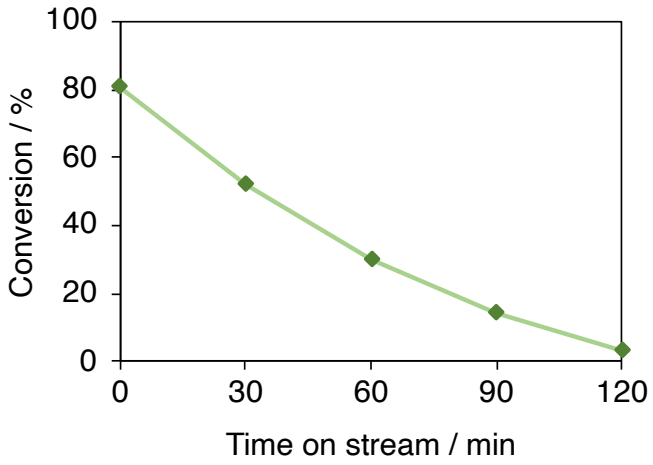

Figure 11 Effect of time on stream on conversion of mandelic acid to 5-phenyl-2-methyl-1,3-dioxolan-4-one over H-Y-30 zeolite in X-Cube flow reactor. Catalyst: Zeolite H-Y-30 (300 mg, 60-80 mesh). Feed: mandelic acid (2 g), paraldehyde (7.6 g, 13 eqv.), mesitylene (0.4 g, internal standard), MeCN (50 ml). Temperature: 80 °C, flow rate: 0.5 ml min^{-1}.

Following on from the initial experiments using the X-Cube flow reactor, further experiments focussing specifically on MePh-DOX (5b-2) were carried out to try to better understand the effects of the conditions and reagent stoichiometry. We chose this substrate because there was very little literature on its polymerisation,[19] so we considered it a good candidate for taking forward into polymerisation studies. This polymerisation work is discussed in the next chapter of this thesis. Our initial experiments suggested that there was a minimum temperature of 80 °C required for high conversion, above which there was no improvement in conversion. We hypothesised that a lack of free acetaldehyde (due to incomplete decomposition of the cyclic trimer) was limiting conversion at low temperatures. At 80 °C and above, conversion was high (>80%), irrespective of temperature. Our results for batch reactions in section 6.2.3 also showed that the ratio of aldehyde to mandelic acid was important, with high excess of aldehyde shown to produce better results. At this point in the project, the sample of H-Y-30 used for our reactions ran out and, due to time constraints, we could not source more material. As a result, the data from Figure 12 onwards uses H-Y-40 as a catalyst. We found that

activity was similar for H-Y-30 and H-Y-40, probably due to similarity in the properties of the catalysts. They are both zeolite Y catalysts from the ZBV series (ZBV 760 and 780, respectively) sold by Zeolyst. HY40 has been subjected to a stronger acid treatment after steaming which results in the higher Si/Al ratio,[24] but both are ultrastabilised zeolite Y catalysts with significant mesoporosity. For further details of zeolite properties, see the Appendices.

Firstly, the influence of temperature was repeated, but this time the temperatures were investigated in decreasing order, starting at 160 °C, to investigate the highest reaction temperatures using a fresh catalyst (i.e. without the negative effects of catalyst aging whilst testing lower temperatures). Conversion at 160 °C was very similar to the previous experiment (Figure 12 – previous experiment shown for comparison). As the temperature was decreased, we observed that the conversion deviated significantly from the previous experiment. When investigating the temperatures in reverse, the total time on stream was longer, due to the longer time required to cool the reactor to a lower temperature compared with heating to higher temperatures (the reactor doesn't have an active cooling mechanism, so requires ambient cooling to decrease the temperature). It seems likely that the additional time on stream caused increased catalyst deactivation, which explains the deviation at temperatures of 120 °C and below in the two experiments.

When conducting these experiments, we also monitored the ratio of cyclic trimer to acetaldehyde. For temperatures of 80–160 °C, analysis of the residual paraldehyde in the product mixtures showed that more than 90% of paraldehyde had dissociated to free acetaldehyde. However, at 40 °C, very little paraldehyde had dissociated. This may explain the low conversion at 40 °C compared with higher temperatures. Comparing with the previous temperature dependence experiment shows that at temperatures of 80-160 °C, residual paraldehyde is similar for both experiments, but at 40 °C, residual paraldehyde is much lower when the temperatures were run in reverse order. This data suggested that paraldehyde dissociation was dependent on both the reactor temperature and the state of the catalyst. Paraldehyde decomposition can be acid-catalysed, so it seems likely based on our results that decomposition was catalysed (at least to some extent) by the zeolite.[22] Some other examples also suggest that decomposition of paraldehyde can be the rate-determining step when used as a source of acetaldehyde, for example, in the synthesis of poly(oxymethylene)[20] and dimethoxymethane.[21]

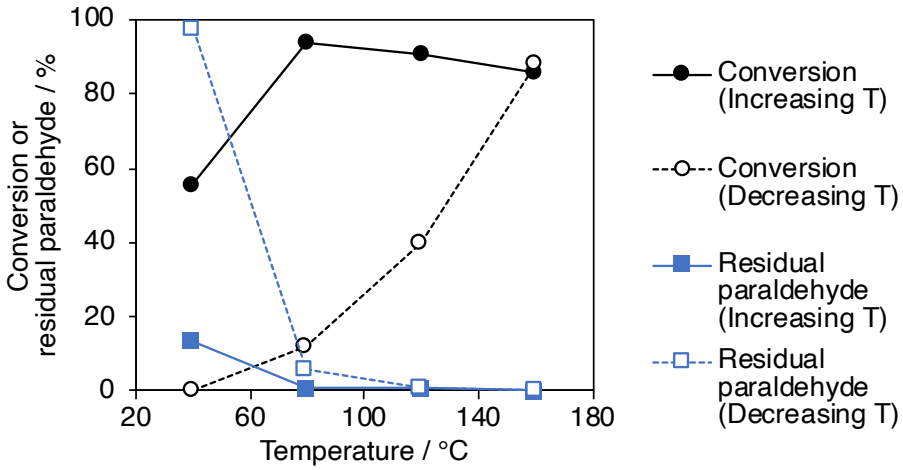

Figure 12 Effect of temperature on conversion of mandelic acid when the temperatures were investigated in increasing order (solid line) or decreasing order (dashed line). Catalyst: Zeolite H-Y-40 (300 mg, 60-80 mesh). Feed: mandelic acid (2 g), paraldehyde (7.6 g, 13 eqv.), mesitylene (0.4 g, internal standard), MeCN (50 ml). Flow rate: 0.5 ml min^{-1}.

BET analysis was carried out on two samples of USY zeolite: the fresh zeolite and the spent catalyst from the experiment shown in Figure 12. The spent zeolite has a lower BET surface area and total pore volume, but still retains a significant micropore volume of 0.15 cm^3 g^{-1}. This suggests that some pore blockage had occurred and that this may be contributing to catalyst deactivation, but this is not sufficient to explain the large decrease in activity. The spent zeolite was not analysed further, but it would have been informative to collect a pXRD spectrum of the spent zeolite. Regeneration (e.g. by calcination) could also be done to remove occluded species deposited during the reactions, followed by repeating the catalytic tests and the BET analysis to investigate whether the deactivation of the zeolite was reversible.

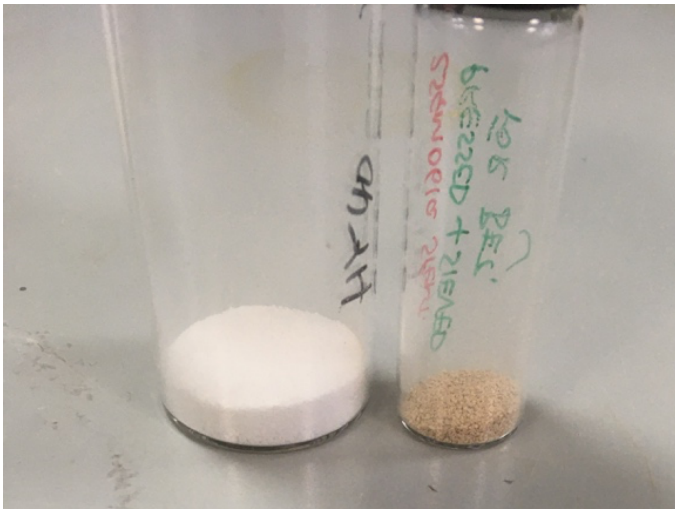

Figure 13 Fresh and spent H-Y-40.

Table 4 Textural properties of fresh and spent zeolite Y.

Zeolite	BET Surface Area / $m^2\ g^{-1}$	S_{micro}[b] / $m^2\ g^{-1}$	V_{micro}[b] / $cm^3\ g^{-1}$	V_{meso}[c] / $cm^3\ g^{-1}$	V_{total}[d] / $cm^3\ g^{-1}$
H-Y-40	810	519	0.21	0.25	0.46
Spent H-Y-40	607	379	0.15	0.21	0.36

(a) EDXRF; (b) t-plot method; (c) $V_{meso} = V_{total} - V_{micro}$; (d) BJH method.

4.2.6 Effect of Reactor Temperature on Cyclic Trimer Dissociation

The X-Cube reactor has two heating blocks with catalyst cartridges ("CatCart") in them. For all the experiments here, the CatCart containing the zeolite was loaded into the second heating block. The CatCart in the first heating block was filled with silicon carbide – an inert material used as a "blank". A further experiment was conducted to investigate whether the temperature of the first heating block (T_1) had any effect on conversion or residual paraldehyde. If the dissociation of the cyclic trimer was not catalyst dependent, then we would expect to see an increase in free paraldehyde when T_1 was increased.

On increasing the temperature of the first catalyst bed, T_1, from 40 °C to 100 °C, with T_2 maintained at 40 °C, there was little change in the residual paraldehyde, remaining at around 13 %. Conversion decreased with time, likely due to catalyst deactivation rather than the increasing T_1. The same experiment was run with T_2 increased to 60 °C. This led to both an increase in conversion and a decrease in the amount of residual paraldehyde compared with T_2 set at 40 °C. Once again, conversion decreased over time and residual paraldehyde remained constant despite increasing T_1 temperature. These results suggest that the dissociation of paraldehyde to acetaldehyde is dependent on the temperature of the zeolite catalyst bed, T_2, but not the temperature of the blank CatCart, T_1. Therefore, the zeolite plays a role in both the initial dissociation of the cyclic trimer and in the formation of DOX from mandelic acid and acetaldehyde. However, at constant T_2 temperature, the amount of paraldehyde present was constant with time whilst conversion decreased steadily, suggesting that catalyst aging or deactivation affected the decomposition of paraldehyde and conversion of mandelic acid differently. We attempted to increase the T_1 temperature much higher, to 160 °C, but we observed no conversion of mandelic acid, and very little dissociation of paraldehyde. This further showed that the dissociation of paraldehyde did not increase with increased T_1 temperature. Additionally, it showed that any dissociation catalysed by the zeolite had also stopped by this stage of the experiment, possibly due to catalyst deactivation.

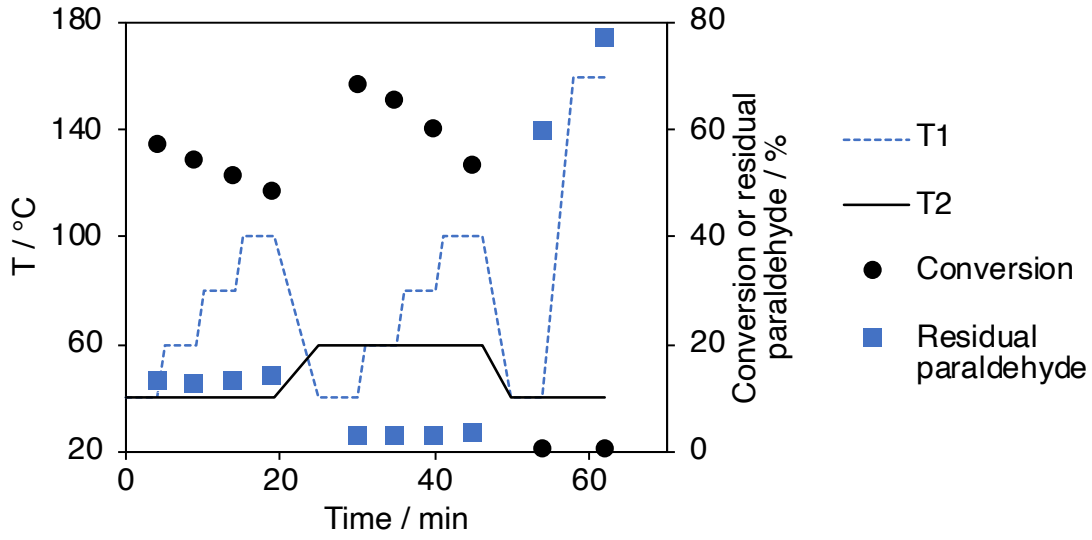

Figure 14 Effect of changing the temperature of the blank catalyst cartridge (T_1) on conversion and paraldehyde decomposition. Catalyst: Zeolite H-Y-40 (300 mg, 60-80 mesh). Feed: mandelic acid (2 g), paraldehyde (7.6 g, 13 eqv.), mesitylene (0.4 g, internal standard), MeCN (50 ml). Temperature: T_1 = 40-160 °C, T_2 = 40-60 °C flow rate: 0.5 ml min^{-1}.

4.2.7 Effect of Time on Stream on Conversion and Cyclic Trimer Dissociation

Changing the reagent stoichiometry had a large effect on conversion in the batch reactions discussed earlier. Figure 15 shows conversion at three different ratios of acetaldehyde to mandelic acid. For each ratio, the reaction temperature was increased from 30 °C to 80 °C, and then held at 80 °C for approximately 80 minutes. As the amount of acetaldehyde was increased, the conversion increased. This was consistent across all temperatures from 30 °C to 80 °C. The amount of residual paraldehyde (i.e. the amount that hasn't been converted to free acetaldehyde) in the product solution is also shown as a percentage of the amount of paraldehyde in the feed. For all ratios, no paraldehyde was observed in the product solutions collected at 40 minutes or earlier. At longer times, the amount of paraldehyde began to increase, but conversion had already decreased to 15% or lower by this point. The data shows that a higher amount of acetaldehyde relative to mandelic acid results in higher conversion. This trend is similar to that observed for batch reactions. As discussed earlier, excess acetaldehyde may be needed in the batch reactions to compensate loss by evaporation and collection in the phase separator. However, this could not be the case here, the flow reactor is sealed so evaporation should not affect the reaction. It also shows that the dissociation is not affected by the initial catalyst deactivation that occurs before about 60 minutes.

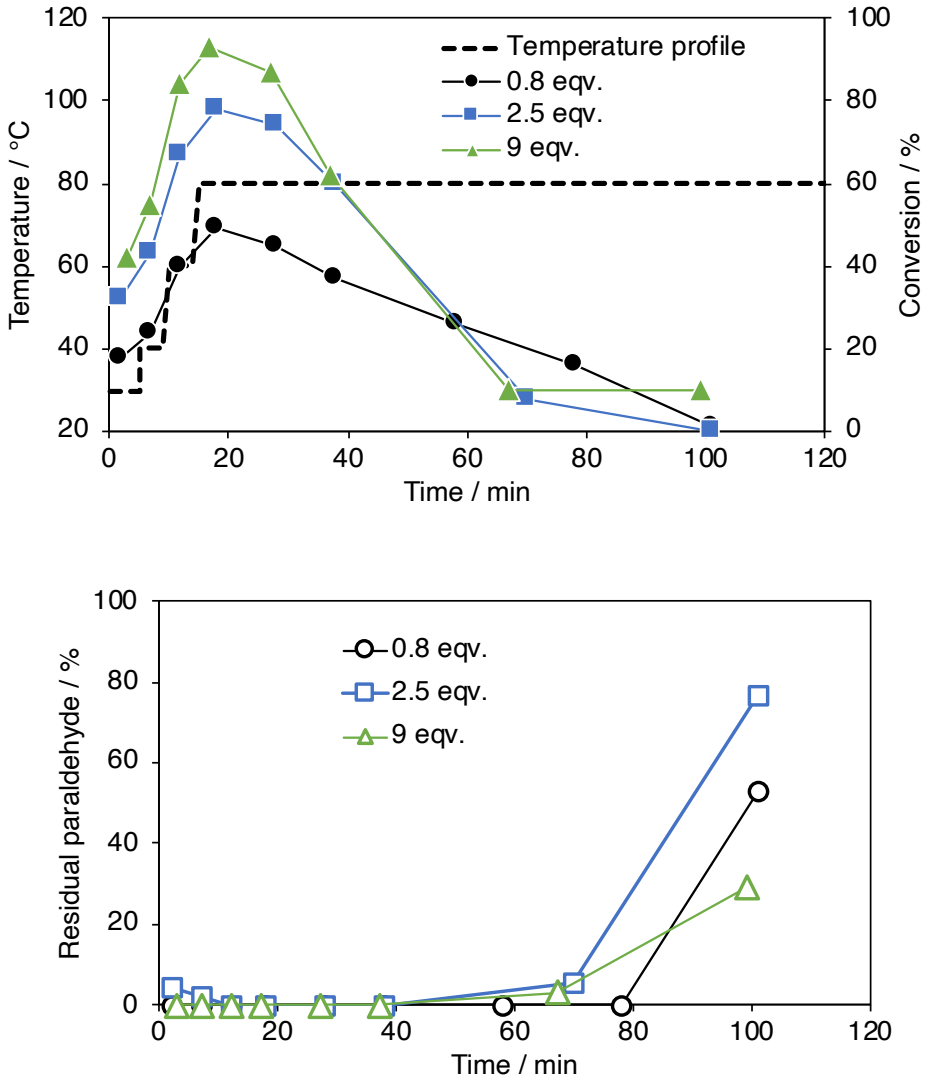

Figure 15 Effect of time on stream for the reaction of mandelic acid with acetaldehyde at with 3 different feed compositions of mandelic acid:acetaldehyde ratio: 0.8 eqv, 2.5 eqv and 9 eqv. Temperature was increased from 30 °C to 80 °C (temperature profile is shown) and then held at 80 °C. Catalyst: Zeolite H-Y-40 (100 mg, 60-80 mesh). Feed: mandelic acid (2 g), mesitylene (0.4 g, internal standard), MeCN (50 ml). Flow rate: 0.5 ml min^{-1}.

To further investigate the effect of time on stream on conversion, an additional experiment at three temperatures was conducted (Figure 16). The rate of decrease in conversion with time on stream was similar at all three temperatures and the decrease started at t = 0, suggesting that the reaction temperature did not influence the rate of catalyst deactivation (which was presumed to cause the decrease in conversion over time). In contrast, there was a lag in the increase in paraldehyde. It began to increase after around 30 minutes and interestingly the trend is very different at 80 °C compared with 100 °C and 120 °C. The slightly higher temperatures resulted in a much more significant decrease in conversion of paraldehyde to acetaldehyde. Catalyst deactivation may be the reason for the decrease over time in both the conversion of mandelic acid to DOX and of paraldehyde to acetaldehyde. It is not clear why the trend in the amount of

paraldehyde measured in the product mixtures was different for different temperatures, as the trends in conversion were similar, presumably due to similar rates of catalyst deactivation. It's also not clear why there is a lag time of around 30 minutes before the paraldehyde conversion decreases, whilst mandelic acid conversion decreases steadily from t = 0. These results do show that the amount of free acetaldehyde was not a contributing factor on the decreased conversion over time, as a large excess of free acetaldehyde was still present after 50 minutes at 80 °C, but conversion had dropped below 20%.

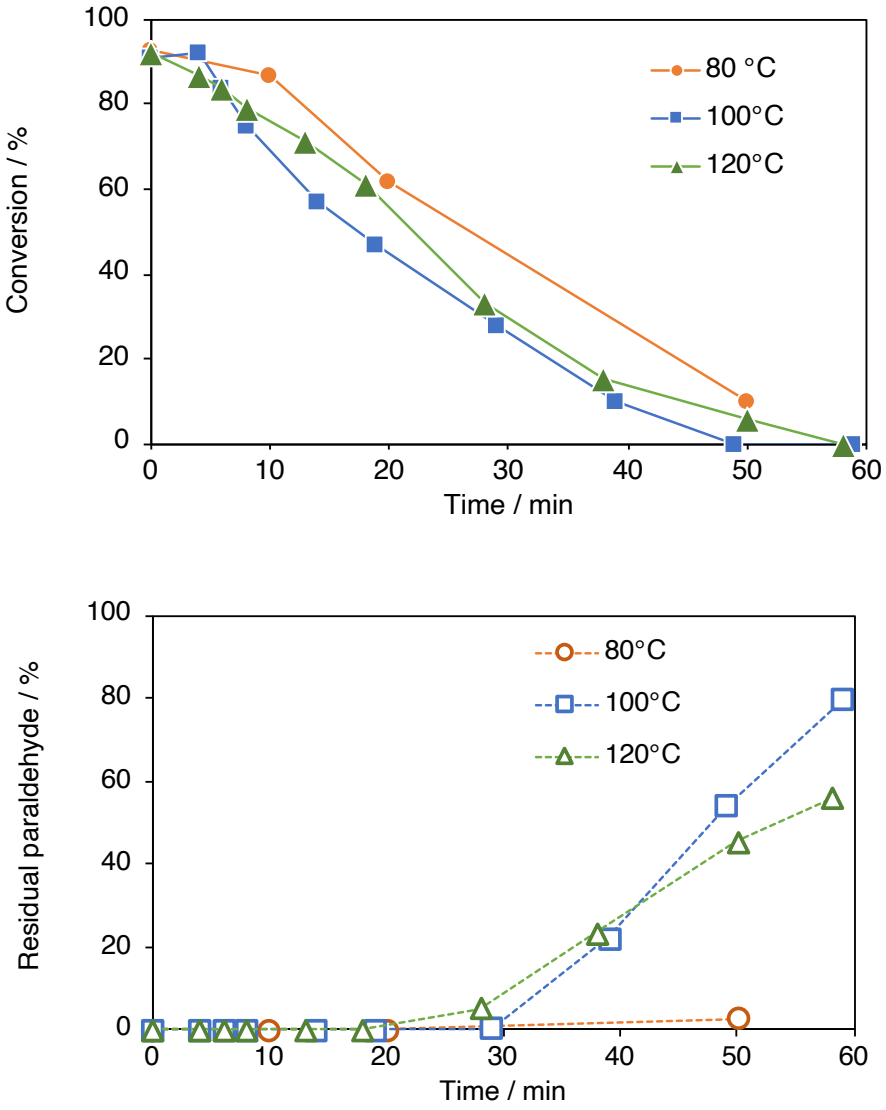

Figure 16 Effect of time on stream on conversion and the amount of residual paraldehyde in the product solution at 80 °C, 100 °C and 120 °C. Catalyst: Zeolite H-Y-40 (100 mg, 60-80 mesh). Feed: mandelic acid (2 g), paraldehyde (12 g, 10 eqv.), mesitylene (0.4 g, internal standard), MeCN (50 ml). Flow rate: 0.5 ml min^{-1}.

In these experiments, at 100 °C and 120 °C, an unknown compound was also observed – see the peak at 5.43 ppm in the ^{1}H NMR spectrum in $CDCl_3$ (Figure 17a). This had not

been previously observed and was only present in the samples taken at 100 °C and 120 °C. This remains unassigned and was not used in the quantitative analysis. Another signal in the methyl region with a 3:1 relative integral to the signal at 5.43 ppm suggests that this unknown could be similar in structure to the DOX. It's possible that this unknown may correspond to the linear form of MePh-DOX, prior to cyclisation (Figure 17b) but this was not confirmed.

(a)

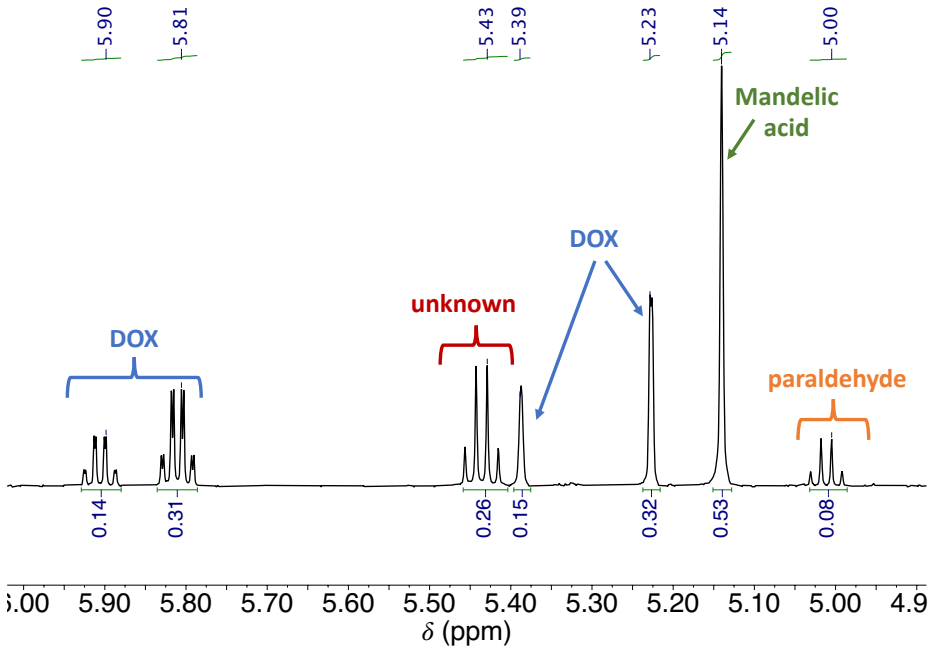

(b)

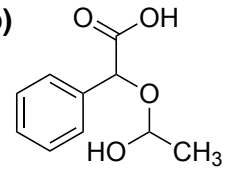

Figure 17 (a) ^{1}H NMR spectrum of eluent solution diluted in $CDCl_3$ showing unknown resonance at 5.43 ppm (quartet). (b) Possible structure of impurity (2-(1-hydroxyethoxy)-2-phenylacetic acid).

4.2.8 Comparison of Synthesis of MePh-DOX (5b-2) in Batch and Flow

We calculated the approximate number of turnovers in some of the reactions in order to compare the batch and flow syntheses (Table 5). These calculations were made on the assumption that selectivity is high (i.e. no byproducts are accounted for). However, as discussed above, some byproducts do form in flow reactions under certain conditions. The reactions utilise an excess of acetaldehyde. As seen earlier, the amount of acetaldehyde is very influential on the conversion of mandelic acid. The different solvent

choice may also influence the reaction. For example, acetonitrile is more polar than cyclohexane and is also known to adsorb onto zeolite Brønsted acid sites – it is commonly used as a probe molecule in characterisation of zeolite acid sites by vibrational spectroscopy.[25] For these reasons, these calculations are useful only as a qualitative comparison. The decrease in conversion with time on stream is reasonably approximated as a linear decrease, and this assumption was used to approximate the amount of mandelic acid converted in 1 hour, based on the flow rate and mandelic acid concentration.

The total amount of mandelic acid converted in batch is lower than in flow at equivalent ratios of mandelic acid to acetaldehyde. The conversion was only comparable when the batch reaction was run with a higher excess of acetaldehyde (60 equivalents). It is clear from the flow results that conversion had completely subsided after 1 hour, showing the catalyst was no longer active. However, in the batch reactions, the catalyst may still have been active. The reaction could have been run for longer or a further charge of mandelic acid and acetaldehyde could have been added to investigate the state of the catalyst at this point in the batch reaction. These results show that the flow process was more efficient than the batch conditions tested, achieving a greater number of mandelic acid turnovers under similar conditions. However, the data is not sufficient to compare the rates of deactivation or the maximum number of turnovers possible in batch with those achieved in flow, due to lack of information about the state of the spent catalyst from the batch reactions.

Table 5 Comparison of conversion of mandelic acid over H-Y-30 in batch and flow after 1 hour.

Reaction	**MA concentration / g ml^{-1}**	**Acetaldehyde eqv.**	**Solvent**	**T* / °C**	**Mandelic acid converted / mmol g_{zeo}^{-1} h^{-1}**
Batch	0.02	12	Cyclohexane (b.p. = 80 °C)	100	10.5
Batch	0.023	60	Cyclohexane (b.p. = 80 °C)	100	40
Flow	0.040	10	Acetonitrile (b.p. = 80 °C)	120	36

* Temperature of hotplate (batch reactions) or heating unit (flow reactions)

4.2.9 Practical Problems

Whist our results show that it is possible to synthesise DOX in a flow reactor, catalyst lifetime was only around two hours and we encountered significant problems associated with poor mandelic acid solubility. This led to frequent blocking of the reactor. DOX monomers are known to be more soluble than mandelide, and most of the blockages were occurring around the HPLC pumps (see Figure 18). The feed solution passes through the HPLC pumps before it reaches either of the two heating blocks, so the blockages were occurring before any product had been formed. Therefore, mandelic acid solubility was the problem here. Reactor blocking might have been reduced by alternative solvent choice or by reducing the mandelic acid concentration, but we did not conduct these experiments.

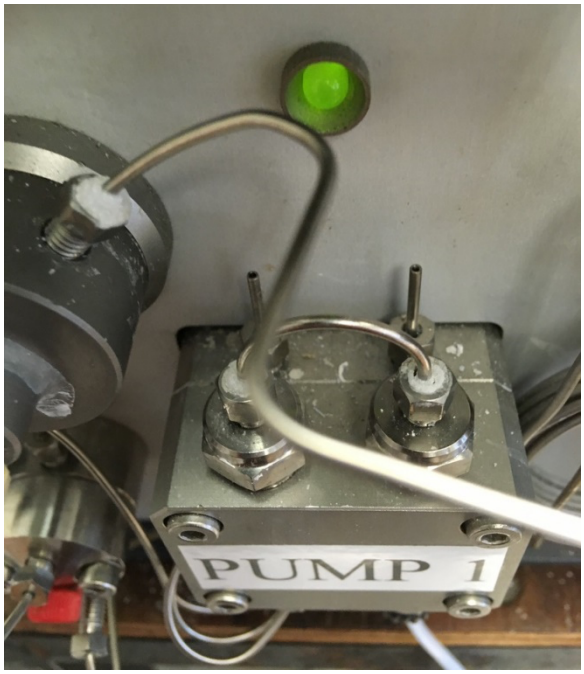

Figure 18 Picture showing solid (presumably mandelic acid) at the junction of the HPLC pumps.

4.3 Conclusions

Following on from attempts to synthesise mandelide over zeolite catalysts, we investigated the synthesis of a series of alternative monomers, the 1,3-dioxolan-4-ones (DOX). Once again, we found that the H-Y-30 catalyst was the most selective, suggesting some structure-activity relationship between this catalyst and mandelic acid. In later experiments, a similar zeolite H-Y-40, was also found to be effective for the same reactions under flow conditions. Compared with the literature synthesis, we found the catalyst loading of H-Y-30 could be decreased relative to that used for *p*-TSA. However, we found that this was only the case for the reaction of acetone with mandelic acid. The literature method for acetone involved using a large excess of acetone in the solvent mix,

whereas the reaction of formaldehyde or acetaldehyde used ratios close to stoichiometric. In batch reactions, the catalyst loading and ratio of aldehyde to mandelic acid were found to be influential on conversion, with a high excess of aldehyde leading to improved results.

In an X-cube flow reactor, the effect of flow rate and temperature was very different depending on the aldehyde or ketone used. This may have been due to differences in reactivity or equilibrium limitations. In the case of formaldehyde and acetaldehyde, cyclic trimers were used as the reagent source. Based on sterics and electronics, it would be expected that formaldehyde would be the most reactive of these two aldehydes. However, we observed the converse in our results. Therefore, this trend suggested that some other factor was more influential on the reaction outcome than aldehyde reactivity. A possible explanation is different rates of dissociation of the two trimers. Conversion increased significantly with increasing temperature. This result was similar to a previous report in the literature for carbonylation of trioxane over H-ZSM-5[13] and suggested that the dissociation of the cyclic trimers may be highly temperature dependent. When acetone was used (to synthesise Me_2Ph-DOX), increasing the temperature had very little effect on conversion, suggesting the amount of acetone or the catalyst loading might have been limiting. Very little difference was observed as temperature was increased from 80 °C to 120 °C for MePh-DOX, with the slight decrease in conversion as temperature increased likely to be due to catalyst deactivation occurring in the timescale of the experiment.

Dissociation of the cyclic trimer, paraldehyde, was temperature dependent between 40 °C and 80 °C. However, this temperature dependence was only observed when heating the zeolite catalyst bed, suggesting that dissociation of paraldehyde may have been catalysed by the zeolite. At temperatures between 30 °C and 80 °C, increasing the ratio of paraldehyde to mandelic acid in the feed increased the conversion at each given temperature. Catalyst deactivation occurred at a similar rate irrespective of paraldehyde ratio and conversion (i.e. number of turnovers). This suggested catalyst deactivation may have been influenced by some other factor than the turnover of mandelic acid to DOX, such as acid site poisoning by the acetamide generated from the acetonitrile solvent.[26]

Monitoring the reaction over time showed that catalyst deactivation occurred fairly rapidly, with a complete loss of conversion after two hours at 80 °C. Textural analysis of a spent catalyst suggested that pore blockage may have been a contributing factor in this deactivation, with a decrease in micropore volume observed relative to a fresh catalyst. The rate of deactivation was similar at 80 °C, 100 °C and 120 °C. However, the dissociation of paraldehyde decreased after 1 hour at 100 °C and 120 °C, but remained

high at 80 °C. This suggested that, whilst earlier experiments showed that paraldehyde dissociation and DOX production were both catalysed by the zeolite, these two processes were influenced differently by catalyst ageing. DOX production decreased over time from the beginning of the reaction, whilst the extent of paraldehyde dissociation began to decrease comparably later in time. This suggests these two processes may be catalysed by different sites on the zeolites, with the sites catalysing DOX production beginning to deactivate earlier in the reaction.

Comparison of the reactions conducted under batch and flow conditions suggested that the flow reactor was more efficient at producing DOX, with a higher overall turnover of mandelic acid after 1 hour under similar conditions. It was only at much higher ratios of acetaldehyde to mandelic acid that the batch conditions were comparable to flow in terms of total turnovers. Despite this apparent improvement relative to the batch reactions, the use of the flow reactor still had significant drawbacks due to poor mandelic acid solubility and the observed catalyst deactivation.

4.4 References

1. Liu, T. Q.; Simmons, T. L.; Bohnsack, D. A.; Mackay, M. E.; Smith, M. R.; Baker, G. L., Synthesis of polymandelide: A degradable polylactide derivative with polystyrene-like properties. *Macromol.* **2007,** *40* (17), 6040-6047.

2. Graulus, G. J.; Van Herck, N.; Van Hecke, K.; Van Driessche, G.; Devreese, B.; Thienpont, H.; Ottevaere, H.; Van Vlierberghe, S.; Dubruel, P., Ring opening copolymerisation of lactide and mandelide for the development of environmentally degradable polyesters with controllable glass transition temperatures. *React. Funct. Polym.* **2018,** *128*, 16-23.

3. Thillaye du Boullay, O.; Marchal, E.; Martin-Vaca, B.; Cossio, F. P.; Bourissou, D., An activated equivalent of lactide toward organocatalytic ring-opening polymerization. *J. Am. Chem. Soc.* **2006,** *128* (51), 16442-3.

4. Bonduelle, C.; Martin-Vaca, B.; Cossio, F. P.; Bourissou, D., Monomer versus alcohol activation in the 4-dimethylaminopyridine-catalyzed ring-opening polymerization of lactide and lactic O-carboxylic anhydride. *Chemistry* **2008,** *14* (17), 5304-12.

5. Cairns, S. A.; Schultheiss, A.; Shaver, M. P., A broad scope of aliphatic polyesters prepared by elimination of small molecules from sustainable 1,3-dioxolan-4-ones. *Polym. Chem.* **2017,** *8* (19), 2990-2996.

6. Xu, Y.; Perry, M. R.; Cairns, S. A.; Shaver, M. P., Understanding the ring-opening polymerisation of dioxolanones. *Polym. Chem.* **2019,** *10* (23), 3048-3054.

7. Buchard, A.; Carbery, D. R.; Davidson, M. G.; Ivanova, P. K.; Jeffery, B. J.; Kociok-Kohn, G. I.; Lowe, J. P., Preparation of stereoregular isotactic poly(mandelic acid) through organocatalytic ring-opening polymerization of a cyclic O-carboxyanhydride. *Angew. Chem. Int. Ed. Engl.* **2014,** *53* (50), 13858-61.

8. Vagenende, M.; Graulus, G.-J.; Delaey, J.; Van Hoorick, J.; Berghmans, F.; Thienpont, H.; Van Vlierberghe, S.; Dubruel, P., Amorphous random copolymers of lacOCA and manOCA for the design of biodegradable polyesters with tuneable properties. *Eur. Polym. J.* **2019,** *118*, 685-693.

9. Tang, L.; Deng, L., Dynamic Kinetic Resolution via Dual-Function Catalysis of Modified Cinchona Alkaloids: Asymmetric Synthesis of α-Hydroxy Carboxylic Acids. *J. Am. Chem. Soc.* **2002,** *124* (12), 2870-2871.

10. Martin, R. T.; Camargo, L. P.; Miller, S. A., Marine-degradable polylactic acid. *Green Chem.* **2014,** *16* (4), 1768-1773.

11. Gazzotti, S.; Ortenzi, M. A.; Farina, H.; Silvani, A., 1,3-Dioxolan-4-Ones as Promising Monomers for Aliphatic Polyesters: Metal-Free, in Bulk Preparation of PLA. *Polymers (Basel)* **2020,** *12* (10).

12. Xu, Y.; Șucu, T.; Perry, M. R.; Shaver, M. P., Alicyclic polyesters from a bicyclic 1,3-dioxane-4-one. *Polym. Chem.* **2020**.

13. Sano, T.; Sekine, T.; Wang, Z.; Soga, K.; Takahashi, I.; Masuda, T., Synthesis of 1,3-dioxolan-4-one from trioxane and carbon monoxide on HZSM-5 zeolite. *Chem. Commun.* **1997,** (19), 1827-1828.

14. Kashyap, B.; Saikia, I.; Phukan, P., Silica sulfate as an efficient recyclable catalyst for protection of α-hydroxy acids with cyclohexanone. *Green Chem. Lett. Rev.* **2012,** *5* (1), 89-95.

15. Shcherbinin, V. A.; Konshin, V. V., Convenient synthesis of O-functionalized mandelic acids via Lewis acid mediated transformation of 1,3-dioxolan-4-ones. *Tetrahedron* **2019,** *75* (26), 3570-3578.

16. Hyoi, K.; Kanazawa, A.; Aoshima, S., Cationic Ring-Opening Co- and Terpolymerizations of Lactic Acid-Derived 1,3-Dioxolan-4-ones with Oxiranes and Vinyl Ethers: Nonhomopolymerizable Monomer for Degradable Co- and Terpolymers. *ACS Macro Lett.* **2019,** *8* (2), 128-133.

17. Jeswani, H. K.; Perry, M. R.; Shaver, M. P.; Azapagic, A., Biodegradable and conventional plastic packaging: Comparison of life cycle environmental impacts of poly(mandelic acid) and polystyrene. *Sci. Total Environ.* **2023,** *903*, 166311.

18. Asabe, Y.; Takitani, S.; Tsuzuki, Y., Studies of Saturated Heterocyclic Compounds. II. The Preparation and PMR Spectroscopic Study of Mono- and Di-substituted-1,3-dioxolan-4-ones. *Bull. Chem. Soc. Jpn.* **1975,** *48* (3), 966-970.

19. Inoue, M.; Kanazawa, A.; Aoshima, S., Living Cationic Ring-Opening Homo- and Copolymerization of Cyclohexene Oxide by “Dormant” Species Generation Using Cyclic Ethers as Lewis Basic Additives. *Macromol.* **2021,** *54* (11), 5124-5135.

20. Peláez, R.; Marín, P.; Ordóñez, S., Synthesis of poly(oxymethylene) dimethyl ethers from methylal and trioxane over acidic ion exchange resins: A kinetic study. *Chem. Eng. J.* **2020,** *396*.

21. Peláez, R.; Marín, P.; Ordóñez, S., Effect of formaldehyde precursor and water inhibition in dimethoxymethane synthesis from methanol over acidic ion exchange resins: mechanism and kinetics. *Biofuel. Bioprod. Bior.* **2021,** *15* (6), 1696-1708.

22. Withey, R. J.; Whalley, E., Pressure effect and mechanism in acid catalysis. Part 11.—Depolymerization of paraldehyde and trioxane. *Trans. Faraday Soc.* **1963,** *59*, 901-906.

23. Additions of Heteroatom Nucleophiles to Carbonyl Compounds and Subsequent Reactions—Condensations of Heteroatom Nucleophiles with Carbonyl Compounds. In *Organic Mechanisms*, 2010; pp 359-395.

24. Kenvin, J.; Mitchell, S.; Sterling, M.; Warringham, R.; Keller, T. C.; Crivelli, P.; Jagiello, J.; Pérez-Ramírez, J., Quantifying the Complex Pore Architecture of Hierarchical Faujasite Zeolites and the Impact on Diffusion. *Adv. Funct. Mater.* **2016,** *26* (31), 5621-5630.

25. Bordiga, S.; Lamberti, C.; Bonino, F.; Travert, A.; Thibault-Starzyk, F., Probing zeolites by vibrational spectroscopies. *Chem. Soc. Rev.* **2015,** *44* (20), 7262-341.

26. Barbosa, L. A. M. M.; van Santen, R. A., Study of the Hydrolysis of Acetonitrile Using Different Brønsted Acid Models: Zeolite-Type and HCl(H2O)x Clusters. *J. Catal.* **2000,** *191* (1), 200-217.

Chapter 5: Evaluation of 2-Methyl-5-phenyl-1,3-dioxolan-4-one as a Monomer for the Synthesis of Poly(mandelic acid) by Ring Opening Polymerisation

5.1 Introduction

5.1.1 Ring Opening Polymerisation of 1,3-dioxolan-4-ones (DOX)

The development of ring opening polymerisation (ROP) of 1,3-dioxolan-4-ones (DOXs) monomers is still relatively new in comparison to lactides or *O*-carboxyanhydrides (OCAs), with reports of DOX polymerisation only occurring in the last 10 years. There is some debate as to whether polymerisation of DOXs proceeds via elimination (Scheme 1a) or retention (Scheme 1b) of the carbonyl of the DOX monomer. These two routes lead to different polymer structures – polyesters or polyesteracetals. Scheme 2 shows the ring opening copolymerisation of the simplest DOX monomer, 1,3-dioxolan-4-one, with L-lactide.[1] The authors reported that a polyesteracetal is formed. They reported that the ^{1}H NMR spectrum of the polymer included a resonance associated with the CH_2 of the acetal group. However, they did not include any MALDI-TOF data and, given that the mass of the repeat unit would differ for polyesters and polyesteracetals, this would have been informative. In contrast, Shaver and coworkers[2] carried out the same reaction and saw no evidence of acetal retention in the final polymer and this was supported by MALDI-ToF data. Therefore, based on present understanding this appears to be the more likely of the two mechanisms.

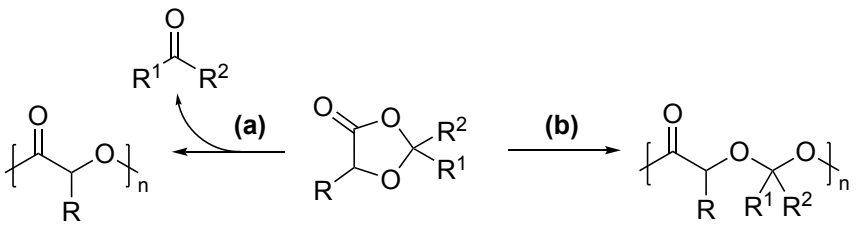

Scheme 1 (a) Elimination of carbonyl from DOX to give polyesters. (b) Retention of carbonyl to give polyesteracetals.

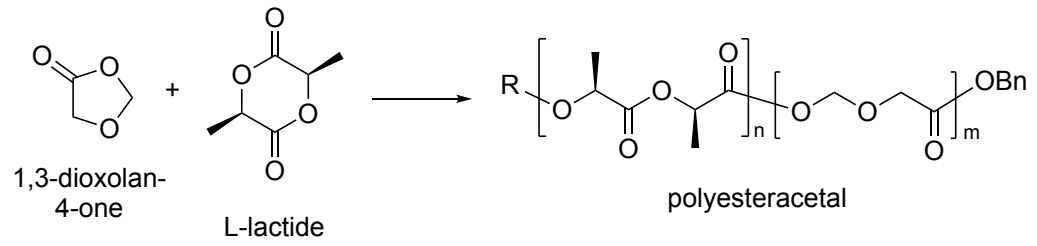

Scheme 2 Synthesis of polyesteracetals from the ring-opening copolymerisation of glycolic acid-derived 1,3-dioxolan-4-one and L-lactide.[1]

In addition to ROP of DOX, Hillmeyer and coworkers[3] have reported the polymerisation of a structurally similar monomer, 1,3-dixoane-4-one, using $ZnEt_2$ (shown in Scheme 3). They found that this monomer could polymerise with or without acetal retention. The mechanism depended on the amount of catalyst present, with low zinc loading leading to acetal retention (giving polyesteracetals) and high zinc loading leading to acetal elimination (giving polyesters).

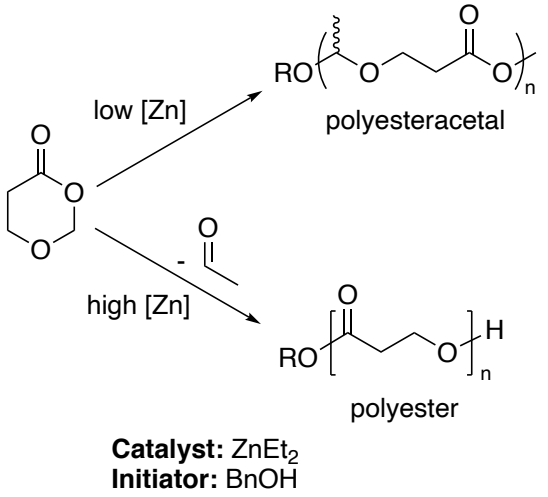

Scheme 3 Ring-opening polymersiation of a 1,3-dioxane-4-one. Reaction outcome was determined by the catalyst loading.[3]

Two more recent publications by Shaver and co-workers have expanded the monomer scope and provided additional insight into the mechanism of DOX polymerisation.[2, 4] In the presence of an Al(salen) catalyst, they were able to polymerise a range of DOX monomers.[2] They found that the Al(salen) catalyst outperformed other catalysts tested, such as tin(octanoate), DBU and $ZnEt_2$, both in terms of monomer conversion and tacticity control. However, experimental molecular weights were much lower than theoretical. A later publication by the same research group[4] suggested that a side reaction occurred between propagating polymer chains and formaldehyde during polymerisation, causing undesirable termination which was at least partly responsible for the discrepancy in molecular weight. As well as this side reaction causing termination of propagating chains, it was also proposed that it creates a new methoxy species that can

act as a new initiator, causing a further negative effect on molecular weight. As a result, experimental molecular weights as low as 10% of theoretical at 99% monomer conversion were observed.[4] Improved control over this side reaction was achieved by tuning the sterics of the salen ligands on the catalyst as well as the use of dynamic vacuum conditions to aid the removal of formaldehyde. However, the effects of this side reaction were not fully eliminated.

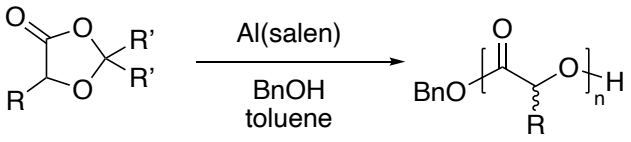

R = Me, Ph, i-Pr, Cy, n-Bu, i-Bu or t-Bu
R' = H or CH_3

Scheme 4 Ring-opening polymerisation of 1,3-dioxolan-4-ones using an Al(salen) catalyst.[2, 4]

Furthermore, these results were obtained for PhDOX (5b-1, Figure 1). The same reactions conducted with Me_2PhDOX (5b-3, Figure 1) required more forcing conditions and did not result in tacticity control. In the case of ^{t}BuPhDOX, no polymerisation was observed and instead the monomer decomposed.[4]

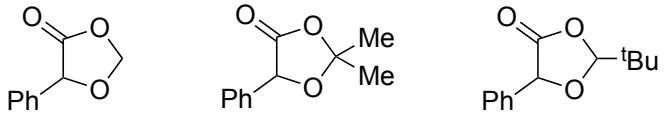

PhDOX **5b-1** | Me_2PhDOX **5b-3** | ^{t}BuPhDOX **5b-5**

Figure 1 DOX monomers of mandelic acid previously reported for ring opening polymerisation (ROP).[2, 4]

DOX monomers of lactic acid have also been polymerised using acid catalysts (Scheme 5).[5] These catalysts were investigated as metal-free alternatives to the $Sn(Oct)_2$ and Al(salen) catalysts previously reported for DOX polymerisation.[2, 4, 6] In the polymerisation of MeDOX (Scheme 5, R' = H) using trifluoroacetic acid (TFA) as catalyst, molecular weight initially increased slowly and reached full conversion after around 48 hours. The molecular weight distribution of the resultant polymer was bimodal with high polydispersity, suggesting the presence of two distinctly different molecular weights and poor control over the polymerisation. Once again, this was attributed to the action of formaldehyde in the reaction mixture. In contrast to the previous work on PhDOX (5b-1) and Me_2PhDOX (5b-3), the authors here found that polymerisation proceeded more readily for Me_3DOX than MeDOX. Polymerisation in the bulk, using *p*-TSA as a catalyst at ca. 5 mol% loading with respect to Me_3DOX, with a neopentanol initiator, yielded the highest molecular weight polymer in this study. Whilst the authors did not comment on it,

observed molecular weights were still fairly low at around 30% of theoretical based on the monomer:initiator ratio and once again they reported a bimodal molecular weight distribution, again indicating poor control of termination reactions.

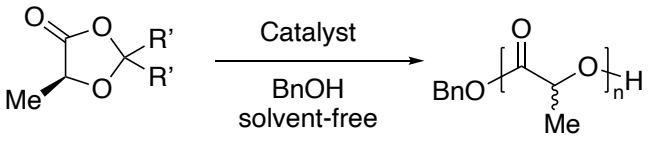

R' = H or CH_3
Catalyst = TfOH, p-TSA, TFA, CSA, DPP

Scheme 5 Organocatalysed ring-opening polymerisation of 1,3-dioxolan-4-ones dervied from L-lactic acid. Catalysts: triflic acid (TfOH), paratoluenesulfonic acid (p-TSA), trifluoroacetic acid (TFA), camphorsulfonic acid (CSA) and diphenylphosphate (DPP).[5]

5.1.2 Coordination-Insertion Mechanism

It has been proposed that ROP of 1,3-dioxolan-4-one monomers catalysed by MeAl(salen) complexes proceeds via a coordination-insertion mechanism (shown in Scheme 6).[2, 4] This mechanism is common amongst ROP of other bioderived cyclic ester monomers, such as lactides and lactones,[7, 8] commencing with coordination of the monomer to the catalyst, followed by cleavage of the ester bond by the initiator. Commonly, the initiator is an alcohol added in a 1:1 ratio with the catalyst. In an ideal reaction, each catalyst:initiator complex will initiate only one polymer chain. Therefore, in a well-controlled reaction, the length of the polymer chain is dictated by the ratio of catalyst to monomer added. Deviation of the experimental molecular weight ($M_{n,exp}$) away from the theoretical molecular weight ($M_{n,theo}$ – calculated based on the monomer:initiator ratio) is usually an indication that the reaction is poorly controlled. This can occur for various different reasons: for example, side reactions such as transesterification can lead to termination of the growing chain before it reaches the desired molecular weight. The presence of water in the reaction mixture can also lead to unwanted initiation and/or termination, with initiation leading to an increase in the number of polymer chains and termination preventing them from reaching the theoretical degree of polymerisation.

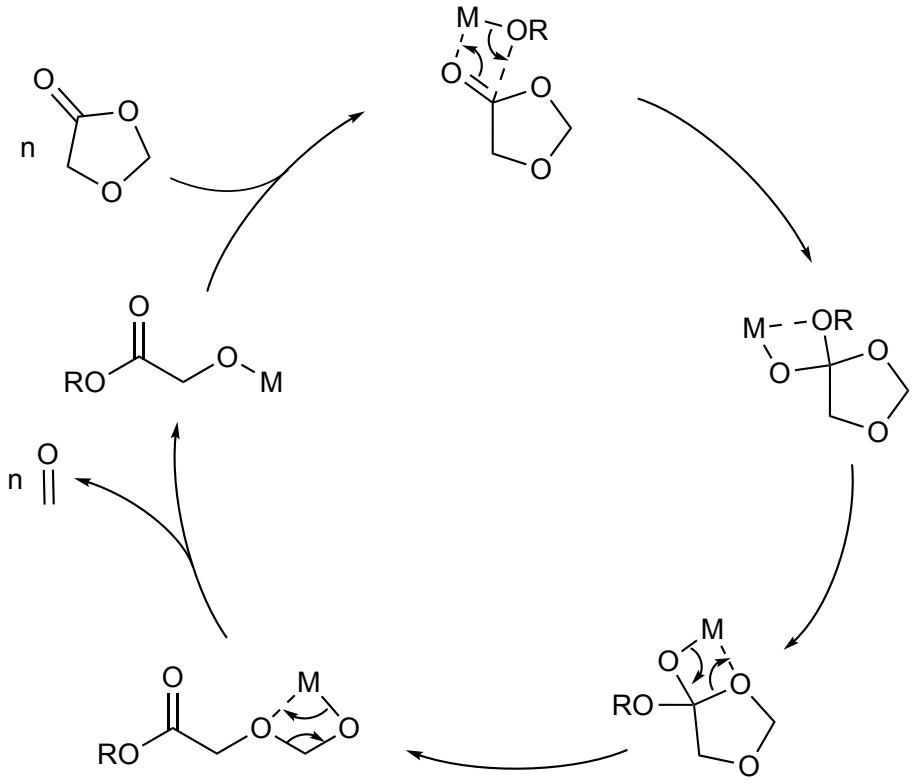

Scheme 6 Mechanism for the coordination–insertion ROP of DOX monomers by MeAl(salen) catalysts proposed in the literature.[2]

5.1.3 Ring Opening Polymerisation of 2-methyl-5-phenyl-1,3-dioxolan-4-one (MePhDOX, 5b-2)

As reported in the previous chapter, DOX monomers were successfully synthesised using zeolites as catalysts under both batch and flow conditions. 2-methyl-5-phenyl-1,3-dioxolan-4-one (PhMeDOX, 5b-2), one of the DOX products of mandelic acid and acetaldehyde reported in the previous chapter of this thesis, has not previously been polymerised to our knowledge.

In this chapter, ROP of 5b-2 monomer has been attempted using catalysts and conditions previously reported in the literature for other DOX monomers. The current literature on ROP of these monomers suggests that the outcome is highly sensitive to the monomer structure. For example, reactivity varies greatly with even small changes in monomer structure, due to changes in sterics of the alpha-hydroxy acid and the Thorpe-Ingold effect (also referred to as the *gem*-dimethyl effect) for DOX monomers of acetone.[2] Furthermore, there are conflicting opinions as to whether polyesters or polyesteracetals form.

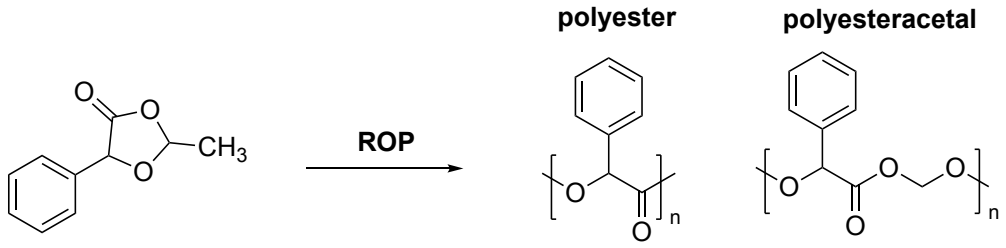

Figure 2 Possible polymers that could form from ring opening polymerisation of MePhDOX (5b-2).

5.2 Results and Discussion

5.2.1 Acid-Catalysed Bulk Polymerisation of MePh-DOX (5b-2)

As discussed above (Scheme 5), the polymerisation of 1,3-dioxolan-4-ones has been reported using acid catalysis.[5] Polymerisation of 5a-1 or 5a-3 in the bulk at 100 °C gave poly(lactic acid). In this work, these conditions were replicated for the ROP of MePh-DOX (5b-2). Three monomer:catalyst:initiator (M:C:I) ratios were tested: 200:10:1, 400:10:1 and 2000:10:1. A colour change from clear colourless liquid to dark brown was observed for each of these three reactions (Figure 3a). Evidence of oligomerisation/polymerisation was only observed at the lowest M:C:I ratio (highest catalyst loading) of 200:10:1. The resonance associated with the methine proton of poly(mandelic acid) (PMA) appears as a broad peak at approximately 6 ppm in the ^{1}H NMR spectra of the crude products (Figure 3b-d). Whilst the NMR spectra suggest polymer formation, conversion was low and attempts to isolate polymeric products by precipitating the crude reaction mixture into cold MeOH were unsuccessful.

The NMR spectra also contained a small signal at around 5.27 ppm, most prominent in Figure 3b. Formation of a precipitate within the liquid products was also observed for this reaction. Analysis of this precipitate gave the NMR spectra shown in Figure 3e and f and the major peaks in these spectra (5.25 ppm in the ^{1}H and all peaks visible in ^{13}C) were consistent with mandelic acid. These results suggested that polymerisation of 5b-2 only occurred at the highest catalyst loading, whilst monomer conversion was low (ca. 15% by relative integration) and monomer decomposition back to mandelic acid occurred simultaneously under these conditions.

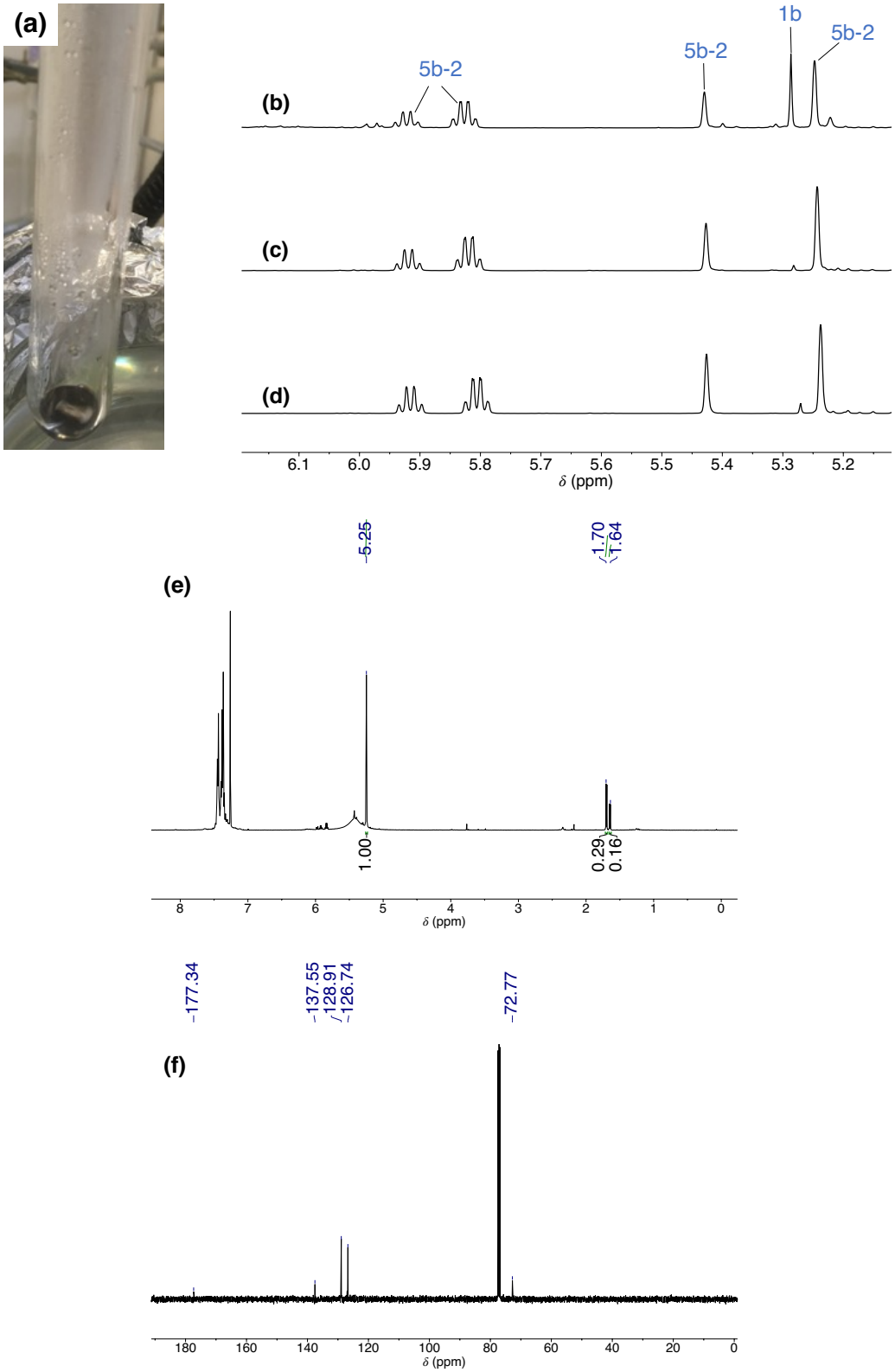

Figure 3 Solvent-free ring opening polymerisation of MePhDOX (5b-2) using p-TSA as catalyst at 100 °C. (a) Colour of liquid product. (b)-(d) ^{1}H NMR spectra (400 MHz, $CDCl_3$) of the crude products at three different monomer:catalyst:initiator ratios: 200:10:1, 400:10:1 and 2000:10:1. (e)-(f) ^{1}H and ^{13}C NMR spectra ($CDCl_3$) of a precipitate formed within the liquid product (200:10:1 reaction).

5.2.2 Polymerisation of MePhDOX (5b-2) using Al(salen) catalysts

An aluminium salen complex (Figure 4) was synthesised according to a previously reported method.[9, 10] This catalyst was previously reported to be active for ROP of PhDOX (5b-1) and Me_2PhDOX (5b-3).[2, 4] We tested this Al(salen) for ROP of 5b-2 in toluene and in solvent-free conditions. The results are summarised in Table 1.

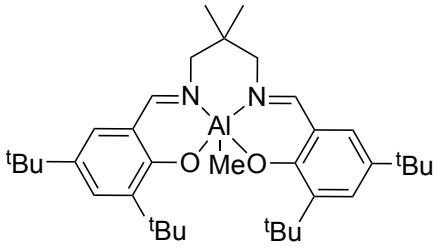

Figure 4 Al(salen) catalyst used in this work.

Table 1 ROP of PhMeDOX catalysed by Al(salen).

Entry	[monomer] / M	M:C:I ratio	Solvent	Temperature / °C	Stirring / rpm	t / h	Conversion[a] / %
1	N/A	None	neat	180	no	43.5	26
2	N/A	17:0:1	neat	180	500	42	28
3	1	100:1:1	toluene	90	500	18	0
4	1	100:1:1	toluene	125	500	18	17
5	1	100:1:1	toluene	125	500	22	19
6	1	100:1:1	toluene	125	500	114	26
7	1	100:1:1	toluene	125	500	137	30
8	N/A	50:1:1	neat	180	500	19	34

Catalyst: Al(salen). Initiator: BnOH.
[a] Conversion determined from crude ^{1}H NMR spectrum in $CDCl_3$ by relative integrals of poly(mandelic acid) and DOX.

Figure 5 shows the ^{1}H NMR spectrum of the crude products obtained from the solvent-free reaction at 180 °C and M:C:I ratio of 50:1:1 (Table 1, entry 8). Mandelic acid conversion was approximately 34%, based on relative integration of the methine resonances of oligomer/polymer (6.0-6.25 ppm) and monomer (5.43, 5.23 ppm). A 1:1 relative integral of acetaldehyde CHO (9.79 ppm) with the polymer methine (6 ppm) suggests the polymer was formed via elimination of acetaldehyde from 5b-2. Polymerisation using Al(salen) catalysts gave higher monomer conversion than p-TSA in section 7.2.1, but this was still modest, with a maximum conversion of 34% (Table 1, entry 8). It was not possible to improve conversion by increasing either reaction

temperature up to 180 °C (Table 1, entries 1, 2, 8) or reaction time up to 5 days (Table 1, entry 8). In contrast to catalysis by p-TSA, decomposition of the monomer to mandelic acid was not observed.

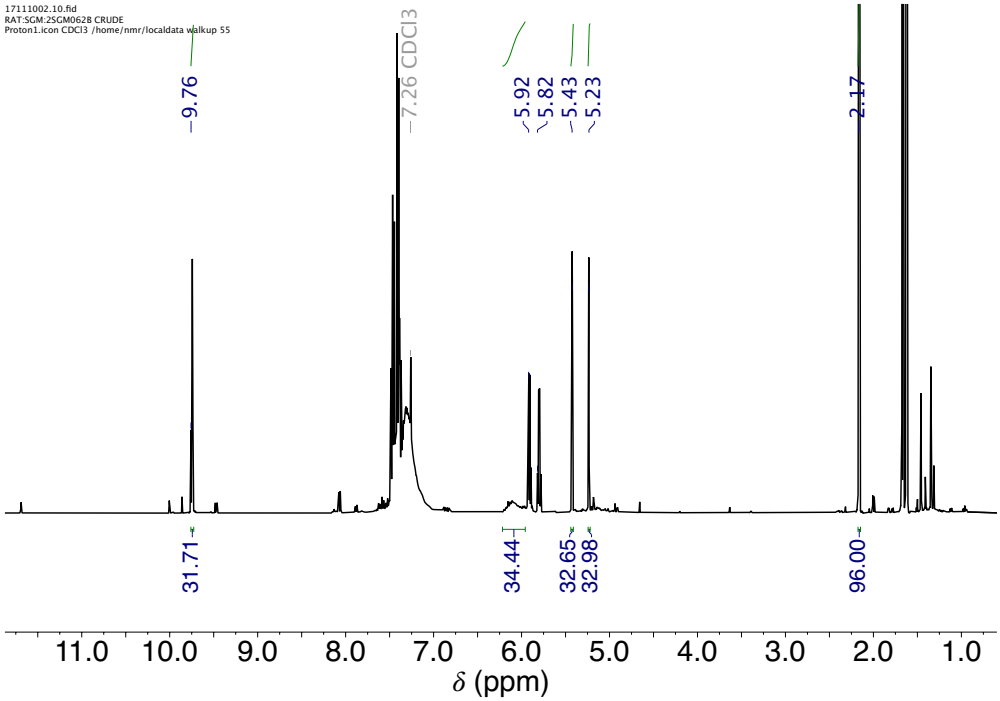

Figure 5 ^{1}H NMR (400 MHz, $CDCl_3$) spectrum of the Al(salen)-catalysed ring-opening polymerisation of PhMeDOX (5b-2) in the absence of solvent. Monomer:catalyst:initiator = 50:1:1, T = 180 °C, t = 19 hours. Table 1, Entry 8.

5.2.3 Polymerisation of MePhDOX (5b-2) using Organocatalysts

The use of organocatalysts for ROP of cyclic monomers such as lactides and OCAs is well known.[8, 11-14] Three different organocatalysts were tested for ROP of MePhDOX (5b-2): dimethylaminopyridine (DMAP), 4-pyrrolidinopyridine and diazabicycloundecene (DBU) (Figure 6).

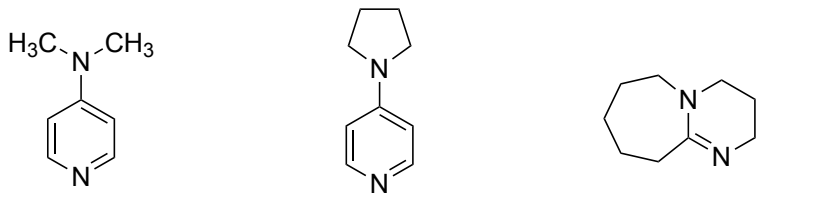

dimethylaminpyridine (DMAP) | 4-pyrrolidinopyridine (PPY) | diazabicycloundecene (DBU)

Figure 6 Chemical structures of organocatalysts used in this work.

Table 2 shows the results of organocatalytic ROP of 5b-2 attempted in this work. Entry 1 shows that conversion of DOX occurred even when only an initiator was present and therefore did not require the presence of a catalyst. This might suggest that there were impurities present in the reaction mixture that were able to catalyse polymerisation. For

example, free mandelic acid that may be able to act as an acid catalyst. No conversion was observed when polymerisation was conducted in refluxing toluene (Table 2, entries 11-13). These results indicate that high temperatures are required for these organocatalysts to be effective, compared with the Al(salen) tested in section 7.2.2, where polymerisation in toluene reached comparable conversion to the equivalent solvent-free conditions.

Table 2 Polymerisation of PhMe-DOX catalysed by organocatalysts.

Entry	Catalyst	M:C:I ratio	Solvent	Temperature / °C	t / h	Conversion[a] / %
1	none	N/A	neat	180	43	26
2	DMAP	17:0:1	neat	180	42	28
3	DMAP	50:1:1	neat	180	16	22
4	DMAP	100:1:1	neat	180	16	24
5	DMAP	200:1:1	neat	180	16	22
6	DMAP	50:1:1	neat	180	44	12
7	DMAP	100:1:1	neat	180	44	19
8	DBU	50:1:1	neat	180	42	15
9	DBU	100:1:1	neat	180	44	28
10	PPY	100:1:1	neat	180	44	14
11	DMAP	50:1:1	toluene	120	21	0
12	DMAP	100:1:1	toluene	120	21	0
13	DMAP	200:1:1	toluene	120	21	0

Catalysts: 4-dimethylaminopyridine (DMAP), diazabicycloundecene (DBU), 4-pyrrolidinopyridine (PPY). Initiator: BnOH.
Conditions: Solvent-free: T = 180 °C, no stirring. Toluene: T = 120 °C, stirred at 500 rpm, [M] = 1 M, toluene (2mL).
[a] Conversion determined from crude ^{1}H NMR spectrum in $CDCl_3$ by relative integrals of poly(mandelic acid) and DOX (in $CDCl_3$).

5.2.4 Incidental Polymerisation under Distillation Conditions

During a vacuum distillation of the 5b-2 monomer, polymer was formed in the distillation flask. The vacuum distillation of MePhDOX was performed whilst stirring over CaH_2. The hotplate was (mistakenly) set to 130 °C, rather than a temperature of 110 °C that was used for proper distillation of 5b-2 (at approximately 7 x 10^{-4} mbar). The formation of the solid shown in Figure 7a occurred over the course of approximately 1 hour. Prior to distillation, 5b-2 was stirred over CaH_2 for approximately 16 hours. Whilst the purpose of

CaH_2 in this context was to remove residual water from the crude monomer, CaH_2 is a known catalyst[15-18] for ROP. In the presence of an initiator, it could have catalysed polymerisation of 5b-2 to give the solid in Figure 7a. Possible initiators that could be present in the crude 5b-2 are water or residual mandelic acid left over after monomer synthesis (the presence of the alpha-hydroxyl group means that mandelic acid can act as ROH initiating species[19]). The presence of hydroxyl-containing impurities is known to adversely affect both ε-caprolactone and lactide ROPs.[20, 21] Hydroxyl-containing impurities (R'OH) include water and lactic acid that may remain present in the catalyst or lactide solutions after purification. Free carboxylic acids are also known to decrease the rate of polymerisation in Sn(octanoate)$_2$-catalysed ROP of ε-caprolactone and lactide ROPs.[22-24] The addition of controlled amounts of octanoic acid resulted in a reduction in overall polymerisation rate, but did not affect the final molecular weight of the polymers.

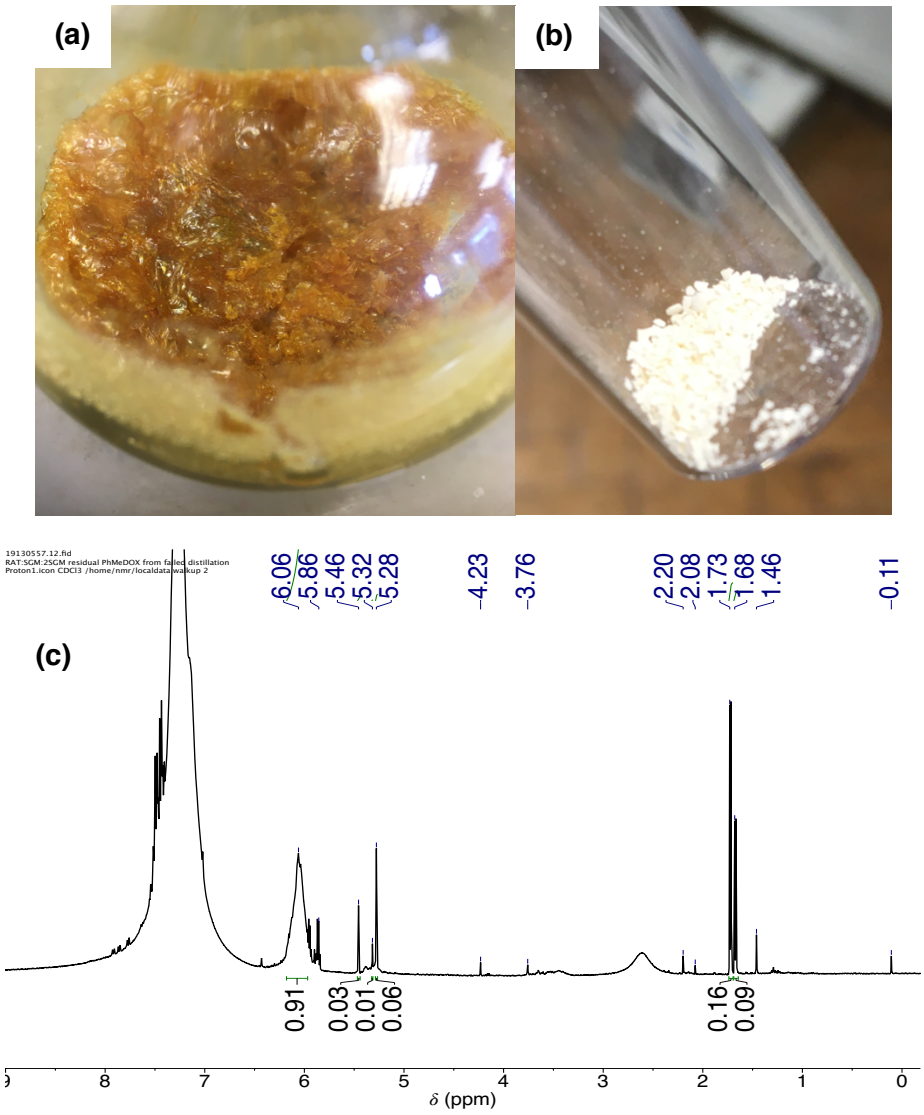

Figure 7 (a) Solid formed during an unsuccessful distillation of 5b-2. (b) White solid recovered by precipitation of the product shown in (a) into cold MeOH. (c) ^{1}H NMR spectrum of the crude product shown in (a).

The polymeric material formed was very viscous, even when heated to 130 °C. This suggests the solvent-free polymerisations attempted may have been problematic even if they had progressed to higher conversion. The increase in viscosity of the material as degree of polymerisation increased would have caused mixing problems. This has been observed previously for the ROP of 5b-1 and mitigated by using diphenyl ether solvent.[4]

The fact that polymerisation occurred under the vacuum conditions used for distillation might suggest that removal of acetaldehyde facilitates the polymerisation reaction, since (after elimination of acetaldehyde from 5b-2 during ring opening) acetaldehyde would have been removed from the round bottom flask via the distillation apparatus. This has previously been observed for the polymerisation of 5b-1, where the presence of formaldehyde inhibits polymerisation.[4] In this case, the use of a dynamic vacuum gave improved results, which was hypothesised to facilitate removal of formaldehyde from the reaction mixture after elimination from 5b-1 during polymer propagation. Carrying out the ROP of 5b-2 in the presence of the known catalysts discussed earlier and using a vacuum to facilitate removal of acetaldehyde therefore may lead to better yields and more control over polymerisation.

However, the primary way in which formaldehyde affected ROP of 5b-1 in the absence of dynamic vacuum (i.e. under the conditions used here in sections 7.2.1-7.2.3) was to increase polydispersity through a side reaction that generates new methoxy initiating species. [4] This differs from our results, since it was found that conversion of 5b-2 was limited, whereas for 5b-1, the reaction proceeded to high conversion but control over molecular weight was compromised.

Our results for 5b-2 more closely reflect what was observed for 5b-3 and 5b-5.[4] More forcing conditions were required to polymerise 5b-3, which may be due to the *gem*-dimethyl effect, increasing the stability of the cyclic monomer. Additionally, in the same publication it was reported that ROP of 5b-5 was unsuccessful, instead forming an unknown decomposition product. Our results suggest that 5b-2 was less reactive towards ROP than 5b-1 and therefore similar issues encountered for 5b-3 and 5b-5 in the literature may apply in our case to 5b-2. Stability of 5b-2 to ring opening, as with 5b-3, could explain the low conversions observed in this work. Furthermore, the *p*-TSA catalysed ROP of 5b-2 resulted in significant decomposition of the monomer, albeit to its precursor mandelic acid rather than an unknown decomposition product as seen with 5b-5.

Scheme 7 shows several examples of reactions of 2,5-diphenyl-1,3-dioxolan-4-one that have been reported in the literature. Reaction with alcohols can yield alkoxyacetates

(Scheme 7a).[25] Addition of controlled amounts (1 eqv.) of an alcohol in the presence of a Brønsted acid (mandelic acid) can yield alkyl mandelate esters (Scheme 7b).[26] Finally, the addition of C-nucleophiles can yield O-functionalised mandelic acid (Scheme 7c).[27, 28] The reaction shown in Scheme 7b is analogous to the initiation of DOX ROP, generating an ester end group and a free α-hydroxyl. The reactions in Scheme 7a and Scheme 7c would be detrimental to ROP, as the α-hydroxyl group would not be free to continue the ROP mechanism. As the reactions in Scheme 7a and Scheme 7c involve the participation of alcohols or water, it is possible that they could occur under the conditions used for DOX ROP. For example, one of these reactions could lead to unknown decomposition products observed in the ROP of 5b-5.[4]

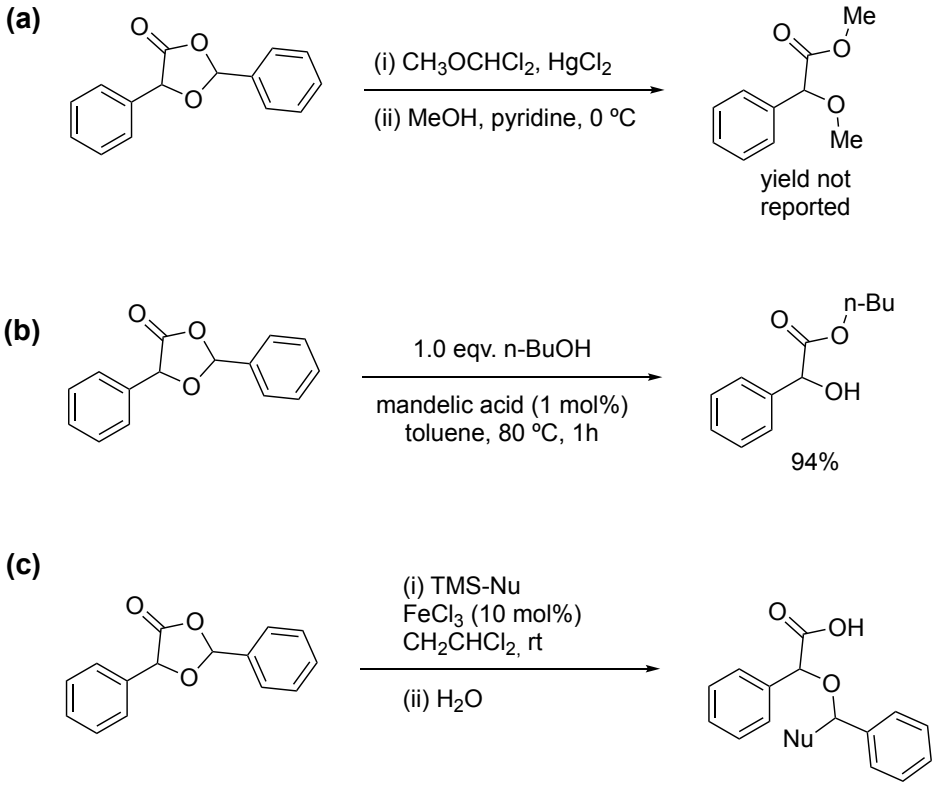

TMS-Nu	Time / h	Yield / %
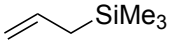	0.5	84
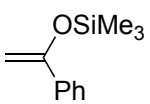	1	55
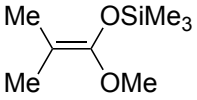	0.5	80

Scheme 7 Reactions reported in the literature for 2,5-diphenyl-dioxolan-4-one with alcohols and nucleophiles. (a) Formation of ester/ether of mandelic acid.[25] (b) Formation of benzyl mandelate.[26] (c) Formation of ethers of mandelic acid with C-nucleophiles.[27, 28]

5.3 Conclusions

ROP of 2-methyl-5-phenyl-1,3-dioxolan-4-one (5b-2) was attempted using conditions previous reported for other DOX monomers.[2, 4, 5] Monomer conversion was low, with a maximum conversion of approximately 34% achieved when using an Al(salen) catalyst. Polymeric material was formed from 5b-2 during a distillation, suggesting that the presence of CaH_2 in the crude monomer could act as a ROP catalyst and/or the use of a vacuum may facilitate polymerisation, for example by removing acetaldehyde after it is eliminated from the monomer. Some similarities could be drawn to earlier work reported, where the polymerisation of 5b-3 required forcing conditions, however higher monomer conversions were observed in comparison to the results reported here for 5b-2. Additionally, attempts to polymerise 5b-5 were reported to be unsuccessful, similar to the observations here for p-TSA catalysed ROP of 5b-2. More work is required to elucidate the exact effect of the structure of 5b-2 and how this prevents ROP, since the results of this work indicate that it undergoes ROP much less readily than 5b-1 and 5b-3 despite its very similar structure.

5.4 References

1. Martin, R. T.; Camargo, L. P.; Miller, S. A., Marine-degradable polylactic acid. *Green Chem.* **2014,** *16* (4), 1768-1773.

2. Cairns, S. A.; Schultheiss, A.; Shaver, M. P., A broad scope of aliphatic polyesters prepared by elimination of small molecules from sustainable 1,3-dioxolan-4-ones. *Polym. Chem.* **2017,** *8* (19), 2990-2996.

3. Neitzel, A. E.; Petersen, M. A.; Kokkoli, E.; Hillmyer, M. A., Divergent Mechanistic Avenues to an Aliphatic Polyesteracetal or Polyester from a Single Cyclic Esteracetal. *ACS Macro Lett.* **2014,** *3* (11), 1156-1160.

4. Xu, Y.; Perry, M. R.; Cairns, S. A.; Shaver, M. P., Understanding the ring-opening polymerisation of dioxolanones. *Polym. Chem.* **2019,** *10* (23), 3048-3054.

5. Gazzotti, S.; Ortenzi, M. A.; Farina, H.; Silvani, A., 1,3-Dioxolan-4-Ones as Promising Monomers for Aliphatic Polyesters: Metal-Free, in Bulk Preparation of PLA. *Polymers (Basel)* **2020,** *12* (10).

6. Martin, R. T.; Camargo, L. P.; Miller, S. A., Marine-degradable polylactic acid. *Green Chem.* **2014,** *16* (4), 1768-1773.

7. Gregory, G. L.; López-Vidal, E. M.; Buchard, A., Polymers from sugars: cyclic monomer synthesis, ring-opening polymerisation, material properties and applications. *Chem. Commun.* **2017,** *53* (14), 2198-2217.

8. Dechy-Cabaret, O.; Martin-Vaca, B.; Bourissou, D., Controlled Ring-Opening Polymerization of Lactide and Glycolide. *Chem. Rev.* **2004,** *104*, 6147-6176.

9. Hormnirun, P.; Marshall, E. L.; Gibson, V. C.; Pugh, R. I.; White, A. J., Study of ligand substituent effects on the rate and stereoselectivity of lactide polymerization using aluminum salen-type initiators. *Proc Natl Acad Sci U S A* **2006,** *103* (42), 15343-8.

10. Nomura, N.; Ishii, R.; Yamamoto, Y.; Kondo, T., Stereoselective ring-opening polymerization of a racemic lactide by using achiral salen- and homosalen-aluminum complexes. *Chemistry* **2007,** *13* (16), 4433-51.

11. Stanford, M. J.; Dove, A. P., Stereocontrolled ring-opening polymerisation of lactide. *Chem. Soc. Rev.* **2010,** *39* (2), 486-94.

12. Williams, C. K., Synthesis of functionalized biodegradable polyesters. *Chem. Soc. Rev.* **2007,** *36*, 1573-1580.

13. Gregory, G. L.; Lopez-Vidal, E. M.; Buchard, A., Polymers from sugars: cyclic monomer synthesis, ring-opening polymerisation, material properties and applications. *Chem. Commun.* **2017,** *53*, 2198-2217.

14. Dove, A. P., Organic Catalysis for Ring-Opening Polymerization. *ACS Macro Lett.* **2012,** *1* (12), 1409-1412.

15. Kawasaki, N.; Nakayama, A.; Higashi, T.; Maeda, Y.; Yamamoto, N.; Aiba, S.-i., Studies on Poly[acrylamide-co-(-caprolactone)]: Synthesis, Characterization and Biodegradability. *Macromol. Chem. Phys.* **2001,** *202* (11), 2231-2238.

16. Colwell, J. M.; Wentrup-Byrne, E.; George, G. A.; Schué, F., A pragmatic calcium-based initiator for the synthesis of polycaprolactone copolymers. *Polym. Int.* **2014,** *64* (5), 654-660.

17. Atz Dick, T.; Couve, J.; Gimello, O.; Mas, A.; Robin, J.-J., Chemical modification and plasma-induced grafting of pyrolitic lignin. Evaluation of the reinforcing effect on lignin/poly(l-lactide) composites. *Polymer* **2017,** *118*, 280-296.

18. Zhong, Z.; Dijkstra, P. J.; Birg, C.; Westerhausen, M.; Feijen, J., A Novel and Versatile Calcium-Based Initiator System for the Ring-Opening Polymerization of Cyclic Esters. *Macromol.* **2001,** *34*, 3863-3868.

19. Buchard, A.; Carbery, D. R.; Davidson, M. G.; Ivanova, P. K.; Jeffery, B. J.; Kociok-Kohn, G. I.; Lowe, J. P., Preparation of stereoregular isotactic poly(mandelic acid) through organocatalytic ring-opening polymerization of a cyclic O-carboxyanhydride. *Angew. Chem. Int. Ed. Engl.* **2014,** *53* (50), 13858-61.

20. A. J. Nijenhuis; Grijpma, D. W.; Pennings, A. J., Lewis Acid Catalyzed Polymerization of L-Lactide. Kinetics and Mechanism of the Bulk Polymerization. *Macromol.* **1992,** *25*, 6419-6424.

21. Duda, A.; Penczek, S.; Kowalski, A.; Libiszowski, J., Polymerizations of ε-caprolactone and L,L-dilactide initiated with stannous octoate and stannous butoxide—a comparison. *Macromol. Symp.* **2000,** *153* (1), 41-53.

22. Kaur, P.; Mehta, R.; Upadhyay, S. N., Role of important parameters in ring opening polymerization of polylactide. *J. Polym. Eng.* **2011,** *31* (2-3).

23. Ryner, M.; Stridsberg, K.; Albertsson, A.-C., Mechanism of Ring-Opening Polymerization of 1,5-Dioxepan-2-one and L-Lactide with Stannous 2-Ethylhexanoate. A Theoretical Study. *Macromol.* **2001,** *34*, 3877-3881.

24. Kowalski, A.; Duda, A.; Penczek, S., Kinetics and mechanism of cyclic esters polymerization initiated with tin(II) octoate, 1. Polymerization ofη-caprolactone. *Macromol. Rapid Commun.* **1998,** *19* (11), 567-572.

25. Martin, C. W.; Lund, P. R.; Rapp, E.; Landgrebe, J. A., Halogenated carbonyl ylides in the reactions of mercurial dihalocarbene precursors with substituted benzaldehydes. *J. Org. Chem.* **1977,** *43*, 1071-1076.

26. Weng, S.-S.; Li, H.-C.; Yang, T.-M., Chemoselective esterification of α-hydroxyacids catalyzed by salicylaldehyde through induced intramolecularity. *RSC Adv.* **2013,** *3* (6), 1976-1986.

27. Shcherbinin, V. A.; Konshin, V. V., Lewis acid-mediated mono- and bis-addition of C -nucleophiles to 1,3-dioxolan-4-ones. *Tetrahedron Lett.* **2018,** *59* (31), 3005-3009.

28. Shcherbinin, V. A.; Konshin, V. V., Convenient synthesis of O-functionalized mandelic acids via Lewis acid mediated transformation of 1,3-dioxolan-4-ones. *Tetrahedron* **2019,** *75* (26), 3570-3578.

Future Work

The use of zeolites in the synthesis of cyclic monomers of mandelic acid has been explored in this thesis. It has been shown that cyclic mandelide can be synthesised using H-Beta zeolite. USY zeolites were also particularly active in the conversion of mandelic acid, but the major products were diarylacetic acids. This thesis provides insight into the effects of zeolite modification and reaction solvent on these reactions.

1,3-dioxolan-4-ones were also successfully synthesised over zeolites in batch and flow conditions. The most active catalysts were once again the USY zeolites. In particular, liquid phase flow reactions were investigated and shown to provide an effective route for the synthesis 2-methyl-5-phenyl-1,3-dioxolan-4-one (MePhDOX).

6.1 Synthesis of Mandelide and Diarylacetic Acids

Our results suggested that framework effects played a role in dictating reaction outcomes in the conversion of mandelic acid. Whilst most zeolites produced a mix of products, zeolite H-Y-30 selectively formed diarylacetic acids. It is hypothesised that the presence mesopores and supercages is critical to the formation of these bulky products. It is likely that mesopores are required to facilitate molecular transport and the supercages were only pores in the tested zeolites large enough to accommodate the products. In addition to hierarchical zeolites containing mesopores, reducing zeolite particle size can also facilitate mass transport by reducing diffusion path lengths from the crystal surface. Further work could investigate different hierarchical zeolites and zeolites with smaller particle sizes (such as nanosized zeolites). The large size of the products in this work may be better suited to pore sizes that are larger than those possessed by zeolites. Mesoporous materials such as mesoporous silicas are also well known as catalysts and their use in conversion of mandelic acid should also be considered.

In the case of H-Beta, the nominal pore widths were smaller than the products of mandelic acid conversion. Thus, observed products over these catalysts were unlikely to have originated from the internal microporosity and acidity of the external surface of H-Beta may be the active sites in these reactions. Passivation of the surface acid sites, for example by adsorption of bulky pyridines, could be used to further investigate the role of internal and external acid sites in these reactions.

6.2 Synthesis of 1,3-Dioxolan-4-ones

Due to the properties of mandelic acid, the synthesis of DOX monomers in flow was limited to liquid phase flow chemistry. In this set up, we encountered significant problems with reactor blocking due to poor mandelic acid solubility in the chosen acetonitrile

solvent and rapid catalyst deactivation. Future work could expand the scope of these reactions in terms of solvent choice in search of improved mandelic acid solubility and catalyst design could be investigated to reduce the rate of catalyst deactivation. Once again, given mandelic acid is the substrate here, products are likely to be large. Therefore, hierarchical zeolites or purely mesoporous materials may also be effective in these transformations.

6.3 Ring Opening Polymerisation of 2-Methyl-5-phenyl-1,3-dioxolan-4-one

Attempts to polymerise MePhDOX under conditions previously reported in the literature resulted in low monomer conversion and, in some cases, monomer decomposition. The scope of the experiments conducted in this project was not sufficient to determine any clear explanation for these results. However, polymeric material was formed from this monomer under the vacuum conditions used for distillation, suggesting that the use of different reaction conditions could lead to more successful polymerisation of this monomer.

Appendices

Appendix 1: Characterisation of Byproducts in Initial Catalyst Screening

1.1.1 Diarylacetic Acids

In our initial experiments, we observed a series of resonances in the ^{1}H NMR spectra at a chemical shift of 5-5.2 ppm (400 MHz, $CDCl_3$) that could not be assigned to the dimer, cyclic dimer or oligomeric products that we expected to observe. These unassigned resonances were found to be the major peaks in the ^{1}H NMR spectra of the products of H-Y-30-catalysed reactions and part of a mixture of resonances in H-Beta-catalysed reactions.

H-Y-30-catalysed reactions were run in a range of aromatic solvents. LC-MS was used to analyse the products (without purification). We observed that the LC-MS chromatograms contained a large peak at a retention time in the range 2-3 min. The retention time and the MS fragments present in the mass spectra varied depending on the reaction solvent. After a further search of the literature, we found that reactions of mandelic acid (or derivatives e.g. hydroxymandelic acid) with aromatics were common. The products of these reactions are diarylacetic acids and spectroscopic data was available in the literature for many of the compounds. Comparison of the spectroscopic data (^{1}H and ^{13}C NMR, mass spectra) from the literature with our results showed that the unknown compounds were diarylacetic acids formed from mandelic acid and the reaction solvent. The mass fragments that we observed matched those in the literature and can be attributed to stable ion fragments of the diarylacetic acid products, as shown in Figure 1 and Figure 2. The stability of these mass fragments is due to the electronic stabilisation of the positive charge by the two aromatic rings in these diaryl products. These two fragments occur due to loss of the solvent aromatic ring (giving a lower m/z fragment) or neutral loss of CO_2 (giving a higher m/z fragment). Some examples of the mass spectra are shown for chlorobenzene, mesitylene and toluene. For a complete summary of the characterisation, see the experimental section.

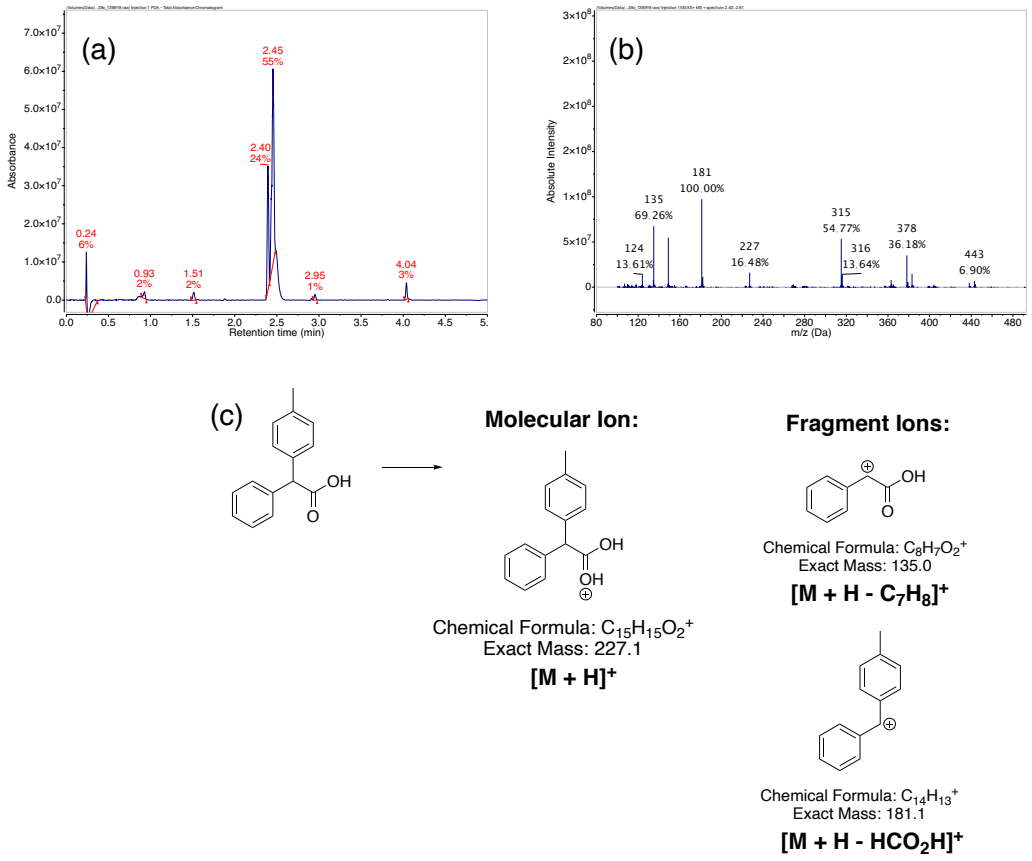

Figure 1 (a)*:* UV chromatogram of a crude reaction mixture from the reaction of mandelic acid in toluene, catalysed by zeolite H-USY-30. (b) ESI-MS positive ion spectrum corresponding to the electrophilic aromatic substitution product (R_T = 2.4-2.6 min). (c) Assignment of mass peaks in the ESI-MS positive ion spectrum at m/z 227 Da (absolute intensity = 16%), 181 Da (absolute intensity = 100%) and 135 Da (absolute intensity = 69%).

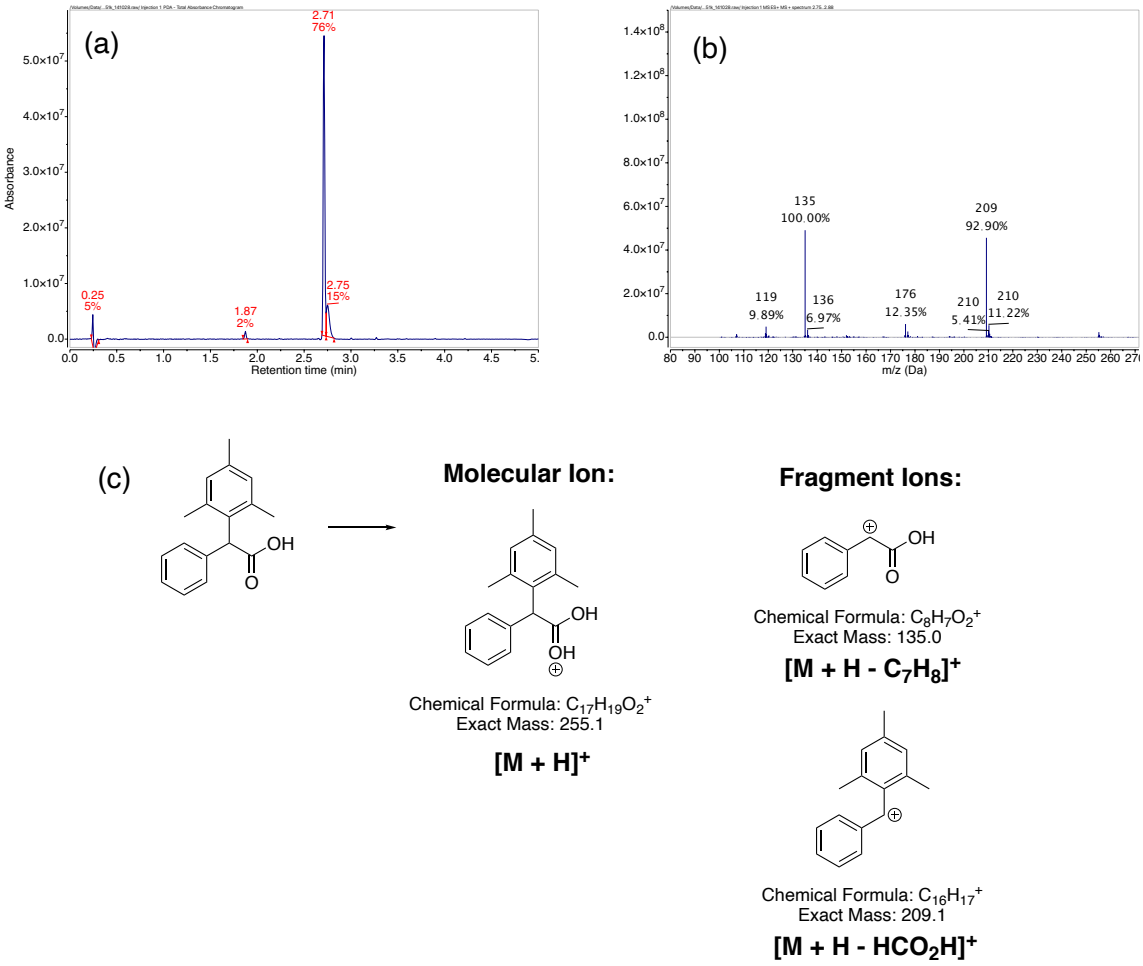

Figure 2 (a) UV chromatogram of a crude reaction mixture from the reaction of mandelic acid in mesitylene, catalysed by zeolite H-USY-30. (b) ESI-MS positive ion spectrum corresponding to the electrophilic aromatic substitution product (R_T = 2.75-2.88 min). (c) Assignment of mass peaks in the ESI-MS positive ion spectrum at m/z 255 Da (low abundance), 209 Da (absolute intensity = 93%) and 135 Da (absolute intensity = 100%).

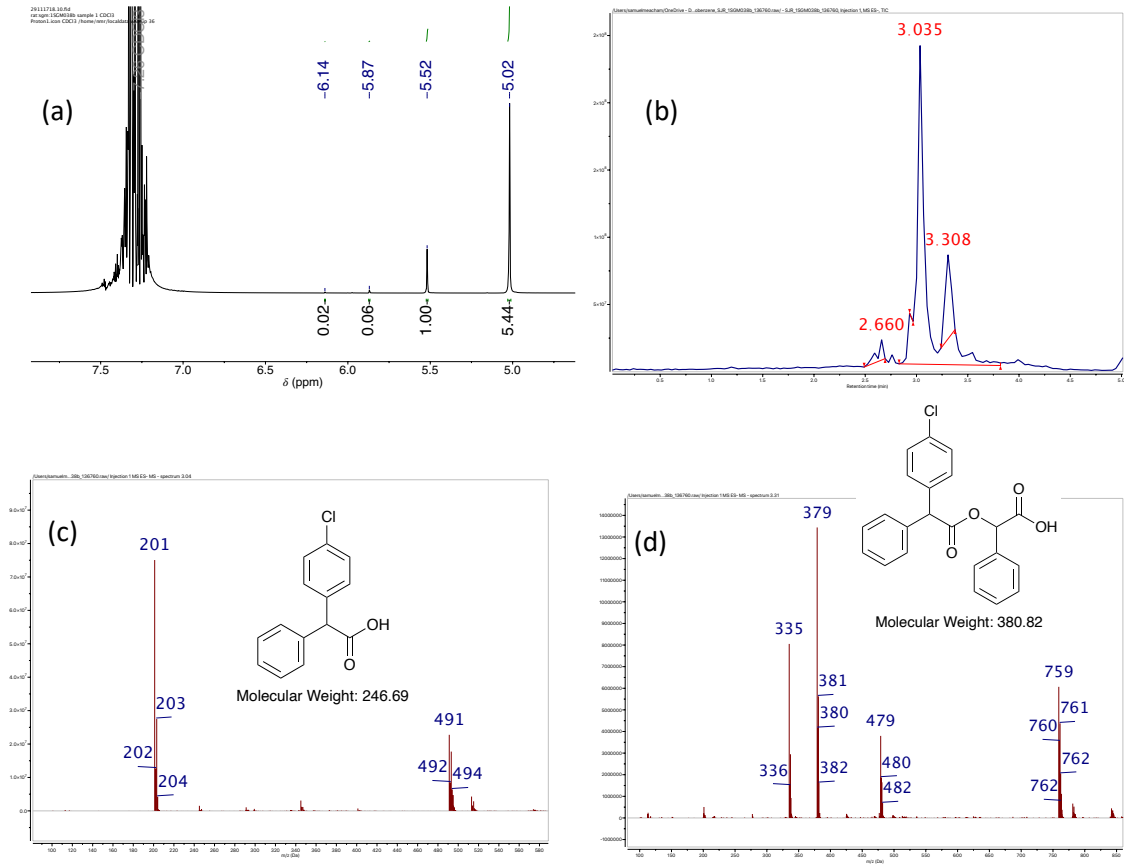

Figure 3 Characterisation data for the product of H-Y-30 catalysed conversion of mandelic acid in chlorobenzene. (a) ^{1}H NMR (400 MHz, $CDCl_3$) of the crude product mixture. (b) UV chromatogram of the crude reaction mixture. (c) ESI-MS spectrum (negative ion) of the peak at R_t = 3.035 min. (d) ESI-MS spectrum (negative ion) of the peak at R_t = 3.308 min.

For the reaction in chlorobenzene (Figure 3), an additional peak at 5.5 ppm in the ^{1}H NMR spectra could not be assigned to a known product. This may be due to a reaction occurring between the diarylacetic acid and mandelic acid to form a dimer. The LC-MS data showed a significant peak at R_t = 3.3 min (Figure 3b) and a mass fragment with m/z 379 (Figure 3d). This mass would be consistent with a dimer structure made up of the diarylacetic acid and mandelic acid. However, the NMR data is not consistent with such a structure, as two different methine environments would be present, whereas the NMR only contained a single additional peak at 5.5 ppm. No further work was done to elucidate the structure corresponding to the peak at 5.5 ppm, and this peak was not included in the quantitative analysis of zeolite-catalysed reactions in chlorobenzene. For all other solvents, no significant unassigned peaks were present.

1.1.2 Benzaldehyde and 2,5-diphenyl-1,3-dioxolan-4-one

After assigning the peaks corresponding to the diarylacetic acids, a series of unassigned peaks still remained in our NMR spectra. These were particularly prominent in the ^{1}H NMR spectra of H-Beta-catalysed reactions and consisted of two pairs of peaks, as seen in Figure 8 (labelled “5”). A further examination of the literature on known reactions of

mandelic acid led us to the synthesis of dioxolanones from mandelic acid and various carbonyl compounds. We found that the NMR data for the compound 2,5-diphenyl-1,3-dioxolan-4-one matched the unassigned peaks in our spectra. This compound is formed by the reaction of mandelic acid with benzaldehyde.[1] It is not clear how the benzaldehyde is formed. In the case of the formation of small amounts of acetaldehyde during the gas-phase production of lactide, the authors suggested the decomposition of methyl lactate or of lactide could produce the acetaldehyde and CO.[2] Another reference suggests acetaldehyde could form by decarboxylation of lactic acid to produce CO_2.[3] A study into the gas phase decomposition of mandelic acid suggested benzaldehyde could form via a stable alpha lactone.[4] We did not attempt to detect the formation of CO or CO_2 during our reactions, so we are unable to comment on the mechanism of benzaldehyde formation. However, what was clear was that benzaldehyde was being formed in our reactions and that it was subsequently reacting with mandelic acid to form 2,5-diphenyl-1,3-dioxolan-4-one.

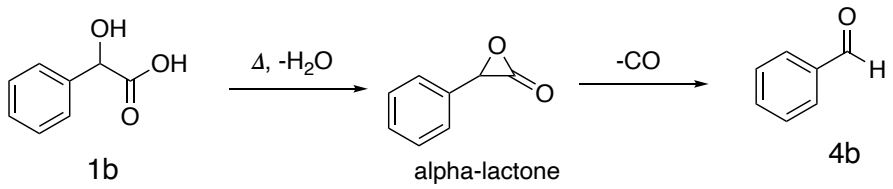

Figure 4 Gas phase decomposition pathway of mandelic acid (1b) to benzaldehyde (4b) proposed in the literature.[4]

We found that the amount of benzaldehyde present in product mixtures was significant when H-Beta was used as a catalyst but only at short reaction times (3 hours or less). After longer reaction times (e.g. overnight), the benzaldehyde had been consumed in the formation of 2,5-diphenyl-1,3-dioxolan-4-one. Figure 5 shows the ^{1}H NMR spectrum of benzaldehyde stacked above an example of a spectrum of a crude product mixture obtained for a H-Beta-75-catalysed reaction. The bottom spectrum shows the significant benzaldehyde peaks at 10 ppm and 7.9 ppm, along with the peaks corresponding to the methine peaks of the solid products (esters and diarylacetic acids) at 5-6.2 ppm. We carried out some of the catalyst screening experiments prior to identifying benzaldehyde as a reaction product. As a result, the initial catalyst tests underestimated the quantity of benzaldehyde, as the reaction solvent was removed by rotary evaporation prior to NMR sample preparation and this process would also remove benzaldehyde (b.p. = 178 °C). Later, to properly quantify benzaldehyde, two NMR samples were run on every crude product mixture. One sample was diluted with NMR solvent without rotary evaporation and one with rotary evaporation to remove the reaction solvent, followed by dissolution in NMR solvent. The sample without rotary evaporation (“sample 1”) was used to quantify

the amount of benzaldehyde relative to one of the non-volatile product peaks (usually the largest peak in a given sample). The sample with rotary evaporation ("sample 2") was then used to quantify the rest of the peaks corresponding to non-volatile products, and total product distribution (including benzaldehyde) calculated based on the two samples. The second sample was necessary to get an accurate measure of the quantities of the solid products, as these peaks would often be lost in the baseline or would overlap in the sample 1 spectra.

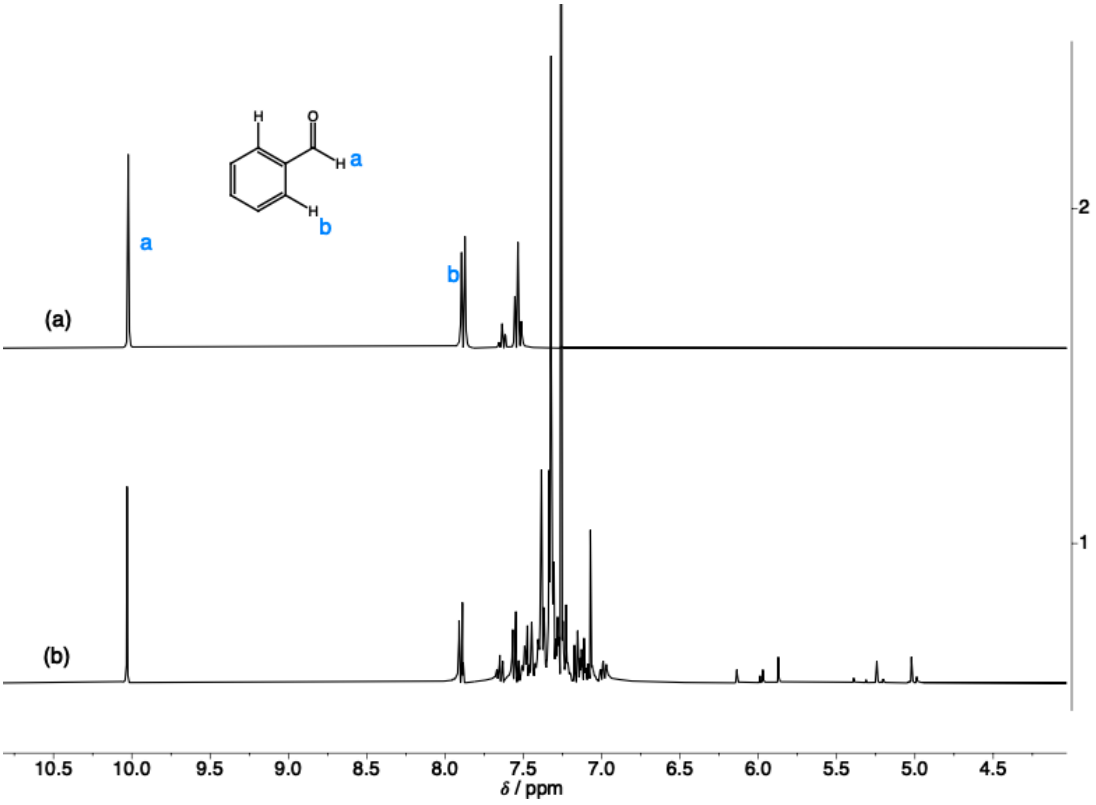

Figure 5 (a) ^{1}H NMR spectrum (400 MHz, $CDCl_3$) of (a) benzaldehyde, (b) product mixture from H-Beta-75-catalysed reaction of mandelic acid. Reaction conditions: 2g mandelic acid, 1.3 g zeolite H-Beta-75, 20 mL mixed xylenes, reflux with Dean Stark trap, Oil bath T = 175°C (T_b + 35 °C), stirring rate = 500 rpm, time = 2 hours.

A reference sample of 2,5-diphenyl-1,3-dioxolan-4-one was synthesised using a slightly modified method from the literature (Figure 6).[1] Brønsted acidic p-TSA catalyst was used in place of Lewis acidic $BF_3.OEt_2$. We successfully synthesised this compound using p-TSA (and later using zeolites), suggesting that the reaction can be catalysed by both Lewis acidic and Brønsted acidic catalysts. ^{1}H and ^{13}C NMR spectra of this reference compound are shown in Figure 7. Figure 8 shows an example spectrum containing the methine peaks of all of the key products (except benzaldehyde) identified in this work to form from mandelic acid in zeolite-catalysed reactions. The peaks corresponding to 2,5-diphenyl-dioxolan-4-one are labelled with the number 5.

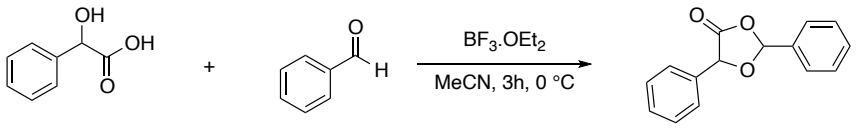

Figure 6 Previously reported synthesis of 2,5-diphenyl-1,3-dioxolan-4-one from mandelic acid and benzaldehyde using a Lewis acid catalyst.[1]

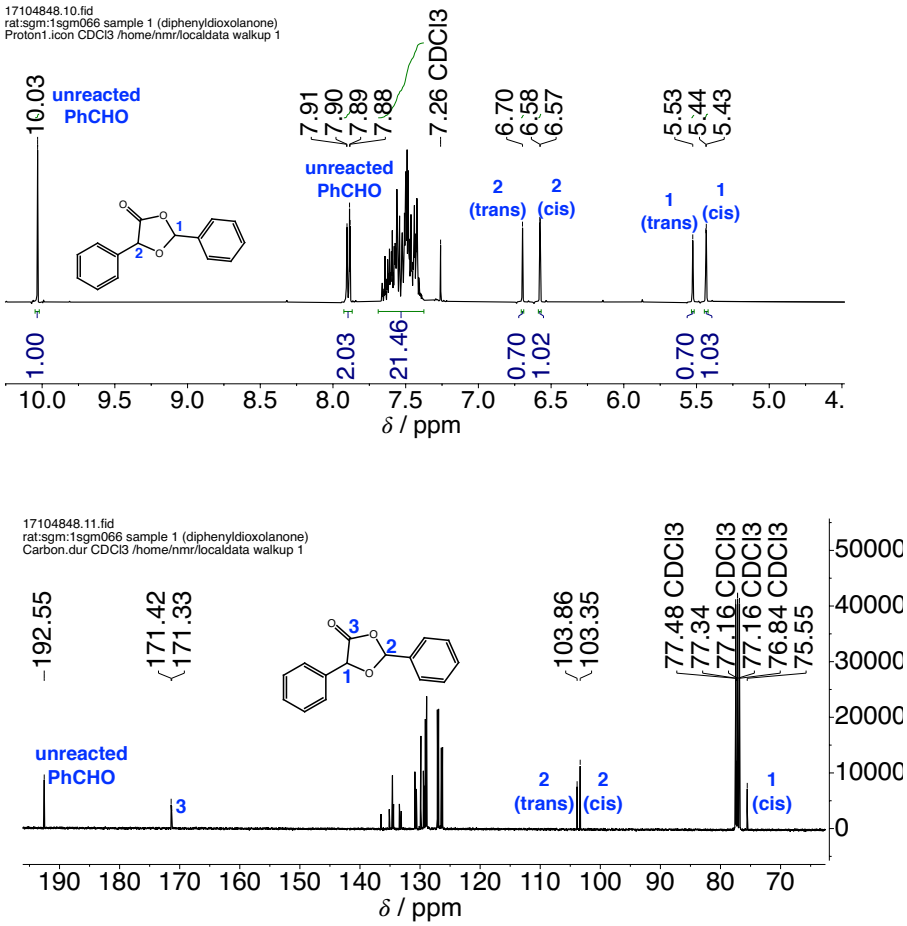

Figure 7 ^{1}H and ^{13}C NMR spectra (400 MHz, $CDCl_3$) of 2,5-diphenyl-1,3-dioxolan-4-one synthesised by reaction of mandelic acid and benzaldehyde in acetonitrile. Conditions: reflux with Dean-Stark trap overnight. 1 g mandelic acid, 0.68 mL benzaldehyde (1 eqv.), 10 ml acetonitrile. Yield approximately 56 %.

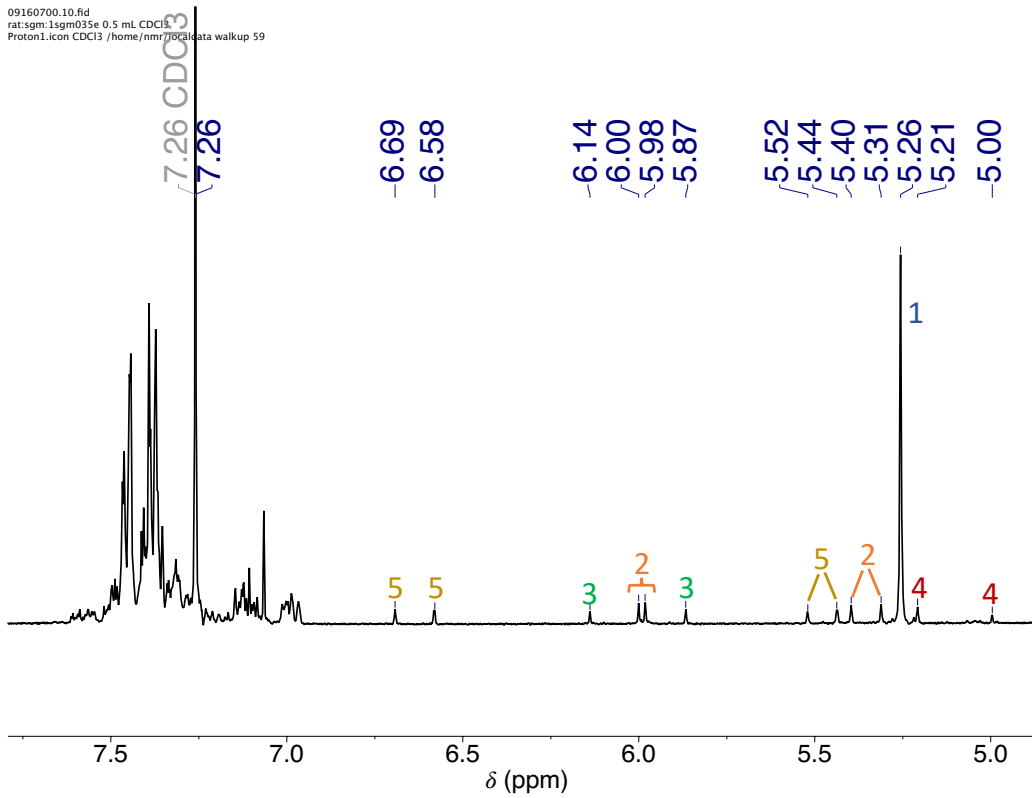

Figure 8 Example ^{1}H NMR spectra (400 MHz, $CDCl_3$) of crude products obtained from a zeolite-catalysed reaction of mandelic acid in mixed xylenes. Methine peaks of the key products are annotated as follows: (1) mandelic acid; (2) mandelic acid dimer (2 stereoisomers, 2 methine environments per isomer); (3) mandelide (*meso*- and *rac*-isomers); (4) diarylacetic acids; (5) *cis*- and *trans*-2,5-diphenyl-1,3-dioxolan-4-one (2 methine environments per isomer).

1.1.3 Brønsted Acid-catalysed Mechanisms for Observed Product Formation

When the reaction was run without catalyst, only a small amount of linear dimer was observed. Similarly, the product distribution when using homogeneous p-TSA catalyst contained products of esterification only, such as the dimer and mandelide. Here, we suggest some possible mechanisms for the formation of the observed products catalysed by Brønsted acidic zeolites. For simplicity, the activation of the substrate by the acidic proton of the zeolite is shown as a formal transfer, for example to activate carbonyl C=O to C-OH^{+}. However, this could be shown with dashed lines rather than formal proton transfer (as shown in Figure 9), and we have not done experiments to ascertain whether cationic intermediates are involved.

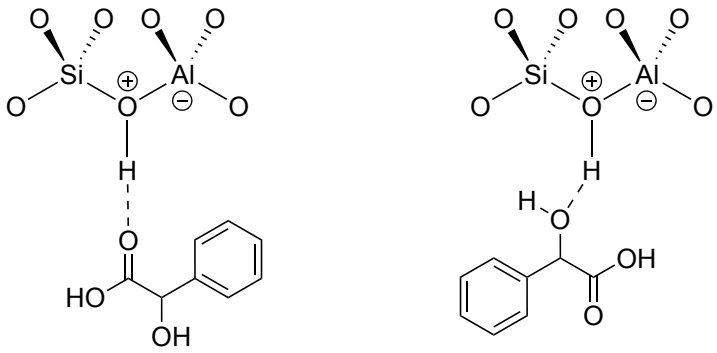

Figure 9 Activation of mandelic acid by Brønsted acidic zeolites.

Figure 10 shows the mechanism of dimerisation of mandelic acid catalysed by a Brønsted acidic zeolite. This reaction is a condensation reaction, liberating a molecule of water. We expect the formation of mandelide, the cyclic dimer of mandelic acid, to occur via a similar mechanism between the hydroxyl group and carboxylic acid group in the dimer to form the lactone ring.

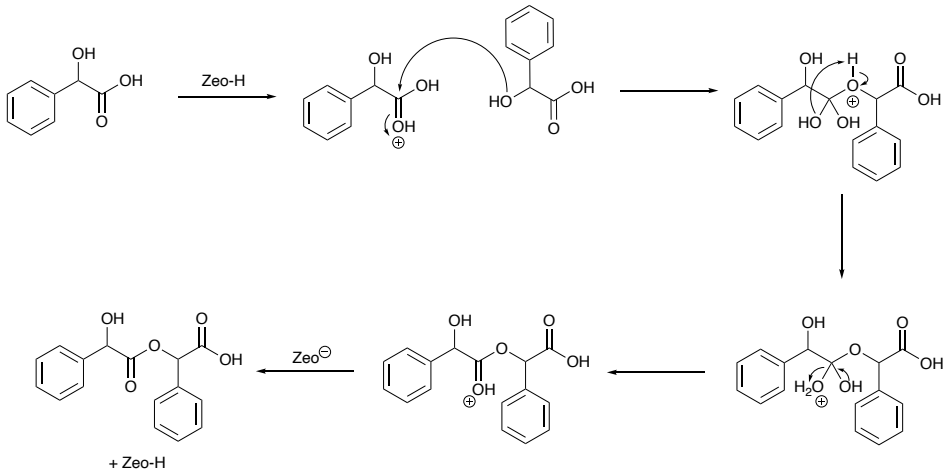

Figure 10 Mechanism of dimerisation of mandelic acid catalysed by Brønsted acidic zeolites.

Figure 11 shows the possible mechanisms by which benzaldehyde may have formed from mandelic acid in zeolite-catalysed reactions. The first is the mechanism suggested for the formation of acetaldehyde from lactide in heterogeneous catalytic production of lactide from methyl lactate.[5, 6] In this mechanism, the cyclic dimer decomposes to two molecules of aldehyde and two molecules of carbon monoxide. In the case of lactide to acetaldehyde, this process was only found to occur at much higher temperatures than those studied here for mandelic acid (>300 °C, gas phase vs ~140 °C, refluxing solvent). If this is the mechanism of benzaldehyde formation, it may suggest a greater instability of the mandelide cyclic monomer compared with lactide, possibly due to the presence of bulky phenyl rings. The pi-system of the phenyl rings may also contribute to the instability of mandelide through donation of electron density towards the lactone groups, making it more susceptible to further decomposition after it has been formed. The other possible

route to benzaldehyde is that seen in the gas phase decomposition of mandelic acid.[4] In this case, an intramolecular cyclisation forms a lactone ring, liberating water. A molecule of CO is then lost to give benzaldehyde. As with the formation of acetaldehyde from lactide, the gas phase decomposition of mandelic acid occurs at much higher temperatures (300-340 °C) than the reaction conditions studied here for mandelic acid to mandelide. This has been studied for a range of different alkyl groups at the 2-position, and it is found that the bulkier phenyl group accelerates decomposition compared with simple alkyls, through a combination of steric and electronic effects. These effects may be at play here in our reactions, where we observed significant amounts of benzaldehyde, whereas under similar conditions, no acetaldehyde is observed in the zeolite-catalysed reaction of lactic acid to make lactide.[7] However, due to the very different conditions used in the reports, it is unclear if either of these mechanisms provides a plausible explanation for the formation of benzaldehyde in our experiments.

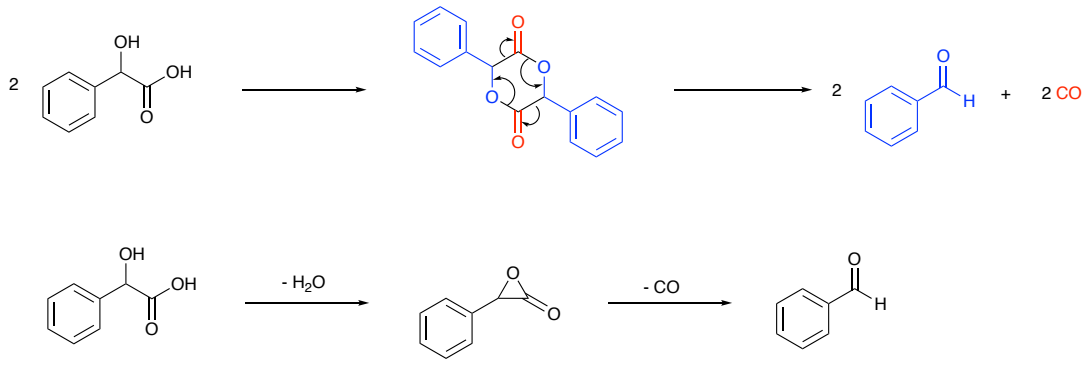

Figure 11 Possible routes to form benzaldehyde from mandelic acid in zeolite-catalysed reactions.

Figure 12 shows a possible mechanism for the acid-catalysed formation of 2,5-diphenyl-1,3-dioxolan-4-one. It's likely that this follows a similar mechanism to the dimerization of mandelic acid to make mandelide, with the slight difference in the initial activation. Here, the aldehyde of benzaldehyde is activated towards nucleophilic attack by the hydroxyl group of mandelic acid, rather than the carbonyl of the ester group in mandelic acid, as shown in Figure 10.

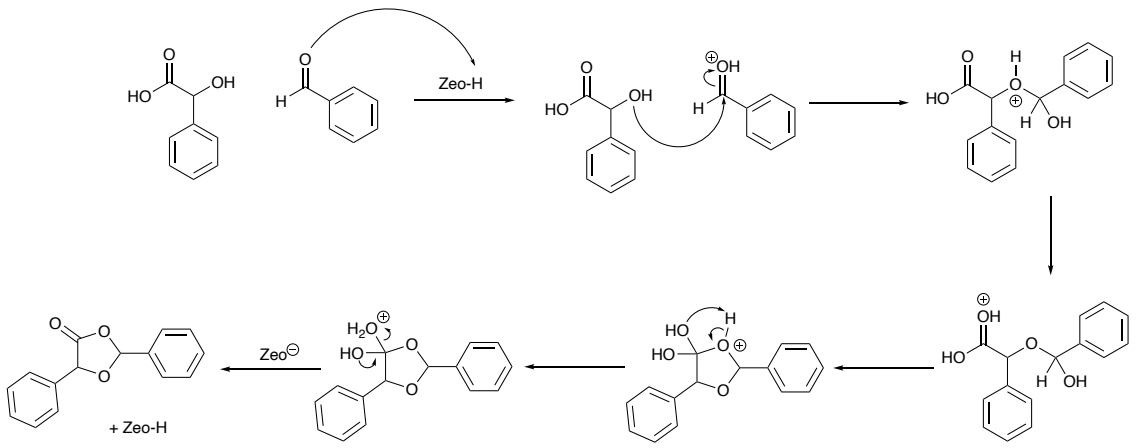

Figure 12 Mechanism of formation of 2,5-diphenyl-1,3-dioxolan-4-one from mandelic acid and benzaldehyde catalysed by Brønsted acidic zeolites.

Figure 13 shows a possible mechanism for formation of diarylacetic acids. In this case, the products could form via a carbocation intermediate through loss of water prior to nucleophilic attack by the aromatic ring or via the concerted mechanism shown in Figure 18, where nucleophilic attack and loss of water occur simultaneously. It's possible the nature of this mechanism could be determined by using enantiopure mandelic acid and analysing the stereochemistry of the products. For example, in the concerted mechanism, you would expect S_N2 inversion to occur and for the products to have the opposite configuration to the mandelic acid starting material (assuming no racemisation of mandelic acid or the products occurs under the reaction conditions). In the case of a carbocation intermediate, sp2 hybridisation of the positively charged carbon center would result in a statistical product mix of both stereoisomers, irrespective of the stereochemistry of the mandelic acid starting material. It may also have been possible to observe a carbocation intermediate via spectroscopic techniques such as solid-state NMR spectroscopy. These investigations were outside the scope of this work.

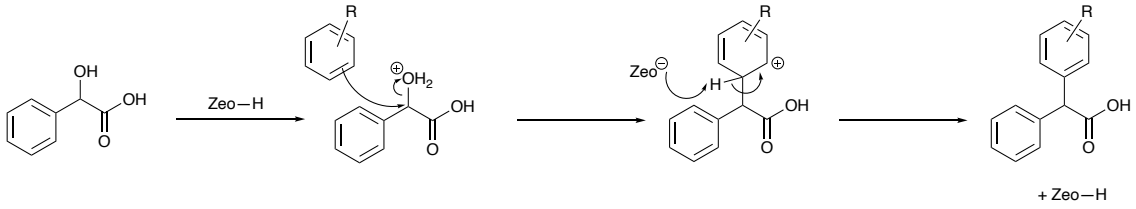

Figure 13 Possible mechanism of diarylacetic acid formation from mandelic acid and aromatic solvents catalysed by Brønsted acidic zeolites.

Appendix 2: BET measurements of Commercial Zeolites

The below table summarises BET measurements measured for the commercial zeolites. Measurements obtained for our samples and measurements reported in the literature are included for comparison.

Table 1 Textural properties of selected commercial zeolites.

Zeolite	V_{total} / $cm^3\ g^{-1}$	V_{micro} / $cm^3\ g^{-1}$	BET Surface Area / $m^2\ g^{-1}$	S_{meso} / $m^2\ g^{-1}$	S_{ext} / $m^2\ g^{-1}$	Ref
H-Beta-12.5	0.43	0.16	560	-	-	This work
H-Beta-75	0.49	0.20	516	126	-	[8]
	0.29	0.19	635	-	-	This work
H-Y-2.5	0.30	0.26	721	-	72	[9]
H-Y-15	0.59	0.36	-	221	-	[10]
	0.54	0.32	760	144	-	[11]
H-Y-30	0.56	0.32	797	171	-	[11]
	0.54	0.27	805	-	261	[12]
H-Y-40	0.52	0.26	734	226	-	[11]
	0.65	0.32	-	394	-	[10]

References

1. Shcherbinin, V. A.; Konshin, V. V., Convenient synthesis of O-functionalized mandelic acids via Lewis acid mediated transformation of 1,3-dioxolan-4-ones. *Tetrahedron* **2019,** *75* (26), 3570-3578.

2. De Clercq, R.; Makshina, E.; Sels, B. F.; Dusselier, M., Catalytic Gas-Phase Cyclization of Glycolate Esters: A Novel Route Toward Glycolide-Based Bioplastics. *ChemCatChem* **2018,** *10* (24), 5649-5655.

3. Murphy, B. M.; Letterio, M. P.; Xu, B., Catalytic dehydration of methyl lactate: Reaction mechanism and selectivity control. *J. Catal.* **2016,** *339*, 21-30.

4. Gabriel Chuchani, I. M., Elimination Kinetics of D,L-Mandelic Acid in the Gas Phase. *J. Phys. Org. Chem.* **1997,** *10*, 121-124.

5. De Clercq, R.; Dusselier, M.; Poleunis, C.; Debecker, D. P.; Giebeler, L.; Oswald, S.; Makshina, E.; Sels, B. F., Titania-Silica Catalysts for Lactide Production from Renewable Alkyl Lactates: Structure–Activity Relations. *ACS Catal.* **2018,** *8* (9), 8130-8139.

6. De Clercq, R.; Dusselier, M.; Makshina, E.; Sels, B. F., Catalytic Gas-Phase Production of Lactide from Renewable Alkyl Lactates. *Angew. Chem. Int. Ed. Engl.* **2018,** *57* (12), 3074-3078.

7. Dusselier, M.; Van Wouwe, P.; Dewaele, A.; Jacobs, P. A.; Sels, B. F., Shape-selective zeolite catalysis for bioplastics production. *Science* **2015,** *349*, 78-80.

8. Lin, R.; Mitchell, S.; Netscher, T.; Medlock, J.; Stemmler, R. T.; Bonrath, W.; Létinois, U.; Pérez-Ramírez, J., Substrate substitution effects in the Fries rearrangement of aryl esters over zeolite catalysts. *Catal. Sci. Tech.* **2020,** *10* (13), 4282-4292.

9. Chapellière, Y.; Daniel, C.; Tuel, A.; Farrusseng, D.; Schuurman, Y., Kinetics of n-Hexane Cracking over Mesoporous HY Zeolites Based on Catalyst Descriptors. *Catalysts* **2021,** *11* (6).

10. Kenvin, J.; Mitchell, S.; Sterling, M.; Warringham, R.; Keller, T. C.; Crivelli, P.; Jagiello, J.; P é rez-Ram í rez, J., Quantifying the Complex Pore Architecture of Hierarchical Faujasite Zeolites and the Impact on Diffusion. *Adv. Funct. Mater.* **2016,** *26* (31), 5621-5630.

11. Keller, T. C.; Arras, J.; Wershofen, S.; Pérez-Ramírez, J., Design of Hierarchical Zeolite Catalysts for the Manufacture of Polyurethane Intermediates. *ACS Catal.* **2014,** *5* (2), 734-743.

12. Lakiss, L.; Vicente, A.; Gilson, J. P.; Valtchev, V.; Mintova, S.; Vimont, A.; Bedard, R.; Abdo, S.; Bricker, J., Probing the Bronsted Acidity of the External Surface of Faujasite-Type Zeolites. *ChemPhysChem* **2020,** *21* (16), 1873-1881.

Appendix 3 – Selective alkylation of mandelic acid to diarylacetic acids over a commercial zeolite

Part of this thesis has been published in the following journal publication.

ChemComm

COMMUNICATION

View Article Online
View Journal | View Issue

Cite this: *Chem. Commun.*, 2023, **59**, 9243

Received 23rd March 2023,
Accepted 3rd July 2023

DOI: 10.1039/d3cc01444d

rsc.li/chemcomm

Selective alkylation of mandelic acid to diarylacetic acids over a commercial zeolite†

Samuel G. Meacham and Russell A. Taylor *

A commercial zeolite is shown to be a highly effective heterogeneous catalyst for the Friedel–Crafts alkyation of mandelic acid with aromatic substrates. The reaction yields mixed diarylacetic acids in one step avoiding the need for inert atmosphere techniques or superacids. The observed reaction pathways are zeolite framework dependent with only the FAU framework giving very high selectivity to the mixed diarylacetic acids.

The Friedel–Crafts (FC) alkylation reaction is catalysed by a wide variety of strong Lewis acids (*e.g.* $AlCl_3$) and Brønsted acids (*e.g.* H_2SO_4), but very commonly stoichiometric, or super-stoichiometric, amounts of these acids are utilised.[1,2] The traditional use of toxic alkylhalide substrates as masked electrophiles also leads to problems with the formation of HX by-products, such as salt formation. As such, the development of improved Friedel–Crafts alkylation procedures for the formation of C–C bonds remains a highly active area of chemical research.[3–5] The use of so-called "π-activated" alcohols has proven to be a successful way to use alcohols as electrophiles (rather than toxic alkylhalides) but the great number of reports in the field utilise transition metal catalysts or metal salts that can be de-activated by the water co-produced and/or are difficult to recycle.[3,6] The use of heterogeneous catalysts for Friedel–Crafts alkylation reactions with alcohols has the potential to overcome the aforementioned limitations, with heteropolyacids and zeolites showing utility in this general transformation.[7–12]

We herein report that a commercial zeolite, H-Y-30 (CBV760 from Zeolyst), selectively converts mandelic acid to diarylacetic acids through an FC alkylation reaction (hydroxyalkylation) in aromatic solvents. Diarylacetic acid moieties are important scaffolds in active pharmaceutical ingredients[13–17] but simple synthetic routes do not exist at present. Homogeneous routes to mixed diarylacetates have been reported from monoaryl precursors, but many of these routes are expensive (*e.g.* Pd plus ligand[18,19]), atom inefficient (*e.g.* stoichiometric metal salts[20,21] or halogenated substrates[18–21]) and/or hazardous to implement (diazo-precursors[22–24]).

On the other hand, diarylacetic acids can be formed with heterogeneous, strong Brønsted acid catalysts. Super-stoichiometric triflic acid supported on PVP can catalyse the formation of diarylacetic acids directly from glycolic acid and aromatics in one step, but the catalyst is air sensitive and requires handling of hazardous, super acid: triflic acid.[25] Similarly, H_2SO_4 supported on silica (in glacial acetic acid) can catalyse the same reaction when using electron rich aromatics, but was unable to convert mandelic acid to a diarylacetic acid.[26]

During the course of our investigations into the zeolite catalysed reactions of mandelic acid, we have discovered that mixed diarylacetic acids can be formed from mandelic acid and aromatic substrates using a commercial acidic zeolite catalyst, without the need for inert atmosphere techniques. Initial catalyst screening results with *p*-toluenesulfonic acid (pTSA) and a variety of acidic zeolite catalysts are shown in Fig. 1.

Using mixed xylenes as substrate and solvent, the overnight reactions were carried out using a phase separator to remove water from the reaction flask (Fig. S1, ESI†). Zeolite catalyst loadings were adjusted to give 3 mol% Al (relative to mandelic acid). Fig. 1 shows that when using a homogeneous catalyst (pTSA) only the linear dimer and cylic dimer, mandelide, were produced at ~80% conversion. The formation of mandelide using pTSA as catalyst is known[27,28] (mixed xylenes, 1 day, 25% or 3 days, 57% yield) and was reproduced under our conditions. However, when using heterogeneous, acidic zeolite catalysts additional products were observed alongside the expected linear dimer and mandelide (Scheme 1). These additional products were: (1) diarylacetic acids from FC alkylations, (2) benzaldehyde, and (3) 2,5-diphenyl-1,3-dioxolan-4-one from the reaction of benzaldehyde with mandelic acid.

From Fig. 1 it is clear that the zeolite framework and Si/Al ratio have a marked effect on conversion and the observed product distribution. Zeolites H-Beta-75 and H-Y-30 were the

Department of Chemistry, Durham University, South Road, Durham DH1 3LE, UK. E-mail: russell.taylor@durham.ac.uk

† Electronic supplementary information (ESI) available. See DOI: https://doi.org/10.1039/d3cc01444d

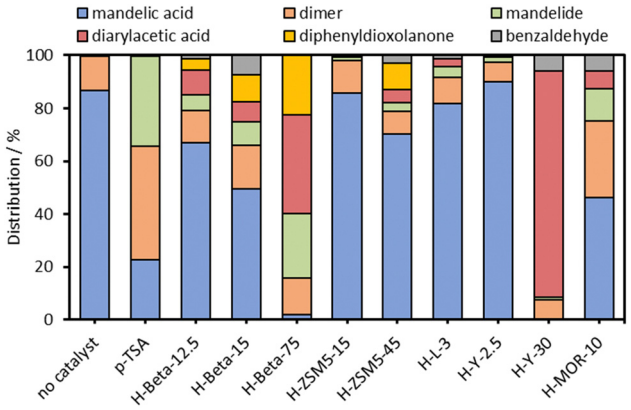

Fig. 1 Effect of zeolite catalyst framework and Si/Al ratio on product distribution. Conditions: 0.5 g mandelic acid in 50 ml mixed xylenes, 3 mol% H^+ (pTSA) or 3 mol% Al (zeolites), reflux with Dean Stark trap overnight (*ca.* 20 hours), stirring rate = 500 rpm.

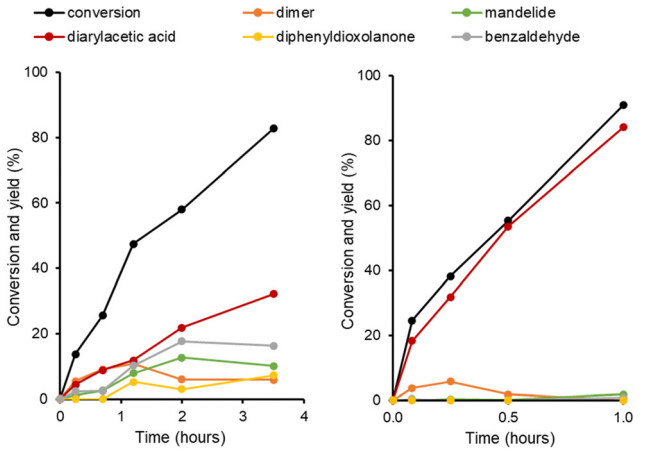

Fig. 2 Effect of reaction time on product distribution for H-Beta-75 (left) and H-Y-30 (right) zeolite-catalysed reaction of mandelic acid. Solvent = mixed xylenes.

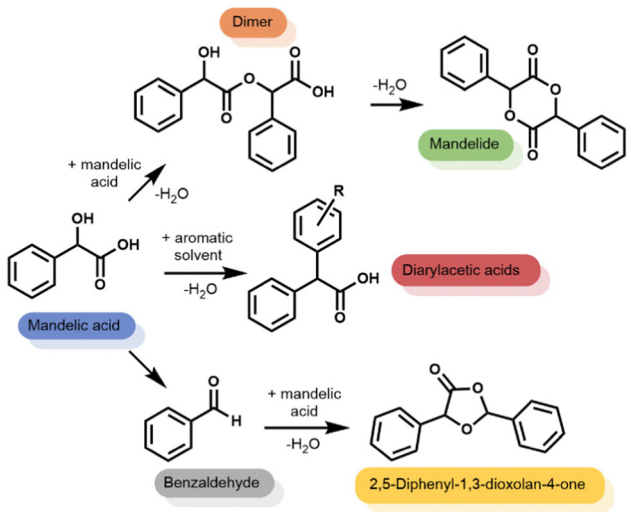

Scheme 1 Range of products observed in zeolite-catalysed reactions of mandelic acid.

most active for mandelic acid conversion under the reaction conditions. For H-Beta, three different Si/Al ratios were tested and we surprisingly observed that the conversion increased from approximately 35% to 98% upon increasing the Si/Al from 12.5 to 75, despite the Al loading remaining constant. In the case of zeolite H-Y-30, very high selectivity for the FC alkylation reaction was observed. The medium pore ZSM-5 zeolites showed lower conversion than the large pore H-Beta, H-Y and H-MOR zeolites, which may be due to the reactant being too large to enter the medium micropore system of ZSM-5.

In order to further understand the reaction pathways occurring with the most active materials, H-Y-30 and H-Beta-75, a series of reaction time profile experiments were carried out, the results of which are shown in Fig. 2. In the case of H-Beta-75, all reaction pathways (shown in Scheme 1) occur simultaneously. At short reaction times, the linear dimer of mandelic acid and the FC alkylation product are the major components. At reaction times longer than 1 hour, the linear dimer concentration decreases as it is converted to the cyclic dimer mandelide. Benzaldehyde is also observed at all reaction times, with the subsequent dioxolanone product only forming at reaction times greater than 1 hour. Between 2 to 3.5 hours, the predominant reaction occurring is the FC Alkylation. For H-Y-30 the major product is the FC alkylation product at all time points measured.

The FC alkylation of mandelic acid catalysed by H-Y-30 was explored further using a range of aromatic solvents (*o*-, *m*-, *p*-xylene, toluene and chlorobenzene). Initial experiments (reflux, phase separator, 1 hour) show that the FC alkylation product dominates across all solvents (Fig. S15, ESI†), but conversion varied from 17% (toluene) up to 92% (*o*-xylene), and selectivity for the FC product varied from 68% (chlorobenzene) to 97% (*o*-xylene). As this variation in selectivity could be due to the different reflux temperatures (and thus variation of selectivity at different conversion levels after 1 hour) or aromatic substituent effects, time profiles were also recorded (Fig. 3A) in order to study product selectivity at near iso-conversion (Fig. 3B). The selectivity to the FC alkylation product still varies at near iso-conversion (Fig. 3B), indicating that the aromatic substituents do cause directing effects and modulation of ring reactivity. Such effects are consistent with carbocation chemistry, suggesting carbocation intermediates may be involved. Screening H-Beta-75 across the same range of reaction solvents still resulted in a broad range of products; notably, in the absence of aromatic solvents, mandelide could be formed as the dominant product over H-Beta-75 (Fig. S16, ESI†). An additional iso-conversion study comparing H-Beta-75, H-Y-30, H-ZSM5-45 and H-MOR-97 show that the high selectivity to diarylacetic acids is framework selective (Fig. S17, ESI†).

These observations show that the product of mandelic acid conversion with aromatics by acidic zeolite catalysts can be tuned by controlling the microenvironment surrounding the active site. Homogenous pTSA yields condensation products of

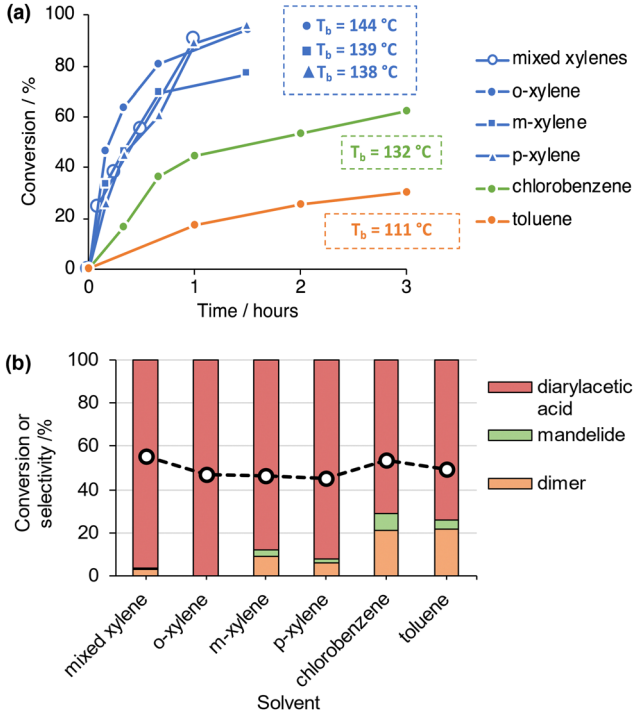

Fig. 3 (a) Effect of reaction time on mandelic acid conversion in various aromatic solvents. (b) Selectivity and conversion to arylation products catalysed by H-Y-30 zeolite. Reactions were run for various time under reflux at the boiling point of each solvent to obtain 45–55% conversion. Aside from *p*-xylene, products are obtained as a mixture of positional isomers, with the para isomer the major product.

dehydration, while zeolites can promote an FC alkylation pathway that is typical of superacids,[25,26] but do so under non-superacid conditions The yield of the FC reaction product is highly dependent on the zeolite framework, indicating that the necessary reaction intermediates for FC alkylation of mandelic acid are stabilised by the FAU framework. In addition, the observation that H_2SO_4 supported on silica (in glacial acetic acid) is unable to convert mandelic acid to a diarylacetic acid in aromatic solvents[26] supports the importance of the zeolite framework in modulating the reaction outcome. The observation of multiple reaction pathways, catalysed by zeolites, for mandelic acid conversion under these reaction conditions is in contrast to a recent report which showed that H-Y-2.6, H-Beta-12.5 and H-Beta-75 were effective catalysts for the production of lactide from lactic acid (in xylenes, under analogous conditions).[29] The only by-products observed in this reported system were linear oligomers of lactic acid, in contrast to our findings. Furthermore, surfactant-templated zeolite Y has been successfully applied for the FC alkylation of indole with "π-activated" alcohols.[11] Indole is, however, an electron-rich nucleophile in FC reactions with a nucleophilicity parameter 9 orders of magnitude greater than toluene and is therefore easily alkylated in FC alkylation reactions.[30,31] In addition, "π-activated" alcohols bearing electron withdrawing groups are notoriously difficult FC electrophiles,[32] all of which highlights the remarkable selectivity exhibited with H-Y-30 for the reported FC alkylation reactions reported here.

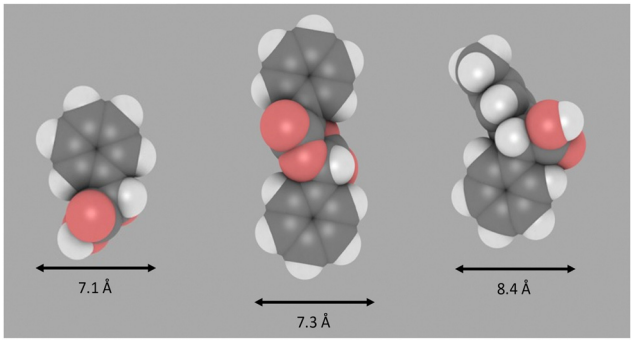

Fig. 4 Approximate diameter perpendicular to long axis of the molecule. Image produced using iRASPA. Left: Mandelic acid, middle: mandelide, right: Alpha arylation product (solvent = *p*-xylene).

To further consider the differences in product selectivity observed across the range of zeolite catalysts tested, the size of some of the key products formed in these experiments were modelled using an approach that has been successfully reported recently.[33,34] Molecular sizes were approximated by first carrying out an energy minimisation of the molecular structures followed by calculating the minimum projection area (from van der Waals radii) as detailed in the ESI† (Section S3). The diameter of mandelic acid (Fig. 4) was found to be approximately 7.1 Å, greater than the largest pore width of both zeolites ZSM-5 (5.7 Å) and H-Beta (6.6 Å), but slightly smaller than that of H-Y (7.4 Å).[35] Mandelide has a similar diameter of 7.3 Å. The largest of all the products are the diarylacetic acids, at 8.4 Å for the product of *p*-xylene and mandelic acid. This is larger than the nominal pore widths of all zeolites tested in this work but could be included within the supercage of zeolite Y (11.2 Å). Hence mandelic acid is very likely excluded from accessing the internal pore system of medium pore (10-membered ring) H-ZSM-5, resulting in low conversion. However, for the large (12-membered ring) zeolites such as Beta, Y and MOR, conversion during screening was observed to be more significant in general (Fig. 1) suggesting improved active site accessibility. For the same zeolite framework, conversion was shown to increase as the Si/Al ratio increases (Fig. 1). This is exemplified for zeolite H-Beta where the conversion increases across three Si/Al ratios (12.5, 15 and 75) but the product distribution remains constant. Likewise, for zeolite H-Y, conversion increases across H-Y-2.5, H-Y-15 and H-Y-30 (5%, 38% and 90% respectively, (1 hour, *p*-xylene, reflux, Fig. S18, ESI†). The formation of benzaldehyde and dioxolanone is not observed for any H-Y catalysts (Fig. S18, ESI†). It has been well established that the high silica zeolite Y materials from Zeolyst (CBV series) are formed by steaming and acid washing and result in hierarchical materials containing mesopores.[36,37] The fact that high silica forms of both Beta and Y, which all have higher mesoporosity (ESI,† Section S4) and give rise to the highest conversion, indicate that the presence of mesopores are critical for high catalytic activity.

Whilst the true origin of the observed selectivity for FC alkylation products is beyond the scope of this work, the following observations are suggestive. We have calculated that diarylacetic acids should be too large to exit (or enter) the micropore system of any of the frameworks tested, likely

excluding the traditional modes of shape selectivity (*reactant*, *product* and *transition*) that are well established in zeolite catalysis.[38–40] Counter intuitively, an inverse relationship of conversion with acid site density is observed for Beta and FAU frameworks, but this is coupled to the hierarchical nature of the high silica forms of FAU and Beta catalysts tested here, which indicates that hierarchical structures are critical to conversion. In addition, the very high selectivity for FC alkylation over high silica, hierarchical H-Y-30, which is not observed over other frameworks or with homogeneous catalysts, indicates that the (heirachical) FAU framework is essential. This suggests that confinement[41] or the nest effect[40] (*i.e.* surface exposed, partial super cages) may be responsible for our observations. We are continuing our investigations to probe this facile procedure and determine the origins of the observed selectivity.

In conclusion, we have shown that the observed product selectivity in the reaction of mandelic acid in aromatic solvents is controlled by the zeolite frameworks, and diarylacetic acids can be formed selectivity over the FAU framework. The findings provide a simple and green approach to this important organic moiety, without the need for super-stoichiometric acid, or corrosive and/or inert conditions.

R. A. T. thanks the EPSRC for generous funding of an EPSRC Manufacturing Fellowship, EP/R01213X/1. S. M. was supported by the EPSRC CDT in Soft and Functional Interfaces, EP/L015536/1.

Conflicts of interest

There are no conflicts to declare.

Notes and references

1 M. Rueping and B. J. Nachtsheim, *Beilstein J. Org. Chem.*, 2010, **6**, 6.
2 M. M. Heravi, V. Zadsirjan, P. Saedi and T. Momeni, *RSC Adv.*, 2018, **8**, 40061–40163.
3 R. Kumar and E. V. Van der Eycken, *Chem. Soc. Rev.*, 2013, **42**, 1121–1146.
4 S. Zhang, M. Vayer, F. Noël, V. D. Vuković, A. Golushko, N. Rezajooei, C. N. Rowley, D. Lebœuf and J. Moran, *Chemistry*, 2021, **7**, 3425–3441.
5 S. Estopiñá-Durán and J. E. Taylor, *Chem. – Eur. J.*, 2021, **27**, 106–120.
6 M. Bandini and M. Tragni, *Org. Biomol. Chem.*, 2009, **7**, 1501–1507.
7 K.-i Shimizu and A. Satsuma, *Energy Environ. Sci.*, 2011, **4**, 3140–3153.
8 Y. Sun and R. Prins, *Appl. Catal., A*, 2008, **336**, 11–16.
9 K. Masuda, Y. Okamoto, S. Y. Onozawa, N. Koumura and S. Kobayashi, *RSC Adv.*, 2021, **11**, 24424–24428.
10 Y. N. Nayak, N. Swarnagowri, Y. F. Nadaf, N. S. Shetty and S. L. Gaonkar, *Lett. Org. Chem.*, 2020, **17**, 491–506.
11 N. Linares, F. G. Cirujano, D. E. De Vos and J. García-Martínez, *Chem. Commun.*, 2019, **55**, 12869–12872.
12 J. R. Cabrero-Antonino, A. Leyva-Pérez and A. Corma, *Angew. Chem., Int. Ed.*, 2015, **54**, 5658–5661.
13 D. M. Brown, B. O. Hughes, C. D. Marsden, J. C. Meadows and B. Spicer, *Br. J. Pharmacol.*, 1973, **47**, 476–486.
14 M. G. Palfreyman, E. S. Palfreyman and M. S. G. Clark, *Eur. J. Pharmacol.*, 1974, **28**, 379–383.
15 B. E. Maryanoff, S. O. Nortey and J. F. Gardocki, *J. Med. Chem.*, 1984, **27**, 1067–1071.
16 I. Roufos, S. J. Hays, D. J. Dooley, R. D. Schwarz, G. W. Campbell and A. W. Probert, Jr., *J. Med. Chem.*, 1994, **37**, 268–274.
17 I. Roufos, S. Hays and R. D. Schwarz, *J. Med. Chem.*, 1996, **39**, 1514–1520.
18 B. Song, T. Himmler and L. J. Gooßen, *Adv. Synth. Catal.*, 2011, **353**, 1688–1694.
19 W. A. Moradi and S. L. Buchwald, *J. Am. Chem. Soc.*, 2001, **123**, 7996–8002.
20 Y. Kim, Y. S. Choi, S. K. Hong and Y. S. Park, *Org. Biomol. Chem.*, 2019, **17**, 4554–4563.
21 P.-S. Lai, J. A. Dubland, M. G. Sarwar, M. G. Chudzinski and M. S. Taylor, *Tetrahedron*, 2011, **67**, 7586–7592.
22 S. Hu, J. Wu, Z. Lu, J. Wang, Y. Tao, M. Jiang and F. Chen, *ChemCatChem*, 2021, **13**, 2559–2563.
23 Y. Xi, Y. Su, Z. Yu, B. Dong, E. J. McClain, Y. Lan and X. Shi, *Angew. Chem., Int. Ed.*, 2014, **53**, 9817–9821.
24 B. Wang, I. G. Howard, J. W. Pope, E. D. Conte and Y. Deng, *Chem. Sci.*, 2019, **10**, 7958–7963.
25 G. K. S. Prakash, F. Paknia, A. Kulkarni, A. Narayanan, F. Wang, G. Rasul, T. Mathew and G. A. Olah, *J. Fluorine Chem.*, 2015, **171**, 102–112.
26 D. L. Moore, A. E. Denton, R. M. Kohinke, B. R. Craig and W. E. Brenzovich, *Synth. Commun.*, 2016, **46**, 604–612.
27 T. Q. Liu, T. L. Simmons, D. A. Bohnsack, M. E. Mackay, M. R. Smith and G. L. Baker, *Macromolecules*, 2007, **40**, 6040–6047.
28 G. J. Graulus, N. Van Herck, K. Van Hecke, G. Van Driessche, B. Devreese, H. Thienpont, H. Ottevaere, S. Van Vlierberghe and P. Dubruel, *React. Funct. Polym.*, 2018, **128**, 16–23.
29 M. Dusselier, P. Van Wouwe, A. Dewaele, P. A. Jacobs and B. F. Sels, *Science*, 2015, **349**, 78–80.
30 H. Mayr, B. Kempf and A. R. Ofial, *Acc. Chem. Res.*, 2003, **36**, 66–77.
31 S. Lakhdar, M. Westermaier, F. Terrier, R. Goumont, T. Boubaker, A. R. Ofial and H. Mayr, *J. Org. Chem.*, 2006, **71**, 9088–9095.
32 V. D. Vuković, E. Richmond, E. Wolf and J. Moran, *Angew. Chem., Int. Ed.*, 2017, **56**, 3085–3089.
33 T. C. Keller, S. Isabettini, D. Verboekend, E. G. Rodrigues and J. Pérez-Ramírez, *Chem. Sci.*, 2014, **5**, 677–684.
34 F. C. Hendriks, D. Valencia, P. C. A. Bruijnincx and B. M. Weckhuysen, *Phys. Chem. Chem. Phys.*, 2017, **19**, 1857–1867.
35 C. Baerlocher and L. McCusker, Database of Zeolite Structures, **https://www.iza-structure.org/databases/**, (accessed 23rd March 2023).
36 K. P. de Jong, J. Zečević, H. Friedrich, P. E. de Jongh, M. Bulut, S. van Donk, R. Kenmogne, A. Finiels, V. Hulea and F. Fajula, *Angew. Chem., Int. Ed.*, 2010, **49**, 10074–10078.
37 J. Kenvin, S. Mitchell, M. Sterling, R. Warringham, T. C. Keller, P. Crivelli, J. Jagiello and J. Perez-Ramirez, *Adv. Funct. Mater.*, 2016, **26**, 5621–5630.
38 S. M. Csicsery, *Zeolites*, 1984, **4**, 202–213.
39 M. E. Davis, *Ind. Eng. Chem. Res.*, 1991, **30**, 1675–1683.
40 T. F. Degnan, *J. Catal.*, 2003, **216**, 32–46.
41 R. Gounder and E. Iglesia, *Chem. Commun.*, 2013, **49**, 3491–3509.

